Microstructure Development and Transport Properties of Portland Cement-fly Ash Binary Systems

-in view of service life predictions

Zhuqing Yu

Microstructure Development and Transport Properties of Portland Cement-fly Ash Binary Systems

-in view of service life predictions

Proefschrift

ter verkrijging van de graad van doctor
aan de Technische Universiteit Delft,
op gezag van de Rector Magnificus Prof. dr. W. R. Hagen;
voorzitter van het College voor Promoties,
in het openbaar te verdedigen op
20 May, 2015 om 10:00 uur

door

Zhuqing YU

Master of Science, Wuhan University of Technology, P.R.China
geboren te Yantai, P.R.China

Dit proefschrift is goedgekeurd door de promotoren:
Prof. dr. ir. K. van Breugel

Copromotor:
Dr. G. Ye

Samenstelling promotiecommissie:

Rector Magnificus,	Technische Universiteit Delft, voorzitter
Prof. dr. ir. K. van Breugel,	Technische Universiteit Delft, promotor
Dr. G. Ye,	Technische Universiteit Delft, copromotor
Prof. dr. R. B. Polder,	Technische Universiteit Delft, TNO Technical Sciences
Prof. dr. ir. Geert De Schutter,	Universiteit Gent, België
Prof. Carmen Andrade,	National Research Council of Spain, Spain
Dr. Martin Hunger,	ENCI B.V., the Netherlands
Prof. Xiaodong Shen,	Nanjing Tech University, P. R. China
Prof.ir. R.P.J. van Hees,	Technische Universiteit Delft, reservelid

Published and distributed by:

Zhuqing Yu
Section Materials & Environment
Faculty of Civil Engineering & Geosciences
Technische Universiteit Delft
Email: yu.zhuqing@hotmail.com

ISBN: 978-94-6186-464-2
Keywords: fly ash, concrete, microstructure development, ageing factor

Printing: Haveka B.V., the Netherlands
Copyright ©2015 Zhuqing Yu

All rights reserved. No part of the material protected by this copyright notice may be reproduced or utilized in any form or by any means, electronic or mechanical, including photocopying, recording or by any information storage and retrieval system, without written consent from the publisher.

To my family

Table of Contents

List of Symbols

A	cross-sectional area of the sample	[m^2]
$A_{C_{s,cl}}$	regression parameter describing the relation between the chloride surface concentration and the w/c ratio	[% relative to binder]
C	chloride concentration	[mol/m^3]
C_s	surface chloride content	[% relative to binder]
C_i	initial chloride concentration in the concrete	[% relative to binder]
$C(x,t)$	chloride concentration at depth x and after time t	[-]
C_{cr}^{c}	characteristic value of the critical chloride concentration	[% relative to binder]
C_{cr}^{d}	design value of the critical chloride concentration	[% relative to binder]
$C^d(x,t)$	design value of chloride concentration at depth x and after time t	[% relative to binder]
$C_{s,cl}^{d}$	design value of the chloride surface concentration	[% relative to binder]
d	pore diameter	[-]
D	chloride diffusion coefficient	[m^2/s]
$D(t)$	chloride diffusion coefficient	[m^2/s]
D_{RCM}	chloride migration coefficient	[m^2/s]
D_0	chloride migration coefficient at the reference time of the concrete (normally 28 days)	[m^2/s]
erf	complement of error function	[-]
g	acceleration due to gravity	[9.81 m^2/s]
k	correction factor	[-]
K	intrinsic permeability	[m^2]
K_{SP}	solubility product constant which is the equilibrium constant for a solid substance dissolving in an aqueous solution	[-]
K_W	water permeability coefficient	[m/s]
$k_{e,cl}^{c}$	environment factor	[-]
$k_{c,cl}^{c}$	curing factor	[-]
$L^{'}$	thickness of the specimen	[mm]
L	thickness of the solid	[m]
n, n_{cl}	ageing factor	[-]
N	number of total images	[-]
p	applied pressure	[-]
Q	rate of fluid flow	[m^3/s]
$\gamma_{C_{cr}}$	partial factor of the critical chloride concentration	[-]
$\gamma_{C_{s,cl}}$	partial factor for the surface concentration	[-]
$R_{cl}^{d}(t)$	design value of the resistance to chloride penetration	[$year/mm^2$]
$R_{cl,0}^{c}$	resistance to chloride penetration determined on the basis of compliance tests	[$year/mm^2$]
t	age of the concrete	[days]
t_0	reference time of the concrete	[days]
t_i^d	service life	[years]

t_d	test duration	[hour]
T	average value of the initial and final temperatures in the anolyte solution	[°C]
U	absolute value of the applied voltage	[V]
v	dynamic viscosity of the fluid	[s/m^2]
$V_{c\text{-}measured}$	volume of unreacted clinker from the image analysis	[-]
$V_{c\text{-}initial}$	initial volume of cement in the mix proportions	[-]
$V_{FA\text{-}measured}$	volume of fly ash from the image analysis	[-]
$V_{FA\text{-}initial}$	initial volume of fly ash in the mix proportions	[-]
x	position in the sample	[m]
x_d	average value of the penetration depth	[mm]
x^d	design value of the cover depth	[mm]
x^c	cover depth to reinforcement	[mm]
$\alpha(cement)$	degree of hydration of cement	[-]
$\alpha(fly\ ash)$	degree of pozzolanic reaction of fly ash	[-]
γ	surface tension of the mercury	[mN/m]
$\gamma_{R_{cl}}$	partial factor for the resistance with respect to chloride ingress	[-]
θ	contact angle between the mercury and the pore wall surface of the material	[-]
ρ	density of the fluid	[kg/m^3]
Δh	hydraulic pressure gradient	[m]
Δt	time interval during which the volume was collected	[s]
ΔV	incremental volume of water read from the graduated tube	[m^3]
Δx	safety margin for the cover depth	[mm]

List of Abbreviations

ACI	American Concrete Institute
AFt	ettringite
AFm	monosulfate aluminate hydrate
$AgNO_3$	silver nitrate
Al_2O_3	alumina oxide
A-S	aluminosilicate
BSE	backscattered electron
C_3A	tricalcium aluminate
C_4AF	ferrite
$CaCO_3$	calcium carbonate, limestone powder
CH	calcium hydroxide
CASH	monosulfoaluminate hydrate
CAH	calcium aluminate hydrate
C_3S	tricalcium silicate
C_2S	dicalcium silicate
$C\underline{S}H_2$	gypsum
C-S-H	calcium silicate hydrate
DEF	delayed ettringite formation
D_{RCM}	chloride migration coefficient
DTA	differential thermal analysis
EDS	energy dispersive spectroscopy
ESEM	environmental scanning electron microscope
MIP	mercury intrusion porosimetry
PSD	particle size distribution
RCM	rapid chloride migration
SE	secondary electron
SiO_2	silica dioxide
TG	thermogravimetric
w/b	water to binder ratio
w/c	water to cement ratio
XRD	X-ray diffraction

Summary

Fly ash is a by-product of burning coal in electric power generating plants. It is commonly known that owing to its pozzolanic properties fly ash is widely used as a partial replacement for Portland cement in concrete. The use of fly ash in concrete not only reduces the landfill costs of fly ash, but also reduces the use of Portland cement in concrete, consequently reduces CO_2 emission per ton concrete. More important, the presence of fly ash improves the durability of concrete and extends the service life of concrete structures. Today, there is a demand for concrete structures with a service life of 80, 100, or even 200 years. In many cases chloride-induced rebar corrosion is assumed to be the dominant mechanism determining the service life of reinforced concrete structures. It is commonly believed that fly ash concrete has a better resistance to chloride penetration than Portland cement concrete, since the microstructure development of Portland cement-fly ash binary systems is different from that of pure Portland cement system. The resistance of concrete to chloride penetration is highly related to their microstructure. The studies on Portland cement-fly ash binary systems (concrete or paste) have been carried out for many years. Most studies are based on experimental results at a relative short curing period (i.e. 3 months) or from different concrete mixtures with different fly ash and Portland cement. The advantage of using fly ash, *however*, becomes evident at later ages, *i.e.* beyond 90 days. Systematic long-term investigations on Portland cement-fly ash binary systems are still limited. In this thesis the research on these binary systems starts from the hydration process (chapter 3), the microstructure development (chapter 4) to transport properties (water permeability and chloride penetration) (chapter 5-chapter 8) in view of service life predictions of concrete structures made with fly ash-blended cements.

In a fly ash cement paste there are two types of chemical reactions: hydration of cement and pozzolanic reaction of fly ash. The pozzolanic reaction of fly ash needs calcium hydroxide (CH), *produced by the hydration of cement*, to occur. The evolution of the amount of CH with time reflects the rate of hydration of cement and pozzolanic reaction of fly ash in binary systems. As discussed in chapter 3 at early ages, *i.e.* before 7 days, the CH content of blended cement paste was higher than that of Portland cement paste. It indicated that the presence of fly ash leaded to faster hydration of cement in binary systems. After about 7 days, the CH content in blended cement paste decreases significantly. It suggests that in binary systems the rate of the pozzolanic reaction of fly ash (consuming CH) is faster than that of the hydration of cement (producing CH). At later ages, *i.e.* beyond 180 days, the CH content in blended cement paste stays at a constant low level. It is inferred that beyond 180 days the rate of the pozzolanic reaction of fly ash in binary systems becomes very slow.

The pozzolanic reaction of fly ash results in a different microstructure development of blended cement paste compared with pure Portland cement paste. In chapter 4 the evolution of the pore structure of Portland cement paste and blended cement paste was investigated at ages up to 3 years. The porosity of blended cement paste was higher than that of pure Portland cement paste, even at an age of 3 years. At later ages, i.e. after about 28 days, the presence of fly ash results in the formation of a large amount of small capillary pores in the range between 10 and 100 nm. At later ages, *i.e.* after 180 days, blended cement paste had a lower connectivity of the pores than Portland cement paste. The pore structure of blended cement paste was refined at later ages while the porosity of blended cement was still higher than that of Portland cement paste (at ages up to 3 years).

The microstructure of paste determines the transport properties. In chapter 5 the water permeability of Portland cement paste and blended cement paste was studies. At early age the pastes containing fly ash exhibit a higher capillary porosity than pure Portland cement paste. The initial water permeability of blended cement paste is higher than that of Portland cement paste. However, after about 180 days blended cement paste is less permeable than pure Portland cement paste, even though the capillary porosity of blended cement paste is higher than that of Portland cement paste. The water permeability of pure cement paste and blended cement paste depends on the connectivity of the pores. At later ages, i.e. after 180 days, the connectivity of the pores of blended cement paste is lower than that of pure Portland cement paste, resulting in a less permeable microstructure.

In chapter 6 the resistance of Portland cement concrete and fly ash concrete to chloride penetration was investigated. Under moist curing conditions the D_{RCM} values of Portland cement concrete made with different w/c ratios (0.4, 0.5 and 0.6) decrease with time at early ages, i.e. from 28 to 180 days. After that the D_{RCM} values of Portland cement concrete increase and then turn to decrease again after around 1 year (Figure 6.6). The possible reason might be the delayed ettringite formation in Portland concrete when limestone powder (as filler) is blended with Portland cement clinker and when it is cured under moist conditions (see chapter 7). The DEF results in a change of the microstructure of hydrated cement paste and an increase of D_{RCM} at later ages. At ages beyond about 28 days the concrete mixtures made with fly ash have better resistance against chloride penetration than Portland cement concrete. Ettringite forms in fly ash concrete at later ages. This ettringite is found in voids initially present in the paste and in the spaces left after the reaction of fly ash particles. Formation of ettringite in empty spaces explains why DEF in fly ash concrete does not lead to expansion and micro-cracking and an associated increase of the D_{RCM} values as observed for Portland cement concrete.

Based on the measured D_{RCM} values for Portland cement concrete and fly ash concrete, the ageing factor n was determined (see chapter 8). It represents how rapidly the chloride migration coefficient of the concrete decreases with time. In DuraCrete the 28 days values of D_{RCM} and n are two important input parameters to predict the service life of concrete structures. An important question is whether new n-values, as those determined in this study, can directly be adopted in the currently used version of DuraCrete for service life predictions. In DuraCrete it is assumed that the chloride diffusion (migration) coefficient of concrete, $D(t)$, decreases considerably with increasing age of the concrete. This decrease is quantified with a constant value of n. It means that $D(t)$ would go to zero as time tends to infinity ($t \rightarrow \infty$), which is known not to be realistic. In reality, the chloride diffusion coefficient $D(t)$ is directly determined by the microstructure of concrete. In fact, the decrease of the diffusion coefficient cannot be described adequately with a constant value of n. A more accurate description of the evolution of the diffusion coefficient $D(t)$ with an not constant value of n, however, will affect the consistency of the currently used version of DuraCrete. A reconsideration of n-values should be accompanied by reconsidering the values of other model parameters values (*e.g. environmental factor* k_e and *curing factor* k_c in DuraCrete), since these parameter, k_e, k_c and n, are mutually interdependent.

Samenvatting

Vliegas is een bijproduct van de verbranding van steenkool in elektriciteitscentrales. Het is algemeen bekend dat, wegens de puzzolane eigenschappen, vliegas veel wordt gebruikt als een gedeeltelijke vervanging van portlandcement in beton. De toepassing van vliegas in beton vermindert niet alleen de kosten van het storten van vliegas, maar vermindert ook het gebruik van portlandcement in beton, dus vermindert de hoeveelheid CO_2 per ton beton. Belangrijker is dat het toepassen van vliegas de duurzaamheid van beton verbetert en de levensduur van betonconstructies verlengt. Tegenwoordig bestaat er behoefte aan betonconstructies met een levensduur van 80, 100 of zelfs 200 jaar. In veel gevallen geldt chloride-geïnduceerde wapeningscorrosie als een van de belangrijkste mechanismen die de levensduur van gewapend betonconstructies bepalen. Het wordt algemeen aangenomen dat vliegascementbeton een betere weerstand heeft tegen chloridepenetratie dan portlandcement beton, aangezien de microstruc-tuurontwikkeling van portlandvliegascement systemen verschilt van die van een zuiver portland-cement systeem. De weerstand van beton tegen chloridepenetratie is sterk gerelateerd aan de microstructuur. Al vele jaren worden er studies verricht aan mengsels met portlandvliegascement (beton of pasta). De meeste studies betreffen experimenteel onderzoek over een relatieve korte verhardingsperiode (tot circa 3 maanden) en onderzoek naar het gedrag van betonmengsels met verschillende soorten vliegas. De voordelen van vliegas worden echter pas goed merkbaar op latere leeftijd, na ongeveer 90 dagen. Systematisch onderzoek naar het gedrag van betonmeng-sels met portlandvliegascement zijn nog steeds beperkt. Dit proefschrift behandelt onderzoek naar het hydratatieverloop (hoofdstuk 3), de microstructuurontwikkeling (hoofdstuk 4) en de ontwikkeling van de transporteigenschappen (waterdoorlatendheid en chloride penetratie) (hoofdstuk 5 - hoofdstuk 8) vliegascementbeton ten behoeven van levensduurvoorspellingen van betonconstructies die zijn gemaakt met vliegascementbeton.

In een vliegascementpasta vinden twee soorten chemische reacties plaats: hydratatie van cement en puzzolane reactie van de vliegas. Voor de puzzolane reactie van vliegas is calciumhydroxide (CH) nodig. Deze kan worden verkregen door de hydratatie van het cement. De ontwikkeling van het CH-gehalte met de tijd weerspiegelt de mate van hydratatie van cement en de puzzolane reactie van vliegas. Zoals besproken in hoofdstuk 3 is op jonge leeftijd, dat wil zeggen vóór 7 dagen, het CH-gehalte van samengestelde cementen hoger dan dat van puur portlandcement. Het gaf aan dat de aanwezigheid van vliegas leidt tot snellere hydratatie van cement in samengestelde systemen. Na ongeveer 7 dagen verminderde het CH-gehalte in samengestelde cementen aanzienlijk. Dat suggereert dat in deze systemen de snelheid van de puzzolane reactie van vliegas (het consumptie van CH) sneller is dan die van de hydratatie van cement (productie van CH). Op latere leeftijd, dat wil zeggen na meer dan 180 dagen, blijft het CH-gehalte in samengestelde cementen op een constant laag niveau. Hieruit is afgeleid dat na 180 dagen de snelheid van de puzzolane reactie van vliegas in portlandvliegascement erg traag wordt.

De puzzolane reactie van vliegas resulteert in een andere microstructuur van pasta’s van samengestelde cementen in vergelijking met puur portlandcementpasta. In hoofdstuk 4 is de ontwikkeling van de poriestructuur van portlandcementpasta en portlandvliegascementpasta onderzocht bij verschillende ouderdom, tot 3 jaar. De porositeit van portlandvliegascementpasta was hoger dan van zuiver portlandcementpasta, zelfs op een leeftijd van 3 jaar. De aanwezigheid van vliegas resulteert op latere leeftijd, d.i. na ongeveer

28 dagen, in de vorming van een grote hoeveelheid kleine capillaire poriën in de range van 10 tot 100 nm. Op nog latere leeftijd, dat wil zeggen na 180 dagen, had portlandvliegascementpasta een lagere *connectiviteit* van de poriën dan portlandcementpasta. De poriënstructuur van portlandvliegascementpasta werd verfijnd op latere leeftijd, terwijl de porositeit van deze pasta's nog steeds hoger was dan die van portlandcement-pasta (op leeftijden tot 3 jaar).

De microstructuur van de cementsteen (eng.: hardened paste) is bepalend voor de transport-eigenschappen van beton. In hoofdstuk 5 is de waterdoorlatendheid van portlandcementpasta en portlandvliegascementpasta bestudeerd. Op vroege leeftijd vertoonde de pasta met vliegas een hogere capillaire porositeit dan zuivere portlandcementpasta. De aanvankelijke waterdoorlatend-heid van portlandvliegascementpasta was hoger dan die van portlandcementpasta. Na ongeveer 180 dagen werd de portlandvliegascementpasta minder doorlatend dan pure portlandcement-pasta, terwijl de capillaire porositeit van portlandvliegascementpasta hoger was dan die van portlandcementpasta. De waterdoorlatendheid van zuivere cementpasta en samengestelde cementpasta hangt af van de connectiviteit van de poriën. Op latere leeftijd, dat wil zeggen na 180 dagen, was de connectiviteit van de poriën van portlandvliegascementpasta lager dan die van zuivere portlandcementpasta, resulterend in een minder permeabele microstructuur.

In hoofdstuk 6 werd de weerstand van portlandcementbeton en vliegasbeton tegen chloride-penetratie onderzocht. Onder vochtige verhardingsomstandigheden namen de D_{RCM} waarden van portlandcementbeton met verschillende w/c-verhoudingen (0,4, 0,5 en 0,6) in de periode van 28 tot 180 dagen in de tijd af. Daarna liepen de D_{RCM}-waarden van portlandcementbeton weer op om vervolgens na ongeveer 1 jaar weer te dalen (figuur 6.6). De mogelijke reden voor dit gedrag zou vertraagde ettringietvorming (delayed ettringite formation: DEF) in portlandcementbeton kunnen zijn indien kalksteenpoeder (als vulstof) is gemengd met portlandcementklinker en wan-neer het materiaal verhardt onder vochtige omstandigheden (zie hoofdstuk 7). Deze vertraagde ettringietvorming resulteert in een verandering van de microstructuur van cementsteen en een toename van D_{RCM}-waarden op latere leeftijd. Portlandvliegascementen zouden van dit verschijnsel minder last hebben. Ettringiet gevormd in vliegascementbeton op latere leeftijd werd aangetroffen in holtes in de cementsteen en in holtes die na de reactie van vliegasdeeltjes waren achtergebleven. Vorming van ettringiet in lege ruimten zou een verklaring kunne zijn waarom DEF in vliegasbeton niet leidt tot expansie en microscheuring en een bijbehorende stijging van de D_{RCM} waarden zoals waargenomen voor portlandcementbeton.

Op basis van de gemeten D_{RCM} waarden voor portlandcementbeton en vliegasbeton is de verouderingsfactor n bepaald (zie hoofdstuk 8). De n-waarde geeft aan hoe snel de chloride migratiecoëfficiënt van het beton afneemt met de tijd. In DuraCrete zijn de 28 daagse waarden van D_{RCM} en n twee belangrijke inputparameters om de levensduur van betonconstructies te voorspellen. Een belangrijke vraag of nieuw bepaalde n-waarden zonder meer in de momenteel gebruikte DuraCrete versie voor de levensduurvoorspellingen kunnen worden ingebracht. In DuraCrete wordt aangenomen dat het chloride diffusie (migratie) coëfficiënt van beton, D(t), aanzienlijk afneemt met de leeftijd van het beton. Deze daling wordt gekwantificeerd met een *constante* waarde van n. In werkelijkheid wordt de chloride diffusiecoëfficiënt D(t) direct bepaald door de microstructuur van beton. Veranderingen in de microstructuur bij hoge ouderdom van het beton laten zich niet beschrijven met een constante waarde van n. In dit proefschrift beschreven experimentele resultaten geven aanknopingspunten voor een herziene formulering van de verouderingsfactor n, waarmee de ontwikkeling van D(t) van de onderzochte betonmengsels in de tijd nauwkeuriger kan worden beschreven. Benadrukt moet worden dat bij herziening of aanpassing van n-waarden ook de

waarden van andere modelparameters in DuraCrete, bijvoorbeeld omgevingsfactor k_e en nabehandelingsfactor k_c, opnieuw geëvalueerd zouden moeten worden, aangezien deze parameters, k_e, k_c en n, onderling van elkaar afhankelijk zijn.

Acknowledgements

Time flies 光阴荏苒，日月如梭, it seems like just yesterday that I came to Delft University of Technology (TUDelft), the Netherlands. Being a PhD student and managing life is difficult. I would never have been able to finish my dissertation without those persons who gave me help and support. It is to them that I owe my deepest gratitude.

This project was carried out in the Microlab, Civil Engineering and Geosciences, TUDelft and financially sponsored by China Scholarship Council (CSC) and TUDelft. CSC and TUDelft are gratefully acknowledged. I also would like to thank Prof. dr. Zhonghe Shui and Prof. Baoguo Ma, Wuhan University of Technology (WHUT), P.R. China. They supported me to apply this PhD position in TUDelft.

I would like to express my deepest appreciation to my promoter Prof. dr. ir. Klass van Breugel for his excellent guidance, patience, and providing me with an excellent atmosphere for doing research. There is nothing more lucky than discussing with an internationally acclaimed professor for 52 times in 5 months. His tireless efforts and constructive comments on this dissertation are highly appreciated.

I would like to give my sincerest acknowledgement to my co-promotor Assoc. Prof. dr. Guang Ye for his excellent supervision. In these five years, his suggestions, patience and encouragement supported me to pursue a doctorate. My dissertation will not be finished without his sparkling ideas and patiently correction.

I would like to thank my dissertation committee of Prof. dr. R. B. Polder, Prof. dr. ir. Geert De Schutter, Prof. Carmen Andrade, Dr. Martin Hunger and Prof. Xiaodong Shen for their time and valuable feedback on this thesis. I would particularly like to acknowledge Prof. dr. ir. Geert De Schutter, Ghent University (UGent), Belgium, for his kind guidance and helpful advice during the monthly meeting at UGent.

I am grateful to Ms. Franca Post, assistant project coordinator, Center for International Cooperation and Appropriate Technology (CICAT) for her strong support during my stay in TUDelft.

I would like to thank all the colleagues and former colleagues of Microlab. My special thanks go to the kindly technicians, Arjan Thijssen for his patiently teaching and help, Gerrit Nagtegaal for his selfless assistance, and John van den Berg for his kind help. Many thanks to secretaries, Nynke Verhulst, Iris Batterham, Claudia Baltussen, and Melanie Holtzapffel for their kind help with the daily administration affaires. I would like to thank Dr. Dessi Koleva and Dr. Branko Savija for reading my thesis and giving me suggestion. I also have to thank Prof. Erik Schlangen, Dr. Henk Jonkers, Virginie Wiktor, Neuyen van Tuan, Mladena Lukovic, Marija Nedeljkovic, Renée Mors, Agus Susanto, Farhad Pargar, Senot Sangadji, Ennery Leon Fuenmayor for their smile and encouragement, especially to Renee for helping the Dutch translation work. Many thanks to Dr. Zhiwei Qian, one of my ex-officemates for his scientific advice and knowledge and many insightful discussions and suggestion. I will forever be thankful to Hua Dong, Peng Gao, Xu Ma for their accompany and care, to Bei Wu (your family), Zhipei Chen and Jiayi Chen (Wenqin) for their support during my last difficult stage in Delft. I am also very grateful to my Chinese colleagues, Fuhai Li, Yun Zhang, Xuliang Hou, Hao Huang, Yong Zhang, Tianshi Lu, Xiaowei Ouyang, Yibin Zuo, Haoliang

Huang, Qi Zhang, Ying Wang etc. for all the great times that we have shared. I still remember the memorable lunch time every day. I would like to thank Jinlong Li, Jitang Fan, Shaoguang Li, Dongya Ren, Zheng Fang, Ye Yuan for their kind help. My special thanks to my friends, Yuan Zhang, Hailing Zhang, Jingang Wang, Xuhong Qiang, Xu Jiang, Quantao Liu and Yue Xiao. We spent unforgettable time in Delft. You brought me laughter, happiness and warmth.

I am deeply thankful to my father and mother for their love, support, and sacrifices. Without them, I cannot finish my dissertation. This last word of acknowledgment I have saved for my dear husband Dr. Ning Li, who shared my tear and happiness, gave me encouragement to finish my PhD work. In these five years, he cooked for me, helped my laboratory works and corrected my thesis, even though he was doing his own PhD work.

Zhuqing Yu（于竹青）

Delft, the Netherlands,
March, 2015

Chapter 1

Introduction

1.1 Background

Concrete is a composite material, obtained by mixing cementitious materials, water and aggregates. Concrete technology was known by the Ancient Romans 2000 years ago and was widely used within the Roman Empire. The Pantheon in Rome, shown in Figure 1.1, is one of the most magnificent concrete structures. This great building has stood there for over 2000 years and it is still in service in Rome. The Pantheon is the largest unreinforced solid concrete dome in the word until now. The 4,535 metric tons weight of the concrete dome was cast by using pozzolans (volcanic ash, volcanic rock) together with burnt limestone, water and light weight aggregate stones. Many researches assumed that the use of pozzolans substantially contributed to the long service life of the structure *[Herring 2002; Pruitt 2013]*.

Figure 1.1: The Magnificent Pantheon

A pozzolan is a siliceous or siliceous and aluminous material. In general, pozzolanic materials come from two sources *[ACI 116R 2005]*: 1) natural pozzolanic materials (volcanic tuffs, diatomaceous earth, *etc.*); 2) artificial pozzolanic materials (industrial by-products: fly ash, silica fume, slags, *etc.*). In the presence of water pozzolans can react chemically with calcium hydroxide to form reaction products *[ACI 116R 2005]*. The process of the reaction of pozzolans is known as pozzolanic reaction. Nowadays pozzolans are commonly used in concrete as replacement of Portland cement and are generally called supplementary cementitious materials. In concrete pozzolans can continue to react for many years, further strengthening the concrete and making it denser and more durable *[Mehta 1981; Cook 1986; Mehta 1987; Rojas 2002]*.

Fly ash is one of the most widely used supplementary cementitious materials in concrete for over 80 years. It is the by-product of burning coal in electric power generating plants. Fly

ash is primarily silicate glass containing silica, alumina, iron and calcium, with high pozzolanic activity. Through its pozzolanic properties fly ash can react chemically with calcium hydroxide released during the hydration of cement and produce calcium silicate hydrate (C-S-H). According to ASTM C 618, the amount of fly ash in concrete may vary from 5% to 65% by mass of total cementitious materials, depending on the source and composition of the fly ash and the performance requirements of the concrete. *In this thesis concrete partially blended with fly ash is hereafter called fly ash concrete.*

The wide use of fly ash in concrete brings many benefits, such as:

- Reducing landfill costs of fly ash;
- Reducing the use of Portland cement in concrete and consequently reducing CO_2 emission per ton concrete;
- Improving the workability of the concrete;
- Reducing water demand *[Davis 1937; Owens 1979]*;
- Improving the durability of concrete and extending the service life of concrete structures *[Collepardi 2000; Edvardsen 2002; Shafiq 2004; Cox 2007; Zhang 2011]*.

Today, there is a demand for concrete structures with a service life of 80, 100, or even 200 years. In many cases chloride-induced rebar corrosion is assumed to be the dominant mechanism determining the service life of reinforced concrete structures *[NEN 6720; NEN-EN 206-1/NEN 8005; NEN 6722; van Breugel 2009]*. In the past few decades, several service life prediction models have been developed for reinforced concrete structures exposed to a chloride environment, such as the North American Life-365 model *[Ehlen 2009]*, the fib Model Code *[Schießl 2006]*, the DuraCrete probabilistic method *[DuraCrete 2000] etc*. In these models Fick's 2nd law, *with modifications*, is adopted to describe the transport of chloride ions into concrete, assuming that diffusion is the dominant transport mechanism. The resistance of the concrete cover to chloride ingress depends on the chloride diffusion coefficient of the concrete.

The DuraCrete project has provided guidelines for durability design and assessment of the service life of concrete structures, and is used for many large projects in Europe and other countries. In the DuraCrete probabilistic method the rapid chloride migration (RCM) test is used as bases for predicting the service life of concrete structures. The chloride migration coefficient of concrete is determined by the RCM test at 28 days and is used to evaluate the resistance of concrete to chloride penetration. The time-dependent chloride migration coefficient *D(t)* is described by the initial value of the chloride migration coefficient (normally measured at 28 days), and the ageing factor *n [Mangat 1994; Maage 1996; Gulikers 2006; van der Wegen 2014]*. The ageing factor *n* represents how rapidly the chloride migration coefficient of the concrete decreases with time. It is dependent on the type of cement and has a considerable effect on the service life calculation *[Matthews 2009 (fib)]*. Due to the pozzolanic reaction of fly ash, the chloride migration coefficient of fly ash concrete decreases substantially with time, particularly at ages beyond 28 days. The large decrease of the migration coefficient at later ages leads to a higher ageing factor of fly ash concrete than that of Portland cement concrete *[DuraCrete 2000; fib 2006]*. In the literature many different values of the ageing factor (*n*-values) for Portland cement concrete and fly ash concrete can be found *[DuraCrete 2000; Polder 2005; fib 2006; CUR-Bouw&Infra 2009; van der Wegen 2014]*. These values, *however*, cannot be used unconditionally since the ageing factor *n* of concrete is influenced by the length of the reference period covered by the measured RCM-values. In this study the *n*-values for Portland cement concrete and fly ash concrete will be discussed based on the RCM-values measured at ages up to 3 years.

As we know, the durability and service life of concrete structures strongly depend on the transport properties of the materials. The relevant transport mechanisms are diffusivity, permeability and absorptivity *[Brown 1993; Bentz 1999]*. Many studies have been carried out on the transport properties (water permeability) of fly ash concrete *[Neville 1995]*, although most results are obtained from experiments on concrete less than 90 days old. The advantage of using fly ash, however, becomes evident at ages beyond 90 days. It is necessary, *therefore*, to investigate the transport properties of fly ash concrete at ages beyond 90 days.

The transport properties of cement-based systems are highly related to their microstructure *[Hughes 1985;* Garboczi *1990]*. In Portland cement-fly ash binary systems the development of the microstructure is different from that in a pure Portland cement system. Thus the study of the microstructure of fly ash-blended systems is considered most relevant for performing reliable predictions of the long-term transport properties.

1.2 Objectives

The main aim of this thesis is to investigate the microstructure development and transport properties of Portland cement-fly ash binary systems in view of service life predictions. For reliable service life predictions of fly ash concrete structures the chloride diffusion coefficient *D(t)* is a crucial parameter. Due to the pozzolanic reaction of fly ash the evolution of *D(t)* of fly ash concrete is different from that of Portland cement concrete. Knowing this, the research focuses on the following aspects:

- With different fly ash dosages and water/binder ratios, the hydration process, microstructure development and transport properties (water permeability and chloride penetration) of Portland cement-fly ash binary systems will be investigated at ages up to 3 years.

- The correlation between microstructure (pore structure) and transport properties will be investigated in order to find out the crucial parameters governing the transport properties of binary systems.

- Based on the measured RCM-results, the ageing factor *n* of Portland cement concrete and fly ash concrete is discussed in view of service life predictions of concrete structures.

1.3 Scope of the Research

In this thesis Portland cement-fly ash binary systems are studied with the following restrictions:

1) No external alkali was used to activate fly ash (the alkali activated fly ash (*geopolymer*) was not considered in this study).

2) The experimental studies on the hydration process, the microstructure development and water permeability were performed on *cement paste*. The experimental study on the chloride penetration was performed on *concrete*.

3) Typical low-calcium fly ash was studied. Two dosages of fly ash were used in this study, *i.e.* 30% and 50% by weight, as replacement of Portland cement (CEM I 425 N).

4) The w/b ratios 0.4 and 0.5 were used to prepare *cement paste*. For *concrete mixtures* three w/b ratios were used, *i.e.* 0.4, 0.5 and 0.6.

5) Test specimens of blended cement paste were cured in sealed condition under a room temperature of around 20°C. Concrete specimens were cured in a fog room at 100% relative humidity and 20°C.

6) In the concrete mixtures no superplasticizer was used.

1.4 Outline of This Thesis

This thesis consists of nine chapters. The structure is shown in Figure 1.2.

- General introduction (chapter 1 and chapter 2)
- Hydration process and microstructure development (chapter 3 and chapter 4)
- Transport properties: water permeability and resistance of concrete to chloride penetration (chapter 5, chapter 6, chapter 7 and chapter 8)
- Conclusions (chapter 9)

Chapter 1 gives a general introduction including the background, objective, scope and outline of this research.

Chapter 2 provides a literature review on the effect of fly ash on hydration, microstructure, transport properties, durability and service life of Portland cement-fly ash binary systems.

In chapter 3 a detailed description of the material used in this study is presented. The hydration process of blended cement paste is investigated at ages up to 3 years. The hydration products are identified by X-ray diffraction (XRD) analysis. The calcium hydroxide content is determined by thermal analysis (TGA). The degree of hydration of cement and of the Pozzolanic reaction of fly ash in blended cement paste are studied using the environmental scanning electron microscope (ESEM).

In chapter 4 the microstructure development of blended cement paste is investigated. The development of the solid phase and the pore phase with time are studied using ESEM observations and mercury intrusion porosimetry (MIP) tests.

In chapter 5 the water permeability of blended cement paste is determined on specimens up to 2 years. Based on the results of pore structure measurements obtained in chapter 4, the crucial pore structure parameter determining the water permeability of blended cement paste is discussed.

In chapter 6 and chapter 7, the resistance to chloride penetration of Portland cement concrete and fly ash concrete is discussed. The factors affecting the resistance of Portland cement concrete and fly ash concrete to chloride penetration are explored. Based on the RCM-results obtained in chapter 6 the ageing factor n describing the effect of ageing of the concrete on the evolution of chloride diffusion (migration) coefficient $D(t)$ is discussed in chapter 8.

In chapter 9 general conclusions and recommendations for further work are presented.

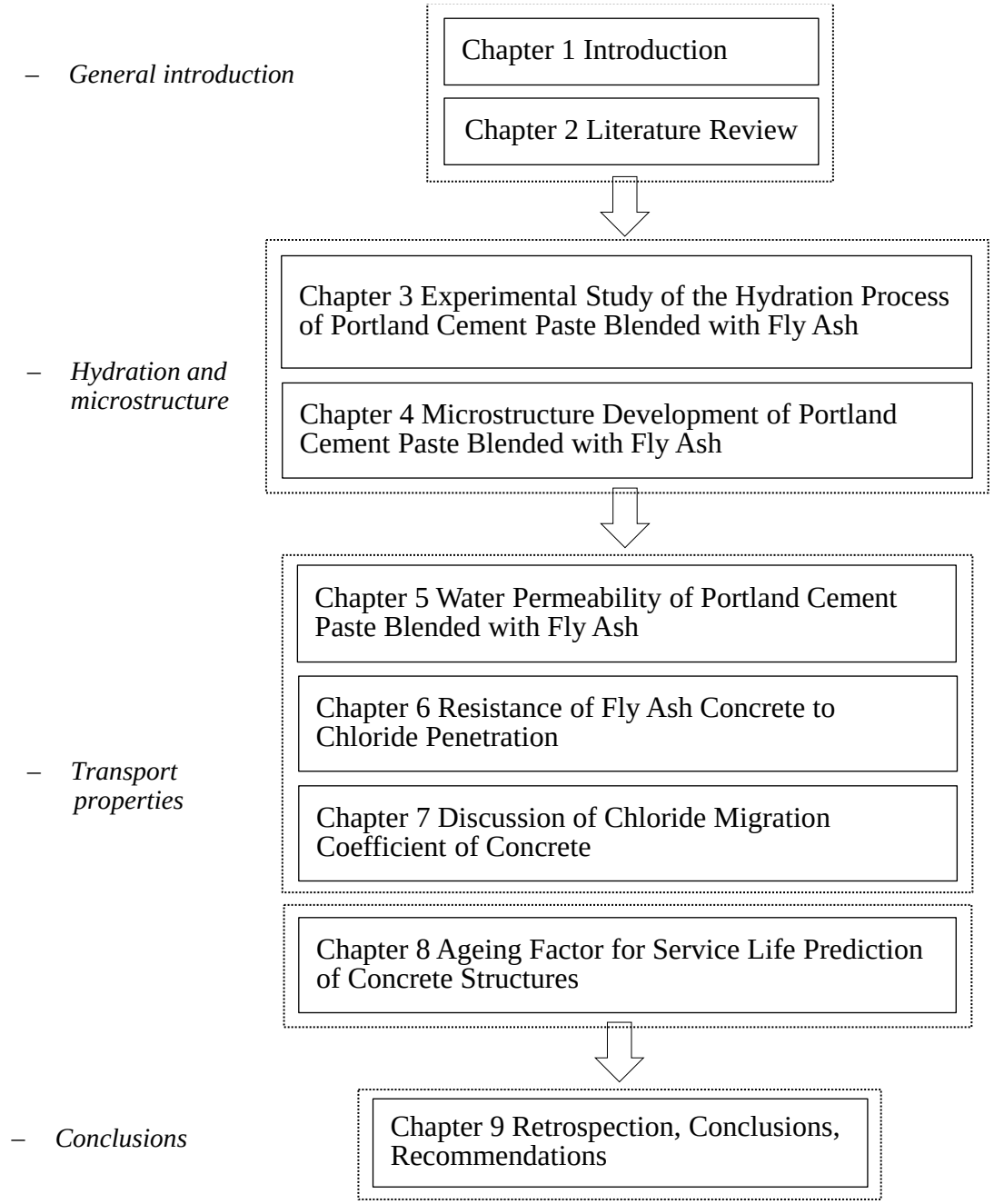

Figure 1.2: Flowchart of this thesis

References

[1] ACI 116R 2005, Cement and Concrete Terminology.

[2] Bentz, D. P., Garboczi E. J., 1999. Effects of cement particle size distribution on performance properties of Portland cement-based materials. Cement and Concrete Research, 1999; 29 (10): 1663-1671.

[3] Brown P.W., Shi Dex, Skalny J.P., 1993. Porosity/permeability relationships. Parts of 'Concrete microstructure porosity and permeability'. D. M. Roy, P. W. Brown, D. Shi, B. E. Scheetz, W. May. Strategic Highway Research Program, National Research Council, Washington, DC 1993. SHRP-C-628.

[4] Collepardi S., Corinaldesi V., Moriconi G., Bonora G., Collepardi M., 2000. Durability of high-performance concretes with pozzolanic and composite cements. Durability of Concrete, 2000; 192: 159-172.

[5] Cook D.J., 1986. Natural pozzolanas, in: R.N. Swamy (Ed.), Cement Replacement Materials, Surrey University Press, 1986, p. 200.

[6] Cox K., De Belie N., 2007. Durability behavior of high-volume fly ash concrete. International Conference on Sustainable Construction Materials and Technologies, 2007; 45-53.

[7] CUR-Bouw&Infra 2009. Duurzaamheid van constructief beton met betrekking tot chloride-geïnitieerde wapeningscorrosie - Leidraad voor het formuleren van prestatie-eisen – Achtergrondrapport (in Dutch), Tudelft, 19 Mei 2009.

[8] Davis R.E., Carlson R.W., Kelly J.W., Davis H.E., 1937. Properties of cements and concretes containing fly ash. J. Am. Concr. Inst., 1937; 33: 577-612.

[9] DuraCrete, 2000. Probabilistic performance based durability design of concrete structures. Contract BRPR-CT95-0132, Project BE95-1347. Document BE95-1347/R17, May 2000.

[10] Edvardsen Carola, Jepsen Marianne Tange, 2002. Chloride migration coefficients from non-steady-state migration experiments at environment-friendly "Green" concrete. Proceedings of the 2nd international RILEM workshop "Testing and modelling the chloride ingress into concrete". Edited by C. Andrade and J. Kropp. 2002; 203-209.

[11] Ehlen, Mark, A., Thomas, Michael D.A., Bentz, Evan C., 2009. Life-365 service life prediction model TM Version 2.0. Concrete International. May 41-46.

[12] Fib Bulletin 34, Model code for service life design. 2006.

[13] Garboczi, E.J., 1990. Permeability, diffusivity, and microstructural parameters: A critical review. Cement Concrete Research, 1990; 20: 591-601.

[14] Gulikers J, 2006. Pitfalls and practical limitation in probabilistic service life modeling of reinforced concrete structures, in Proceedings of the Eurocorr 2006, Maastricht 25-28 September 2006.

[15] Herring Benjamin, 2002. The Secrets of Roman Concrete Imagine building Structures that last 2,000 years. How Did they do it? CONSTRUCTOR, September 2002: 13-16.

[16] Hughes D.C., 1985. Pore Structure and Permeability of Hardened Cement Paste. Mag. Concr. Res., 1985; 37(133): 227-233.

[17] Maage, M., Helland, S., Poulsen, E., Vennesland, O., Carlsen, J.E., 1996. Service life prediction of existing concrete structures exposed to marine environment. ACI Materials Journal, 1996; 93(6): 602-608.

[18] Mangat PS, Molloy BT, 1994. Prediction of long term chloride concentration in concrete. Materials and Structure, 1994; 27 (168):338-346.

[19] Matthews Stuart, 2009. Structural concrete. Textbook on behavior, design and performance. Second edition Volume 3. Fib CEB-FIP.

[20] Mehta, P. K., 1981. Studies on blended portland cement containing Santorin-earth. Cement and Concrete Research, 1981; 11: 507-518.

[21] Mehta, P. K., 1987. Natural pozzolans: supplementary cementing materials for concrete. CANMET-SP-86-8E, Canadian Government Publishing Center, Supply and Services, Ottawa, Canada, K1A0S9.

[22] NEN 6720:1995 nl TGB 1990 - Voorschriften Beton - Constructieve eisen en rekenmethoden (VBC 1995).

[23] NEN-EN 206-1 Beton – Deel 1: Specificatie, eigenschappen, vervaardiging en conformiteit.

[24] NEN 8005:2008 nl Nederlandse invulling van NEN-EN 206-1: Beton - Deel 1: Specificatie, eigenschappen, vervaardiging en conformiteit.

[25] NEN 6722: 1989 Voorschriften Beton. Uitvoering (VBU 1988), met correctieblad van mei 1989.

[26] Neville, A. M., 1995. Properties of concrete. 4th and final Ed., Longman's, London.

[27] Owens P.L., 1979. Fly ash and its usage in concrete. Concr. J. Concr. Soc., 1979; 13: 21-26.

[28] Polder, R.B. and Rooij, M.R. de, 2005. Durability of marine concrete structures – field investigations and modeling. HERON, 2005; 50 (3): 133-154.

[29] Pruitt Sarah, 2013. The secrets of ancient roman concrete, http://www.history.com/news/the-secrets-of-ancient-roman-concrete.

[30] Rojas M.F., Cabrera J., 2002. The effect of temperature on the hydration rate and stability of the hydration phases of metakaolin–lime–water systems. Cement and Concrete Research, 2002; 32: 133-138.

[31] Schießl P, Bamforth P, Baroghel-Bouny, V, Corley G, Faber M, Forbes J, Gehlen C, et al., 2006. Model code for service life design. fib bulletin 34, 2006.

[32] Shafiq N., 2004. Effect of fly ash on chloride migration in concrete and calculation of cover depth required against the corrosion of embedded steel reinforcement. Structural Concrete, 2004; 5 (1): 5-9.

[33] van Breugel, K., Polder, R., 2009. Probability-based service life design of structural concrete, in Proc. 2nd Int. RILEM Workshop on Concrete Durability and Service Life Planning-ConcreteLife'09, Haifa, Israel, 2009; 383-391.

[34] van der Wegen G.J.L., Boutz M.M.R., Sarabèr A.J., van Eijk R.J., 2014. Ageing coefficient of fly ash concrete and its impact on durability. AMS '14 - Proceedings of the 1st International Conference on Ageing of Materials & Structures, edited by K. van Breugel, E.A.B. Koenders, ISBN: 978-94-6186-314-0, p. 171-178, 26-28 May 2014, Delft, The Netherlands.

[35] Zhang Wu-man, Ba Heng-jing, Chen Shang-jiang, 2011. Effect of fly ash and repeated loading on diffusion coefficient in chloride migration test. Construction and Building Materials, 2011; 25(5): 2269-2274.

Chapter 2

Effects of Fly Ash on Hydration, Microstructure, Transport Properties and Service Life of Portland Cement-fly Ash Binary Systems - A Literature Review

2.1 Introduction

Fly ash is widely applied as a mineral admixture in Portland cement concrete to improve its long-term properties and prolong the service life of concrete structures *[Malhotra 1999; 2002]*. For instance, the use of fly ash in concrete can significantly improve the resistance of concrete to chloride ingress *[Neville 1995]*. The transport properties of concrete mainly depend on the microstructure of the cement paste *[Audenaert 2006; Boel 2006]*. Chloride ions penetrate into concrete through interconnected pores of the paste.

It is well known that the pore structure of cement paste blended with fly ash is affected by the pozzolanic reaction of fly ash. The properties of fly ash and its utilization in the practice have been extensively reviewed in literature. In those reviews, the effects of fly ash on hydration and microstructure development and the transport properties (permeability and diffusion) have been emphasized. The main findings presented in literature are reported in this chapter in detail.

2.2 Properties of Fly Ash

Fly ash, also called pulverised fuel ash (PFA), is a by-product of the combustion of coal in power plants in a temperature range of 1300°C-1500°C. It is generally collected from chimneys of powdered coal-fired plants. The fly ash particles are more or less spherical and range in diameter from less than 1 μm to about 200 μm *[Fraay 1990]*.

Two classes of fly ash are specified in *ASTM C618* according to the amount of calcium, silica, alumina and iron oxide: *viz.* class F and class C. Table 2.1 presents the typical chemical composition of Portland cement and of these two classes of fly ash. It shows that fly ash has similar chemical composition as Portland cement. Normally, class F fly ash is considered an ideal cementitious material in concrete since it has higher pozzolanic activity than class C fly ash. Class F fly ash is generally low in lime, usually under 15%, and contains a larger share of silica, alumina and iron (> 70%) than Class C fly ash. *In this study class F fly ash is used.*

From the mineralogical point of view, fly ash consists of three types of components: crystalline minerals (quartz, mullite, spinel, *etc.*), unburnt carbon particles and non-crystalline (amorphous) aluminosilicate glass *[Ward 2006]*. The amorphous phase is formed during the

quick cooling process. It is a vitreous or glassy solid with pozzolanic activity. In contrast, the crystalline mineral is formed during the slow cooling process and does not participate in the pozzolanic reaction *[Brouwers 2003]*. Figure 2.1 shows cartoons of the structure of the crystalline (a) and amorphous structure (b) of silica (SiO_2). In a two-dimensional presentation the chemical bonding in crystalline silica shows a regular lattice. In amorphous silica, the atoms build up an irregular lattice and the chemical bonds are easily broken by hydroxyl ions.

Table 2.1: Chemical characteristics of Portland cement, class F fly ash and class C fly ash [Papadakis 1999; Papadakis 2000]

Chemical composition	Portland Cement (%)	Class F fly ash (%)	Class C fly ash (%)
SiO_2	20.10	53.50	39.21
Al_2O_3	4.25	20.40	16.22
Fe_2O_3	3.49	8.66	6.58
CaO	63.20 (1.48 free)	3.38 (0.36 free)	22.78 (5.18 free)
SO_3	2.88	0.60	4.30
LOI	0.86	2.20	2.10
Glass phase content (%)	–	75	50

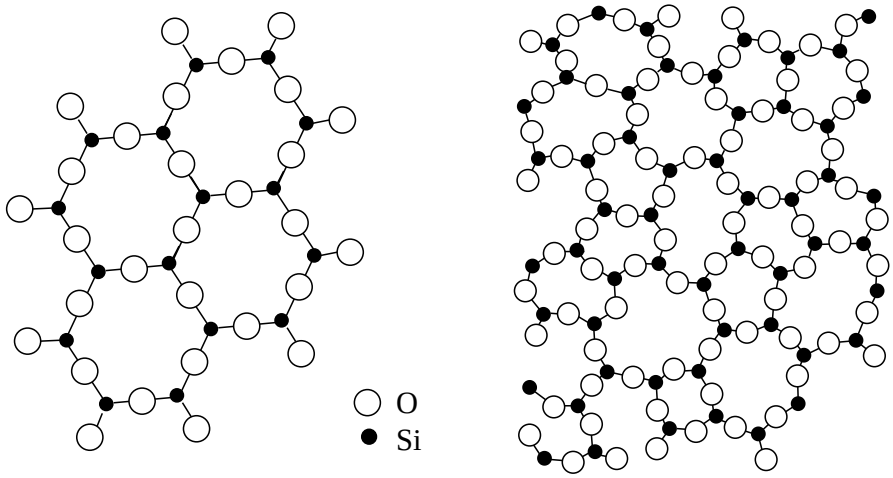

(a) Crystalline silica *(b) Amorphous silica*

Figure 2.1: Crystalline (a) and amorphous (b) silica (SiO_2) structures in two-dimensions [Best 1990]

2.3 Utilization of Fly Ash

In the United States about 131 million tons of fly ash is produced annually from 460 coal-fired power plants *[Mayda 2012]*. Besides the United States, the production of fly ash is growing fast in many other countries, especially in the developing countries. In India there were 90 million tons of fly ash in the year 2011 and the amount will be 180 million tons by 2014 *[Gupta 2013]* and reach 225 million tons by 2017 *[Kumar 2005]*, respectively. In China more than 375 million tons of fly ash were produced in 2009 *[Yang 2010]*. It will reach around 580 million tons by 2015 *[National development and reform commission of China 2010]*. Due to insufficient understanding of the properties of fly ash, the utilization efficiency is still low. Normally, fly ash is treated as a waste product and disposed in landfills. Because of scarcity of land the cost for landfill gradually increases. Thus the treatment and utilization of fly ash has become an urgent issue for society.

At present, there are various ways to utilize fly ash *[Ahmaruzzaman 2010]*. In agriculture, fly ash has been used to improve soil fertility and its productivity *[Kishor 2010]*. Henning *[Henning 1974]* and Tapkin *[Tapkin 2008]* found that asphalt mixtures blended with fly ash have high stability. In the concrete industry fly ash is commonly used as a replacement of Portland cement, ranging from 15 to 20 percent by mass of the total cementitious material. Recent research has shown that mixtures with 50 percent fly ash or even more still have high performance *[Mehta 2004]*.

In the year of 2001, about 33 percent of all the fly ash in the United States was reused and this value increased to 43% in 2008 *[Chemical & Engineering News 2009]*. The Chinese government reported that at least 60% of fly ash was reused in 2008 *[Asian coal ash association 2010]*. Nevertheless, the amount of unused fly ash is still rising.

2.4 Hydration and Microstructure of Cement Paste Blended with Fly Ash

In a fly ash cement paste there are two types of chemical reactions: *hydration of cement and pozzolanic reaction of fly ash*. The pozzolanic reaction of fly ash is the chemical reaction between fly ash and the calcium hydroxide that is produced during the hydration of cement and forms reaction products, *mainly calcium silicate hydrate [Helmuth 1987]*. It is supposed that the pozzolanic reaction of fly ash leads to a more uniform microstructure of concrete *[Stutzman 1995; Chindaprasirt 2007]* and makes concrete less permeable and more durable.

2.4.1 Hydration in cement paste blended with fly ash

2.4.1.1 Chemical reactions of Portland cement

Once Portland cement is mixed with water, a set of chemical reactions is initiated. The chemical reactions of Portland cement have been described by many authors *[Mindess 1981; Taylor 1997; Odler 1998]* and they can be summarized as follows:

- *Hydration of tricalcium silicate (C_3S) and dicalcium silicate (C_2S) produces calcium hydroxide (CH) and calcium silicate hydrates:*

$$2C_3S + 5.6H \rightarrow C_3S_2H_3 + 2.6CH \quad (2.1)$$

$$2C_2S + 3.6H \rightarrow C_3S_2H_3 + 0.6CH \quad (2.2)$$

$C_3S_2H_3$ is the most often found form of calcium silicate hydrates. It is normally denoted as, simply, *C-S-H*, since the stoichiometry of C-S-H in cement paste is in fact not fixed.

- *Hydration of tricalcium aluminate (C_3A) with gypsum ($C\underline{S}H_2$) produces ettringite (AFt: $C_6A\underline{S}_3H_{32}$):*

$$C_3A + 3C\underline{S}H_2 + 26H \rightarrow C_6A\underline{S}_3H_{32} \quad (2.3)$$

$$2C_3A + C_6A\underline{S}_3H_{32} + 4H \rightarrow 3C_4A\underline{S}H_{12} \quad (2.4)$$

Once all gypsum is consumed, ettringite can further react with remaining C_3A and forms monosulfatealuminate hydrate (AFm: $C_4A\underline{S}H_{12}$).

- *Hydration of ferrite (C_4AF)*

$$C_4AF + 3C\underline{S}H_2 + 30H \rightarrow C_6(A,F)\underline{S}_3H_{32} + (A,F)H_3 + CH \quad (2.5)$$

$$C_4AF + C_6(A,F)\underline{S}_3H_{32} + 2CH + 23H \rightarrow 3C_4(A,F)\underline{S}H_{18} + (A,F)H_3 \quad (2.6)$$

During the hydration of ferrite (C_4AF) similar products can be formed as formed by the C_3A reactions *[Taylor 1997]*. One important difference is that some of the aluminum in the reaction products is substituted by iron.

2.4.1.2 Pozzolanic reaction of fly ash

The aluminosilicate (*A-S*) glass in fly ash is responsible for the pozzolanic activity of the ash. Aluminosilicate glass mainly consists of amorphous silicon dioxide (SiO_2) and aluminum oxide (Al_2O_3) *[Fraay 1989; Papadakis 1999]*. The *A-S* glass is chemically attacked by OH^- ions, then the silicon and aluminum ions are detached from the A-S glass framework to produce calcium silicate hydrate and calcium aluminate hydrates *[Fraay 1989; Pietersen 1993]*. The reactions of amorphous SiO_2 and Al_2O_3 are the following:

- *Pozzolanic reaction of silica dioxide*

The pozzolanic reaction of silicon dioxide (*S*) can be described with Equation 2.7 *[Helmuth 1987]*:

$$xCH + yS + zH \rightarrow C_xS_yH_{x+z} \quad (2.7)$$

Based on experimental data Young and Hansen proposed the pozzolanic reaction equation of SiO_2 as shown in Equation 2.8 *[Young 1986]*. In this equation the Ca/Si ratio is about 1.5.

$$1.5CH + S + 2.3H \rightarrow C_{1.5}SH_{3.8} \quad (2.8)$$

In the CEMHYD3D model [1] the formation of pozzolanic C-S-H is described with Equation 2.9 *[Bentz 1997]*. The Ca/Si in this equation is about 1.1:

$$1.1CH + S + 2.8H \rightarrow C_{1.1}SH_{3.9} \quad (2.9)$$

It has been reported that the Ca/Si ratio in C-S-H of fly ash blended cements decreases with increasing the ratio of fly ash to cement clinker *[Taylor 1997]*. Williams found that in binary systems C-S-H produced by the pozzolanic reaction of fly ash has a slightly lower Ca/Si ratio than that generated from the hydration of Portland cement *[Williams 2002]*. The

[1] CEMHYD3D model: a three-dimensional cement hydration and microstructure development model developed at the National Institute of Standards and Technology.

value of Ca/Si ratio in Equation 2.9 is reasonable. Equation 2.9 can be used to describe the reaction of SiO_2 in Portland cement-fly ash binary systems.

- *Pozzolanic reaction of aluminum oxide*

Theoretically, there are two kinds of reaction of aluminum oxide (*A*) in Portland cement-fly ash binary systems as shown in Equations 2.10 and 2.11 *[Papadakis 1999]*:

$$A + C\bar{S}H_2 + 3CH + 7H \rightarrow C_4A\bar{S}H_{12} \quad (2.10)$$

$$A + 4CH + 9H \rightarrow C_4AH_{13} \quad (2.11)$$

In the presence of gypsum, the reaction of amorphous Al_2O_3 with gypsum forms monosulfoaluminate hydrate phase (C-A-S-H). After all the gypsum in binary systems is used up, Al_2O_3 reacts with calcium hydroxide to form calcium aluminate hydrate (C-A-H).

2.4.1.3 Effect of fly ash on the degree of hydration of cement

The effect of fly ash on the rate of hydration of cement in blended cement paste includes the following aspects:

- *The dilution effect*
  It is generally accepted that the rate of hydration of cement increases with increasing effective water/cement (w/c) ratio. This is called the dilution effect *[Taylor 1997]*. In binary systems the effective w/c ratio is increased due to the replacement of cement by fly ash *[Lawrence 2003; Wang 2009]*.

- *The physical effect*
  The physical effect of fly ash on the rate of hydration of cement is related to specific surface area of the fly ash particles *[Wei 1985]*. In binary systems calcium ions are adsorbed on the surface of fly ash particles. This results in a decrease of the concentration of calcium ions in the solution. In order to maintain the equilibrium concentration of calcium ions in the solution, more calcium ions are produced resulting in an acceleration of the hydration of cement. Furthermore, as a result of high specific surface area, fly ash particles provide additional nucleation sites for hydration products to precipitate on *[Wang 2009]*. This also accelerates the hydration of cement in binary systems.

- *The chemical effect*
  In cement paste blended with fly ash calcium hydroxide (CH) produced from the hydration of cement (see Equations 2.1 and 2.2) is consumed by the pozzolanic reaction of fly ash (see Equations 2.9, 2.10 and 2.11). According to basic thermodynamics the reduction of the concentration of [CH] contributes to an acceleration of the hydration of cement.

In Figure 2.2 the CH content of cement paste blended with fly ash, *with fly ash dosages of 0%, 20% and 30%*, is presented (expressed as g CH/100 g cement) *[Weng 1997]*. At an early age, from 1 day to 2 days, the CH content of all pastes increases with age. In the early stage of hydration up to about 10 days, the blended cement pastes have a higher CH content

than the reference sample. This indicates that in the presence of fly ash hydration of cement at early ages is accelerated. Beyond 2 days the CH content in the reference sample hardly changes, whereas the CH content in blended cement pastes starts to decrease. CH is then consumed in the pozzolanic reaction of fly ash. Figure 2.3 shows the degree of hydration of cement in the reference paste and the blended cement pastes *[Lam 2000]*. It is clear that for ages up to 3 months the degree of hydration of cement of the blended cement pastes (25% and 55% fly ash) is higher than that of the reference paste.

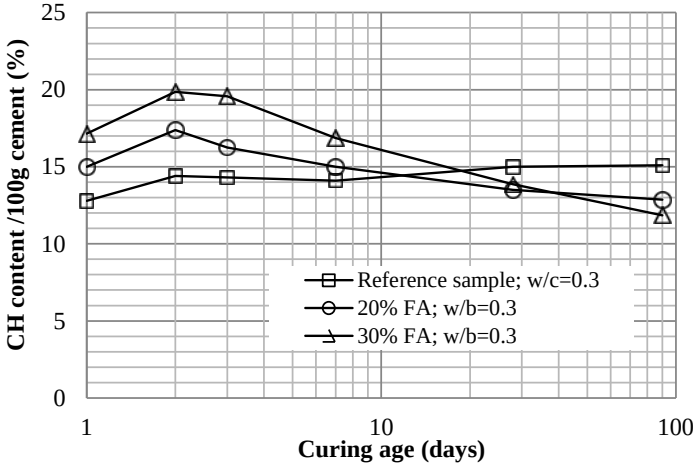

Figure 2.2: The CH content of Portland cement paste (reference sample) and blended cement paste [Weng 1997]

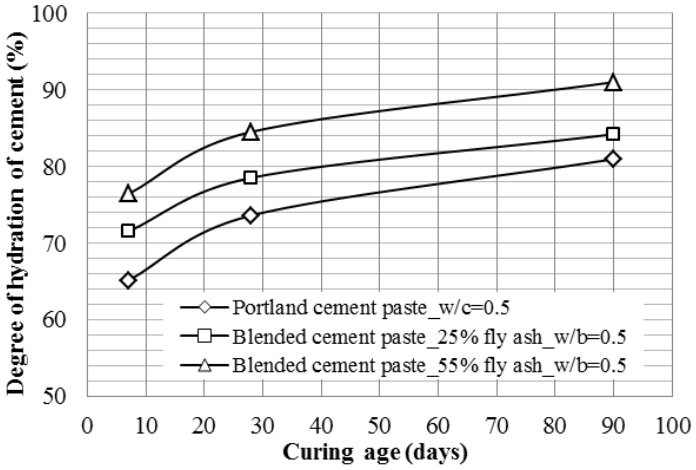

Figure 2.3: The degree of hydration of cement of Portland cement paste (reference sample) and blended cement paste [Lam 2000]

2.4.1.4 Degree of pozzolanic reaction of fly ash

As the result of cement hydration, the alkalinity of pore water in cement paste increases *[Neville 1995]*. From the study of Fraay *[Fraay 1989]*, the glass phases in fly ash particles starts to dissolve when the pH of the pore water exceeds 13.2. Then fly ash is activated and reacts with calcium hydroxide (CH). Table 2.2 shows the degree of pozzolanic reaction of fly ash in blended cement paste *[Lam 2000; Zhang 2000; Sakai 2005; Baert 2009; Ben Haha*

2010]. The test results shown in Table 2.2 vary widely because different test methods were used to get the results.

Table 2.2: The degree of pozzolanic reaction of fly ash in blended cement paste (%)

No.	Fly ash dosage (%)	w/b ratio	Method	Ref.	Age (days)							
					0	1	7	28	91	180	270	360
1	20	0.40	A	*Sakai 2005*	-	-	0.00	5.10	18.00	24.00	26.30	26.60
2	40				-	-	0.00	5.10	13.00	17.60	19.60	18.30
3	60				-	-	0.00	3.70	9.00	12.00	13.00	12.60
4	35	0.50	B	*Ben Haha 2010*	-	2.00	8.00	21.00	30.00	-	-	-
5	35		C		9.00	7.00	9.00	12.00	18.00	-	-	-
6	25	0.19	D	*Lam 2000*	-	-	5.09	13.71	17.54	-	-	-
7	45				-	-	4.85	10.84	14.80	-	-	-
8	25	0.24			-	-	5.65	13.94	22.56	-	-	-
9	45				-	-	5.28	12.81	16.45	-	-	-
10	25	0.30			-	-	6.67	14.41	24.58	-	-	-
11	55				-	-	4.98	11.21	17.03	-	-	-
12	25	0.50			-	-	6.40	12.23	29.52	-	-	-
13	55				-	-	5.26	9.82	19.41	-	-	-
14	40	0.33	D	*Zhang 2000*	-	-	16.53	28.00	32.20	36.24	-	-
15	50				-	-	15.90	24.88	30.70	33.02	-	-
16	60				-	-	15.56	21.95	25.40	28.59	-	-
17	50	0.40	D	*Baert 2009*	-	0.47	5.57	13.70	15.14	16.31	-	-
18	67				-	0.00	8.05	10.21	12.22	14.00	-	-

Note:
A: Selective dissolution: 2M HCL+5% Na_2CO_3
B: Image analysis (IA)
C: Selective dissolution: EDTA and NaOH
D: Selective dissolution: picric acid - methanol solution and water

As observed from Table 2.2 at early age, up to around 7 days, the pozzolanic reaction of fly ash does not occur and the glass phases are still in the initial alkali attack stage *[Berry 1989; Wong 1999]*. With increasing time, the pozzolanic reaction of fly ash starts to develop and the degree of pozzolanic reaction increases. This process normally takes months or years. From Table 2.2 it can be seen that after 1 year around 70 - 80% fly ash has not reacted yet *[Sakai 2005]*.

From Table 2.2 also the effect of fly ash dosage and w/b ratio on the degree of pozzolanic reaction of fly ash in blended cement paste can be obtained. It is clear that at each age the degree of pozzolanic reaction of fly ash decreases with increasing fly ash dosage (with the same w/b ratio) *[Lam 2000; Zhang 2000; Sakai 2005; Baert 2009]*. However, the data of Lam *[Lam 2000]*, shown in Table 2.2, is insufficient to investigate the effect of fly ash on the degree of pozzolanic reaction of fly ash in binary systems at ages beyond 3 months.

2.4.2 Microstructure of cement paste blended with fly ash

In this section the microstructure in cement paste blended with fly ash is studied. First the solid phase will be discussed and then the pore phase.

2.4.2.1 Solid phase

Figure 2.4 and Figure 2.5 show the backscattered electron (BSE) images of Portland cement paste and blended cement paste, respectively. In the BSE image different phases can be distinguished on the basis of their grey level in the image.

In Portland cement paste the unhydrated cement grains appear bright; the calcium hydroxide phase shows light grey and the other hydration products (mainly C-S-H) look as various shades of darker grey *[Scrivener 1988; Ye 2003]*. The pore phase appears uniformly black due to the low average atomic number of the epoxy that is filling the pores. Similar to Portland cement paste, the main solid phases of blended cement paste are classified as hydration products (CH, C-S-H, C-A-H and C-A-S-H) and unreacted phases (unhydrated cement grain and unreacted fly ash particles). From the BSE image observation (Figure 2.5) it is difficult to distinguish C-A-H, C-A-S-H and C-S-H. The unreacted fly ash particles are normally recognized as spherical particles.

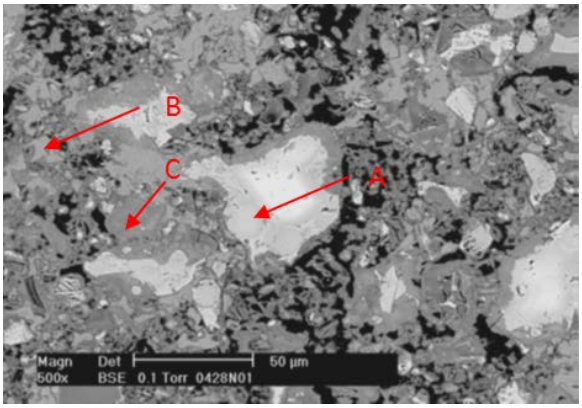

A: *Unhydrated cement grain*
B: CH
C: Other hydration products (mainly C-S-H)

Figure 2.4: BSE image of Portland cement paste (w/c=0.4; 28 days) [Ye 2003]

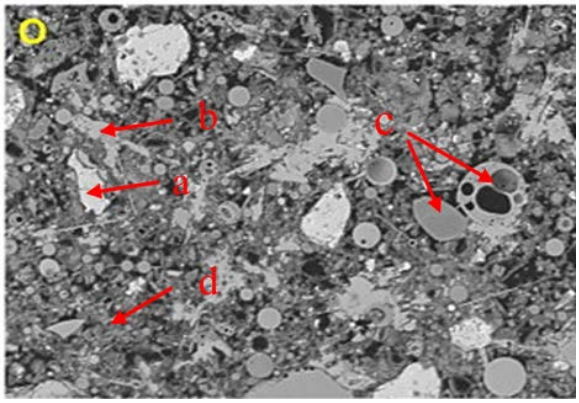

a: Unhydrated cement grain
b: CH
c: Unreacted fly ash
d: Hydration products other than CH

Figure 2.5: BSE image of blended cement paste (28 days) [Ben Haha 2010]

2.4.2.2 Pore phase

The hydrated cement paste is a porous material. Normally, the pores in hydrated cement paste are classified into capillary pores and gel pores as shown in Table 2.3 *[Mindess 1981]*.

Capillary pores

The pores, *ranging from 10 nm to 10 μm*, are defined as capillary pores. The capillary pores are the residual unfilled spaces between cement grains. They act as free space for the precipitation of hydration products. The capillary pores determine the permeability of concrete. Strength has often been correlated to the capillary porosity. Drying shrinkage also depends on the capillary porosity *[Tanabe 2009]*.

Gel pores

The finer pores, *ranging from 0.5 nm to 10 nm*, constitute the internal porosity of the C-S-H phase and are named gel pores. At low relative humidity the shrinkage of cement paste is determined by the desorption of water from the gel pores *[Tanabe 2009]*. The pores with diameter smaller than 0.5 nm are formed by the interlayer spaces of C-S-H gel.

Table 2.3: Classifications of pores in hydrated cement paste [Mindess 1981]

Type of pore	Description	Diameter	Paste properties affected
Capillary pores	large	50 nm-10 μm	Permeability; strength
	Medium	10 nm-50 nm	Permeability; strength; shrinkage (at high RH, >80%)
Gel pores	Small	2.5 nm-10 nm	Shrinkage (to 50% RH)
	Micro-pores	0.5 nm-2.5 nm	Shrinkage; creep (at all RH)
Interlayer spaces	Structural	<0.5 nm	Shrinkage; creep (at all RH)

RH: Relative Humidity

2.5 Pore Structure and Permeability of Cement Paste Blended with Fly Ash

As stated by Neville *[Neville 1995], durability of concrete largely depends on the ease with which fluids, both liquids and gases, can enter into, and move through, the concrete. This is commonly referred to as permeability of concrete*. The permeability of concrete is mainly controlled by the pore structure of the hydrated cement paste *[Larbi 1993; Neville 1995]*. In this section a review is presented on the pore structure and water permeability (water transport) of binary systems.

2.5.1 Pore Structure

Mercury intrusion porosimetry (MIP) is a common technique used for characterizing the pore structure of cement paste *[Diamond 1971; Aligizaki 2006]*. Both the porosity and the pore size distribution of cement paste can be obtained with this technique.

In general, the total porosity of paste is increased by the addition of fly ash and with increasing fly ash dosage *[Neville 1995; Poon 1997; Chindaprasirt 2005]*. That might be due to higher w/c ratio and lower gel/space ratio in cement paste blended with fly ash *[Poon 1997]*. It has been reported by Wang *[Wang 2004]* that the hydration products produced by pozzolanic reaction of fly ash fill the pores. This reduces not only the pore volume, but also the pore size. Furthermore, it was stated by Fraay *[Fraay 1989]* that after 1 year cement paste blended with 30% fly ash has a finer pore structure and a smaller capillary porosity than Portland cement paste (reference sample), although the total porosity (*high volume of Hg*, see Figure 2.6) in the two pastes is similar. In other words, the pore structure of binary systems is refined by the pozzolanic reaction of fly ash at later ages *[Mindess 1981; Fraay 1989; Bijen*

1996; Rilem report 38 2007]. However, a comprehensive understanding of the pore structure of blended cement paste at later ages is still missing.

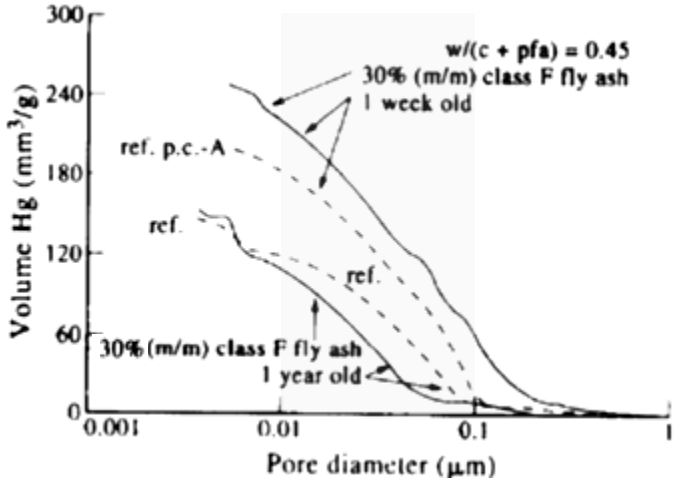

Figure 2.6: Pore size distribution of cement paste blended with fly ash and reference sample [Fraay 1989; Bijen 1996] (Note: Dashed line: reference sample, Portland cement paste; Real line: cement paste blended with fly ash; 30% (m/m): 30% class F fly ash)

2.5.2 Water permeability

Water permeability determines the rate at which water flows through a saturated specimen of concrete (porous medium) under an externally applied hydraulic gradient *[ACI 1963]*. The permeability of concrete mainly depends on the permeability of the cement paste *[Nawy 2008]*. The pores in aggregate do not contribute to the permeability of concrete because the pores in aggregate are usually discontinuous and aggregate particles are enveloped by the cement paste *[Collins 1986; Neville 1995]*. With progress of hydration of cement the pore spaces are gradually filled with hydration products resulting in a decrease of the water permeability of the paste *[Neville 1995]*.

As a result of the slow pozzolanic reaction of fly ash (see Table 2.2) in concrete, initially, fly ash concrete has a higher permeability than Portland cement concrete with a similar w/b ratio. At later ages, *however*, fly ash concrete is less permeable than Portland cement concrete *[Fraay 1989]*. It was reported by Naik *[Naik 1994]* that beyond 91 days concrete blended with 50% fly ash (w/b=0.35) has a lower water permeability than Portland cement concrete.

It was stated by Powers *[Powers 1958]* that the capillary porosity has a substantial effect on the permeability of cement paste (see Figure 2.7). The resistance to flow through the capillary pores is much smaller than that through the gel pores. Besides capillary porosity, other pore parameters, *viz.* pore size and connectivity of the pores are all important parameters playing role in the transport properties of the paste (concrete) *[Aligizaki 2006]*. In blended cement paste the pozzolanic reaction of fly ash results in a different pore structure of the paste compared to pure Portland cement paste. That will influence the transport properties of binary systems. At present, there is still no a clear understanding of the correlation between the pore structure and transport properties of binary systems, especially not after long-term curing periods.

In order to establish the correlation between pore structure and transport properties, measurements of the pore structure and water permeability of binary systems will be performed. Results are discussed in chapter 4 and 5.

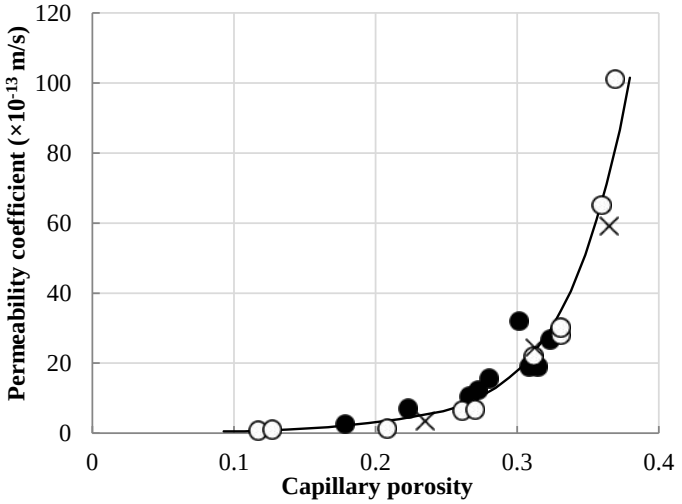

Figure 2.7: Permeability and capillary porosity of cement paste. Different symbols designate different cements [Powers 1958]

2.6 Chloride Transport Mechanism

The transport of chloride ions in concrete is the primary cause of corrosion of steel reinforcement. The movement of (free) chloride ions in pores of the concrete is mainly driven by three different mechanisms: diffusion, convection and ionic migration *[Xi 1997]*. In this literature review the diffusion and migration of chloride ions are presented.

2.6.1 Diffusion

Diffusion of chloride ions in concrete is the movement of chloride ions under a concentration gradient or chemical potential from an area of high concentration to an area of low concentration without a pressure differential *[Tang 2012]*. It takes place only through a continuous network of pores and is controlled by Fick's 2nd law *[Neville 1995]*.

$$\frac{\partial C}{\partial t'} = \frac{\partial}{\partial x}\left(D \frac{\partial C}{\partial x} \right) \tag{2.12}$$

where:

C = chloride concentration at a distance x from the reference point, mol/m^3.
D = chloride diffusion coefficient, m^2/s.
x = position in the sample, m.
t' = time, s.

Among the parameters in Equation 2.12, the chloride diffusion coefficient *D* represents the capacity of concrete to resist chloride penetration and is used as input parameter in models for predicting service life of reinforced concrete structures. The chloride diffusion coefficient can be determined with diffusion tests, such as the AASHTO T259 test (Salt Ponding Test) *[AASHTO T259 1980]*, the Bulk Diffusion Test (NordTest NTBuild 443) *[Nordtest Method 1995]*.

Figure 2.8 shows the chloride diffusion coefficient of Portland cement concrete with different fly ash dosages and w/b ratios at an age of the concrete of 84 days *[Yuan 2009; Nath 2011]*. It is clear that the chloride diffusion coefficient is largely influenced by the w/b ratio for both Portland cement concrete and fly ash concrete. Based on Yuan's study *[Yuan 2009]*, fly ash concrete with a fly ash content of 20% has a lower chloride diffusion coefficient than Portland cement concrete after 84 days (*42 days curing + 42 days exposure*). However, as reported by Nath *[Nath 2011]*, the chloride diffusion coefficient of concrete made with 30% or 40% fly ash is higher than that of Portland cement concrete after 84 days (*28 days curing + 56 days exposure*). The difference between these two experimental results is mainly caused by the different curing and testing periods that were used. In Yuan's research the curing period was 42 days, which is longer than 28 days used by Nath. A long curing age is beneficial for the resistance of fly ash concrete to chloride ingress.

From the above survey, it can be concluded that it is not easy to compare the chloride diffusion coefficients of concretes because various procedures are used to determine these coefficients, including the difference in curing period (*prior to testing*) and exposure period. Although the diffusion test is a realistic representation of natural diffusion, the diffusion test is time consuming (normally 35-90 days of exposure duration) *[AASHTO T259 1980; Nordtest Method 1995]*. Instead of the time consuming diffusion test, an accelerated migration test, viz. rapid chloride migration (RCM) test is suggested to determine the resistance of concrete against chloride penetration.

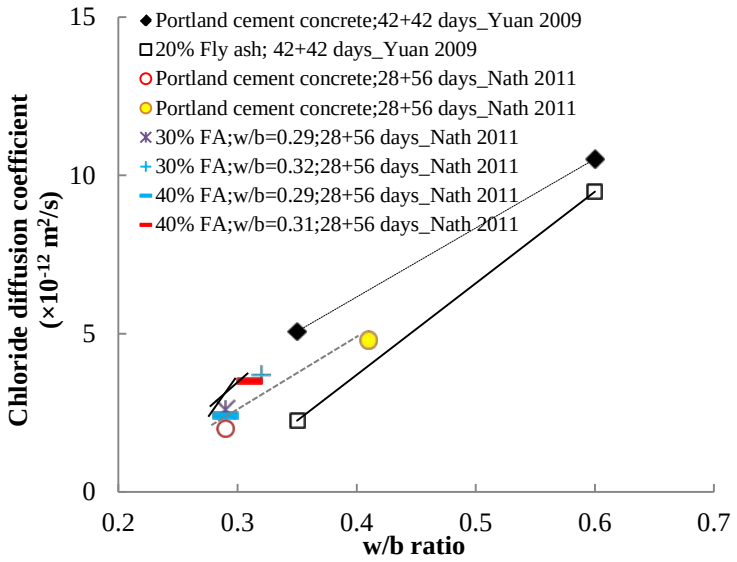

Figure 2.8: The chloride diffusion coefficient of Portland cement concrete and fly ash concrete [Yuan 2009; Nath 2011] Note: "42+42 days" means "42 days of curing +42 days of exposure period"

2.6.2 Migration

Migration of chloride ions is the movement of chloride ions under the action of an external electrical field. A number of migration tests have been proposed in the past to determine the chloride migration coefficient, such as the Rapid Chloride Permeability test (AASHTO T277-RCPT or ASTM C1202) *[ASTM C1202 1994]*, the Electrical Migration Techniques, the Rapid Chloride Migration (RCM) test *[Tang 1992] etc*. The duration of the migration test is only a few hours to less than a week.

At present the RCM test is used worldwide because of its simplicity and the short duration of the test. A detailed explanation of this method will be given in chapter 6. In this section the chloride migration coefficients of Portland cement concrete and fly ash concrete, obtained in the RCM test, are reviewed.

Chloride Migration coefficient of Portland cement concrete

Figure 2.9 shows the chloride migration coefficient (D_{RCM}) of Portland cement concrete as measured at different ages of concrete. The RCM test is usually obtained from concrete mixtures at an age of 28 days. At early age the D_{RCM} value of Portland cement concrete made with a w/c ratio from 0.4 to 0.5 decreases with time, resulting from continuous hydration of cement. With a high w/c ratio of 0.7, however, the D_{RCM} value increases from 28 days to 1 year *[Tang 1996]*. An increase of the D_{RCM} value of Portland cement concrete after a certain age is also observed in other mixtures *[Tang 1996; Obla 2003; van Dalen 2005; Audenaert 2007; Gailius 2008]*, as shown in Figure 2.9.

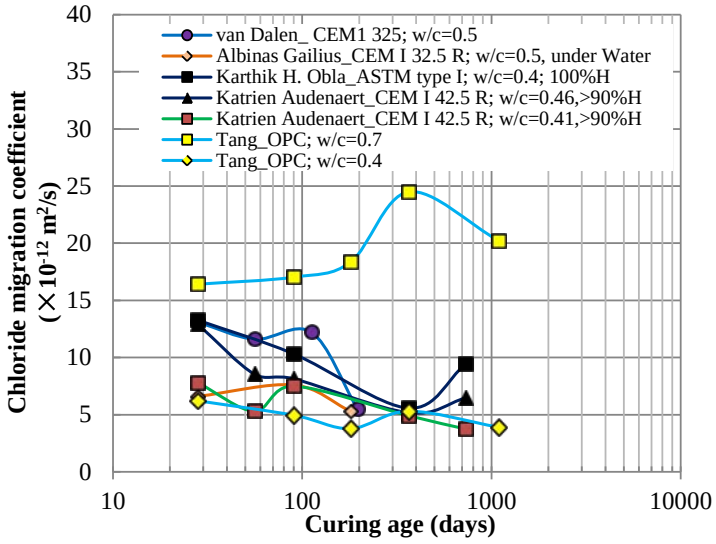

Figure 2.9: Chloride migration coefficient of Portland cement concrete

It should be mentioned that the Portland cement concrete specimens, of which results are presented in Figure 2.9, were all cured in a saturated lime bath (20 °C, 100% humidity) or under water (20 °C). For such properly cured Portland cement concretes, the chloride migration coefficient was expected to decrease with increasing age of the concrete. For the results shown in Figure 2.9 this is not always the case. At present, there is no satisfactory explanation given in literature for this anomaly in test results. This phenomenon has often been ascribed to experimental errors. If this was the reason, however, it is strange that other

mixtures behave differently. In view of long-term performance predictions of Portland cement concrete it is necessary to find out the reasons why the chloride migration coefficient of Portland cement concrete increases at later age.

Chloride migration coefficient of fly ash concrete

Figure 2.10 shows the effect of fly ash on the chloride migration coefficient of concrete. Figure 2.10b shows that the D_{RCM} value of fly ash concrete decreases with increasing time up to 180 days. The anomaly observed in the results of Portland cement concrete is not observed in fly ash concrete.

As observed in Figure 2.10a at an early age of 28 days fly ash concrete (w/b=0.4) has a lower D_{RCM} value than Portland cement concrete if 10 and 20 percent of Portland cement is replaced by fly ash *[Neithalath 2010]*. Figure 2.10b shows that at 28 days the fly ash concrete mixture (30% fly ash; w/b=0.5) has a higher D_{RCM} value than Portland cement concrete *[Gailius 2008]*. It was found by Cox *[Cox 2007]* that at 28 days concrete blended with 50% or 67% fly ash has a much higher D_{RCM} value than Portland cement concrete with the same w/b ratio. It is believed that at 28 days fly ash concrete with a high fly ash content, *i.e.* more than 30%, has a more porous structure than Portland cement concrete since many fly ash particles have not reacted yet.

At later ages, *i.e.* beyond 28 days, the D_{RCM} value of fly ash concrete is much lower than that of Portland cement concrete. With progress of the pozzolanic reaction of fly ash the pore structure of paste is refined, resulting in good resistance of fly ash concrete to chloride ingress. Besides this, the packing effect of fly ash particle and pozzolanic reaction accounting for the eventual disappearance of the interfacial transition zone[2] in fly ash concrete also contribute to lower D_{RCM} values of fly ash concrete *[Mehta 2004]*. In this research the relationship between the pore structure and D_{RCM} value of fly ash concrete will be discussed in chapter 6.

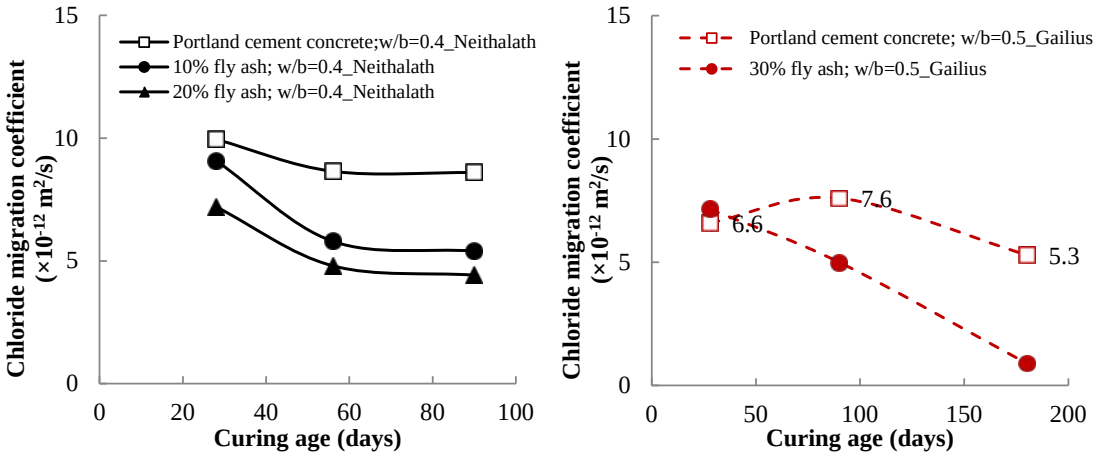

Figure 2.10: The effect of fly ash on the chloride migration coefficient of concrete [Gailius 2008; Neithalath2010]

[2] Interfacial transition zone: *i.e. ITZ,* is the area between the aggregate and cement paste, with high w/c ratio and therefore with more available space that permits the formation of highly porous hydration products containing large crystals of calcium hydroxide and ettringite. In fly ash concrete with progress of pozzolanic reaction of fly ash, the calcium hydroxide phase is consumed to form more dense reaction products, like C-S-H, and the size of the capillary pores in the transition zone decreases. The presence of fly ash in concrete, *therefore*, reduces the ITZ thickness and eliminates the weak link in the concrete microstructure.

2.7 Service Life of Concrete Structures

In marine environment the service life of reinforced concrete structures mainly depends on deterioration due to reinforcement corrosion *[Costa 1999]*. Corrosion caused by chloride penetration leads to the deterioration of bridges, marine structures and industrial plants. In Europe, around 5 billion Euros are spent on maintenance of the infrastructure due to reinforcement corrosion annually *[Klinghoffer 2000]*. During the past few years, several computer models have been developed to predict the service life of concrete structures exposed to chlorides. Among them we mention here the North American Life-365 model *[Bentz 2014]*, the Croatian CHLODIF model *[Krstic 1994]* and the DuraCrete probabilistic method *[DuraCrete 2000]*. The DuraCrete methodology will be reviewed in more detail in this section.

2.7.1 Probabilistic concept for service life design

For service life design of concrete structures the limit state concept is utilized, comprising a function for the load *S* and a function for the resistance *R*, which can be expressed as *g(x,t)=R(t)-S(t) [DuraCrete 2000; Teplý 2002]*. The resistance *R* and the load *S* are both represented as time-dependent stochastic variables. Figure 2.11 shows the evolution of the probability of failure of a structure with elapse of time as function of changing values of the resistance *R* and the load *S*.

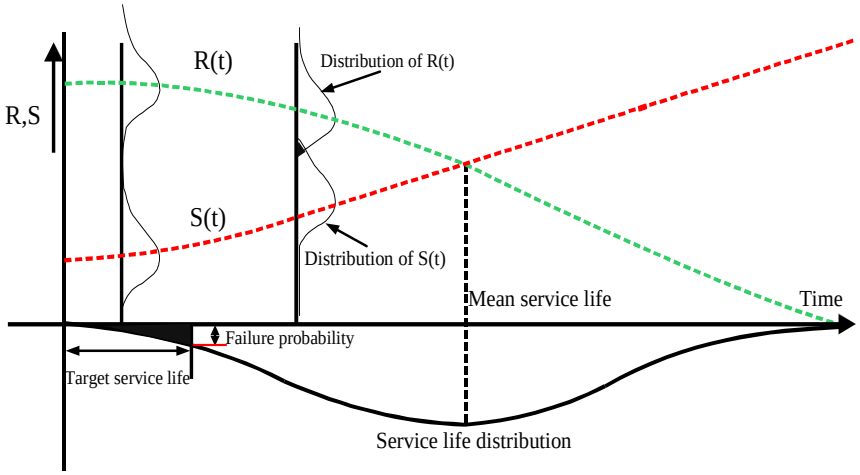

Figure 2.11: Evolution of the probability of failure of a structure with elapse of time as function of changing values of the resistance R and load S [DuraCrete 2000; Siemes 2000]

2.7.2 The DuraCrete model

The DuraCrete model involves a limit state for the initiation of chloride-induced corrosion. In a simplified form it says that the structure is considered to fail as soon as a critical chloride concentration at the steel surface of the reinforcing bars is reached. The Equation 2.13 based on Fick's second law of diffusion, is applied to calculate the chloride content at a certain depth and time.

$$C(x,t) = C_s - (C_s - C_i)\,erf\left[\frac{x}{\sqrt{\{4\,k\,D(t)\,t\}}}\right] \tag{2.13}$$

where:

$C(x,t)$ = chloride concentration at depth x and after time, t.
C_S = surface chloride content.
C_i = initial chloride concentration in the concrete.
k = correction factor, which depends on the binder type, the environment and the curing conditions.
x = depth in concrete.
erf = error function.
$D(t)$ = apparent chloride diffusion coefficient at time t.

In Equation 2.13 $D(t)$ is the time-dependent apparent chloride diffusion coefficient. $D(t)$ depends on the initial value of the chloride diffusion coefficient (D_0) and the ageing factor n, with which the evolution of the diffusion coefficient is described as shown in Equation 2.14 *[Maage 1996; Gulikers 2006]*:

$$D(t) = D_0\left(\frac{t_0}{t}\right)^n \tag{2.14}$$

where:

D_0 = chloride diffusion coefficient at the reference time t_0 (usually 28 days) of the concrete *[Maage 1996]*.
n = ageing factor. It depends on the type of binder and the rate of cement hydration.
t = age of the concrete.

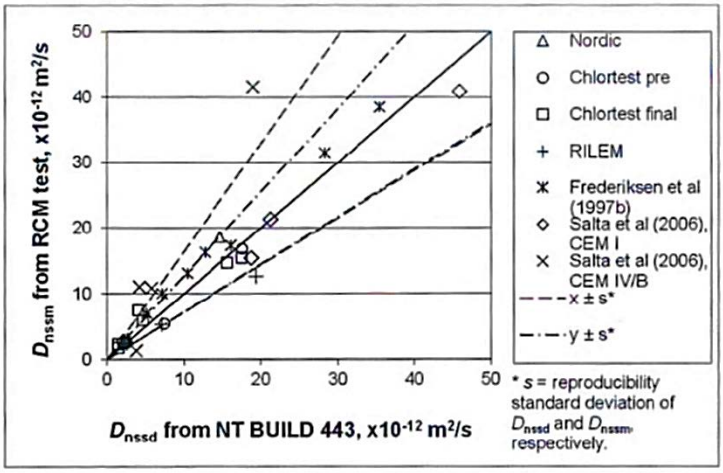

Figure 2.12: Relationship between the diffusion coefficient obtained from diffusion tests and migration coefficient from RCM test. s=standard deviation of the reproducibility of chloride migration coefficient (D_{nssm})(y axis shown in figure) and chloride diffusion coefficient (D_{nssd}) (x axis shown in figure) [Tang 2012]

As mentioned in section 2.6 the resistance of concrete to chloride ingress can be determined both by the chloride diffusion test and the chloride migration test. It was reported *[Tang 2012]* that there is a strong linear correlation between chloride diffusion coefficients from the diffusion test (NT Build 443) and chloride migration coefficients from the migration test (RCM test) as shown in Figure 2.12. Thus it is considered justified to use the less time consuming RCM test instead of the diffusion test for determining the resistance to chloride ingress in concrete.

2.7.3 Service life of fly ash concrete

Until now, many studies *[Collepardi 2000; Shafiq 2004; Cox 2007]* have been performed showing that fly ash as a partial replacement of Portland cement is able to improve the resistance of concrete to chloride ingress because of continuing densification of the microstructure of blended cement paste. Figure 2.13 shows the effect of pulverized fuel ash (PFA) content on the chloride content measured at the depth of 26-31 mm in the concrete for different strength grades *[Thomas 1991]*. The concrete specimens were exposed to the tidal zone of a marine exposure site for two years. The results show that for each of the mixtures the chloride content at the depth 26-31 mm decreases significantly with increasing the PFA content. Eventually, for PFA concrete structures it takes a long time for chloride ions to penetrate the concrete cover to reach the steel surface.

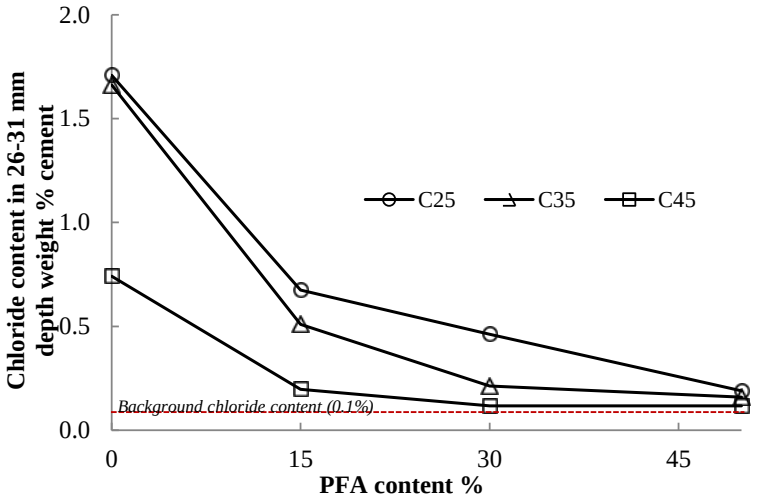

Figure 2.13: Effect of PFA dosage on chloride ion penetration into concrete. Curing conditions: 1 day moist curing + 27 days air-stored curing at 20°C and 65% relative humidity. Exposure conditions: two years' marine exposure. Note: PFA is pulverized fuel ash; C25 (w/c=0.44-0.68), C35 (w/c=0.37-0.57), C45 (w/c=0.32-0.49) are strength grades [Thomas 1991]

2.8 Summary

2.8.1 Conclusions

In this chapter the properties of fly ash and the use of fly ash in concrete were briefly reviewed. The effects of fly ash on hydration, microstructure and transport properties of Portland cement-fly ash binary systems were summarized. Based on this literature survey, the following conclusions can be drawn.

1. Conclusion related to hydration and microstructure

    - Due to the presence of a glass phase in fly ash, a pozzolanic reaction of fly ash takes place when calcium hydroxide is released during the hydration of Portland cement.
    - The effect of fly ash on the hydration of cement consists of a dilution effect, a physical effect and a chemical effect. At early ages, the presence of fly ash accelerates the hydration of cement, reflected by a high calcium hydroxide content in blended cement paste (see Figure 2.2). In blended cement paste (with the same w/b ratio) the degree of pozzolanic reaction of fly ash decreases with increasing fly ash dosage.
    - The hydration products produced by the pozzolanic reaction of fly ash are mainly calcium silicate hydrate (C-S-H) and calcium aluminate hydrates (C-A-H), which are essentially the same as those produced by Portland cement.
    - Although the pore structure of binary systems is refined by the pozzolanic reaction of fly ash at later ages, the blended cement paste still exhibits a *higher* capillary porosity than Portland cement paste. Obviously, in binary systems the development of the pore structure is different from that of pure Portland cement system.

2. Conclusion related to transport properties

    - After an age of 3 months, fly ash concrete mixtures made with 50% fly ash appears to be less permeable than Portland cement concrete (see section 2.5.2).
    - The chloride migration test is less time-consuming than the diffusion test, and is suitable for determining the resistance of concrete to chloride ingress.
    - The fly ash concrete mixtures made with 10% to 30% fly ash have a lower chloride migration coefficient than Portland cement concrete at later ages, *i.e.,* beyond 28 days (see Figure 2.10).

3. Conclusion related to service life predictions of fly ash concrete structures

    - In marine environment, chloride-induced corrosion is assumed the dominant mechanism determining the service life of reinforced concrete structures.
    - Fly ash, *as a partial replacement of Portland cement*, is able to improve the resistance of concrete to chloride ingress and to extend the service life of concrete structures.

2.8.2 Problem statement

From the literature review it can be concluded that in Portland cement-fly ash binary systems the pore structure is refined at later ages due to pozzolanic reaction of fly ash. This will influence the transport properties of concrete and service life of concrete structures. Nevertheless, with regard to the effect of fly ash on the long-term performance of concrete, there are still some tedious problems that need to be investigated.

- Long term evolution of microstructure and transport properties

  Effect of fly ash
  It is well known that the addition of fly ash contributes to the improvement of long-term properties of concrete. However, most studies on the hydration and *microstructure* development are limited to short-term tests, 3 or 6 months. That is not sufficient to characterise the transport properties of cement paste blended with fly ash comprehensively. More long-term experimental results about the resistance to chloride penetration are required in view of service life predictions. Therefore, the effect of fly ash on the hydration process, microstructure development, water permeability and resistance to chloride ingress of Portland cement-fly ash binary systems has to be studied for longer periods, up to at least 3 years.

  Portland cement concrete
  The chloride migration coefficient of *Portland cement concrete* increases at later ages (*after around 90 days*) and the resistance of concrete to chloride penetration decreases. This phenomenon influences the long-term performance of Portland cement concrete. Some possible causes will be studied explaining why the chloride migration coefficient of Portland cement concrete increases at later ages.

- Ageing factor of fly ash concrete in view of service life prediction

  In the DuraCrete methodology for service life predictions the time-dependent chloride diffusion coefficient *D(t)* is described with an ageing factor *n*. Due to the pozzolanic reaction of fly ash the evolution of the microstructure of blended cement paste is different from that of Portland cement paste. This will influence the evolution of *D(t)* and eventually the ageing factor *n*. The values for the ageing factor *n* of Portland cement concrete and fly ash concrete have not been reported based on the *D(t)* measured at a relative long-term period. In this study, the ageing factor *n* for Portland cement concrete and fly ash concrete, determined from the measured *D(t)* at ages up to 3 years, will be discussed.

References

[1] AASHTO T259: Standard method of test for resistance of concrete to chloride ion penetration. American Association of State Highway and Transportation Officials, Washington, D.C., U.S.A., 1980.

[2] Ahmaruzzaman, M., 2010. A review on the utilization of fly ash. Progress in Energy and Combustion Science, 2010; 36(3): 327-363.

[3] Aligizaki K.K., 2006. Pore structure of cement-based materials-testing, Interpretation and Requirement. Taylor & Francis, New York. ISBN: 0419228004.

[4] American Concrete Institute (ACI), 1963. Admixtures for concrete. Journal of ACI Proceedings, 1963; 60(11): 1512.

[5] Asian coal ash association, China fly ash utilization in China, Available at http://www.asiancoalash.org/research/ (click on Fly Ash Utilization in China-2010).

[6] ASTM C1202, 1994. Standard test method for electrical indication of chloride's ability to resist chloride. Annual Book of ASTM Standards V 04.02, ASTM, Philadelphia, pp. 620-625.

[7] Audenaert, K., 2006. Transport mechanisms in self-compacting concrete in relation with carbonation and chloride penetration (in Dutch). Doctoral Thesis, Magnel Laboratory for Concrete Research, Ghent University, Belgium, pp.370.

[8] Audenaert Katrien, Boel Veerle, De Schutter Geert, 2007. Chloride migration in self-compacting concrete. CONSEC'07 Tours, France Concrete under Severe Conditions: Environment & Loading F. Toutlemonde et al.

[9] Baert, Gert, 2009. Physico-chemical interactions in portland cement-(high volume) fly ash binders. 2009, Universiteit Gent, Belgium.

[10] Ben Haha M., De Weerdt K., Lothenbach B., 2010. Quantification of the degree of reaction of fly ash. Cement and Concrete Research, 2010; 40: 1620-1629.

[11] Bentz, Dale P., 1997. Sebastien Remond. Incorporation of fly ash into a 3-D cement hydration microstructure model. 1997, Building and Fire Research Laboratory, National Institute of Standards and Technology, Gaithersburg, Maryland, US.

[12] Bentz E. C., Thomas M. D. A., 2014. Life-365 service life prediction model™ and Computer Program for Predicting the Service Life and Life-Cycle Cost of Reinforced Concrete Exposed to Chlorides. Version 2.2.1, January 15, 2014. Produced by the Life-365™ Consortium III.

[13] Berry EE, Hemmings RT, Langley WS, Carette GG., 1989. Beneficiated fly ash: hydration, microstructure, and strength development in Portland cement. In: Proceedings of the First International Conference on Fly ash, Silica Fume, Slag, and Natural Pozzolan in Concrete, SP-114. Detroit, USA; 1989: 241-273.

[14] Best Ben, 1990. Lessons for Cryonics from Metallurgy and Ceramics. http://www.benbest.com/cryonics/lessons.html

[15] Bijen J., 1996. Benefits of slag and fly ash. Construction and Building Materials, 1996; 10(5): 309-314.

[16] Boel, V., 2006. Microstructure of self-compacting concrete in relation with gas permeability and durability aspects" (in Dutch). Doctoral Thesis, Magnel Laboratory for Concrete Research, Ghent University, Belgium, pp.320.

[17] Brouwers H.J.H., van Eijk R.J., 2003. Chemical reaction of fly ash. Proceedings of the 11th International Congress on the Chemistry of Cement (ICCC) "Cement's Contribution to the Development in the 21st Century. SBN Number: 0-9584085-8-0. Editors: Dr. G. Grieve and G. Owens. 11-16 May 2003, Durban, South Africa.

[18] Chindaprasirt P, Jaturapitakkul C, Sinsiri T., 2005. Effect of fly ash fineness on compressive strength and pore size of blended cement paste. Cement & Concrete Composites, 2005; 27(4): 425-428.

[19] Chindaprasirt Prinya, Jaturapitakkul Chai, Sinsiri Theerawat, 2007. Effect of fly ash fineness on microstructure of blended cement paste. Construction and Building Materials, 2007; 21(7): 1534-1541.

[20] Chemical & Engineering News, 23 February 2009, "The Foul Side of 'Clean Coal'", p. 44.

[21] Collepardi S., Corinaldesi V., Moriconi G., Bonora G., Collepardi M., 2000. Durability of high-performance concretes with pozzolanic and composite cements. Durability of Concrete, 2000; 192: 159-172.

[22] Collins, J.F., Derucher, Jr., K.N., and Korfiaris, G.P., 1986. Permeability of concrete mixtures Part 1: literature review. Civil Engineering for Practicing and Design Engineers, 1986; 5: 579-638.

[23] Costa, A., Appleton, J., 1999. Chloride penetration into concrete in marine environment - Part I1: prediction of long term chloride penetration. Materials and Structures, 1999; 32: 354-359.

[24] Cox, K., De Belie, N., 2007. Durability behavior of high-volume fly ash concrete. International Conference on Sustainable Construction Materials and Technologies, pp 45-53.

[25] Diamond S., 1971. A critical comparison of mercury porosimetry and capillary condensation pore size distributions of Portland cement pastes. Cement and Concrete Research, 1971; 1(5): 531-545.

[26] DuraCrete, 2000. DuraCrete Final Technical Report R17, Document BE95-1347/R17, The European Union – Brite EuRam III, DuraCrete – Probabilistic Performance based Durability Design of Concrete Structures, CUR, Gouda.

[27] Fraay A.L.A., Bijen J.M., de Haan Y.M.,1989. The reaction of fly-ash in concrete-a critical-examination. Cement and Concrete Research, 1989; 19: 235-246.

[28] Fraay, A.L.A., 1990. Fly ash a pozzolan in concrete. PhD thesis, Delft University of Technology.

[29] Gailius Albinas, Kosior-Kazberuk Marta, 2008. Monitoring of concrete resistance to chloride penetration. Materials Science (MEDŽIAGOTYRA), 2008; 14(4): 350-355.

[30] Gulikers J, 2006. Pitfalls and practical limitation in probabilistic service life modeling of reinforced concrete structures, in Proceedings of the Eurocorr 2006, Maastricht 25-28 September 2006.

[31] Gupta, Pardeep Kumar, 2013. High volume fly ash concrete road. International Journal of Emerging Technology and Advanced Engineering, 2013; 3(3): 852-856.

[32] Helmuth R., 1987. Fly ash in cement and concrete. Skokie: Portland cement association, 203.

[33] Henning, N.E., 1974. Evaluation of lignite fly ash as a mineral filler in asphaltic concrete. Report No. Item 2 (73). Twin city testing and engineering laboratory, St.Paul, Minnesota.

[34] Kishor, Prem, Ghosh A.K., Kumar, Dileep, 2010. Use of fly ash in agriculture: a way to improve soil fertility and its productivity. Asian Journal of Agricultural Research, 4: 1-14.

[35] Klinghoffer Oskar, Frølund Thomas, Poulsen Ervin, 2000. Rebar corrosion rate measurements for service life estimates. Paper presented at the ACI Fall Convention 2000, Toronto, Canada, Committee 365 "Practical Application of Service Life Models".

[36] Krstic V., 1994. Numerical model of durability calculation for reinforced concrete structures. Master Thesis, Faculty of Civil Engineering University of Zagreb, Zagreb, Croatia, 1994. (in Croatian).

[37] Kumar. Vimal., Mathur. Mukesh., Sinha. Shashank Shekhar. 2005. A case study: manifold increase in fly ash utilisation in india. Fly Ash India, New Delhi.

[38] Larbi L.A., 1993. Microstructure of the interfacial zone around aggregate particles in concrete. Heron, 1993; 38(1): 69.

[39] Lam L., Wong Y.L., Poon C.S., 2000. Degree of hydration and gel/space ratio of high-volume fly ash/cement systems. Cement and Concrete Research, 2000; 30: 747-756.

[40] Lawrence Philippe, Cyr Martin, Ringot Erick, 2003. Mineral admixtures in mortars: effect of inert materials on short-term hydration. Cement and Concrete Research, 2003; 33: 1939-1947.

[41] Maage, M., Helland, S., Poulsen, E., Vennesland, O., Carlsen, J.E., 1996. Service life prediction of existing concrete structures exposed to marine environment. ACI Materials Journal, 1996; 93(6): 602-608.

[42] Malhotra, V. M., 1999. Making concrete greener with fly ash. Concrete International, 1999; 21(5): 61-66.

[43] Malhotra, V.M., Mehta, P.K., 2002. High-performance, high-volume fly ash concrete. Supplementary Cementing Materials for Sustainable Development, Inc., Ottawa, Canada, pp, 101.

[44] Mayda Chris., 2012. A regional geography of the united states and Canada: toward a sustainable future. Rowman & Littlefield Publishers, 8 Aug.

[45] Mehta P. Kumar, 2004. High-performance, high-volume fly ash concrete for sustainable development. Edited by Kejin Wang, Proceedings of the international workshop on sustainable development and concrete technology, 3-14. Beijing, China. May 20-21, 2004.

[46] Mindess S., Young J. F., 1981 Concrete (Englewood, NJ: Prentice-Hall).

[47] Naik, Tarun R., Singh, Shiw S., Hossain, Mohammad M., 1994. Permeability of concrete containing large amounts of fly ash. Cement and Concrete Research, 1994; 24(5): 913-922.

[48] National development and reform commission of Chin, 2010. Implementing scheme of mainly solid waste utilization. Beijing.

[49] Nath Pradip, Sarker Prabir, 2011. Improvement of durability and service life of concrete using class f fly ash, Proceedings of the Concrete 2011 Conference, Oct 12 2011. Perth, WA: The Concrete Institute of Australia.

[50] Nawy, Edward G., 2008. Concrete Construction Engineering Handbook. 2nd Edition. CRC Press.

[51] Neithalath, Narayanan, Jain Jitendra, 2010. Relating rapid chloride transport parameters of concretes to microstructural features extracted from electrical impedance. Cement and Concrete Research, 2010; 40: 1041-1051.

[52] Neville, A. M., 1995. Properties of concrete. 4th and final Ed., Longman's, London.

[53] Nordtest Method: Accelerated chloride penetration into hardened concrete, Nordtest, Espoo, Finland, Proj. 1154-94, 1995.

[54] Obla, Karthik H., Hill, Russell L., Thomas, Michael D. A., Shashiprakash, Surali G., Perebatova, Olga, 2003. Properties of concrete containing ultra-fine fly ash. Materials Journal, 2003; 100(5): 426-433.

[55] Odler, I., 1998. Hydration, setting, and hardening of Portland cement in Lea's chemistry of cement and concrete, 4th ed. Edited by P. C. Hewlett. Arnold, London, U.K., pp.241.

[56] Papadakis Vagelis G., 1999. Effect of fly ash on Portland cement systems Part I. Low-calcium fly ash. Cement and Concrete Research, 1999; 29:1727-1736.
[57] Papadakis Vagelis G., 2000. Effect of fly ash on Portland cement systems Part II. High-calcium fly ash. Cement and Concrete Research, 2000; 30:1647-1654.
[58] Pietersen, H.S., 1993. Reactivity of fly ash and slag in cement. Ph.D. Thesis (Delft University of Technology, Delft).
[59] Poon, C. S., Wong, Y. L., and Lam, L., 1997. The influence of different curing conditions on the pore structure and related properties of fly ash cement pastes and mortars. Construction and Building Materials, 1997; 11: 383-393.
[60] Powers TC., 1958. Structures and physical properties of hardened portland cement paste. Journal American Ceramic Society, 1958; 41: 5-15.
[61] Rilem report 38, 2007. Durability of self-compacting concrete. Edited by G. De Schutter and K. Audenaert. Rilem TC 205-DSC; State-of-the-Art Report. April 2007. ISBN: 978-2-35158-048-6.
[62] Sakai Etsuo, Miyahara Shigeyoshi, Ohsawa Shigenari, Lee Seung-Heun, Daimon Masaki, 2005. Hydration of fly ash cement. Cement and Concrete Research, 2005; 35: 1135-1140.
[63] Scrivener K.L., Gariner E.M., 1988. Microstructural gradients in cement paste around aggregate particles Mater Res Soc Sympos Proc, 1988; 114: 77-85
[64] Siemes, T., Schiessl, P., Rostam, S., 2000 Future developments of service life design of concrete structures on the basis of DuraCrete, In: Service life prediction and ageing management of Concrete Structures, ed. D. Naus, RILEM, 167-176.
[65] Shafiq N., 2004. Effect of fly ash on chloride migration in concrete and calculation of cover depth required against the corrosion of embedded steel reinforcement. Structural Concrete, 2004; 5 (1): 5-9.
[66] Stutzman Paul E., Centeno Lilia, 1995. Compositional Analysis of Beneficiated Fly Ashes. NISTIR 5598.
[67] Tanabe Tada-aki, Sakata Kenji, Mihashi Hirozo，Sato Ryoichi, Maekawa Kochi, Nakamura Hikar, 2009. Creep, shrinkage and durability mechanics of concrete and concrete structures, Volume 1. ISBN: 978-0-415-48508-1.
[68] Tang Luping, Lars-Olof Nilsson, 1992. Rapid determination of chloride diffusivity of concrete by applying an electric field. ACI Materials Journal, 1992; 89(1): 49-53.
[69] Tang, L., 1996. Chloride transport in concrete-measurement and prediction. Doctoral thesis, publication P-96:6, Dept. of Building Materials, Chalmers Universities of Technology, Gothenburg, Sweden.
[70] Tang Luping, Lars-Olof Nilsson, P.A.Muhammed Basheer, 2012. Resistance of concrete to chloride ingress-testing and modeling. ISBN: 9780415486149. Spon Press.
[71] Tapkin, S., 2008. Improved asphalt aggregate mix properties by Portland cement modification. Canadian journal of civil engineering, 2008; 35: 27-40.
[72] Taylor HFW., 1997. Cement chemistry. London: Thomas Telford.
[73] Teplý B., 2002. Modelling of deterioration effects on concrete structures. Acta Polytechnica, 2002; 42 (3): 8-12.
[74] Thomas M. D. A., 1991. Marine performance of PFA concrete. Magazine of Concrete Research, 1991; 43(156): 171-185.
[75] van Dalen, Sander M., 2005. Experimenteel onderzoek naar de RCM-methode (In Dutch). Master Thesis. Delft University of Technology.
[76] Wang A., Zhang C., Sun W., 2004. Fly ash effects III. The micro aggregate effect of fly ash. Cement and Concrete Research, 2004; 34: 2061-2066.
[77] Wang Xiao-Yong, Lee Han-Seung, 2009. Simulation of a temperature rise in concrete incorporating fly ash or slag. Materials and Structures, 2009; 43: 737-754.
[78] Ward Colin R., French David, 2006. Determination of glass content and estimation of glass composition in fly ash using quantitative X-ray diffractometry. Fuel, 2006; 85: 2268-2277.
[79] Wei Fajun, Grutzeck M.W., Roy D.M., 1985. The retarding effects of fly ash upon the hydration of cement pastes: the first 24 hours. Cement and Concrete Research, 1985; 15: 174-184.
[80] Weng Jeff Kaimao, Langan B.W., Ward M.A., 1997. Pozzolanic reaction in portland cement, silica fume, and fly ash mixtures. Canadian journal of civil engineering, 1997; 24: 754-760.
[81] Williams P. Jason, Biernacki Joseph J., Walker Larry R., Meyer Harry M., Claudia J. Rawn, Jianming Bai, 2002. Microanalysis of alkali-activated fly ash-CH pastes. Cement and Concrete Research, 2002; 32: 963-972.
[82] Wong, Y.L., L. Lam, C.S. Poon, F.P. Zhou, 1999. Properties of fly ash-modified cement mortar-aggregate interfaces. Cement and Concrete Research, 1999; 29(12): 1905-1913.
[83] Xi Y., 1997. Mathematical modeling of chloride diffusion in concrete. Published in Mechanisms of chemical degradation of cement-based systems, Edited by Scrivener K.L., Young J.F.. ISBN: 0419215700, p. 397.
[84] Yang Ailun, Rashid Kang, Zhao Xingmin, Huang Xu, Zhou Hanhua, Su Miaohan, Tang Hongyuan, Li Fei, 2010. The true cost of coal – an investigation into coal ash in China. A Greenpeace report.

[85] Ye Guang, 2003. The microstructure and permeability of cementitious materials. PhD Thesis. Delft University of Technology.

[86] Young J. F., Hansen W., 1986. Volume relationship for C-S-H formation based on hydration stoichiometry. MRS Proceedings, Volume 85. Mater. Res. Soc. Symp. Proc, (Boston, MA, 1986) ed. L.J. Struble and P.W. Brown (Pittsburgh, PA: Materials Research Society) pp 313-22.

[87] Yuan Qiang, 2009. Fundamental studies on Test methods for the transport of chloride ions in cementitious materials. Gent University. PhD thesis.

[88] Zhang, Ya Mei, Sun, Wei, Yan, Han Dong, 2000. Hydration of high-volume fly ash cement pastes. Cement Concrete Composites, 2000; 22: 445-452

Chapter 3

Experimental Study of the Hydration Process of Portland Cement Paste Blended with Fly Ash

3.1 Introduction

As the most soluble hydration product formed during the hydration of cement, calcium hydroxide (CH) is considered a weak link in Portland cement concrete. If the concrete is constantly exposed to running soft water, the CH phase will leach out (dissolve), increasing the porosity and thus making the concrete more vulnerable to further leaching and chemical attack, eventually reducing the service life of concrete structures. In fly ash concrete, however, CH is consumed by the pozzolanic reaction of fly ash to produce reaction products, mainly calcium silicate hydrates (C-S-H). The formation of additional C-S-H in fly ash concrete contributes to strength development and the improvement of durability. The CH content of paste influences the pozzolanic reaction of fly ash, the microstructure development and transport properties of Portland cement-fly ash binary systems.

The main objective of this chapter is to determine the CH content of cement paste blended with fly ash at ages up to 3 years by thermogravimetric analysis (TGA). In order to investigate the effect of fly ash on the hydration process of blended cement paste at later ages, the hydration products are identified by X-ray diffraction (XRD) technique and the rate of hydration of cement and of the pozzolanic reaction of fly ash in blended cement paste are determined by backscattered electron (BSE) image analysis. The results obtained in this chapter will lead to a better understanding of microstructure development and transport properties of binary systems at later ages.

3.2 Materials

The materials used in this study are Portland cement (CEM I 42.5 N), fly ash and de-ionized water. The Portland cement and fly ash used for all experiments are taken from the same batches.

3.2.1 Chemical composition of Portland cement and fly ash

Portland cement (CEM I 42.5 N) used in the experiments was produced by ENCI, The Netherlands. The fly ash is a low-calcium fly ash (Class F fly ash). Table 3.1 shows the chemical composition of the Portland cement and fly ash as determined by X-ray fluorescence (XRF) spectrometry method.

Table 3.1: Chemical composition of Portland cement and fly ash (% by mass)

Chemical Composition	CEM I 42.5 N	Fly Ash
SiO_2	20.36	48.40
Al_2O_3	4.96	31.40
CaO	64.40	7.14
free-CaO	0.60	-
Fe_2O_3	3.17	4.44
P_2O_5	0.18	1.90
K_2O	0.64	1.64
MgO	2.09	1.35
SO_3	2.57	1.18
Na_2O	0.14	0.72
Total	99.11	98.17

3.2.2 Mineral composition

Portland cement

The mineral composition of Portland cement is calculated with the Bogue equation *[Taylor 1997]* and presented in Table 3.2.

Table 3.2: Mineral composition of Portland cement (% by weight)

Phase	Weight (%)
C_3S	67.1
C_2S	5.9
C_3A	7.8
C_4AF	9.6

Fly ash

The mineral composition of the fly ash is identified by X-ray diffraction (XRD) technique. Figure 3.1 shows the XRD pattern of the fly ash. The main crystalline phases are mullite (M) and quartz (Q). By using an XRD-Rietveld refinement method, the mineral compositions are determined. Corundum (α-Al_2O_3) is used as standard sample. The Rietveld method is a technique proposed by Hugo Rietveld *[Rietveld 1969]* for the characterization of crystalline materials and the quantitative analysis of multiphase materials. In this technique, the method of least squares is used to refine a theoretical line profile until it matches the measured patterns *[Kariya 2004]*. The detailed procedure of the Rietveld refinement is described by Rodriguez-Carvajal *[Rodriguez-Carvajal 1993]*. Based on this method, the crystalline phases of the fly ash is calculated, including 13.48% mullite and 13.71% quartz by weight. The glass phase of the fly ash is 72.81%.

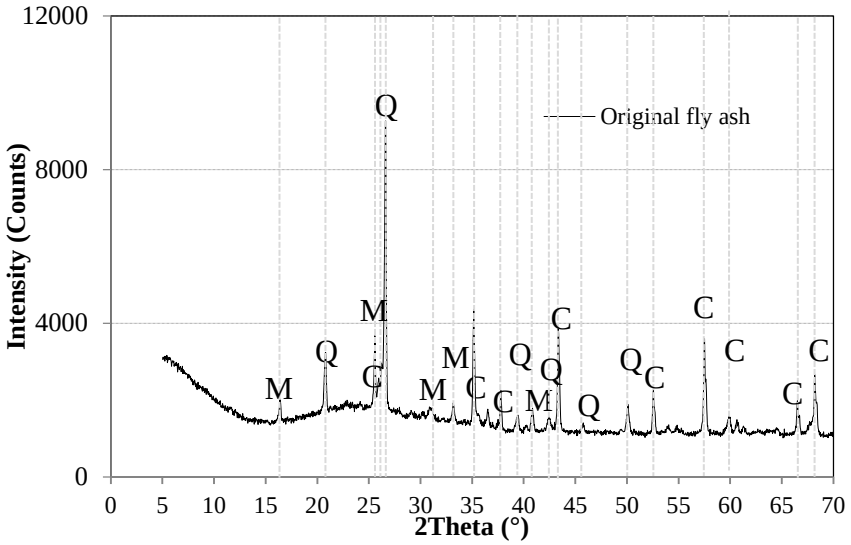

Q: Quartz; C: Corundum (α-Al_2O_3); M: Mullite;

Figure 3.1: XRD pattern of fly ash

3.2.3 Particle size distribution

The particle size distribution of cement and fly ash plays an important role in the hydration process and the development of the microstructure. Figure 3.2 shows the particle size distribution curves of Portland cement and fly ash measured by laser diffraction. The mean particle sizes, *D50*, of fly ash and cement are 21 μm and 17 μm, respectively.

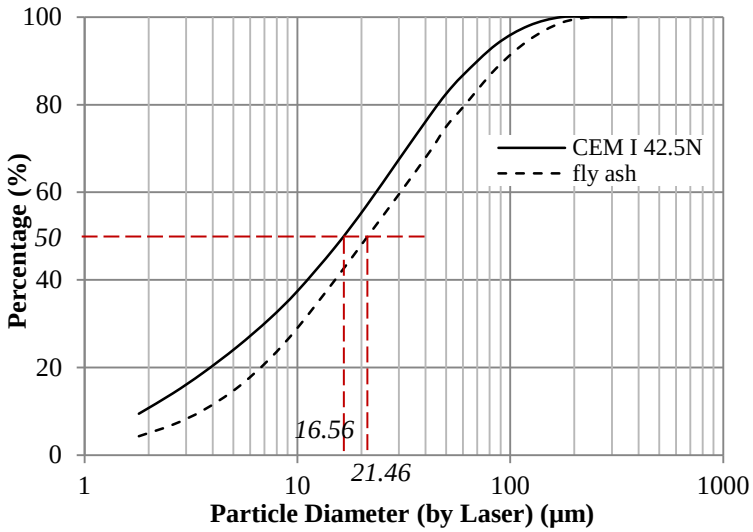

Figure 3.2: The particle size distribution of Portland cement and fly ash

3.2.4 Microstructure

Figure 3.3 shows the backscattered electron (BSE) images of fly ash particles obtained from environmental scanning electron microscope (ESEM). Two types of fly ash particles are observed, hollow particles and solid particles. Except fly ash particles, also un-burnt (UB) coal particles are found. In general, fly ash particles have a spherical shape and can be distinguished clearly from the irregular cement particles.

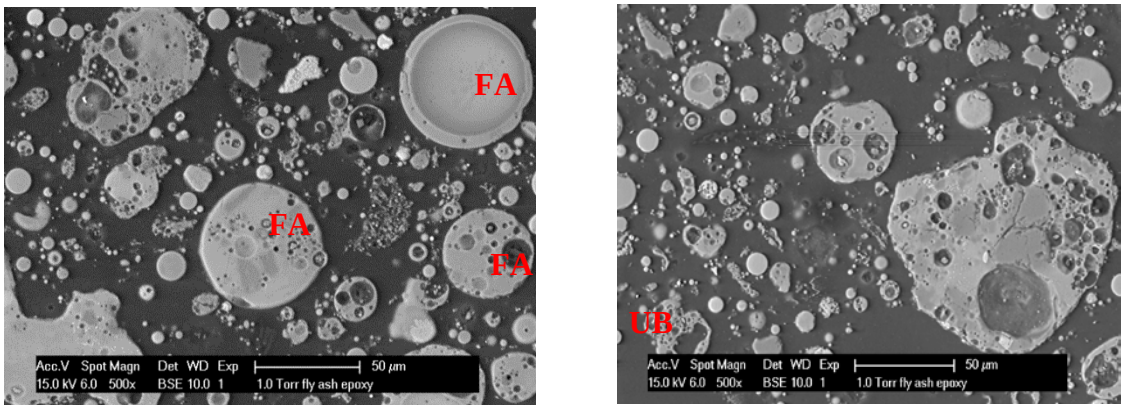

FA: fly ash; UB: un-burnt coal

Figure 3.3: BSE images of fly ash particles

3.3 Mixture Compositions

Four kinds of mixtures are considered in this study. The Portland cement paste is prepared as reference sample with the water/cement ratio of 0.4. The fly ash dosages in blended mixtures are 30% and 50% by weight of binder and w/b=0.4. For cement paste blended with 30% fly ash the water/binder (cement and fly ash) ratios are 0.4 and 0.5. De-ionized water is used to prevent any effect of ions from tap water on the properties of the paste. The mixture compositions are summarized in Table 3.3.

Table 3.3: Mixture compositions used in this study

Specimens name	Cement (%)	Fly ash (%)	w/b	w/c
Portland cement paste	100	0	-	0.4
Cement paste blended with 30% fly ash	70	30	0.4	-
Cement paste blended with 50% fly ash	50	50	0.4	-
Cement paste blended with 30% fly ash	70	30	0.5	-

3.4 Survey of Type of Experiments

The hydration products of blended cement paste at ages up to 3 years were identified by X-ray diffraction (XRD) technique. The effect of fly ash on the CH content in blended cement paste was determined by thermogravimetric analysis (TGA). The rate of hydration of cement and of the pozzolanic reaction of fly ash in blended cement paste was estimated by backscattered electron (BSE) image analysis.

3.4.1 Sample preparation for XRD, TGA and ESEM

The XRD, TGA and ESEM studies were performed on Portland cement paste (as reference sample) and cement paste blended with fly ash. All samples were prepared in a three-liter Hobart mixer at room temperature around 20 ± 2 ºC. After 3 minutes mixing, the specimens were poured in a plastic bottle (ϕ 33×70 mm) and sealed in order to prevent moisture loss and rotated slowly for 24 hours to minimize the effects of settlement and bleeding. After that, all the specimens were cured at 20 ± 2 ºC.

At an age of 1 day, 7 days, 28 days, 90 days, 180 days, 365 days (1 year), 730 days (2 years) and 1095 days (3 years), the specimens were demoulded from the plastic bottles and crushed into small pieces. After that, the specimens were frozen by immersion in liquid nitrogen for 5 minutes to stop hydration. The specimens were then dried in a freeze-dryer. Water loss was recorded each 24 hours until the loss of water reached a value of less than 0.05%/day. Figure 3.4 shows the dried specimens. It should be noted that the freeze drying method was used to prevent damage to the pore structure of cement paste *[Ye 2003]*.

Figure 3.4: Cement paste blended with fly ash after stopping hydration and drying

3.4.2 Testing procedures

X-ray diffraction

The dried paste samples were gently ground by hand until the particle size was smaller than 125 μm. After grinding, the powder samples used for XRD were placed in an aluminium sample holder as shown in Figure 3.5. XRD analyses were performed using a Philips X' pert diffractometer system with Cu Kα radiation (see Figure 3.6). Scans were run from 5 to 70° 2θ, with a step size of 0.02° 2θ and a dwell time of 2 seconds per step.

(a) *(b)*

Figure 3.5: Sample deposition for XRD test (a) Aluminum sample holder; (b) Sample holder with sample

Figure 3.6: Philips X' pert diffractometer system

Thermogravimetric analyses (TGA)

The powder samples were put in an aluminum oxide (Al_2O_3) crucible and heated from 40 °C to 1100 °C in a thermoanalyzer TG-449-F3-Jupiter instrument (see Figure 3.7). The heating rate was 10°C per minute. The measurement was carried out in argon (inert) atmosphere.

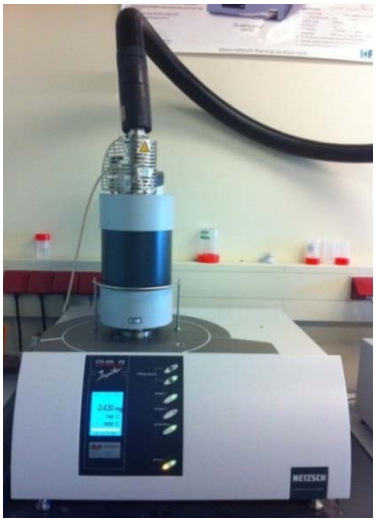

***F**igure 3.7: TG-449-F3-Jupiter® for Thermogravimetric analysis*

Environmental scanning electron microscope

The crushed paste samples with different sizes were collected in a plastic bottle for ESEM tests. The samples were put in a vacuum chamber and then evacuated at 30 mbar for 1 hour. With the vacuum pump still running, liquid epoxy was fed from a cup outside the vacuum chamber to the top of the samples via a plastic tube. The upper face of the sample was covered with epoxy. After about 10 minutes, air was let gradually into the vacuum chamber to push the epoxy further into the pore system of the samples. The impregnated sample was cured at atmospheric pressure at 40 ºC for 24 hours. Then the samples were ready for cutting, grinding and polishing. Figure 3.8 shows an example of the sample ready for the ESEM studies.

The microstructure characteristics of cement paste blended with fly ash were studied by performing back-scattered electrons (BSE) mode. The observations were conducted with a Philips-XL30-ESEM (see Figure 3.9) in a gaseous (water vapour) environment (no conductive coating is needed). An acceleration voltage of 20 kV was used. The size of the reference region of each image is 248 μm in length and 188 μm in width. The magnification is 500× and the image size is 1424 × 968 pixel. Thus, the resolution of each image is 0.18 μm/pixel.

Figure 3.8: Sample for BSE images observation

Figure 3.9: Philips-XL30-ESEM system for microstructural observation

3.4.3 TGA-test for determination of the calcium hydroxide content in paste

As mentioned in introduction (section 3.1), calcium hydroxide (CH) is considered as one of the major phases in the hardened Portland cement paste. The presence of fly ash in blended cement paste leads to a lower CH content caused by its pozzolanic reaction. The amount of CH of the paste can be determined by TGA-test *[Midgley 1979]*.

A typical weight-loss versus temperature curve obtained from TGA-measurements for Portland cement paste (w/c=0.4; at 28 days) is shown in Figure 3.10. Three characteristic endothermic effects are observed. The first endothermic effect, in the temperature range from 100 to 320 °C, is attributed to the dehydration of calcium silicate hydrate (C-S-H) and calcium aluminate hydrate (C-A-H) *[Bhatty 1985; Marsh 1988; Vedalakshmi 2003]*. The temperature for the dehydration of C-S-H/C-A-H mainly depends on the CaO to SiO_2 ratio in the hydrated cement paste. The second endothermic effect, with peak temperature between 420 and 550 °C, is due to the decomposition of CH in cement paste. The decomposition reaction is shown in Equation 3.1:

$$\begin{aligned} &\textit{Chemical reaction}: \quad Ca(OH)_2(s) \rightarrow CaO(s) + H_2O(g) \\ &\textit{Molar weight}: \qquad 74\ g/mol \quad 56\ g/mol \quad 18\ g/mol \end{aligned} \tag{3.1}$$

During the decomposition of CH the weight loss comes from the loss of water. This weight loss (m_{H2O}) can be determined by a graphical technique, proposed by Marsh *[Marsh 1988]* (see Figure 3.10). Within the TG curve the onset and offset points of the decomposition curve of CH are determined, which are the intersections of two tangent lines. They are defined as initial baseline and final baseline, respectively. By the onset and offset points (Temperature axis), the mid-point T_0 is created. The weight loss m_{H2O} is defined as the distance between two intersections generated by the vertical line from T_0 with initial and final baselines. Then the content of CH (m_{CH}) is calculated:

$$m_{CH} = m_{H_2O} \times \frac{74}{18} \tag{3.2}$$

where: 74 and 18 are the molar weight of $Ca(OH)_2$ and H_2O (see Equation 3.1).

The third endothermic effect around 700 °C indicates the decarbonation of calcium carbonate ($CaCO_3$) in cement paste. In the period of the decarbonation of calcium carbonate the weight loss comes from the loss of carbon dioxide (see Equation 3.3).

$$\begin{aligned} &\textit{Chemical reaction}: \quad CaCO_3(s) \rightarrow CaO(s) + CO_2(g) \\ &\textit{Molar weight}: \qquad 100\ g/mol \quad 56\ g/mol \quad 44\ g/mol \end{aligned} \tag{3.3}$$

Calcium carbonate is present as mixed-in mineral admixture or from the carbonation of the paste during sample preparation *[Bhatty 1985; Marsh 1988]*. The weight loss of carbon dioxide (m_{CO2}) can be determined in the same way as the weight loss of water due to the decomposition of CH. The content of $CaCO_3$, m_{CaCO3}, is then calculated by Equation 3.4, where 100 and 44 are the molar weight of $CaCO_3$ and CO_2:

$$m_{CaCO_3} = m_{co_2} \times \frac{100}{44} \tag{3.4}$$

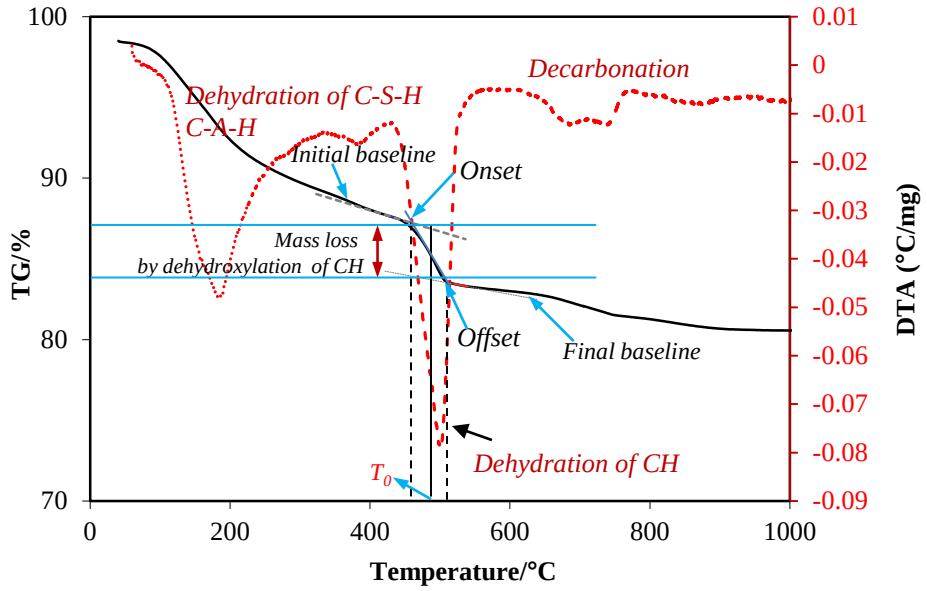

Figure 3.10: Method used to calculate the CH content of paste [Marsh 1988]

3.4.4 Assessment of the rate of hydration of cement and pozzolanic reaction of fly ash by image analysis

BSE image analysis technique is widely used for determination of the degree of hydration of cement in cement paste *[Scrivener 2004]*. It can also be used to determine the degree of pozzolanic reaction of fly ash in Portland cement-fly ash binary systems *[Ben Haha 2010]*. However, the accuracy of the results is limited by the resolution of the images.

Degree of hydration of Portland cement

A typical BSE image of Portland cement paste (w/c=0.4; at 7 days) and its grey level histogram are shown in Figure 3.11. Phases with different density show different grey levels. The grey level histogram indicates that the main phases are present, *i.e.* unhydrated cement (anhydrous), hydration products (CH, HP) and pores. The unhydrated cement phase in cement paste can easily be segmented as shown in Figure 3.12. In the same way the unhydrated cement phase in blended cement paste is also segmented as shown in Figure 3.14 (a).The degree of hydration of cement, α_c, can be calculated from the remaining unhydrated cement. It is the ratio of reacted cement relative to the original amount of cement as shown in Equation 3.5:

$$\alpha_c = \frac{V_{reacted}}{V_{initial}} = 1 - \frac{V_{c-measured}}{V_{c-initial}} \tag{3.5}$$

where:

$V_{c-measured}$ = volume of unreacted clinker from the image analysis.

$V_{c-initial}$ = initial volume of cement in the mix proportions.

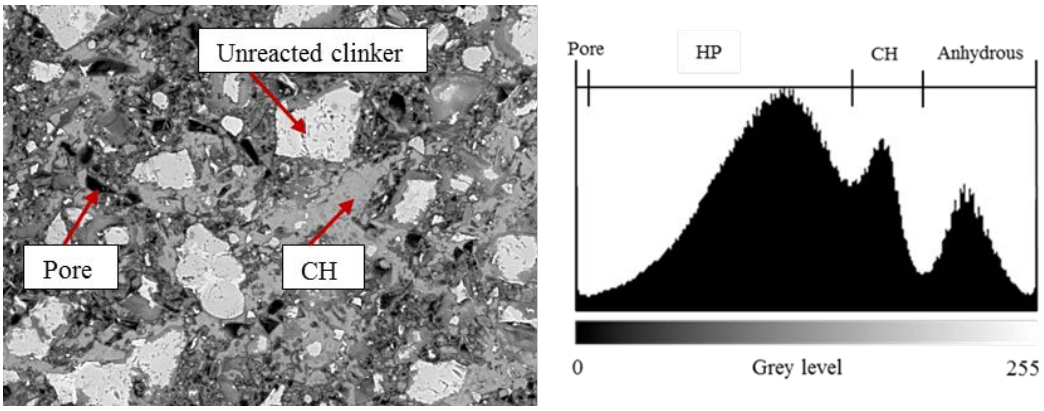

Figure 3.11: A typical BSE image (500×) of cement paste at 7 days and its grey level histogram (Pore: Porosity; HP: hydration products other than Portlandite; CH: Portlandite; Anhydrous: unhydrated cement)

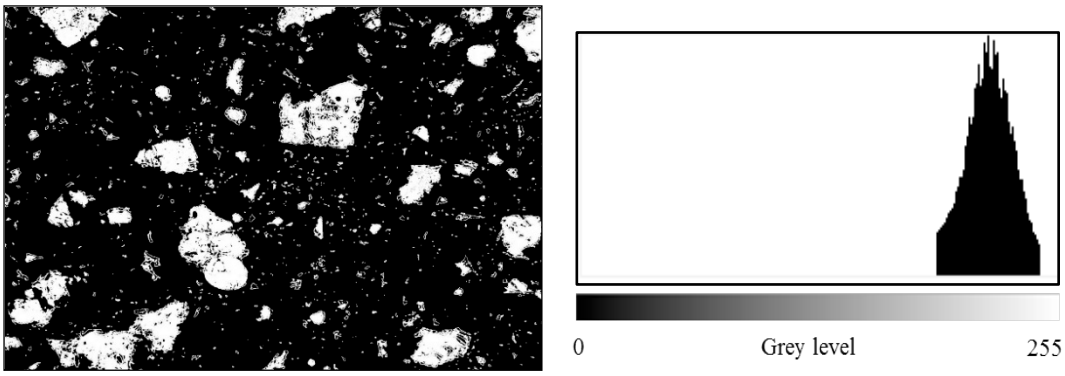

Figure 3.12: Segmented images for unhydrated cement

Degree of pozzolanic reaction of fly ash

A typical BSE image of cement paste blended with fly ash (30% fly ash; w/b=0.4; at 7 days) and the corresponding grey level histogram are shown in Figure 3.13. Compared to Portland cement paste the phases in blended cement paste are more complicated to distinguish, because the grey levels of fly ash particles overlap those of C-S-H and CH (Figure 3.13). Therefore, it is not possible to distinguish the unreacted fly ash phase based on grey level histogram *only*. However, by using a combination of image analysis techniques, the grey level threshold together with area selection tool *[Ma 2013]*, the unreacted fly ash particles can be selected from original BSE image (see Figure 3.13). It is shown in Figure 3.14 (b).

Similar to the calculation of the degree of hydration of cement, the degree of pozzolanic reaction of fly ash, α_{FA}, is obtained with Equation 3.6:

$$\alpha_{FA} = \frac{V_{reacted}}{V_{initial}} = 1 - \frac{V_{FA-measured}}{V_{FA-initial}} \tag{3.6}$$

where:

$V_{FA-measured}$ = volume of fly ash from the image analysis.

$V_{FA-initial}$ = initial volume of fly ash in the mix proportions.

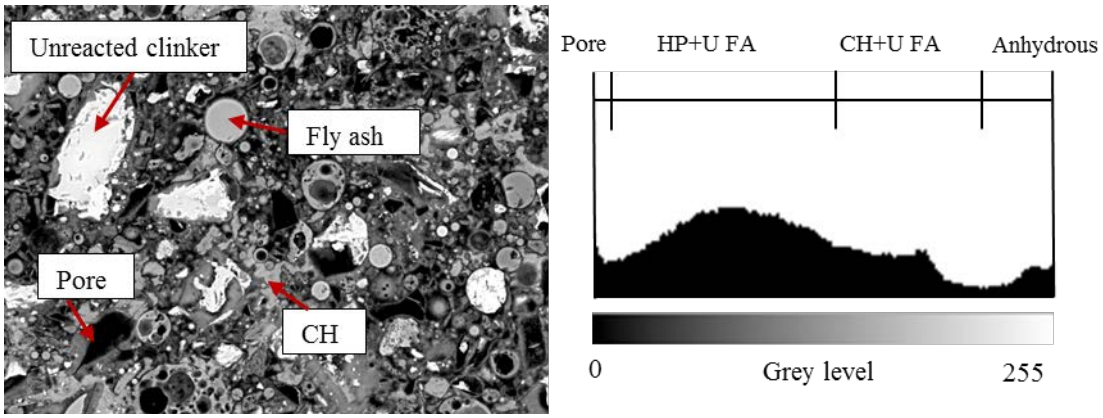

Figure 3.13: A typical BSE image (500×) of cement paste after 7 days and its grey level histogram (Pore: Porosity; HP: hydration products other than Portlandite; CH: Portlandite; U FA: unreacted fly ash; Anhydrous: unhydrated cement clinker)

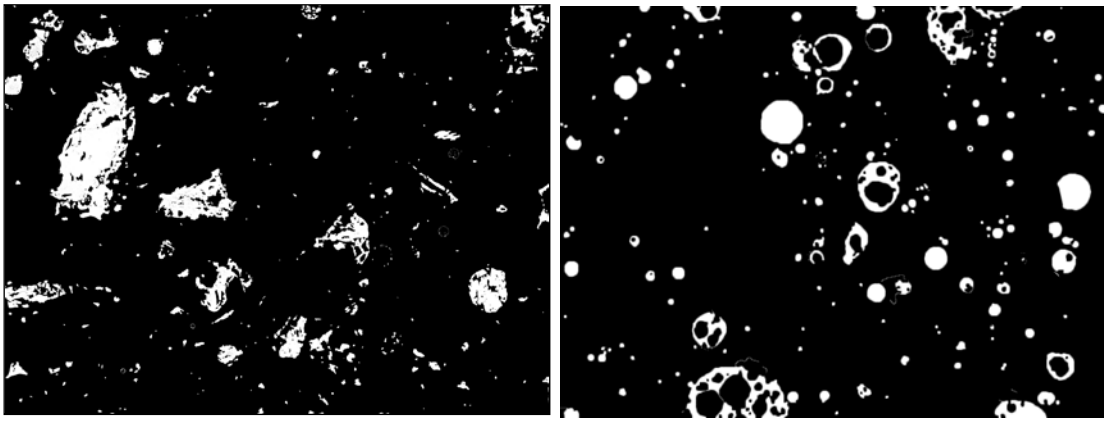

(a) (b)

Figure 3.14: Segmented BSE images (a) unhydrated cement clinker; (b) unreacted fly ash particles

3.5 Experimental Results

3.5.1 Identification of hydration products in blended cement paste cured for 3 years

Figure 3.15 and Figure 3.16 show the XRD patterns of Portland cement paste and cement paste blended with fly ash (30% fly ash; w/b=0.4) at ages from 1 day to 1095 days (3 years), respectively. The main peaks in Portland cement paste represent the hydration product (CH) and unhydrated cement minerals (alite, belite and ferrite). In blended cement paste the mineral phases of fly ash (mullite and quartz) are also detected. As expected, with increasing ages up to 3 years, the intensities of the cement mineral phases decrease and the intensity of CH increases.

As shown in Figure 3.15 and 3.16 the characteristic peak of monocarbonate ($2\theta = 11.7°$) is identified for both Portland cement paste and blended cement paste, particularly at later ages. It has been reported that carboalummate hydrate phase, *i.e. monocarbonate*, may be formed during the hydration of cement in cement paste containing limestone powder (under sealed curing conditions) *[Bushnell-Watson 1985; Ramachandran 1988], but* it is not formed in pure Portland cement paste.

In this study no limestone powder was used. However, in both Portland cement paste and blended cement paste the characteristic peak of $CaCO_3$ around $2\theta = 29.4$ °(PDF 72-1937) is clearly observed. The presence of $CaCO_3$ results from the addition of limestone powder to the Portland cement. As we know, limestone powder, *viz.* $CaCO_3$, is allowed as minor additional constituent in cement up to 5% of the cement clinker *[EN 197-1 1992; Tennis 2011]*. The amount of $CaCO_3$ in this cement is around 2.4 percent of total binder (information from cement supplier).

The formation of monocarbonate is in agreement with the findings of Taylor *[Taylor 1997]*: the monocarbonate results from the reaction of $CaCO_3$ with the alumina phases (C_3A) in Portland cement according to Equation 3.7 *[Soroka 1977; Kakali 2000; Lothenbach 2008; De Weerdt 2011]*:

$$3CaO \cdot Al_2O_3 + CaCO_3 + 11H_2O \rightarrow \left(3CaO \cdot Al_2O_3\right) \cdot CaCO_3 \cdot 11H_2O \tag{3.7}$$

Clear XRD patterns of low angles from 5° to 20° for Portland cement paste and cement paste blended with fly ash are shown in Figure 3.17 and Figure 3.18. In Portland cement paste the peak of monocarbonate is observed at ages beyond 90 days. The relative peak intensity of monocarbonate becomes stronger with an increase in age of the paste. In blended cement paste the monocarbonate is observed at ages beyond 7 days as shown in Figure 3.18. It means that the addition of fly ash promotes the reaction of $CaCO_3$ with C_3A in blended cement paste. That is probably because the content of aluminium oxide in fly ash is much higher than that in Portland cement. As shown in Table 3.1 the content of aluminium oxide in fly ash is 31%. It is higher than 5% in Portland cement (see Table 3.1).

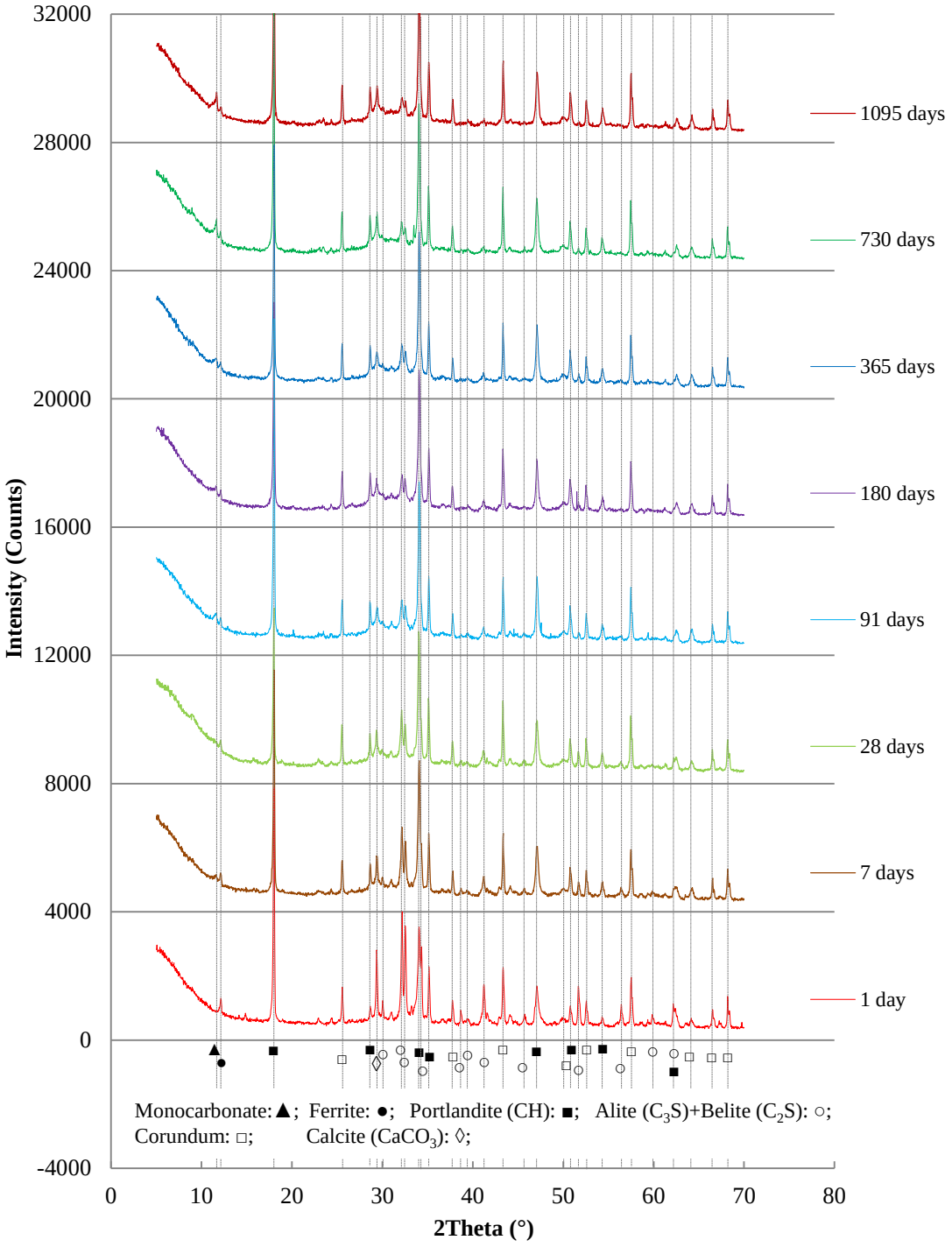

Figure 3.15: The measured XRD patterns of Portland cement paste at ages from 1 day to 3 years

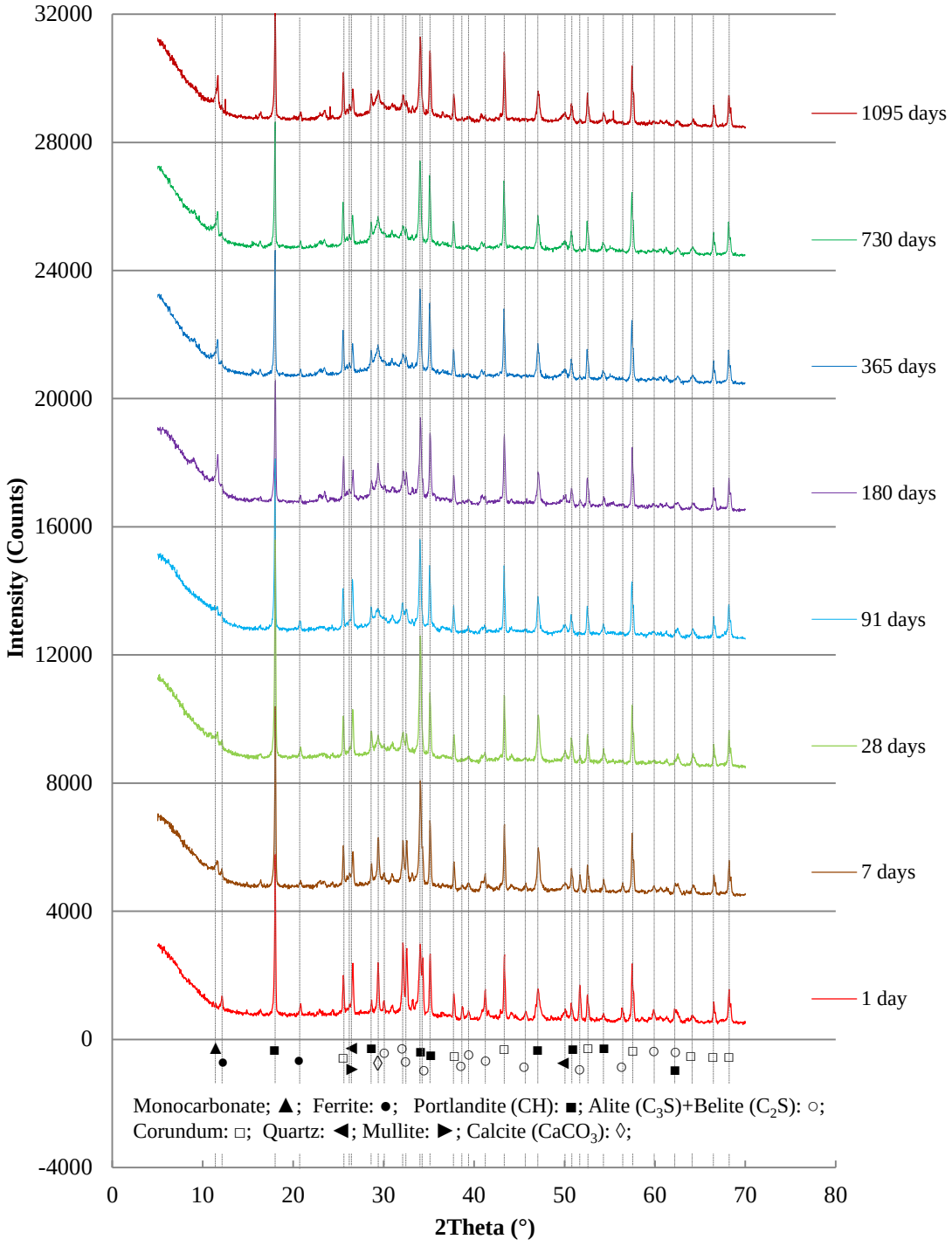

Figure 3.16: The measured XRD patterns of cement paste blended with fly ash at ages from 1 day to 3 years (30% fly ash; w/b=0.4)

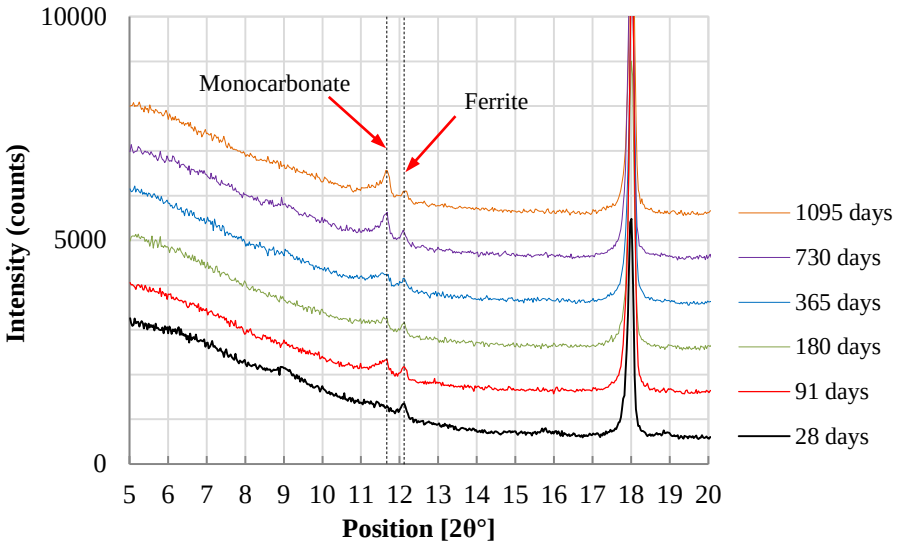

Figure 3.17: XRD patterns for Portland cement paste (w/c=0.4) at ages from 28 days to 3 years

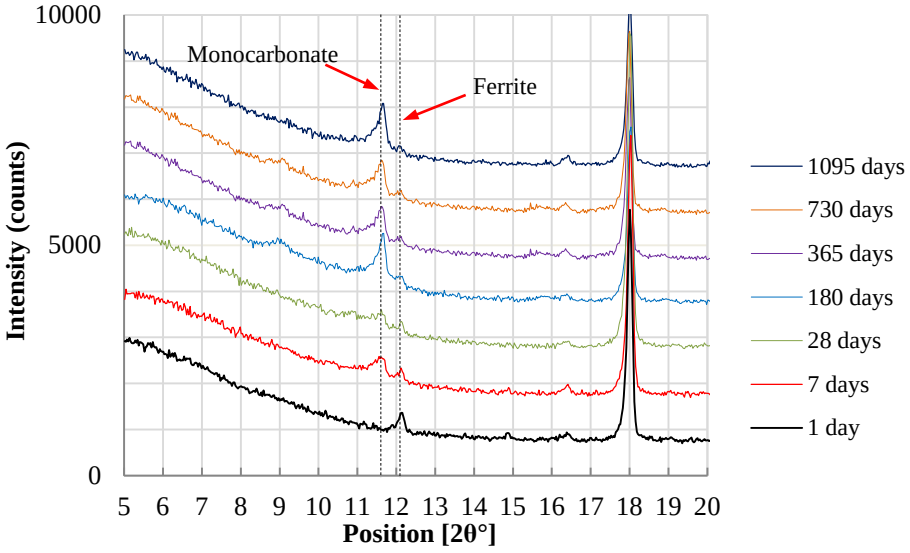

Figure 3.18: XRD patters for cement paste blended with fly ash (30% fly ash; w/b=0.4) at ages from 1 day to 3 years

3.5.2 Calcium hydroxide content in cement paste blended with fly ash

Effect of fly ash content

Figure 3.19 shows the amount of CH in cement pastes made with different fly ash dosages (0%, 30% and 50%) as a function of time. The calculated CH content is presented in gram/gram cement (g/gcement). It can be seen that the CH content of all pastes increases significantly at early age from 1 day to 7 days. The CH content of pastes is higher the higher the fly ash content. Beyond 28 days the CH content of Portland cement paste increases slowly. As a result of the pozzolanic reaction of fly ash a decrease in the CH content of blended cement paste is observed beyond 7 days for mixture with 50% fly ash and beyond 28 days for mixture with 30% fly ash, respectively. Beyond 180 days, the CH content of blended cement paste hardly changes.

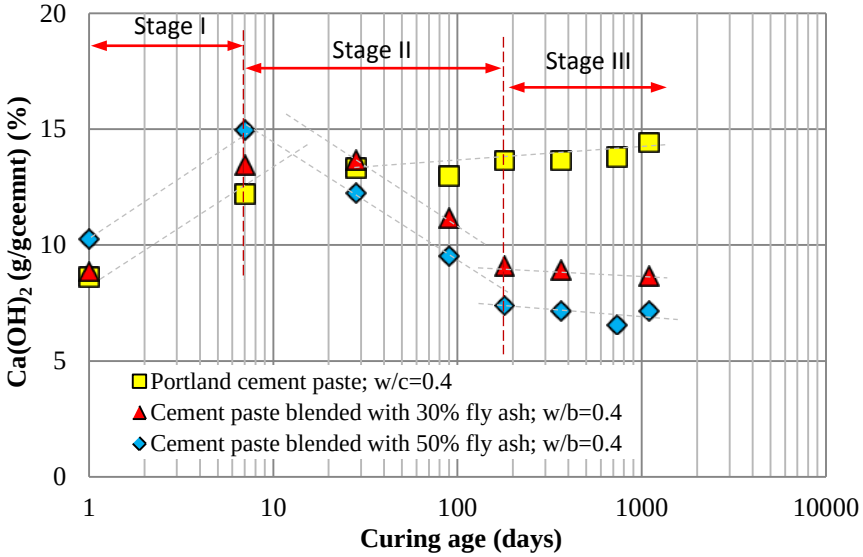

Figure 3.19: The CH content of pastes made with different fly ash dosages at ages up to 3 years

Effect of w/b ratio

Figure 3.20 shows the CH content in blended cement paste with 30% fly ash made with two w/b ratios, 0.4 and 0.5 At early age, from 1 day to 7 days, a w/b ratio of 0.5 leads to an increase of the CH content. At later ages, from 7 days up to 3 years there is no big difference in the CH content between blended cement paste made with w/b ratio of 0.4 and 0.5.

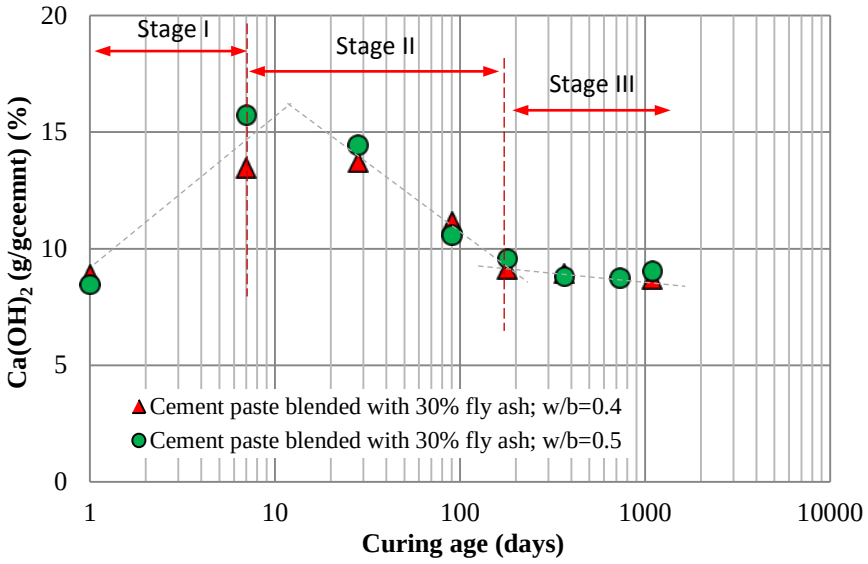

Figure 3.20: The CH content of blended cement pastes made with different w/b ratios at ages up to 3 years

Based on the above mentioned results (Figure 3.19 and Figure 3.20), it can be concluded that three stages can be distinguished in the development of the CH content in blended cement paste:

1) *Stage I.* At early age, *i.e.* before 7 days, the presence of fly ash leads to faster hydration of cement in binary systems. This is indicated by a high CH content in blended cement paste regardless of fly ash dosage (30% and 50%) and w/b ratios (0.4 and 0.5). The reasons for this have been discussed in the literature review (the dilution effect and physical effect of fly ash).
2) *Stage II.* After about 7 days, the CH content in blended cement paste decreases significantly. It suggests that in binary systems the rate of the pozzolanic reaction of fly ash (*consuming CH)* is faster than that of the hydration of cement (*producing CH)*. The blended cement paste made with 50% fly ash consumes more CH than that with 30% fly ash.
3) *Stage III.* At later ages, *i.e.* beyond 180 days, the CH content in blended cement paste stays at a constant low level. It is inferred that beyond 180 days, in binary systems the rate of pozzolanic reaction of fly ash is becoming very slow.

3.5.3 Degree of hydration of Portland cement-fly ash binary systems

In binary systems, *i.e.* pastes, the degree of hydration of cement and the degree of the pozzolanic reaction of fly ash at ages up to 3 years are investigated, respectively.

Degree of hydration of cement

The degree of hydration of cement in Portland cement paste and blended cement paste is shown in Figure 3.21. The experimental results for Portland cement paste are in accordance with those reported by Ye *[Ye 2003]*. The error bars indicate the standard deviations of the experimental results, ranging from 1.2% to 10.5%.

As observed from Figure 3.21, the degree of hydration of cement in all pastes increases with increasing curing age. The degree of hydration of cement in blended cement paste is higher than that in pure Portland cement paste. In blended cement paste with a w/b ratio of 0.5 the degree of hydration of cement is higher than in pastes with a w/b ratio of 0.4 (see Figure 3.21 (b)).

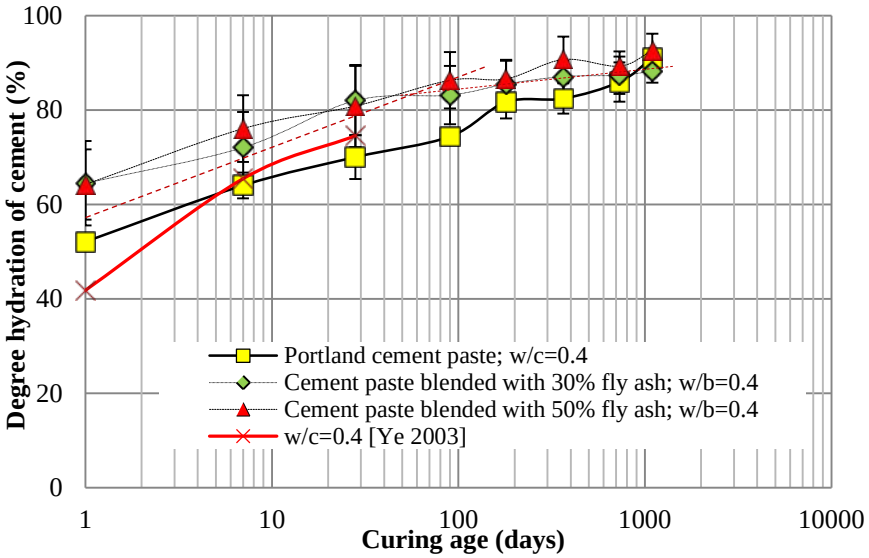

(a) for different fly ash dosages

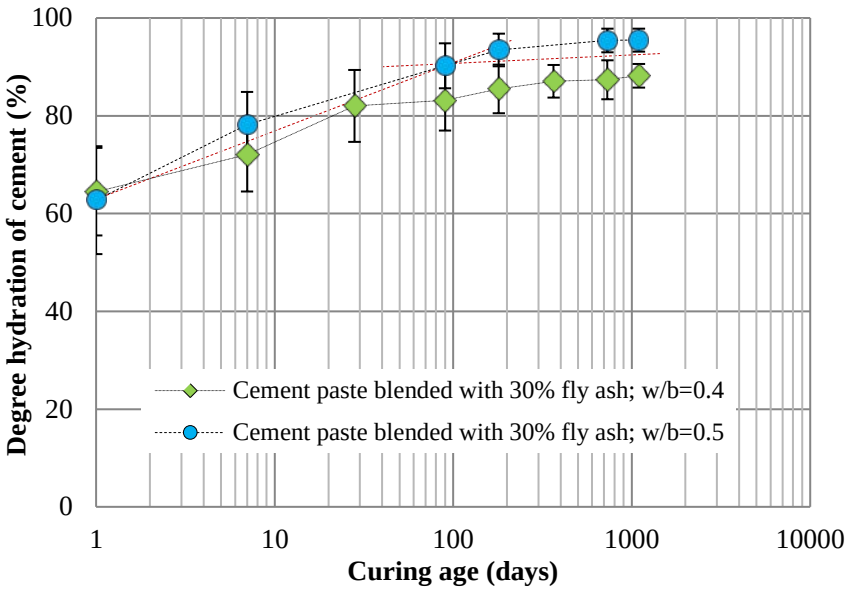

(b) for different w/b ratios

Figure 3.21: Degree of hydration of cement in Portland cement-fly ash binary systems (a): made with different fly ash dosages; (b): with different w/b ratios

Degree of pozzolanic reaction of fly ash

Figure 3.22 shows the degree of pozzolanic reaction of fly ash in cement paste blended with fly ash at ages up to 3 years. The experimental results are compared with those reported by Ben Haha *[Ben Haha 2010]*. Like in our tests, also Ben Haha used BSE image analysis to determine the degree of pozzolanic reaction of fly ash in binary systems. At ages from 28

days to 90 days, the values measured in our experiments are about 15% - 20% higher than those found by Ben Haha *[Ben Haha 2010]*. Several reasons have been suggested for the observed difference, such as the type of cement and of fly ash (fineness), the number and quality of BSE images and the method of image analysis.

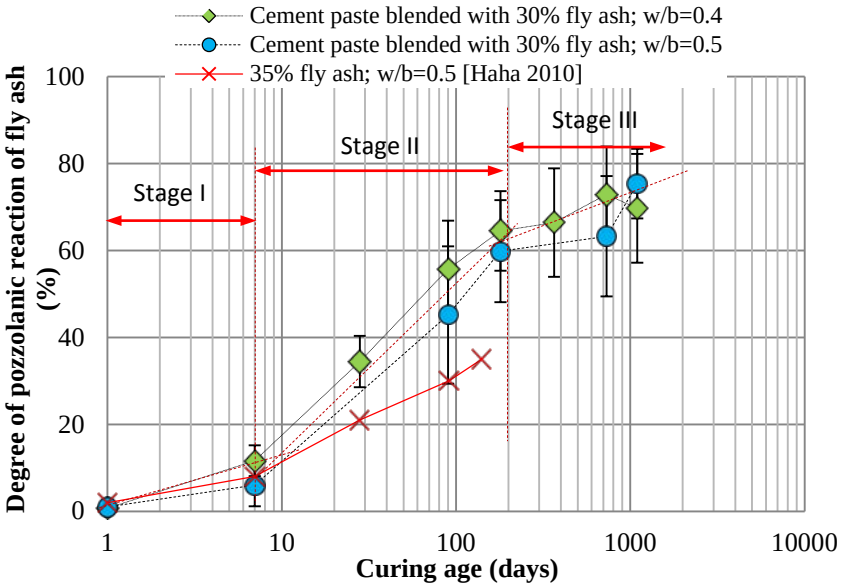

Figure 3.22: Degree of hydration of pozzolanic reaction of fly ash in Portland cement-fly ash binary systems made with different w/b ratios

In Figure 3.22 it can be seen that the degree of the reaction of fly ash in the blended cement paste made with a w/b ratio of 0.5 is lower than that in the blended cement paste made with a w/b ratio of 0.4. A high w/b ratio of 0.5 dilutes the concentration of calcium ions in the pore solution and slows down the pozzolanic reaction of fly ash in binary systems.

In the pozzolanic reaction of fly ash also three stages in the development of the degree of pozzolanic reaction of fly ash can be distinguished (see Figure 3.22).

1) *Stage I*. During the first stage, *i.e.* before 7 days, the pozzolanic reaction of fly ash in binary systems starts slowly. Only a small amount of fly ash has reacted, mainly resulting from the reaction of small fly ash particles *[Berry 1990; 1994; Lam 2000]*.
2) *Stage II*. At ages from 7 days to 180 days, the degree of pozzolanic reaction of fly ash increases significantly. This goes along with a reduction of CH content in blended cement paste (see Figure 3.20).
3) *Stage III*. Beyond 180 days the progress of the pozzolanic reaction of fly ash is slow.

From Figure 3.21 and Figure 3.22 it can be seen that in binary systems the addition of fly ash increases the degree of hydration of cement. During the second stage, *i.e.* from 7 days to 180 days, the rate of pozzolanic reaction of fly ash is faster than that of hydration of cement. The ongoing pozzolanic reaction of fly ash results in a more dense structure of binary systems. Figure 3.23 shows a schematic description of the evolution of hydration of cement and of pozzolanic reaction of fly ash in binary systems In chapter 4, the microstructure development in cement paste blended with fly ash will be investigated at ages up to 3 years.

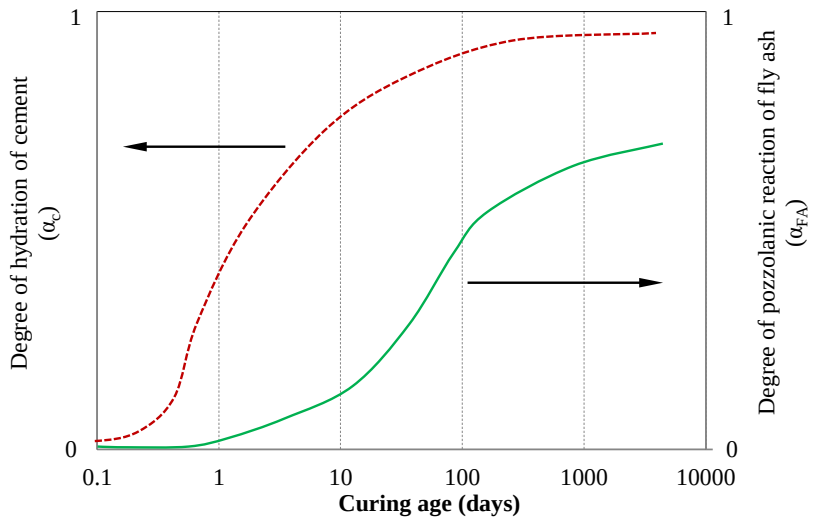

Figure 3.23: Degree of hydration of cement and degree of pozzolanic reaction of fly ash in blended cement paste

3.6 Concluding Remarks

In this chapter, the reaction of fly ash in binary systems is studied at ages up to 3 years. Based on the experimental results and discussions above, the following conclusions have been drawn:

1. The formation of monocarbonate in Portland cement paste and blended cement paste is due to the presence of limestone powder ($CaCO_3$) in the Portland cement. It has been reported by *[Klemm 1990]* that in moist conditions $CaCO_3$ can slowly react with calcium monosulfoaluminate hydrate or calcium aluminate hydrate to form ettringite and monocarbonate. The formation of ettringite in concrete at later ages is detrimental. It will influence the long-term performance of concrete. In chapter 7 the effect of the reaction of $CaCO_3$ on the resistance of concrete to chloride ingress is investigated.

2. The development of CH content in binary systems can be described by three stages. These three stages are:
   I. Early age, *i.e.* before 7 days. In this stage CH content increases significantly due to the hydration of cement. Blended cement paste has a higher CH content than Portland cement paste with the same w/b ratio.
   II. From 7 days to 180 days, the CH content in blended cement paste decreases significantly. In binary systems the rate of the pozzolanic reaction of fly ash (*consuming CH*) is faster than that of the hydration of cement (*producing CH*).
   III. At later ages, *i.e.* after 180 days, the CH content in binary systems hardly changes. This is indicated by a slow pozzolanic reaction of fly ash in binary systems.

3. At later ages, *i.e.* after 180 days, the degree of hydration of cement in binary systems hardly changes. In this phase the degree of the reaction of fly ash increases slowly. As will be shown in the next chapter the ongoing pozzolanic reaction of fly ash contributes to densification of structure in binary systems.

References

[1] Ben Haha M., De Weerdt K., Lothenbach B., 2010. Quantification of the degree of reaction of fly ash. Cement and Concrete Research, 2010; 40: 1620-1629.

[2] Berry E.E., Hemmings R.T., Cornelius B.J., 1990. Mechanism of hydration reactions in high volume fly ash pastes and mortars. Cement and Concrete Composites, 1990; 12: 253- 261.

[3] Berry E.E., Hemmings R.T., Zhang M.H., Cornelious B.J., Golden D.M., 1994. Hydration in high-volume fly ash binders. ACI Mater J 9, 1994; 1: 382-389.

[4] Bhatty J.I., Reid K.J., 1985. Use of thermal analysis in the hydration studies of a Type I Portland cement produced rom mineral tailings. Thermochimica Acta, 1985; (91): 95-105.

[5] Bushnell-Watson SM, Sharp JM, 1985. The detection of the carboaluminate phase in hydrated high alumina cements by differential thermal analysis. Thermochimica Acta, 1985; 93: 613-616.

[6] De Weerdt K., Ben Haha M., Le Saout G., Kjellsen K.O., Justnes H., Lothenbach B., 2011. Hydration mechanisms of ternary Portland cements containing limestone powder and fly ash. Cement and Concrete Research, 2011; 41: 279-291.

[7] European standards EN 197-1 Cement Composition. June 2000.

[8] Kakali G, Tsivilis S, Aggeli E, Bati M., 2000. Hydration products of C_3A, C_3S and Portland cement in the presence of $CaCO_3$. Cement and Concrete Research, 2000; 30(7): 1073-1077.

[9] Kariya Takeaki, Kurata Hiroshi, 2004. Generalized Least Squares. ISBN: 978-0-470-86697-9.

[10] Lam L., Wong Y.L., Poon C.S., 2000. Degree of hydration and gel/space ratio of high-volume fly ash/cement systems. Cement and Concrete Research, 2000; 30: 747-756.

[11] Lothenbach B, Le Saout G, Gallucci E, Scrivener K., 2008. Influence of limestone on the hydration of Portland cements. Cement and Concrete Research, 2008; 38(6): 848-860.

[12] Ma Yuwei, 2013. Microstructure and engineering properties of alkali activated fly ash - as an environment friendly alternative to Portland cement. PhD Thesis. Delft University of Technology.

[13] Marsh B.K., Day R.L., 1988. Pozzolanic and cementitious reactions of fly ash in blended cement pastes. Cement and concrete research, 1988; 18(2): 301-310.

[14] Midgley H.G. 1979. The determination of calcium hydroxide in set Portland cements. Cement and Concrete Research, 1979; 9(1): 77-82.

[15] Ramachandran VS, 1988. Thermal analysis of cement components hydrated in the presence of calcium carbonate. Thermochimica Acta, 1988; 127: 385-394.

[16] Rietveld H. M., 1969. A profile refinement method for nuclear and magnetic structures. Journal of Applied Crystallography, 1969; 2 (2): 65-71.

[17] Rodriguez-Carvajal Juan, 1993. Recent advances in magnetic structure determination by neutron powder diffraction. Physica B: Condensed Matter, 1993; 192 (1-2): 55-69.

[18] Scrivener K.L., 2004. Backscattered electron imaging of cementitious microstructures: understanding and quantification. Cement and Concrete Composites, 2004; 26: 935-945.

[19] Soroka, I., Stern, N., 1977. The effect of fillers on strength of cement mortars. Cement and Concrete Research, 1977; 7(4): 449-456.

[20] Taylor HFW., 1997. Cement chemistry. London: Thomas Telford.

[21] Tennis P. D., Thomas M. D. A., Weiss W. J., 2011. State-of-the-art report on use of limestone in cements at levels of up to 15%. Portland Cement Association, PCA R&D Serial No. SN3148.

[22] Vedalakshmi R., Sundara Raj A., Srinivasan S., Ganesh Babu K., 2003. Quantification of hydrated cement products of blended cements in low and medium strength concrete using TG and DTA technique. Thermochimica Acta, 2003; 407: 49-60.

[23] Ye Guang, 2003. The microstructure and permeability of cementitious materials. PhD Thesis. Delft University of Technology.

Chapter 4

Microstructure Development of Portland Cement Paste Blended with Fly Ash[3]

4.1 Introduction

The hydration of cement goes along with continuous evolution of the microstructure of cement paste and reduction of porosity. The transport properties of cement paste are mainly controlled by their microstructure development *[Garboczi 1990]*. In cement paste blended with fly ash the pozzolanic reaction of fly ash consumes calcium hydroxide and changes the pore structure of paste *[Mindess 1981; Bijen 1996]*. In this study the effect of fly ash on the transport properties is observed no sooner than after about 3 months (see chapter 5). Although the effect of fly ash on the pore structure of blended cement paste has been studied by many researchers, *however*, most research results are limited to a short curing period, *e.g.* 3 months *[Marsh 1985; Cook 1986; Jiang 1999; Zeng 2012]*. This is insufficient to explain the transport properties of Portland cement-fly ash binary systems at later ages.

The objective of this chapter is to study the microstructure development of blended cement paste at ages up to 3 years. The solid phases are observed by environmental scanning electron microscope (ESEM). The pore structure of blended cement paste is determined by mercury intrusion porosimetry (MIP).

4.2 Methods

The ESEM technique, used in this chapter for the analysis of the solid phases of blended cement paste with time, has been described in section 3.4.2. The detailed MIP test procedures and determination of the pore parameters are shown in the following sections.

4.2.1 Mercury intrusion porosimetry

Mercury intrusion porosimetry (MIP) is a widely used technique to characterize the pore structure of cement-based materials *[Cook 1999; Ye 2003]*. A wide range of pore sizes, *varying from 0.001 μm to 1000 μm*, can be measured with the MIP technique *[Feldman 1983]*. Although MIP is a fast method to determine the pore structure, the result from MIP is

[3] This chapter is partially based on:

1) Zhuqing Yu, Guang Ye. The pore structure of cement paste blended with fly ash. Construction and Building Materials 45 (2013) 30-35.

influenced by some specific pore structure characteristics, such as pore shape, the ink-bottle effect, damage of the fine structure during pressuring, surface tension and contact angle, sample preparation and drying treatment *[Diamond 1971; Cook 1993; Ye 2003]*.

MIP is based on the principle that the mercury does not wet most substances and will not spontaneously penetrate into pores by capillary action, but by applying an external pressure. Assuming the pores are cylindrical, the relation between the pore size and the applied pressure can be expressed by the Washburn equation *[Washburn 1921]*:

$$p = -\frac{4\gamma \times \cos\theta}{d} \tag{4.1}$$

where:

p = applied pressure.
d = pore diameter.
γ = surface tension of the mercury, *mN/m*.
θ = contact angle between the mercury and the pore wall surface of the material.

4.2.2 Mercury porosimetry procedure

In this study, MIP measurements were performed with a Micrometrics PoroSizer® 9320 with a maximum intrusion pressure of 207 MPa (see Figure 4.1). The contact angle and surface tension of mercury were 139° and 480 mN/m, respectively *[Ye 2003]*. For these pressures the measured pore size is in the range from 0.007 µm to 400 µm.

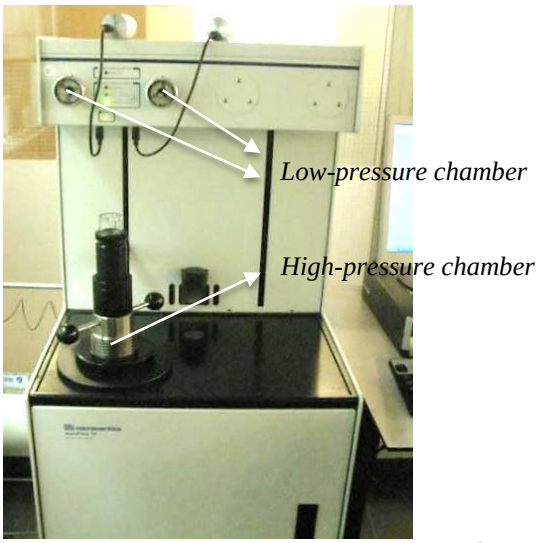

Figure 4.1: Micrometrics PoroSizer® 9320

Figure 4.2: Mercury penetrometer

As shown in Figure 4.1, the apparatus has two low-pressure chambers and one high-pressure chamber. Firstly, the mercury penetrometer (see Figure 4.2), together with paste sample, is put into a low-pressure chamber. The chamber is evacuated and the sample is surrounded by mercury. With increasing pressure, mercury is pressed into the big pores of the samples. This stage would cease when the applied pressure on the mercury has gradually increased to 0.170 MPa. Thereafter, the mercury penetrometer with the sample is put into the high-pressure chamber. The applied pressure in that chamber reaches 207 MPa. If the network of pores is continuous, mercury can penetrate through the smallest pore necks of the system and penetrate the bulk sample volume. If the pore network is not continuous, mercury may penetrate into the sample volume by breaking through pore walls.

After reaching the highest pressure (207 MPa), *i.e. the end of intrusion procedure*, the extrusion procedure starts. With gradual decrease of the applied pressure mercury is desorbed until a equilibrium pressure is reached.

4.2.3 Determination of pore parameters

As described in chapter 2 the details of the pore structure of cement paste are decisive for the permeability of concrete. The porosity, pore size, connectivity of the pores, pore size distribution and critical pore width are main pore structure parameters characterizing the pore structure of hydrated cement paste. Based on the results of MIP tests the determination of these pore structure parameters is briefly discussed in this section.

Capillary pore geometry

From the geometry point of view, the capillary pores in cement paste can be classified into continuous pores, continuous pores with ink-bottle pores (open pores with smaller entrances), dead-end pores with ink-bottle pores and isolated pores (Figure 4.3). The isolated pores are not connected with each other, and do not contribute to the permeability of cement paste.

Through the MIP technique the isolated pores cannot easily be detected. The volume of the isolated pores is, *therefore*, not included in the calculation of the total porosity of pastes.

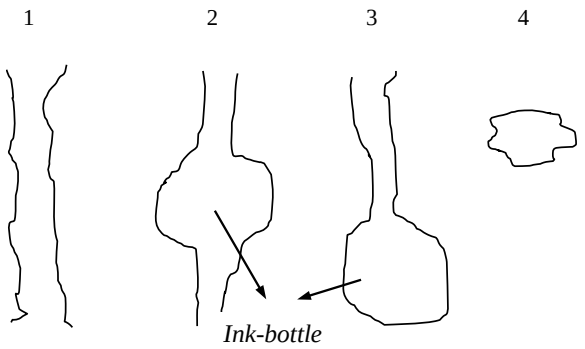

Figure 4.3: Classification of capillary pores geometry; a) Continuous pore; b) Continuous pore with ink-bottle pore; c) Dead-end pore with ink-bottle pore; d) Isolated pore [Ye 2003]

Total porosity

Figure 4.4 schematically shows the process of mercury intrusion and extrusion in a porous system. During the intrusion period all continuous pores, *including the ink-bottle pores*, are filled with mercury. Accordingly, the total intrusion volume, *i.e. total porosity*, is obtained.

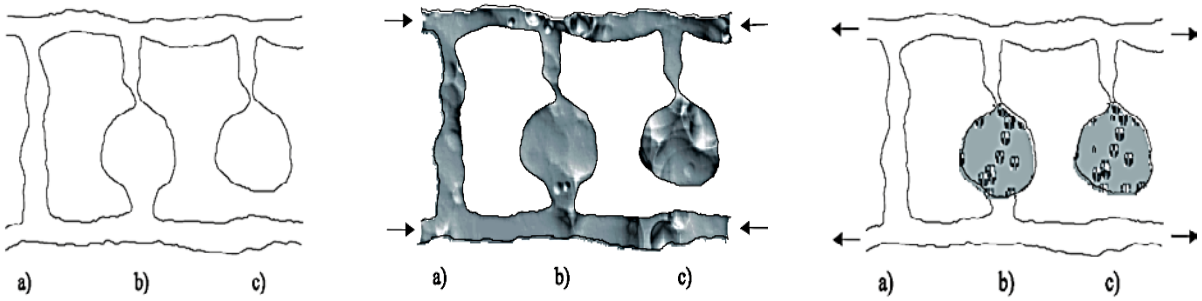

(a) Initial status (b) End of intrusion (c) End of extrusion

Figure 4.4: Schematic illustration of mercury intrusion and extrusion (Arrows indicate the flow direction of mercury) [Ye 2003]

Figure 4.5 shows a typical cumulative pore size distribution (PSD) curve obtained in MIP tests. The total porosity of this particular sample, *covering pores from 0.007 µm to 400 µm*, is 27.6%.

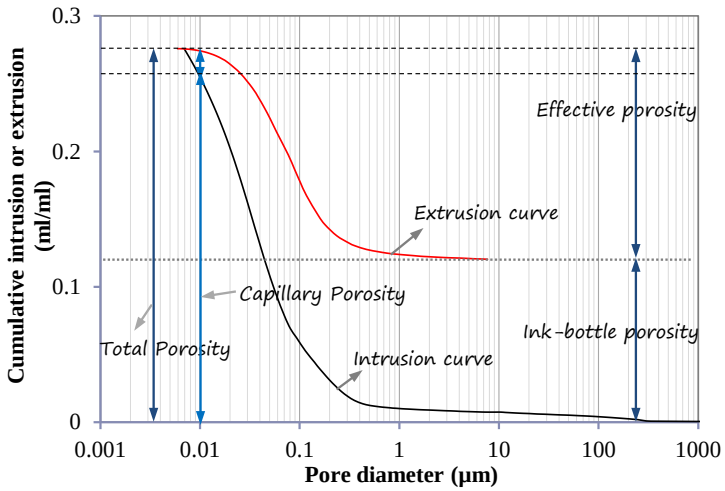

Figure 4.5: A typical cumulative pore size distribution curve (Cement paste blended with 30% fly ash; w/b=0.4 at 7 days)

Ink-bottle porosity

When the pressure is released the mercury is sucked out of the pores except from the ink-bottle pores (Figure 4.4 (c)). That is because the ink-bottle pores cannot be emptied through the smaller pore entrances during retraction of mercury, leaving entrapped mercury in the wide inner pores *[Aligizaki 2006]*. The volume of mercury removed during extrusion is defined as effective porosity. It is the fraction of the bulk volume of cement paste consisting of *only open and effective pores [Aligizaki 2006]*. The volume of mercury left during extrusion is ink-bottle porosity. As shown in Figure 4.5 the ink-bottle porosity is the pore volume that is left after subtracting the effective pores volume from the total cumulative pore volume:

$$Total\ porosity = Effective\ porosity + Inkbottle\ porosity \tag{4.2}$$

Capillary porosity

As mentioned in Table 2.3 the pores, *ranging from 0.01 μm to 10 μm*, are defined as capillary pores *[Mindess 1981]*. Based on the measured MIP-results the cumulative pore volume of the pores, *ranging from 10 μm to 400 μm*, is limited. In this study the capillary porosity is simply described as the cumulative pore volume of the pores larger than 0.01 μm. In Figure 4.5 the capillary porosity of this particular sample, *covering pores from 0.01 μm to 400 μm*, is 25.4%.

Effective capillary porosity

The term effective *capillary* porosity is used for the volume of the effective capillary pores. It is calculated as:

$$Capillary\ porosity = Effective\ capillary\ porosity + Inkbottle\ porosity \tag{4.3}$$

The permeability of cement paste is strongly related to the effective capillary porosity, *since* connected effective pores provide a continuous channel of communication with the ambient environment.

Connectivity of the pores

Generally, connectivity of the pores, *C*, is defined as the volume fraction of capillary pores that make up a connected path through the sample, divided by the total volume fraction of capillary pores *[Garboczi 1990]*. The connectivity of the pores determines the permeability of cement paste *[Aligizaki 2006]*. Figure 4.6 schematically shows a porous cement-based material containing connected pores and disconnected pores. The connectivity of the pores can be described with Equation 4.4:

$$Connectivity\ of\ pores(C)\% = \frac{Connected\ pores\ volume}{Capillary\ pores\ volume} \times 100 = \frac{②}{①+②+③} \times 100 \tag{4.4}$$

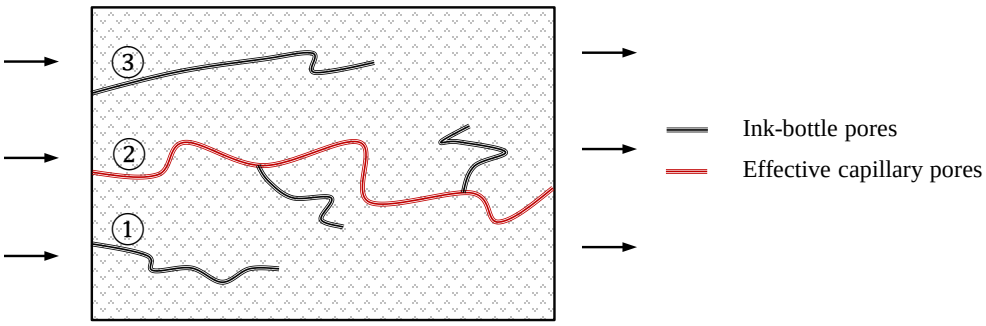

Figure 4.6: Schematic diagram of a porous cement-based material. ① and ③ present the volume of the disconnected pores; ② presents the volume of the connected pores

During the MIP tests the disconnected pores are often considered ink-bottle pores as shown in Figure 4.6. The (ink-bottle) pores, *which have a narrow entrance*, are ineffective to water flow *[Neville 1995]*. Taking into account of the effect of ink-bottle pores on water permeability, the connectivity of pores, in this study, is represented by the fraction of pores

with respect to the capillary pores volume constituted only by the effective capillary pores. It can be described as:

$$Connectivity\ of\ \ the\ pores\ (\%) = \frac{Effective\ \ capillary\ porosity}{Capillary\ porosity} \times 100 = (1 - \frac{Inkbottle\ porosity}{Capillary\ porosity}) \times 100 \qquad (4.5)$$

Figure 4.7 shows the flow of water in a porous material with and without ink-bottle pores, respectively. It is assumed that these two porous materials have the same effective capillary porosity. From Figure 4.6 it can be seen that the porous material with ink-bottle pores has lower connectivity of the pores compared to that porous material without ink-bottle pores, as calculated by Equation 4.4.

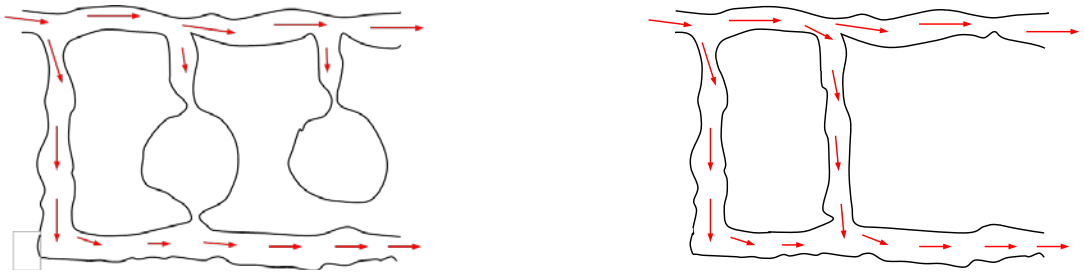

(a) (b)

Figure 4.7: Water flow relevant to permeability in a porous material with (a) and without ink-bottle pores (b) (Arrows indicate the flow direction of water)

Pore size distribution

The pore size distribution (PSD) curve is derived from the cumulative PSD curve and is essentially a plot of *dV/dlogd* (V: Pore fraction) against *d* (d: Pore diameter). The differential PSD curve derived from the cumulative PSD curve *presented in Figure 4.5* is shown in Figure 4.8 (b). This curve shows several peaks. In general, two peaks are found in cement paste *[Diamond 1971; Feldman 1984; Cook 1999; Ye 2003]*. The 1st peak corresponds to the capillary pores, 0.01 µm to 10 µm and the 2nd peak corresponds to the gel pores, 0.5 nm to 10 nm. The definition of capillary pores and gel pores was given in Table 2.3 (see chapter 2).

At early hydration, *e.g.* 1 day, the capillary pore space is fully connected, and only one peak is observed (Figure 4.8 (a)). As hydration proceeds, more hydration products fill up the pore space and the pore diameter of the capillary pores decreases *[Cook 1999]*. The 1st peak moves to smaller pore diameters and a 2nd peak appears as shown in Figure 4.8 (b). At later hydration ages, the capillary pores are blocked with hydration products and become disconnected. The 1st peak disappears and the 2nd peak becomes dominant as shown in Figure 4.8 (c). The pore size at the 2nd peak is generally smaller than 0.1 µm.

Critical pore width

The critical pore width (d_{cr}) of the pore structure is defined as the smallest diameter of continuous pores throughout the cement paste sample *[Cook 1999; Ouellet 2004]*. It is determined on the basis of the pore size distribution curve. Researchers have found that the

permeability of cement paste is also related to the critical pore width *[Mehta 1980; Winslow 1994; Ye 2003]*.

At early age, the critical pore width is represented by the 1st peak as shown in the differential PSD curve (Figure 4.8 (a)). If two peaks (1st peak and 2nd peak) are found in the PSD curve, the highest peak is defined as the critical pore width (Figure 4.8 (b)). When hydration proceeds the 1st peak disappears and the 2nd peak becomes the critical pore width (Figure 4.8 (c)). In Figure 4.8, the d_{cr} value of the samples at an age of 1 day, 7 days and 3 years is 0.430 µm, 0.0306 µm and 0.0266 µm, respectively.

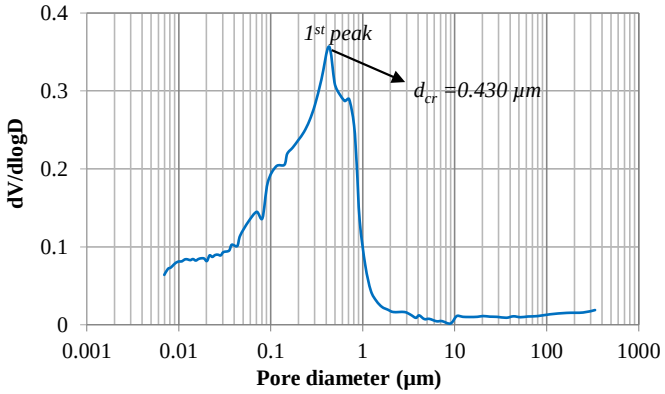

(a) PSD curve of blended cement paste after 1 day curing

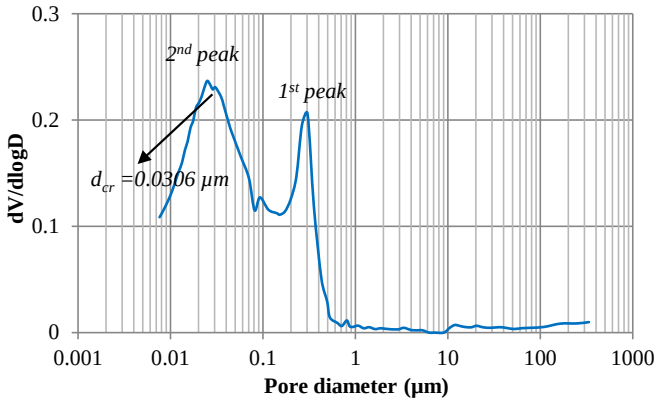

(b) PSD curve of blended cement paste after 7 day curing

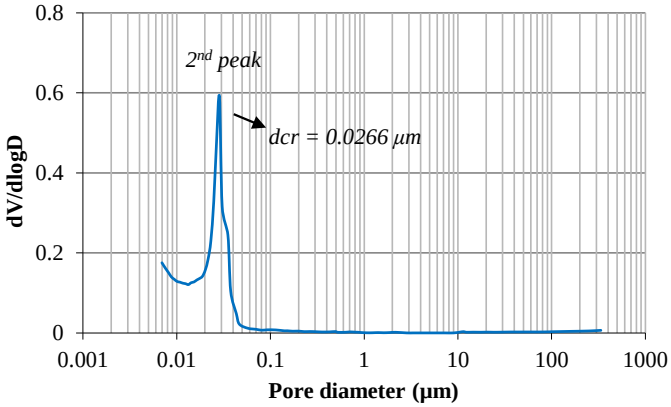

(c) PSD curve of blended cement paste after 3 years curing

Figure 4.8: Differential pore size distribution curves of blended cement paste (30% fly ash; w/b=0.4) after (a): 1 day; (b): 7 days; (c): 3 years of curing

4.3 Results and Discussion

4.3.1 Solid phases of cement paste blended with fly ash

Figure 4.9 shows BSE images of cement paste blended with fly ash at different ages. For comparison the images obtained from Portland cement paste are shown in Figure 4.10. It is easy to distinguish the phase of reaction products, pores and unreacted cement and fly ash (spherical shape) from their grey levels in the images. From the BSE images the following observations can be made:

1) As observed from Figure 4.9, in blended cement paste hollow fly ash particles with a thin shell can easily be identified, especially at early age. With progress of the pozzolanic reaction of fly ash the hollow fly ash particles react with calcium hydroxide to form reaction products, leaving voids in the paste. After around 180 days, some circular pores are found in blended cement paste, *but not* in Portland cement paste. They are surrounded by dense reaction products or unreacted fly ash. In this study, the circular voids are defined as *empty cavities*. The presence of these *empty cavities* contributes to an increase of the porosity of blended cement paste.

2) In blended cement paste it is also found that reacted hollow fly ash particles are able to provide extra space for the accommodation of reaction products, including both hydration products of cement and reaction products of fly ash. Figure 4.11 shows the BSE images of partially reacted hollow fly ash particles at later ages, *i.e.* after 90 days. The images show that the reaction products fill up the hollow fly ash particles.

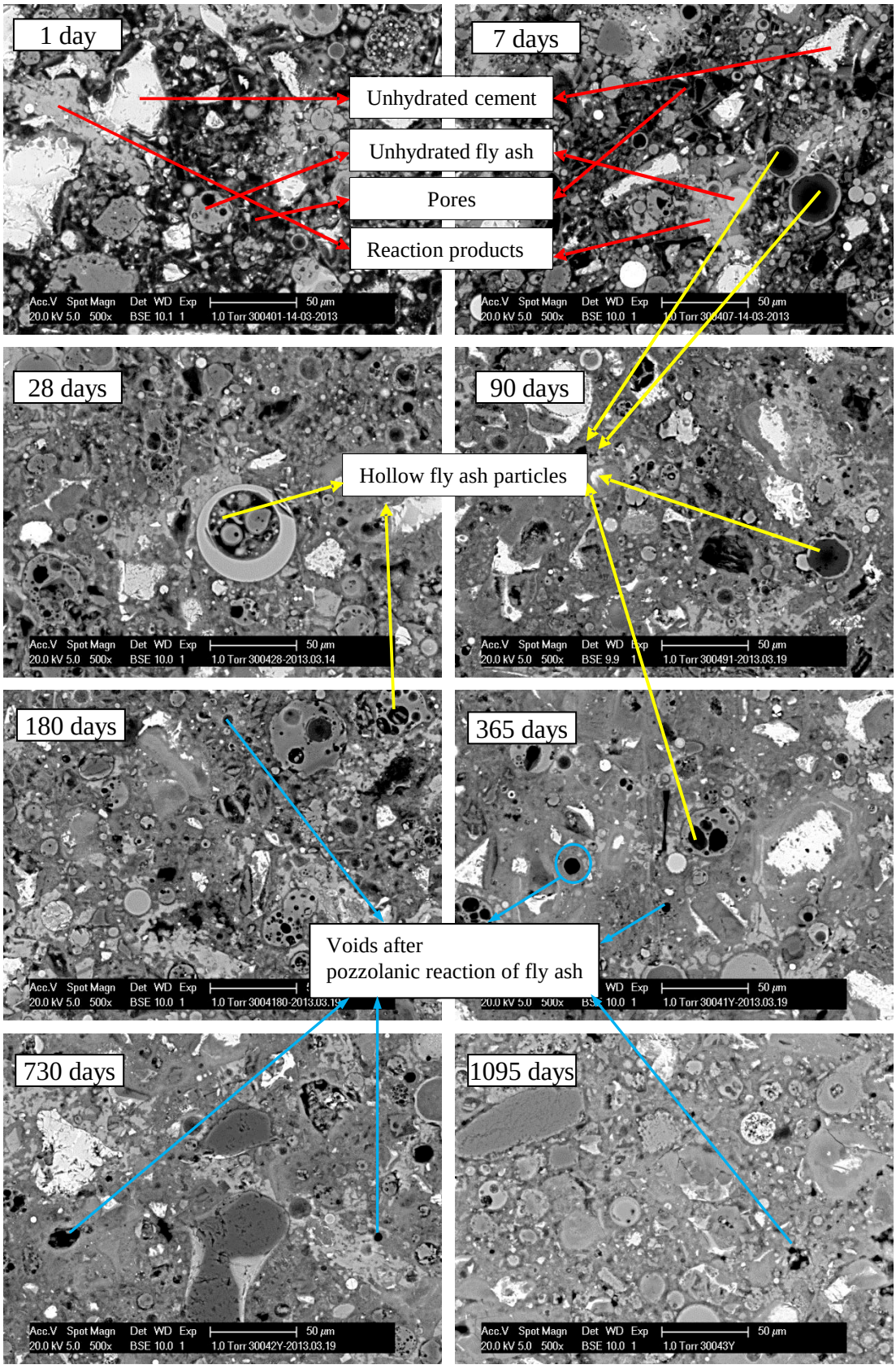

Figure 4.9: BSE images of cement paste blended with fly ash (30% fly ash; w/b=0.4) (Magnification: 500×)

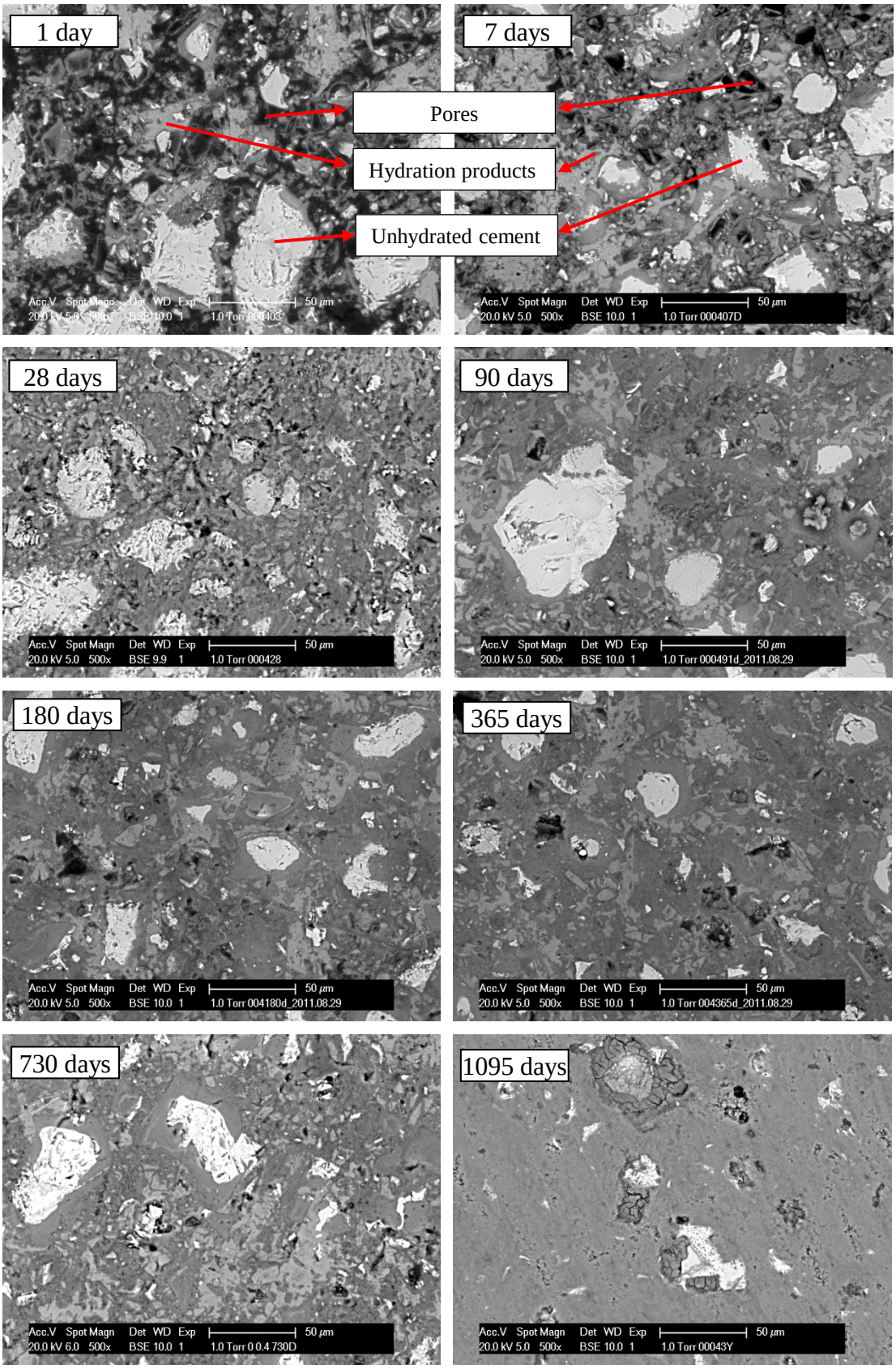

Figure 4.10: BSE images of Portland cement paste (w/c=0.4) (Magnification: 500×)

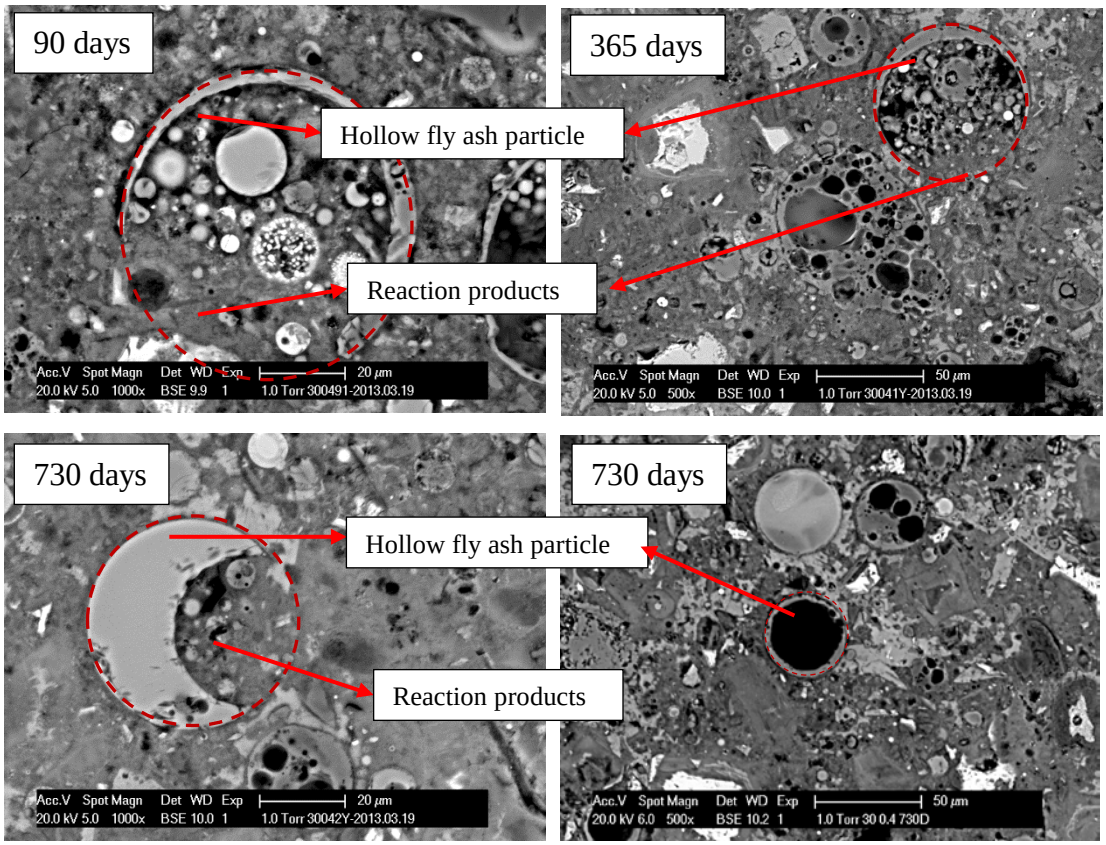

Figure 4.11: BSE images of reacted fly ash particles

4.3.2 Pore structure of cement paste blended with fly ash

The evolution of the cumulative and differential pore size distribution (PSD) curves from 1 day to 3 years for blended cement paste, *30% fly ash, w/b=0.4*, are shown in Figure 4.12. The PSD curves obtained from Portland cement paste and other blended cement pastes (30% fly ash, w/b=0.5; 50% fly ash, w/b=0.4) can be found in Appendix A.

From the cumulative PSD curves of Figure 4.12, it can be observed that the total porosity of blended cement paste decreases with time. From the differential PSD curves, only one peak, *viz.* 1st peak, is observed at early age, *e.g.* 1 day. After about 7 days, the 2nd peak appears at smaller pore sizes (0.025 μm). With progress of the hydration of cement and the pozzolanic reaction of fly ash, the 1st peak becomes less dominant and disappears after 28 days, while the 2nd peak becomes more dominant.

In the following sections, the effect of fly ash on some main pore structure parameters is discussed. These pore structure parameters are porosity (total porosity, capillary porosity and ink-bottle porosity), connectivity of the pores and critical pore width.

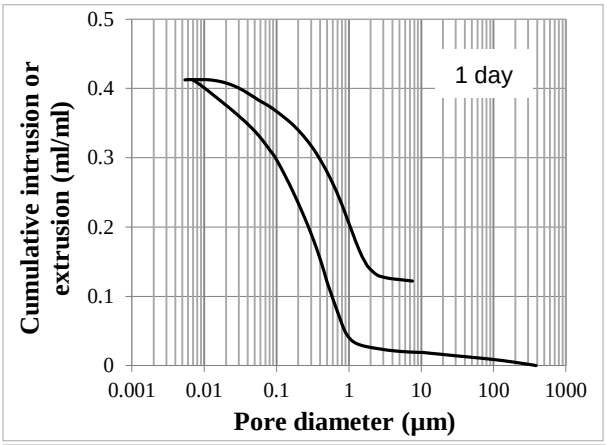
1 day
Cumulative intrusion or extrusion (ml/ml)
Pore diameter (μm)

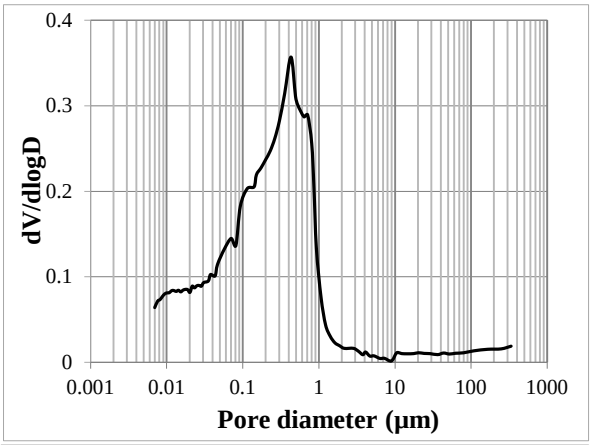
dV/dlogD
Pore diameter (μm)

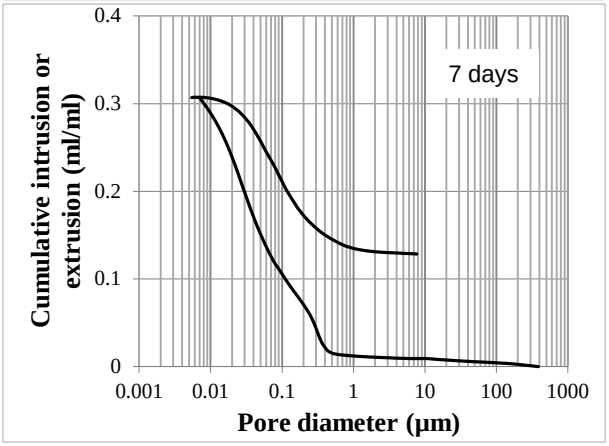
7 days
Cumulative intrusion or extrusion (ml/ml)
Pore diameter (μm)

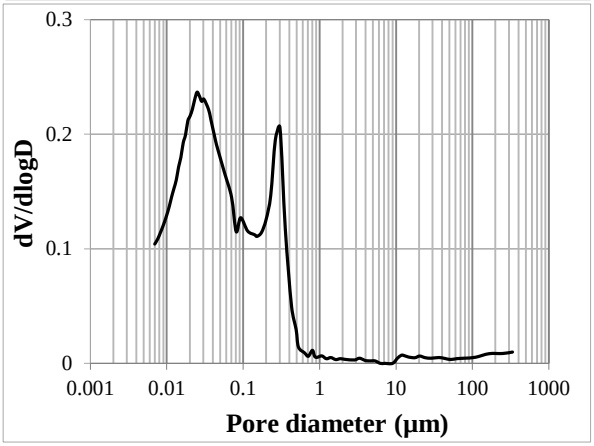
dV/dlogD
Pore diameter (μm)

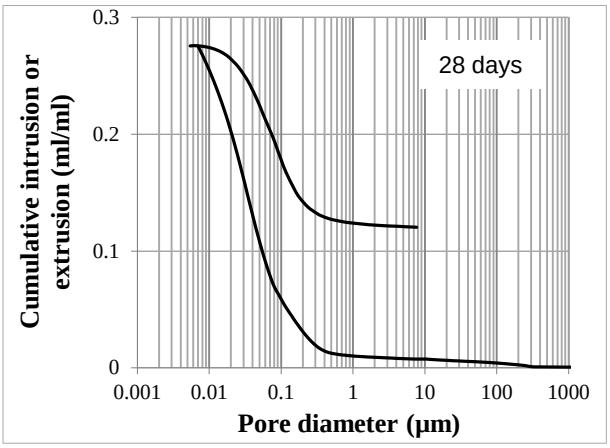
28 days
Cumulative intrusion or extrusion (ml/ml)
Pore diameter (μm)

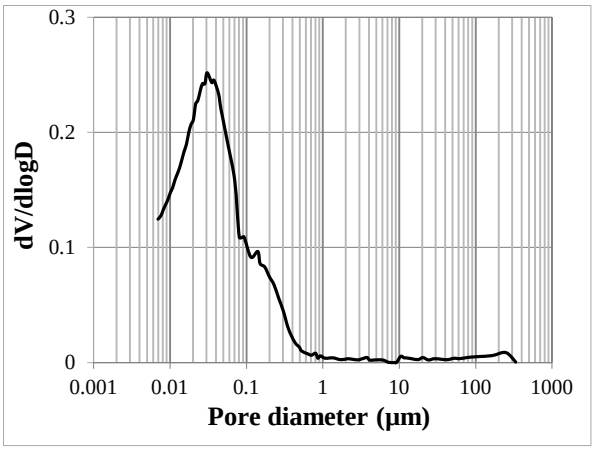
dV/dlogD
Pore diameter (μm)

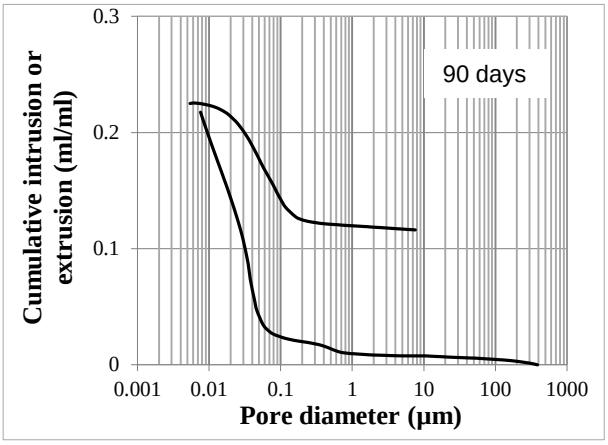
90 days
Cumulative intrusion or extrusion (ml/ml)
Pore diameter (μm)

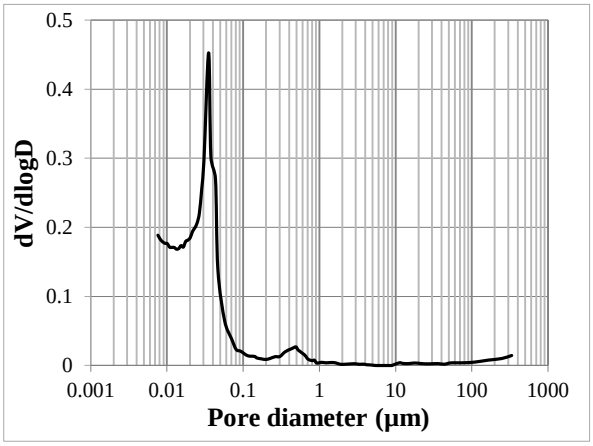
dV/dlogD
Pore diameter (μm)

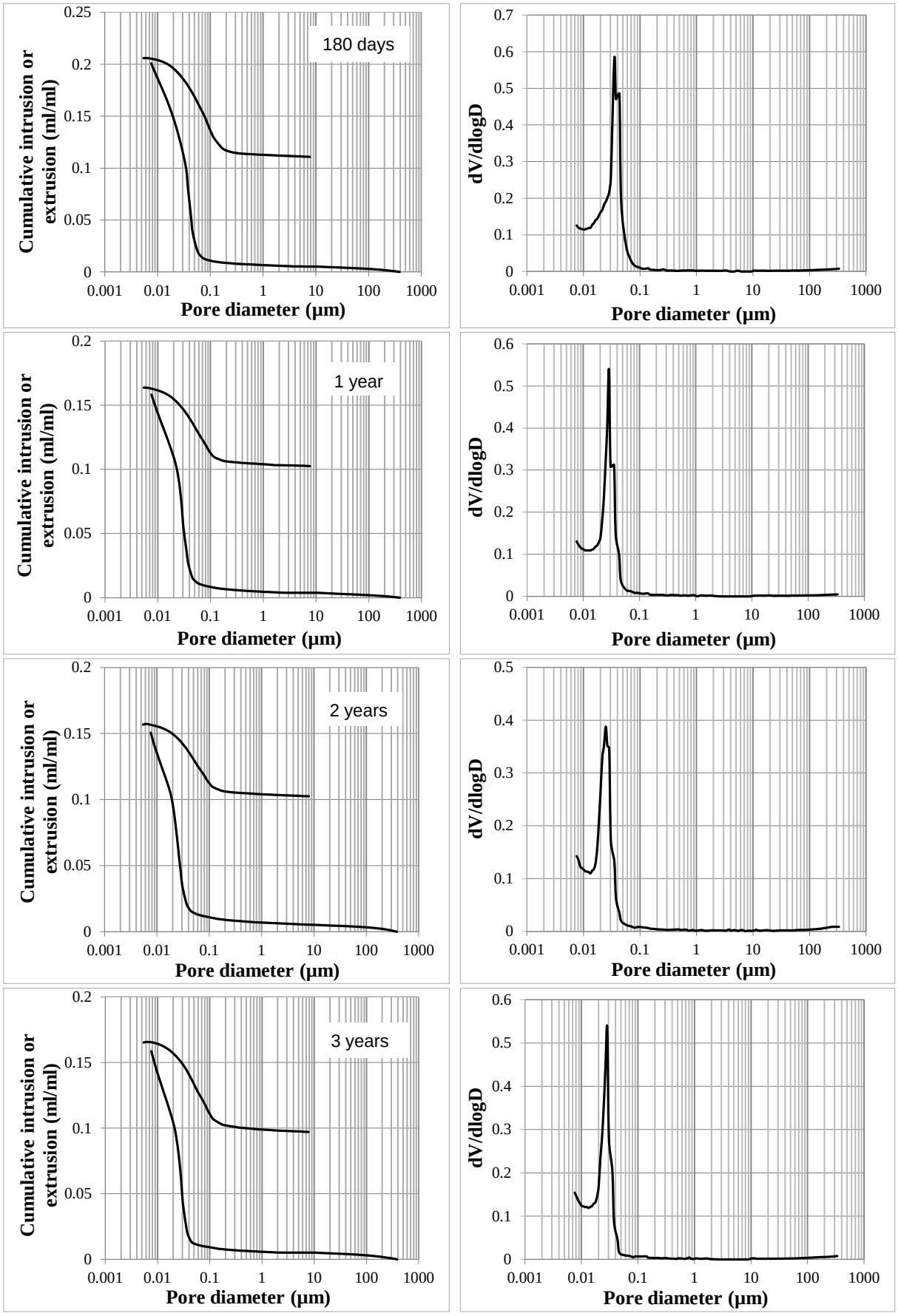

Figure 4.12: Cumulative and differential PSD curves of cement paste blended with fly ash (30% fly ash; w/b=0.4)

4.3.2.1 Total porosity

The total porosity of Portland cement paste and blended cement paste is shown in Figure 4.13 and 4.14. In the following the effect of curing age, fly ash content and w/b ratio on the total porosity of paste will be discussed in more detail.

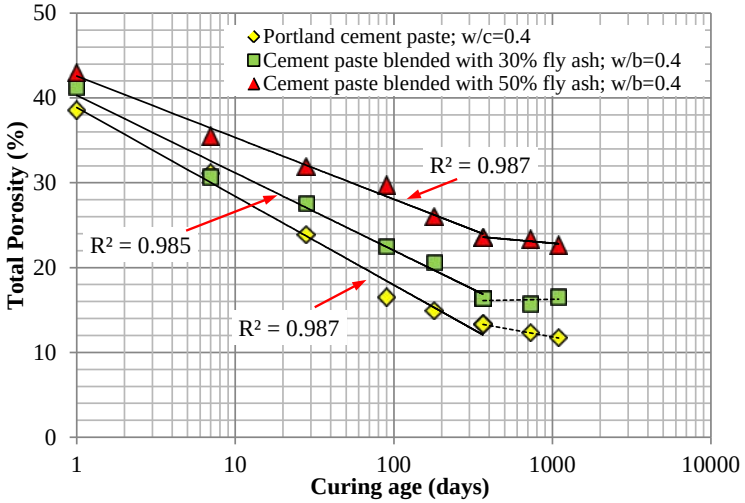

Figure 4.13: Total porosity of cement pastes made with different fly ash contents at different ages of the paste, w/b=0.4

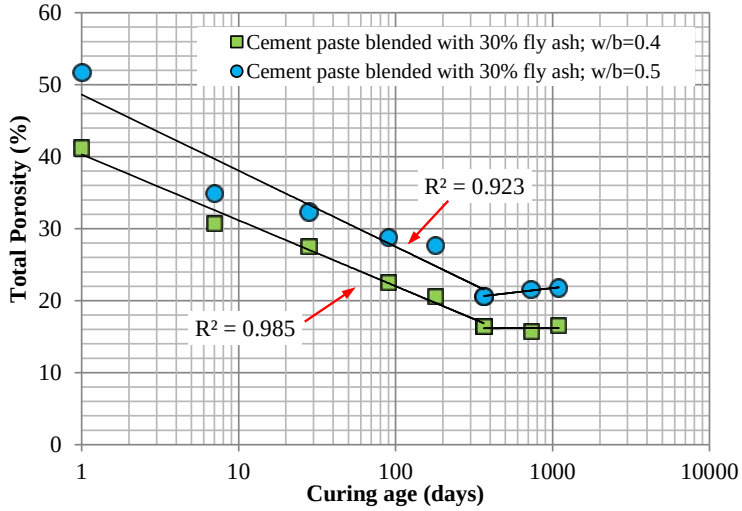

Figure 4.14: Total porosity of cement pastes made with 30% fly ash and w/b= 0.4 and 0.5 at different ages of the paste

Effect of curing period on the total porosity of cement paste

As hydration proceeds the total porosity of Portland cement paste, *w/c=0.4*, decreases continuously with time (Figure 4.13). If plotted on a semi-logarithmic scale a good linear relation between total porosity and time is found at ages from 1 day to 1 year. The R-squared value is 0.99. Similar to the total porosity of Portland cement paste the total porosity of blended cement paste (30% and 50% fly ash; w/b=0.4) decreases linearly with increasing time from 1 day to 1 year if plotted on a semi-logarithmic scale.

After about 1 year, *up to 3 years*, the total porosity of Portland cement paste decreases only slightly (see Figure 4.13). Figure 4.13 shows that in the same period the evolution of the total porosity with time of blended cement paste (30% and 50% fly ash; w/b=0.4) is similar to that for Portland cement paste.

Effect of fly ash content on the total porosity of cement paste (w/b=0.4)

As shown in Figure 4.13 blended cement paste has a higher total porosity than Portland cement paste. The total porosity of paste with a fly ash content of 50% is higher than the paste with a fly ash content of 30%.

As discussed in chapter 3 the degree of pozzolanic reaction of fly ash is much lower than the degree of hydration of cement. Less reaction products are generated in blended cement paste, resulting in a higher total porosity compared to pure Portland cement paste. The higher the fly ash content, the lower rate of the pozzolanic reaction of fly ash in blended cement paste (see Table 2.2). Hence, blended cement paste with 50% fly ash has a higher total porosity than paste with 30% fly ash.

Effect of w/b ratio on the total porosity of blended cement paste (30% fly ash)

In Figure 4.14 the total porosity of blended cement paste with w/b ratio of 0.5 is higher than that of the mixture with w/b ratio of 0.4. Like for w/b=0.4, also for w/b=0.5 a linear relation between total porosity and time is found at ages up to 1 year if plotted on a semi-logarithmic scale. At ages from 1 year to 3 years the total porosity of blended cement paste (30% fly ash; w/b=0.5) has a slight decrease as well as that of the mixture with w/b of 0.4.

During the hydration of cement and the pozzolanic reaction of fly ash the remaining water occupies the pore space, resulting in an increase of the total porosity.

4.3.2.2 Capillary porosity

The pores in cement paste can be classified into capillary pores and gel pores (see Table 2.3). The pores with diameters larger than 0.01 μm (10 nm) are defined as capillary pores, and the pores with diameters less than 10 nm are gel pores. Due to the small size of the gel pores, which are only an order of magnitude larger than the size of the water molecules (~ 3 Å), and due to the strong absorption of water molecules at the reaction products, the movement of water in gel pores does not contribute much to the permeability of cement paste *[Hearn 1994; Aligizaki 2006]*. In this section only the capillary porosity of blended cement paste and Portland cement paste will be discussed.

Figure 4.15 and 4.16 show the capillary porosity of the paste mixture. It can be seen that the effect of curing period, fly ash content and w/b ratio on the capillary porosity of paste is similar as their effect on the total porosity.

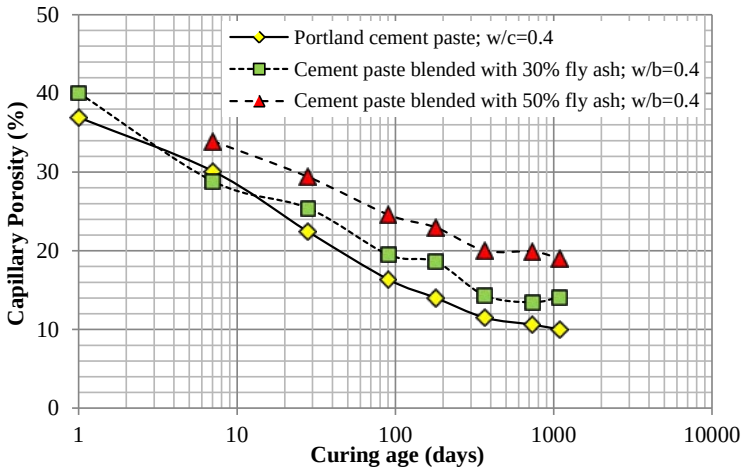

Figure 4.15: Capillary porosity of cement pastes made with different fly ash contents at different ages of the paste, w/b=0.4

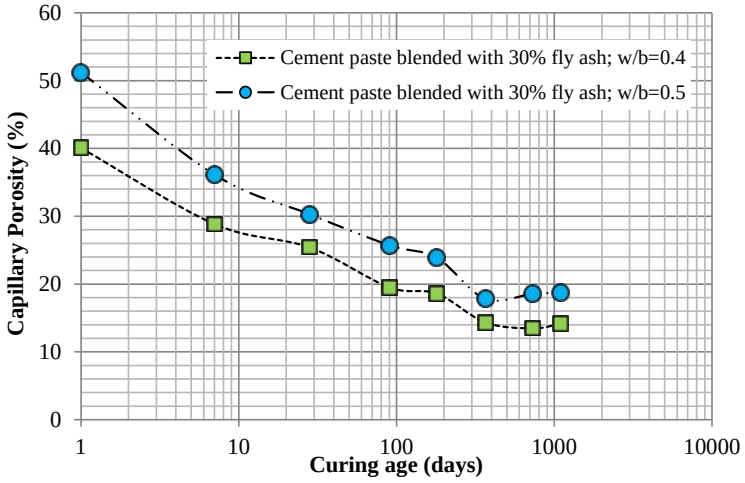

Figure 4.16: Capillary porosity of cement pastes made with 30% fly ash and w/b= 0.4 and 0.5 at different ages of the paste

Characterization of capillary pore size

In order to study the effect of pore size of blended cement paste on the permeability, *in this research*, the capillary pores are classified into small capillary pores (10 - 100 nm) and large capillary pores (>100 nm).

- *Volume of small capillary pores, 10-100 nm*

Based on the cumulative PSD curves of paste (see Figure 4.12 and Appendix 1-3), the volume of small capillary pores, *10-100 nm*, is determined as shown in Figure 4.17 and 4.18. From Figure 4.17 it can be seen that the volume of small capillary pores of Portland cement paste (w/c=0.4) increases with time at early ages up to 28 days, and then decreases from 28 days to 3 years. For blended cement paste, the volume of small capillary pores increases at early ages as well. The subsequent decrease in the volume of small capillary pores is visible from *28 days* for the paste made with 30% fly ash and w/b=0.4 and from *90 days* for the paste made with 50% fly ash, w/b=0.4.

As shown in Figure 4.17 the mixtures with fly ash have a larger volume of small capillary pores, particularly after 28 days. The higher the fly ash content, the larger volume of small capillary pores in blended cement paste. As shown in Figure 4.18 the effect of w/b ratio on the volume of small capillary pores of blended cement paste becomes significant at ages beyond 90 days. With the same fly ash content of 30% the mixture with w/b ratio of 0.5 has a larger volume of small capillary pores than mixture with w/b ratio of 0.4.

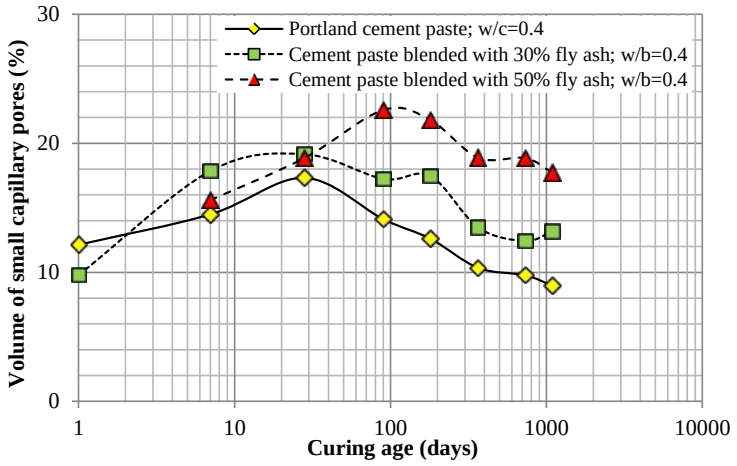

Figure 4.17: Volume of small capillary pores (10-100 nm) of cement pastes made with different fly ash contents at different ages of the paste, w/b=0.4

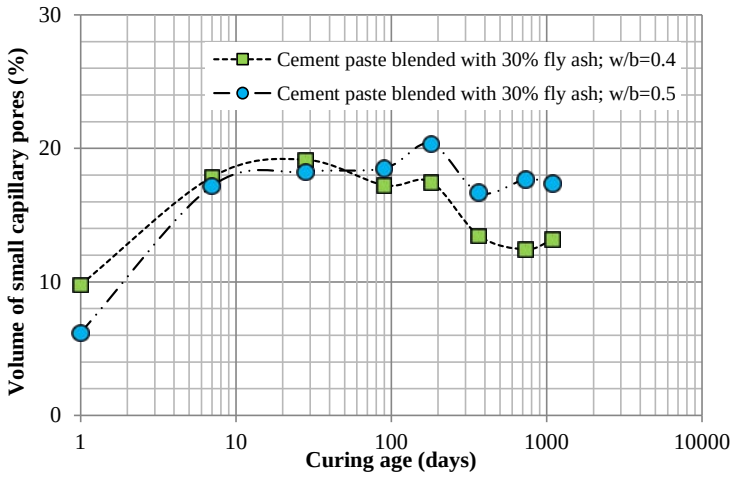

Figure 4.18: Volume of small capillary pores (10-100 nm) of cement pastes made with 30% fly ash and w/b= 0.4 and 0.5 at different ages of the paste

- *Volume of large capillary pores, >100 nm*

Figure 4.19 and 4.20 show the volume of large capillary pores, *>100 nm*, of the paste. As shown in Figure 4.19 the volume of large capillary pores of both pure cement paste and blended cement paste decreases sharply with time to about 2% at 90 days. After that it reduces slightly further to a constant value of around 1%.

At ages up to 90 days, in general, the mixtures with fly ash have a higher volume of large capillary pores. With the same w/b ratio of 0.4 the volume of large capillary pores of the blended cement paste with 50% fly ash is higher than that of paste with 30% fly ash (Figure

4.19). Likewise, the blended cement paste with high w/b ratio of 0.5 has a larger volume of large capillary pores than the mixture with w/b ratio of 0.4 (Figure 4.20).

After an age of 90 days the effect of fly ash content and w/b ratio on the volume of large capillary pores is hardly noticeable.

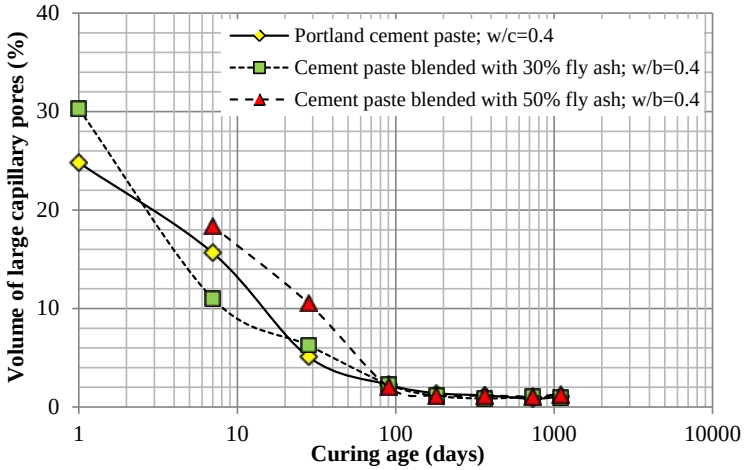

Figure 4.19: Volume of large capillary pores (>100 nm) of cement pastes made with different fly ash contents at different ages of the paste, w/b=0.4

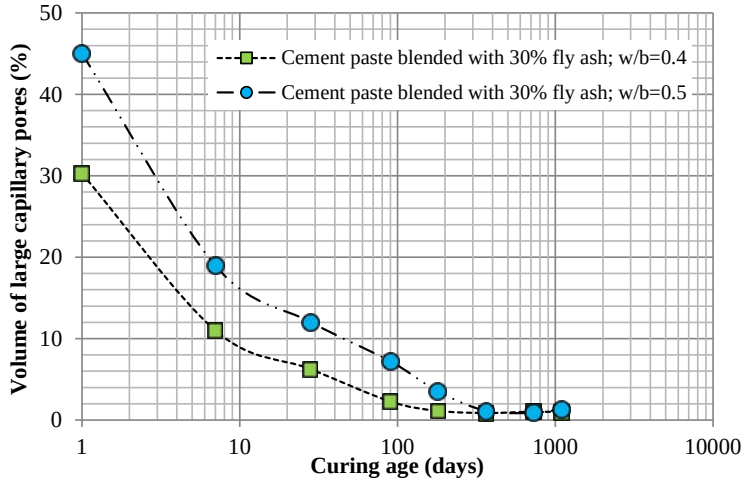

Figure 4.20: Volume of large capillary pores (>100 nm) of cement pastes made with 30% fly ash and w/b= 0.4 and 0.5 at different ages of the paste

Based on the data shown in Figures 4.17 - 4.20 it can be concluded that:

1) At early ages, *from 1 day to 28 days*, the volume of large capillary pores decreases considerably. Hydration products precipitate in large pores, *meanwhile* resulting in an increase of the volume of small capillary pores.
2) From 90 days to 3 years, the volume of large capillary pores of all mixtures hardly changes (Figure 4.19). In the same period the volume of small capillary pores of blended cement paste is much larger than that of Portland cement paste (see Figure 4.17). It means that at later ages fly ash results in the formation of a large amount of small capillary pores in the range between 10 and 100 nm.

4.3.2.3 Ink-bottle porosity

With increasing age of the paste, the pore space of cement paste is gradually filled with hydration products. This results in the reduction of the volume of capillary pores (see Figure 4.15 and 4.16). At the same time a reduction of the ink-bottle porosity is observed for Portland cement paste. As shown in Figure 4.21 from 1 day to 3 years the ink-bottle porosity of Portland cement paste decreases from 12.75% to 5.8%. There is, *however*, a difference between Portland cement paste and blended cement paste. As shown in Figure 4.21 the ink-bottle porosity of blended cement paste does not exhibit a significant decrease with time. For the paste made with 30% fly ash and w/b=0.4 the ink-bottle porosity decreases by only 2.5%, from 12.2% to 9.71%.

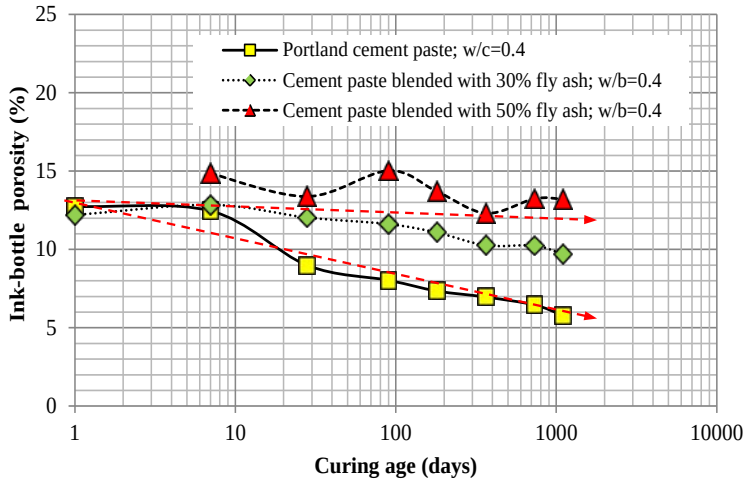

Figure 4.21: Ink-bottle porosity of cement pastes made with different fly ash contents at different ages of the paste, w/b=0.4

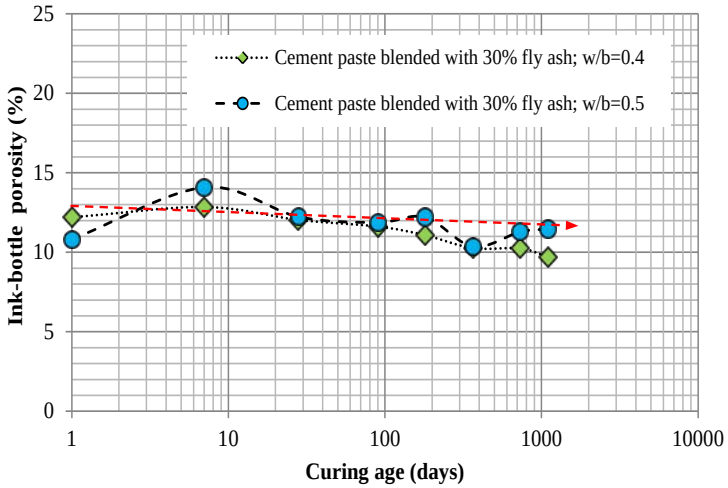

Figure 4.22: Ink-bottle porosity of cement pastes made with 30% fly ash and w/b= 0.4 and 0.5 at different ages of the paste

Effect of fly ash content on the ink-bottle porosity of cement paste (w/b=0.4)

Figure 4.21 shows that, in general, the ink-bottle porosity of the mixtures with fly ash is higher than that of Portland cement paste. This is more pronounced at ages after 28 days. The paste with a high fly ash content of 50% has a higher ink-bottle porosity than the paste with 30% fly ash.

Effect of w/b ratio on the ink-bottle porosity of blended cement paste (30% fly ash)

Figure 4.22 shows that there is no change in the ink-bottle porosity of the pastes between the blended cement paste (30% fly ash) made with two w/b ratios of 0.4 and 0.5.

For the evolution of the ink-bottle porosity in blended cement paste the following explanation is proposed:

As previously discussed in section 4.3.1 (solid phases), at later ages some *empty cavities* are identified in blended cement paste. They result from the pozzolanic reaction of hollow fly ash particles. These *empty cavities* are mostly surrounded by a shell of reaction products or unreacted fly ash (see Figure 4.9). In blended cement paste these *empty cavities* can act as ink-bottle pores as shown in Figure 4.23.

The schematic diagram of the pozzolanic reaction of one hollow fly ash particle in blended cement paste is illustrated in Figure 4.24. Before the reaction the void in the hollow fly ash particle is considered an isolated pore. Even with pressure mercury cannot enter into that pore. After a certain time of pozzolanic reaction the thin shell of the hollow fly ash particle is completely consumed and replaced by reaction products (produced by cement and fly ash). It is believed that the reaction products are porous, and that the size of the pores in the shell of reaction products is usually smaller than the actual cavity. During the MIP test mercury can penetrate through the reaction products and the “isolated pore” is gradually filled with mercury. After the process of extrusion, the pore will remain filled with mercury. The isolated pore now performs like an ink-bottle pore. Accordingly, the mixture blended with 50% fly ash (w/b=0.4) has higher ink-bottle porosity than the mixture with 30% fly ash (w/b=0.4) (see Figure 4.21).

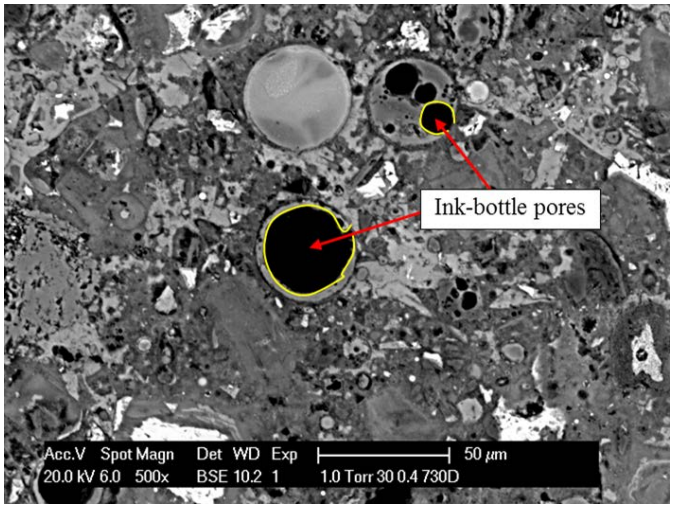

Figure 4.23: Ink-bottle pore formed due to the reaction of hollow fly ash particles

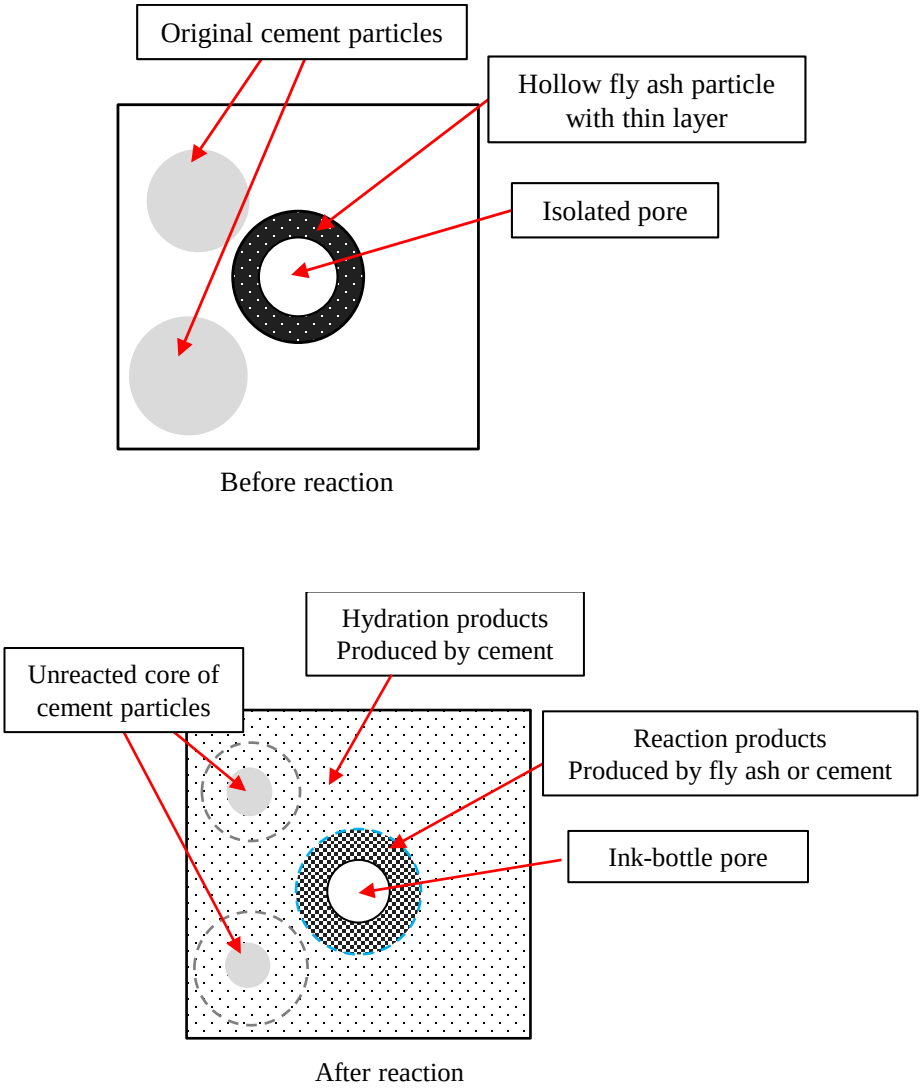

Figure 4.24: The schematic diagram of the pozzolanic reaction of one hollow fly ash particle

4.3.2.4 Effective capillary porosity

The effective capillary porosity is the volume of the effective capillary pores of paste. Figure 4.25 and 4.26 show the effective capillary porosity of the paste mixtures. From these two figures it can be seen that the effective capillary porosity of both Portland cement paste and blended cement paste decreases with time. At later ages, *i.e.* after about 1 year, the effective capillary porosity of all mixtures hardly changes.

From Figure 4.25 it can be observed that the effect of fly ash content (0%, 30% and 50%) on the effective capillary porosity of pastes with w/b=0.4 is not significant. The effective capillary porosity of mixture with 30% fly ash is similar to that of pure Portland cement paste at ages up to 3 years. The effective capillary porosity of the paste with 50% fly ash is only 2% higher than that of Portland cement paste.

As shown in Figure 4.26 the effective capillary porosity of blended cement paste with w/b ratio of 0.5 is higher than mixture with w/b ratio of 0.4

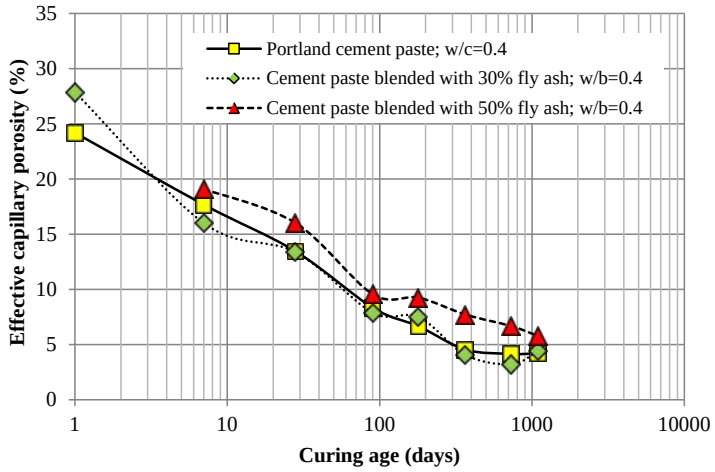

Figure 4.25: Effective capillary porosity of cement pastes made with different fly ash contents at different ages of the paste, w/b=0.4

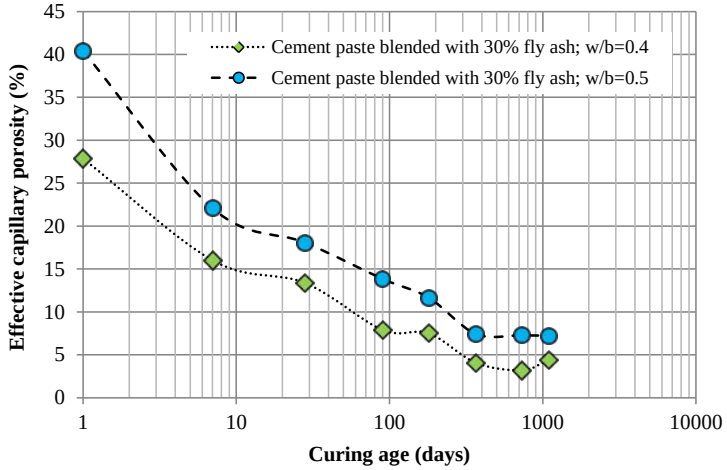

Figure 4.26: Effective capillary porosity of cement pastes made with 30% fly ash and w/b= 0.4 and 0.5 at different ages of the paste

4.3.2.5 Connectivity of the pores

Figure 4.27 and 4.28 show the evolution of the connectivity of the pores of Portland cement paste and blended cement paste as a function of time.

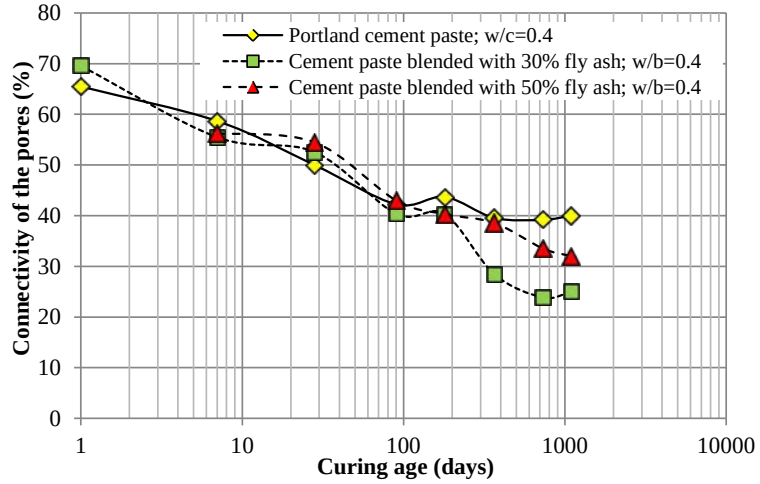

Figure 4.27: Connectivity of the pores of cement pastes made with different fly ash contents at different ages of the paste

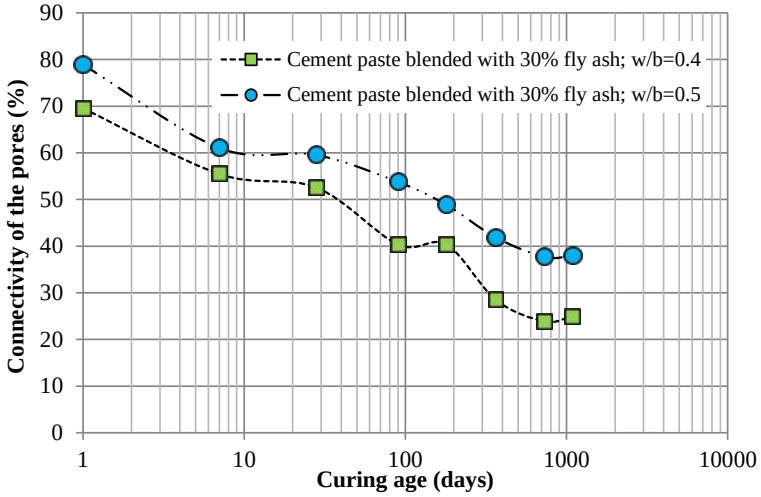

Figure 4.28: Connectivity of the pores of blended cement pastes made with different w/b ratios at different ages of the paste

Effect of curing period

For Portland cement paste Figure 4.27 shows that the connectivity of the pores, as determined with Equation 4.4, decreases with increasing age of the paste, from initially 65.5% at 1 day to 43% at 90 days. In the period from 90 days to 3 years connectivity of the pores of Portland cement paste hardly changes. For blended cement paste, *however*, connectivity of the pores continues to decrease with time, also after 90 days (Figure 4.27).

Effect of fly ash content

From Figure 4.27 it can be seen that from 1 day to 90 days

The connectivity of the pores of blended cement paste made with fly ash content of 30% and 50% is similar to that of Portland cement paste. At later ages, *i.e.* after 90 days, the connectivity of the pores of mixtures with fly ash is smaller than that of pure Portland cement paste. In this period the connectivity of the pores of the blended cement paste with 30% fly ash is lower than that of the blended cement paste with 50% fly ash.

As described in Figure 4.7 (section 4.2.3) the connectivity of the pores of paste is influenced by the ink-bottle pores. With similar effective capillary porosity in Portland cement paste and blended cement paste (see Figure 4.25), the mixtures with fly ash have more ink-bottle pores (see Figure 4.21). Blended cement paste, *therefore*, has a lower connectivity of the pores, particularly at ages beyond 180 days.

Effect of w/b ratio

As shown in Figure 4.28 blended cement paste with a w/b ratio of 0.5 has a larger connectivity of pores than paste with a w/b ratio of 0.4.

As discussed in section 4.2.3 the connectivity of the pores of paste is of utmost importance for the permeability of paste. In chapter 5 the relation between the connectivity of the pores and water permeability of (blended) cement paste will be presented.

4.3.2.6 Critical pore width

The critical pore width of the pore structure of the cement paste is obtained from the differential pore size distribution (PSD) curves (*see Figure 4.12 and Appendix 1-3*). The critical pore widths at an age of 1 day and 7 days are much larger than those at later ages. Figure 4.29 presents the critical pore width of four mixtures in two figures.

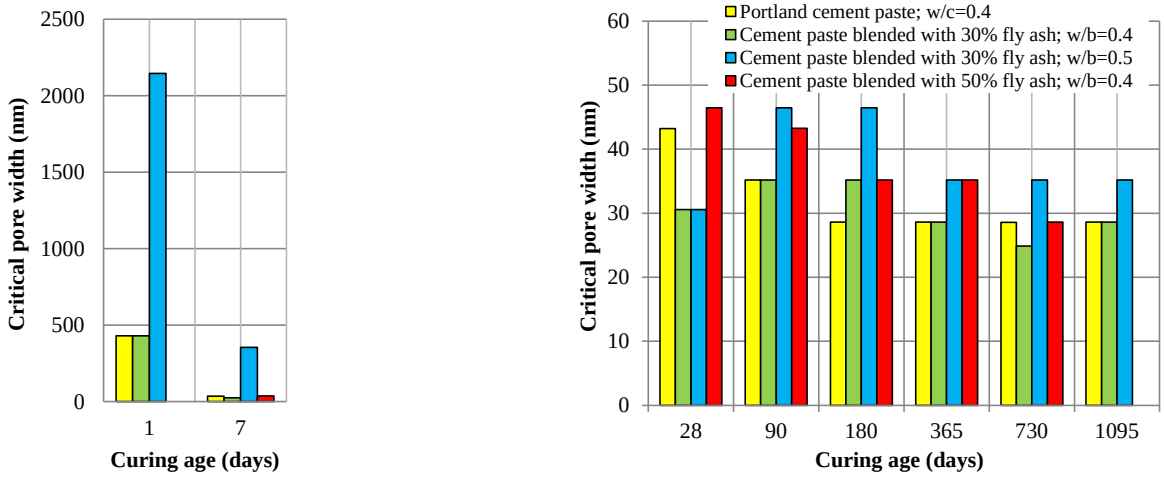

Figure 4.29: Critical pore width of the pastes at different ages

From 1 day to 7 days, the critical pore width of both Portland cement paste and blended cement paste shows a dramatic decrease. After that the change in the critical pore width is insignificant with increasing age of the paste, except in case of the blended cement paste with

a w/b ratio of 0.5. For all the mixtures it holds that in the period from 28 days to 3 years reaction products block the capillary pores and the mercury goes through big C-S-H gel pores to reach the capillaries. The critical pore width varies from 25 nm to 45 nm, which is a little bigger than the pore size of the gel pores (<10 nm) defined by Mindess *[Mindess 1981]*. In other words at later ages, *i.e. after 28 days*, the presence of fly ash does not change the critical pore width of the pore structure of the pastes.

4.4 Conclusions and Remarks

In this chapter the effect of fly ash on microstructure development of blended cement paste, especially the development of its pore structure, is studied at ages up to 3 years. From the experimental results and discussions in this chapter the following conclusions have been drawn.

BSE image observations

1. BSE images show that at ages up to 3 years blended cement paste is more porous than Portland cement paste. In blended cement paste, *30% fly ash; w/b=0.4*, some circular voids surrounded by reaction products are observed at later ages, around 180 days. The formation of those circular voids results from the pozzolanic reaction of hollow fly ash particles (with a thin shell). Furthermore, the partially or fully reacted hollow fly ash particles provides extra space for the accommodation of reaction products.

MIP test

1. Total porosity
   The total porosity of both Portland cement paste and blended cement paste decreases linearly with time (if plotted on a semi-log scale) at ages from 1 day to 1 year. After about 1 year the total porosity of paste decreases only slightly (Figure 4.13). The regression equations and the values of R^2 for the evolution of the total porosity of all mixtures with time are listed in Appendix B.

   The mixtures with fly ash have a higher total porosity than pure Portland cement paste at ages from 1 day to 3 years. With the same w/b ratio (0.4), the paste made with 50% fly ash has a higher total porosity than mixture with 30% fly ash.

   The total porosity of blended cement paste (30% fly ash) with a high w/b ratio of 0.5 is higher than that of blended cement paste with a w/b ratio of 0.4.

2. Capillary porosity
   The evolution of the capillary porosity of blended cement paste with time is similar to that of the total porosity. The effect of fly ash content and w/b ratio on the capillary porosity is similar as their effect on the total porosity.

   The capillary porosity consists of the volume of large capillary pores (>100 nm) and small capillary pores (10 - 100 nm). The volume of large capillary pores of blended cement paste sharply decreases in the period from 1 day to 28 days. In the same period the volume of small capillary pores increases. In the period from 90 days to 3 years blended cement paste has a larger volume of small capillary pores than Portland

cement paste, but the volume of large capillary pores hardly changes. It means that at later ages the presence of fly ash results in the formation of a large amount of small capillary pores in the range between 10 and 100 nm.

3. Ink-bottle porosity
   As shown in Figure 4.9 some fly ash particles are hollow. Before the reaction of fly ash the voids in hollow fly ash particles are considered isolated pores. With progress of the pozzolanic reaction of fly ash the voids act as ink-bottle pores.

   At ages beyond 28 days the ink-bottle porosity in blended cement paste is higher than that in Portland cement paste. With the same w/b ratio of 0.4 the blended cement paste with 50% fly ash has a higher ink-bottle porosity than mixture with 30% fly ash.

   The change of w/b ratio from 0.4 to 0.5 hardly affects the ink-bottle porosity of blended cement paste (30% fly ash).

4. Effective capillary porosity
   The effective capillary porosity is the volume of the effective capillary pores of paste. The effective capillary porosity of all mixtures decreases with time, and hardly changes after about 1 year.

   The effect of fly ash content (0%, 30% and 50%) on the effective capillary porosity is not significant. The effective capillary porosity of mixture with 30% fly ash is similar to that of pure Portland cement paste at ages up to 3 years. The effective capillary porosity of paste with 50% fly ash is only around 2% higher than that of Portland cement paste.

   The effective capillary porosity of blended cement paste with w/b ratio 0.5 is higher than that of mixture with w/b ratio 0.4

5. Connectivity of the pores
   With similar effective capillary porosity, the paste containing a larger volume of ink-bottle pores has a lower connectivity of the pores (see Figure 4.7). With the same w/b ratio of 0.4, the effective capillary porosity of mixture with fly ash is similar to that of pure Portland cement paste at ages up to 3 years (Figure 4.25). However, blended cement paste has a higher ink-bottle porosity than Portland cement paste (Figure 4.21).

   At later ages, *i.e.* after 180 days, blended cement paste has a lower connectivity of the pores than Portland cement paste. The pore structure of blended cement paste is refined at later ages while the porosity of blended cement is still higher than that of Portland cement paste (at ages up to 3 years).

6. Critical pore width
   The critical pore width of the pore structure of Portland cement paste and blended cement paste decreases significantly at early ages up to around 7 days. If the remaining continuous pores in paste are the gel pores, *however*, the critical pore width of both Portland cement paste and blended cement paste varies from 25 to 45 nm. In other words, at later ages, *i.e. after 28 days*, the presence of fly ash does not change the critical pore width of the pore structure of the pastes.

References

[1] Aligizaki K.K., 2006. Pore structure of cement-based materials-testing. Interpretation and Requirement. Taylor & Francis, New York. ISBN: 0419228004.

[2] Bijen J., 1996. Benefits of slag and fly ash. Construction and Building Materials, 1996; 10(5): 309-314.

[3] Cook David J., Cao Huu T., Coan Everett P., 1986. Pore structure development in portland cement/fly ash blends. MRS Proceedings, 1986; 86.

[4] Cook R.A., Hover K.C., 1993. Mercury porosimetry of cement-based materials and associated correction factors. ACI Materials Journal, 1993; 90(2): 152-161.

[5] Cook, R.A., Hover, K.C, 1999. Mercury porosimetry of hardened cement paste. Cement and Concrete Research, 1999; 31 (2): 933-943.

[6] Diamond S., 1971. A critical comparison of mercury porosimetry and capillary condensation pore size distributions of Portland cement pastes. Cement and Concrete Research, 1971; 1(5): 531-545.

[7] Feldman R.F., 1983. Significance of porosity measurements on blended cement performance. Proceedings of the CANMETIACI. First International Conference on the Use of Fly Ash, Silica Fume, Slag and other Mineral By-Products in Concrete. Montebello, Quebec. July 31 - August 5, 1983.

[8] Garboczi, E.J., 1990. Permeability, diffusivity, and microstructural parameters: A critical review. Cement Concrete Research, 1990; 20: 591-601.

[9] Hearn N., Hooton R.D., Mills R.H., 1994. Pore structure and permeability. Significance of tests and properties of concrete and concrete making materials, 4th Edition, P.Klieger, J.F. Lamond (eds), ASTM STP 169C, American society for testing and materials, West Conshohocken, PA, PP. 240-262.

[10] Jiang Linhua, Guan Yugang, 1999. Pore structure and its effect on strength of high-volume fly ash paste. Cement and Concrete Research, 1999; 29: 631-633.

[11] Marsh B.K., Day R.L., Bonnet D.G., 1985. Pore structure characteristics affecting the permeability of Cement paste containing fly ash. Cement and concrete research, 1985; 15: 1027-1038.

[12] Mehta P.K., Manmohan D., 1980. Pore size distribution and permeability of hardened cement pastes. In proceedings of the 7th international congress on the chemistry of cement, Paris, 1980, vol. III, pp. VII-1-VII-5.

[13] Mindess S., Young J. F., 1981 Concrete (Englewood, NJ: Prentice-Hall).

[14] Neville, A. M., 1995. Properties of concrete. 4th and final Ed., Longman's, London.

[15] Ouellet Serge, Bussière Bruno, Benzaazoua Mostafa, Aubertin Michel, Belem Tikou, 2004. Effect of binder type and mixing water chemistry on microstructural evolution of cemented paste backfill. 57th Canadian geotechnical conference & 5th joint CGS/IAH-CNC conference. Session 4G, 23-30. 24-27 October 2004, Quebec City, Quebec.

[16] Washburn E.W., 1921. In Proc. The National Academy of. Sciences, PNASA, 1921, p.7-21.

[17] Winslow D.N., Cohen M.D., Bentz D.P., Snyder K.A., Garboczi E.J., 1994. Percolation and pore structure in mortars and concrete. Cement and concrete research, 1994; 24(1): 25-37.

[18] Ye Guang, 2003. The microstructure and permeability of cementitious materials. PhD Thesis. Delft University of Technology.

[19] Zeng Qiang, Li Kefei, Teddy Fen-chong, Patrick Dangla, 2012. Pore structure characterization of cement pastes blended with high-volume fly-ash. Cement and Concrete Research, 2012; 42: 194-204.

Chapter 5

Water Permeability of Portland Cement Paste Blended with Fly Ash[4]

5.1 Introduction

The service life and durability of concrete structures strongly depend on the transport properties of the concrete *[Brown 1993; Bentz 1999]*. These transport properties depend primarily on the pore structure of the hydrated cement paste *[Hughes 1985; Garboczi 1990; Neville 1995]*. Water permeability is the most important indicator for durability of concrete. The water acts as a carrier of aggressive agents, such as chloride ions, sulphate ions and acid that can activate many chemical reactions, speeding up the degradation process of concrete structures.

In this chapter the effect of fly ash on the water permeability of blended cement paste is investigated at ages of the cement paste up to 2 years. The results show that at later ages blended cement paste is less permeable than pure Portland cement paste. This mainly results from the refinement of the pore structure caused by the pozzolanic reaction of fly ash. Based on the correlation between the results of water permeability tests and pore structure measurements, the crucial pore parameter governing the water permeability of blended cement paste is discussed.

5.2 Materials and Experimental Method

5.2.1 Materials

The materials and mixture compositions of cement paste used for the water permeability measurements are the same as those used in chapter 3 and chapter 4 (see Table 3.3).

5.2.2 Method used to determine water permeability coefficient of cement paste

Water permeability of cement paste is determined by measuring the rate of steady flow through a saturated specimen under a hydrostatic pressure gradient. The measured flow rate is

[4] This chapter is partially based on:

1) Zhuqing Yu, Guang Ye. The pore structure and water permeability of cement paste blended with fly ash over a long period up to one year. Concrete Repair, Rehabilitation and Retrofitting III: 3rd International Conference on Concrete Repair, Rehabilitation and Retrofitting, ICCRRR-3, 296-301, 3-5 September 2012, Cape Town, South Africa.

used to calculate the water permeability coefficient by using Darcy's equation *[Powers 1955; Banthia 1989]*, *viz.*

$$Q = \frac{K\rho g}{\nu} \cdot \frac{A}{L} \cdot \Delta h \tag{5.1}$$

where:

Q = rate of fluid flow, m^3/s.
K = intrinsic permeability, m^2.
Δh = hydraulic pressure gradient, m.
L = thickness of the solid, m.
A = cross-sectional area of the sample, m^2.
ν = dynamic viscosity of the fluid, s/m^2.
ρ = density of the fluid, kg/m^3.
g = acceleration due to gravity, $9.81\ m^2/s$.

The intrinsic permeability K (m^2) can be transformed to a water permeability coefficient K_w (m/s) using the following equation:

$$K_w = \frac{K\rho g}{\nu} \tag{5.2}$$

For water at 20°C, the term $\rho g/\nu$ equals 9.79×10^6 $m^{-1}s^{-1}$ ($\approx 10^7$). When a steady-state flow Q is reached, the coefficient of permeability of the paste, K_w, can be determined directly by combining Equation 5.1 and Equation 5.2:

$$K_w = \frac{LQ}{A \cdot \Delta h} \tag{5.3}$$

When "permeability" is mentioned in this study, it refers to the water permeability coefficient K_w (m/s).

Test set-up

The test set-up used for the experiments is shown schematically in Figure 5.1. The set-up for water permeability measurements consists of a regulated air-pressure source, an air/water converter, three parallel permeability cells, several valves and tubes (see Figure 5.1). The air/water converter was used to convert air pressure (0.7 MPa in this study) to water pressure. The compressed air enabled water to penetrate into the specimens fast enough to avoid a possible pore structure change caused by ongoing reaction. The air pressure should not be so high that it may cause damage to the pore structure of the tested material. During the test water was supplied from the bottom of the specimens (cell 1-3) by the air/water converter (Figure 5.1). Water penetrated the specimens and accumulated in the calibrated tubes that were connected on the top of each cell. The total volume of the calibrated tube was 2.2 ml with a measurement accuracy of 0.01 ml. By monitoring the volume change in each graduated

tube during a certain time interval, the water permeability of the cement paste can be calculated.

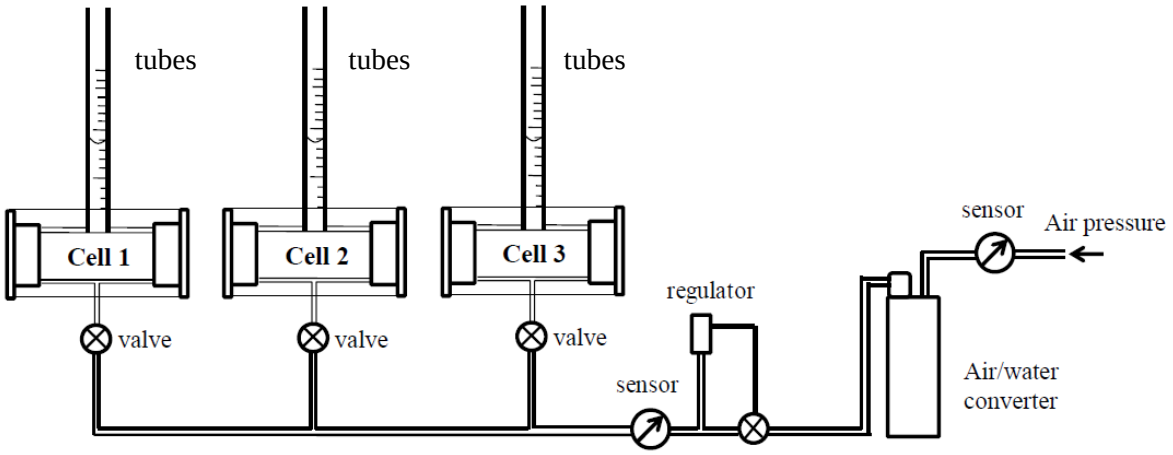

Figure 5.1: The water permeability test set-up in laboratory [Ma 2013]

Calculation of water permeability

In this experiment the diameter of the specimen was 95 mm (0.095 m). Thus the water exposed area A was 0.007088 m^2. *L* is the thickness of the sample, taken as the average of 10 thickness measurements. The outlet pressure was the atmospheric pressure (top of the cell), taken as 0.1013 MPa, which is equal to a water column of 10.34 m, noted as h_1. The inlet pressure is 0.7 MPa. The equivalent water column h_2 can be calculated as:

$$h_2 = \frac{0.7}{0.1013} \times 10.34 = 71.43\ (m) \tag{5.4}$$

Then the hydraulic head Δh can be calculated as:

$$\Delta h = h_2 - h_1 = 71.43 - 10.34 = 61.09\ (m)$$

The flow rate *Q* for each reading during a certain time interval can be calculated as follows:

$$Q = \frac{\Delta V}{\Delta t} \tag{5.5}$$

where:

Q = flow rate, m^3/s.
ΔV = incremental volume of water read from the calibrated tube, m^3.
Δt = time interval during which the volume was collected, *s*.

The steady-state flow is determined by plotting the total volume of collected water versus time. When the resulting curve is linear over the last 10 or more readings (with a time interval of 1-3 hours between each reading), the steady state flow is assumed to have been reached. The time required to reach a steady-state flow varied from several minutes to several hours, depending on the mixture and age of the specimens. The flow rate Q was taken as the average volumetric flow rate over the last ten readings. The detailed information about the apparatus can be obtained in references *[Ye 2003; Ma 2013]*.

5.2.3 Specimen preparation

After 2 minutes mixing, the paste samples were cast in Room Temperature Vulcanized (RTV) silica rubber rings with a diameter of 95 mm (Figure 5.2). The thickness of the specimen is around 15 mm. After 24 hours, the specimens were demoulded, sealed (in order to prevent moisture loss) and cured at room temperature of around 20°C. At an age of 28 days, 90 days, 180 days, 1 year and 2 years, three samples were immersed in water followed by vacuum saturation for around 17 hours.

Also specimens at an age of 3 years were tested. However, under a hydraulic pressure of 0.7 MPa only a little amount of water could penetrate through the paste samples.

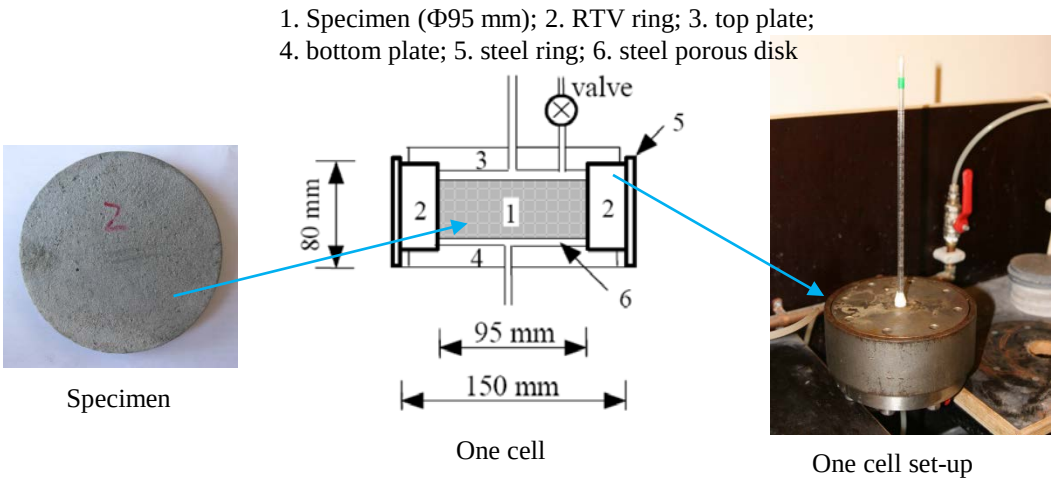

Figure 5.2: One specimen cell for water permeability test

5.3 Experimental Results and Discussions

5.3.1 Results of water permeability

The water permeability coefficient of Portland cement paste and blended cement paste is shown in Figure 5.3 and 5.4. Parameters considered are fly ash content (Figure 5.3) and w/b ratio (Figure 5.4). The standard deviations of the permeability measurements are shown as well.

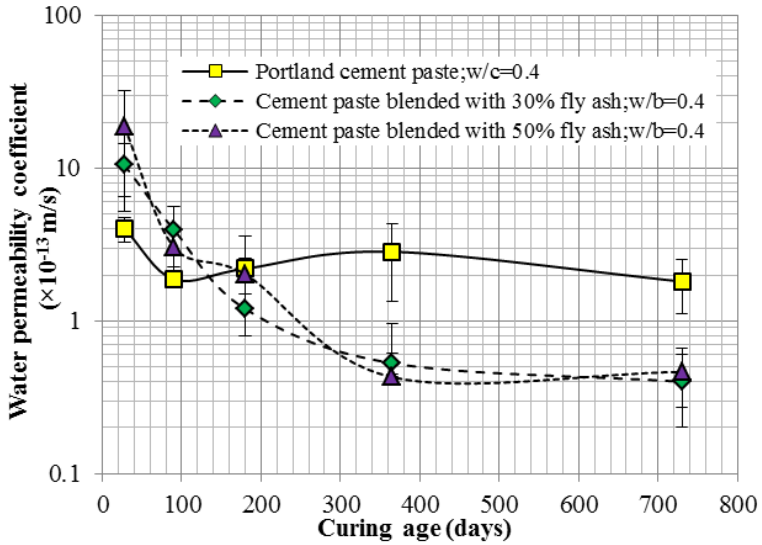

Figure 5.3: The water permeability coefficient of cement paste (w/b=0.4) made with different fly ash contents (0%, 30% and 50%)

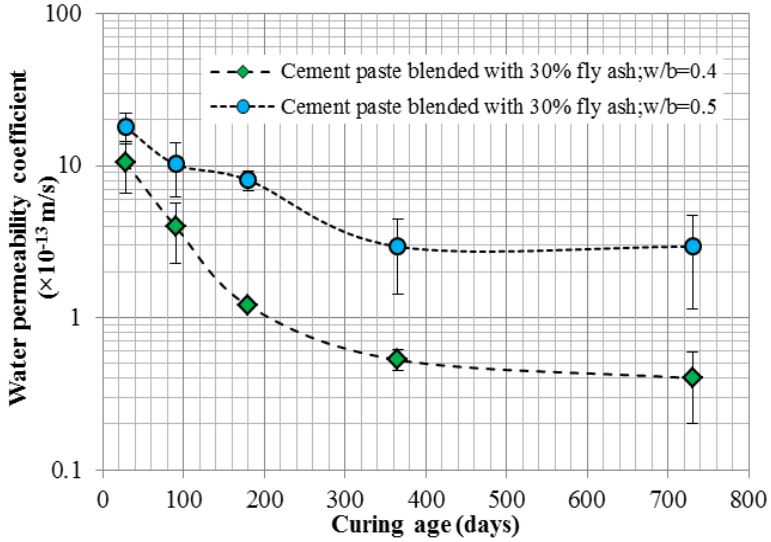

Figure 5.4: The water permeability coefficient of blended cement paste (30% fly ash) made with two w/b ratios (0.4 and 0.5)

Effect of curing period on the water permeability of cement paste

For Portland cement paste, as shown in Figure 5.3, the water permeability decreases from 28 days to 90 days. That results from continuous hydration of cement. After that the water permeability of Portland cement paste has a slight increase. At later ages, *i.e.* after about 1 year, the water permeability starts to decrease. The evolution of the water permeability of Portland cement paste appears to be similar to the evolution of the chloride migration coefficient of Portland cement concrete, as mentioned in Figure 2.9. When the standard deviations of the permeability measurements are taken into account, *however*, after 90 days the water permeability of Portland cement paste hardly changes.

Figure 5.3 shows that the water permeability of blended cement paste decreases significantly from 28 days to 1 year and then hardly changes at later ages, *i.e.* after about 1 year.

Effect of fly ash content on the water permeability of cement paste (w/b=0.4)

The effect of fly ash on the water permeability depends on age of paste as shown in Figure 5.3. In the period from 28 to 90 days the water permeability of mixtures with fly ash is higher than that of pure Portland cement paste. After about 180 days blended cement paste has a lower water permeability coefficient than Portland cement paste. The permeability of mixtures with 30% and 50% fly ash are almost the same.

Effect of w/b ratio on the water permeability of blended cement paste (30% fly ash)

In Figure 5.4 the development of the water peremablity coefficient of paste with w/b ratio 0.4 and 0.5 show a silimar trend. The blended cement paste with w/b ratio 0.5 is more permeable than mixture with a w/b 0.4.

5.3.2 Discussions

As mentioned in the literaure review (chapter 2), the permeability of cement paste depends on the capillary porosity *[Powers 1958]*. Figure 5.5 shows the capillary porosity of all mixtures at ages from 28 days to 730 days (2 years). It can be seen that the capillary porosity of pastes decreases with increasing age of the paste (Figure 5.5a and 5.5b). That is indicated by densifying the microstructure of pastes with progress of hydration of cement and pozzolanic reaction of fly ash. This results in a decrease of the water permeability of paste with time (see Figure 5.3).

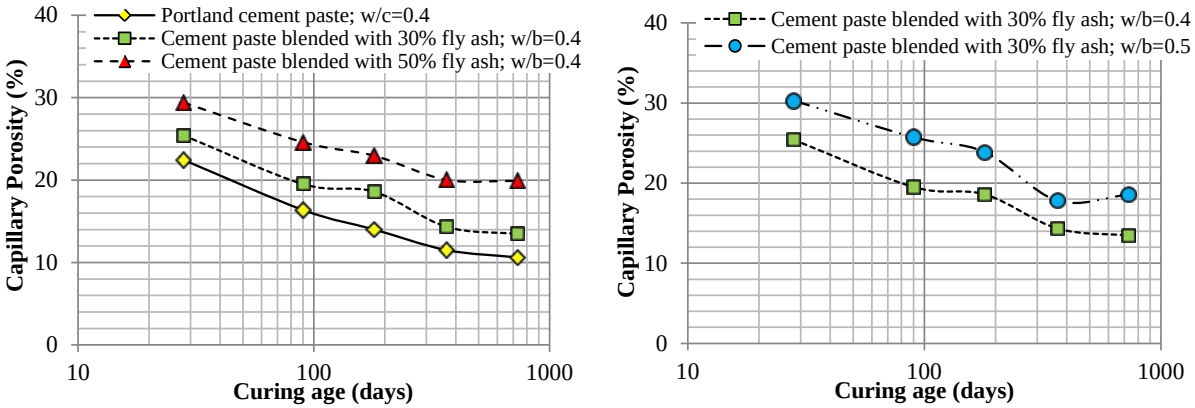

Figure 5.5: Capillary porosity of pastes at ages from 28 days to 730 days (2 years)
(a): cement pastes made with 0%, 30% and 50% fly ash and w/b=0.4
(b): cement pastes made with 30% fly ash and w/b= 0.4 and 0.5

Figure 5.5a shows that at ages from 28 days to 2 years the capillary porosity of mixtures with fly ash is higher than that of Portland cement paste. It is generally assumed that samples with higher capillary porosity are more permeable. This, *however*, appears not to be the case for blended cement paste. The relationship between the capillary porosity and the water permeability of blended cement paste depends on age of the paste. Two subsequent stages can be distinguished:

At ages from 28 days to 90 days

In the period from 28 to 90 days blended cement paste is more permeable than Portland cement paste (see Figure 5.3). The higher permeability of blended cement paste is considered by the higher capillary pores.

At ages after 180 days

At ages beyond 180 days blended cement paste has a *lower* water permeability than pure Portland cement paste, *even though* the capillary porosity of blended cement paste is higher than that of Portland cement paste (see Figure 4.15).

It is obvious that the water permeability of blended cement paste is not only determined by the capillary porosity of the paste. It is also, *or mainly*, determined by the connectivity of the pores of the paste. After an age of 180 days blended cement paste has a lower *connectivity of the pores* than Portland cement paste (see Figure 4.27). In the following section the correlation between water permeability and connectivity of the pores is investigated.

5.4 Correlation Between Water Permeability and Connectivity of the Pores

As mentioned in chapter 4 connectivity of the pores in cement paste is the fraction of pores with respect to the pore volume consisting of only open and effective pores. Figure 5.6 plots the relationship between water permeability coefficient (K_w) and connectivity of the pores (C) for cement pastes. It can be seen that the water permeability of paste increases with increasing connectivity of the pores. As evident from the trend-line a power function ($K_w = a\ e^{b \times C}$) with $R^2 = 0.8233$ holds for the water permeability and the connectivity of the pores.

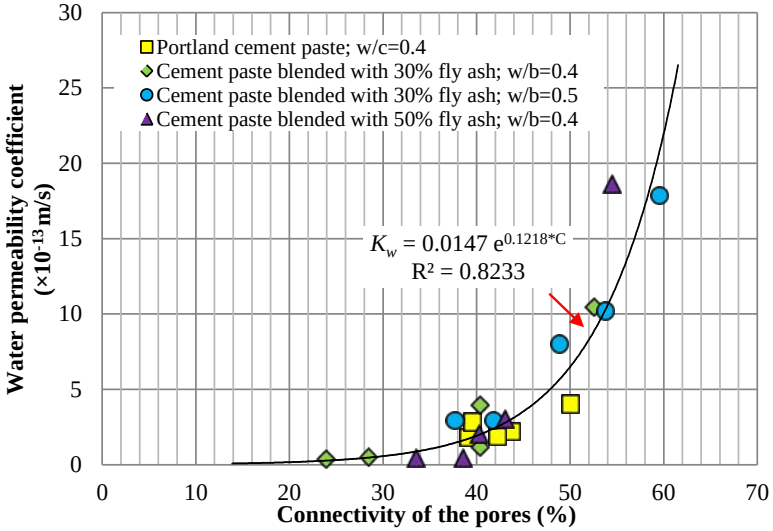

Figure 5.6: The correlation between water permeability coefficient and connectivity of the pores for Portland cement paste and blended cement paste

The above results indicate that the connectivity of the pores is the crucial factor determining the water permeability of paste. Schematic diagrams (2D) of water flow in Portland cement paste and blended cement paste is shown in Figure 5.7. It is assumed that the hollow fly ash particles have fully reacted after a certain time, for example, after 1 year. The voids left after the reaction of hollow fly ash particles then act as ink-bottle pores, resulting in an increase of the capillary porosity, *but* not necessarily in an increase of the permeability (as mentioned in Figure 4.7). With progress of the pozzolanic reaction of fly ash more ink-bottle pores are produced, reducing the connectivity of the pores, and, *hence*, reducing the permeability. At later ages, *i.e.* after 180 days, the connectivity of the pores of blended cement paste is lower than that of Portland cement paste. As a result blended cement paste is less permeable than Portland cement paste, even if its capillary porosity is high. An overview of the results of water permeability test and pore structure parameters measurements for Portland cement paste and blended cement paste is shown in Table 5.1.

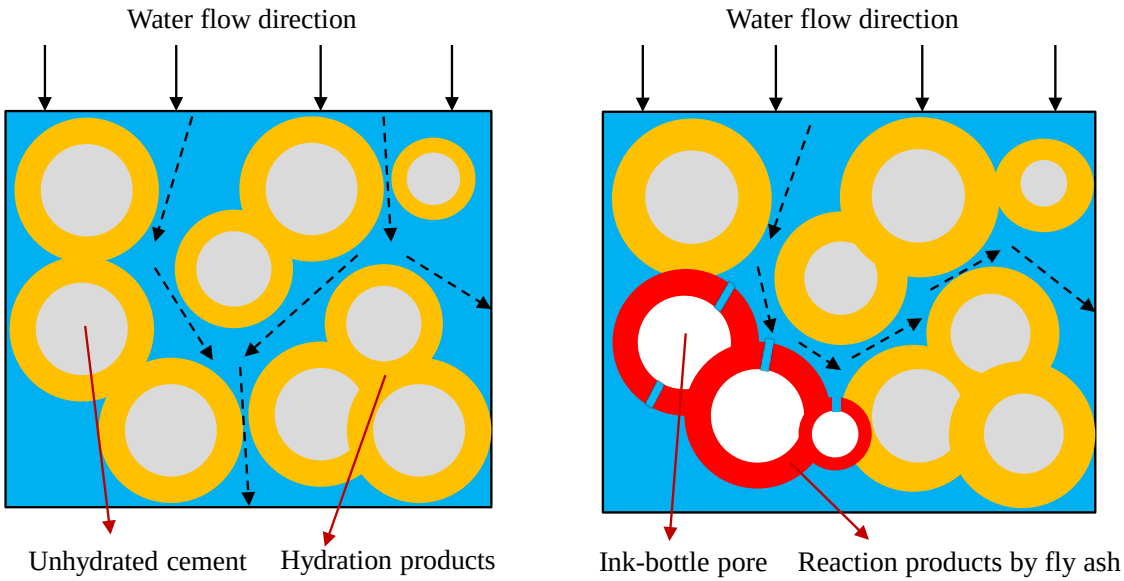

(a) Portland cement paste (b) Blended cement paste

Note: the rate of hydration of cement is accelerated in blended cement paste (see Figure 3.21); the ink-bottle pores are air-filled

Figure 5.7: The schematic diagram (2D) of water flow in Portland cement paste (a) and blended cement paste (b) at later ages

Table 5.1: Measured water permeability coefficient, connectivity of the pores, ink-bottle porosity and capillary porosity of cement paste at ages from 28 days to 2 years

Mixtures	Ages	B	C	D	E
Portland cement paste w/c=0.4	28	4.02	50.0	9.0	22.4
	90	1.87	42.2	8.0	14.7
	180	2.20	43.7	7.4	14.0
	365	2.84	39.6	7.0	11.5
	730	1.81	39.2	6.5	10.6
Cement paste blended with 30% fly ash; w/b=0.4	28	10.47	52.6	12.0	25.4
	90	3.97	40.4	11.6	19.5
	180	1.20	40.3	11.1	18.6
	365	0.53	28.5	10.3	14.3
	730	0.40	23.9	10.3	13.5
Cement paste blended with 50% fly ash; w/b=0.4	28	18.63	54.5	13.4	29.4
	90	3.05	43.0	15.0	26.4
	180	2.02	40.3	13.7	23.0
	365	0.43	38.6	12.3	20.0
	730	0.46	33.5	13.2	19.9
Cement paste blended with 30% fly ash; w/b=0.5	28	17.89	59.6	12.2	30.3
	90	10.20	53.8	11.9	25.7
	180	8.02	48.9	12.2	23.9
	365	2.94	41.8	10.4	17.8
	730	2.94	37.7	11.3	18.6

Note:
A: Age (days); B: Water permeability coefficient $\times 10^{-13}$ (m/s); C: Connectivity of the pores (%);
D: Ink-bottle porosity (%); E: Capillary porosity (%);

5.5 Concluding Remarks

In this chapter the water permeability of blended cement paste is studied at ages up to 2 years. The crucial pore structure parameter governing the water permeability of blended cement paste was discussed. The major conclusions of this chapter are presented below:

1. The water permeability of blended cement paste decreases with time up to 1 year. After 1 year the water permeability of blended cement pastes considered in this study hardly changes.

2. At early age the pastes containing fly ash exhibit a higher capillary porosity than pure Portland cement paste. The initial water permeability of blended cement paste is higher than that of Portland cement paste. However, after about 180 days blended cement paste is less permeable than pure Portland cement paste, even though the capillary porosity of blended cement paste is higher than that of Portland cement paste.

3. As expected the blended cement paste with a w/b ratio 0.5 has a higher water permeability coefficient than paste with a w/b ratio 0.4 at ages up to 2 years. A lower w/b ratio results in a finer pore structure and a lower water permeability.

4. The water permeability of pure cement paste and blended cement paste depends on the connectivity of the pores. At later ages, *i.e.* after 180 days, the connectivity of the pores of blended cement paste is lower than that of pure Portland cement paste, resulting in a less permeable microstructure.

References

[1] Banthia, N., Mindess, S., 1989. Water permeability of cement paste. Cement and Concrete Research, 1989; 19(5): 727-736.

[2] Bentz, D. P., Garboczi E. J., 1999. Effects of cement particle size distribution on performance properties of Portland cement-based materials. Cement and Concrete Research, 1999; 29 (10): 1663-1671.

[3] Brown P.W., Shi Dex, Skalny J.P., 1993. Porosity/permeability relationships. Parts of 'Concrete microstructure porosity and permeability'. D. M. Roy, P. W. Brown, D. Shi, B. E. Scheetz, W. May. Strategic Highway Research Program, National Research Council, Washington, DC 1993. SHRP-C-628.

[4] Garboczi, E.J., 1990. Permeability, diffusivity, and microstructural parameters: A critical review. Cement Concrete Research, 1990; 20: 591-601.

[5] Hughes D.C., 1985. Pore structure and permeability of hardened cement paste. Mag. Concr. Res., 1985; 37(133): 227-233.

[6] Ma Yuwei, 2013. Microstructure and Engineering Properties of Alkali Activated Fly Ash - as an environment friendly alternative to Portland cement. PhD Thesis. Delft University of Technology.

[7] Neville, A. M., 1995. Properties of concrete. 4th and final Ed., Longman's, London.

[8] Powers T. C., Copeland L E., Hayes J. C., Mann H. M., 1955. Permeability of Portland cement paste. Portland Cement Association, 1955; 285-289.

[9] Powers, TC., 1958. Structures and physical properties of hardened portland cement paste. Journal American Ceramic Society, 1958; 41: 5-15.

[10] Ye Guang, 2003. The microstructure and permeability of cementitious materials. PhD Thesis. Delft University of Technology

Chapter 6

Resistance of Fly Ash Concrete to Chloride Penetration[5]

6.1 Introduction

In chapter 5 the water permeability of cement paste blended with fly ash was investigated. At later ages, *i.e.* after 180 days, blended cement paste is less permeable than Portland cement paste. This is mainly attributed to the decrease of the connectivity of the pores in blended cement paste. The pore structure plays an important role in the durability of concrete as well *[Neville 1995]*. In this chapter the effect of fly ash on the resistance of concrete to chloride penetration is studied. The rapid chloride migration (RCM) test is used to determine the evolution of the chloride migration coefficient of the concrete with time, *up to 3 years*. For comparison the RCM test is also performed on Portland cement concrete.

6.2 Materials and Method

6.2.1 Materials properties

The Portland cement and fly ash used for preparing concrete mixtures are the same as those used for the experimental studies presented in chapter 3 (Table 3.1). Tap water is used for mixing concrete. Graded river sand with a maximum grain size of 4 mm and gravel with a maximum grain size of 16 mm are used as fine and coarse aggregates, respectively. The sizes and morphologies of different aggregates are shown in Figure 6.1.

6.2.2 Mixture compositions

Portland cement concrete was casted with three water/cement ratios, 0.4, 0.5 and 0.6. For fly ash concrete fly ash dosages were 30% and 50% by weight, based on the total weight of the binder. The water/binder ratios were 0.4, 0.5 and 0.6. Because of its proneness to bleeding the fly ash concrete mixture with 50% fly ash and w/b=0.6 was excluded. The mixture compositions are given in Table 6.1.

---

[5] This chapter is partially based on:

1) Zhuqing Yu, Guang Ye. Chloride penetration and microstructure development of fly ash concrete. The 2nd international conference "Microstructure related durability of cementitious composites". Amsterdam, 11-13 April 2012.

2) Zhuqing Yu, Guang Ye. A discussion of service life prediction of fly ash concrete based on DuraCrete. International Congress on Durability of Concrete, Trondheim, Norway. 18-21 June 2012.

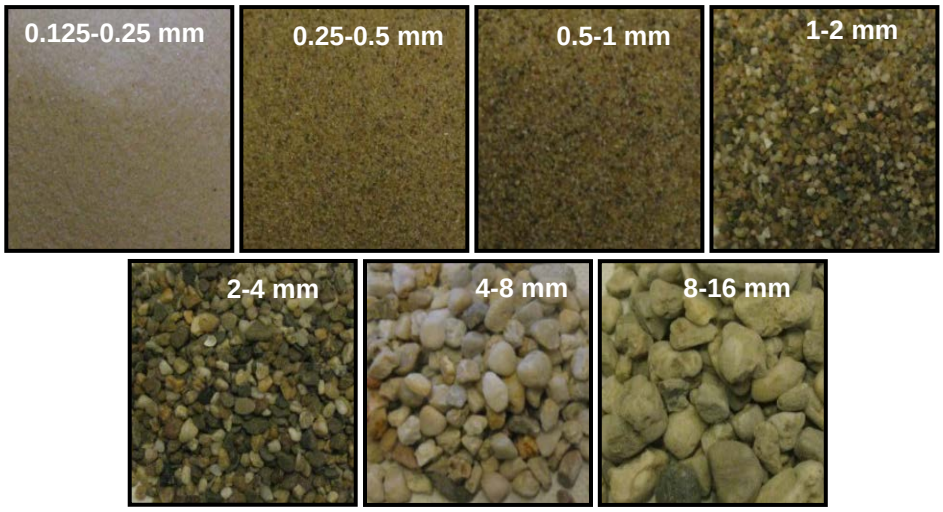

Figure 6.1: The morphology of different sizes of aggregates

Table 6.1: Mixture compositions of Portland cement concrete and fly ash concrete (kg/m^3)

Mixture	CEM I 42.5 N	Fly ash	Tap water	Masonry sand 0/2	Sand 0/4	Gravel 4/16
OPC-04	390	0	156	178	498	1103
OPC-05	390	0	195	178	498	1103
OPC-06	390	0	234	178	498	1103
FA-30-04	273	117	156	178	498	1103
FA-30-05	273	117	195	178	498	1103
FA-30-06	273	117	234	178	498	1103
FA-50-04	195	195	156	178	498	1103
FA-50-05	195	195	195	178	498	1103

6.2.3 Test method and specimen preparation

At present several standard test methods are used to evaluate the resistance of concrete to chloride ingress. These test methods are categorized in diffusion tests, migration tests and indirect tests based on resistivity or conductivity *[Rilem Report 38 2007]*. In this chapter the migration test will be considered. As discussed in chapter 2 the rapid chloride migration (RCM) test is a test where an external electrical field is applied to accelerate chloride penetration in concrete. The RCM test is described in NT Build 492 standard *[NT Build 492 1999]*. Specimen preparation for the RCM test is as follows:

- After mixing for 2 minutes the concrete is cast in a cylindrical mold with a diameter of 100 mm and height of 300 mm (Figure 6.2 a).
- After 24 hours the specimens are demoulded and immediately cured in a fog room at 20°C ± 1°C to prevent loss of moisture from the concrete (Figure 6.2 b and c).
- At an age of 28 days, 91 days, 180 days, 1 year, 2 years and 3 years, three slices with a diameter of 100 mm and a thickness of 50 mm were sawn from the central section of the cylinder by using a water-cooled diamond saw (Figure 6.3). The top and bottom slices were thrown away.

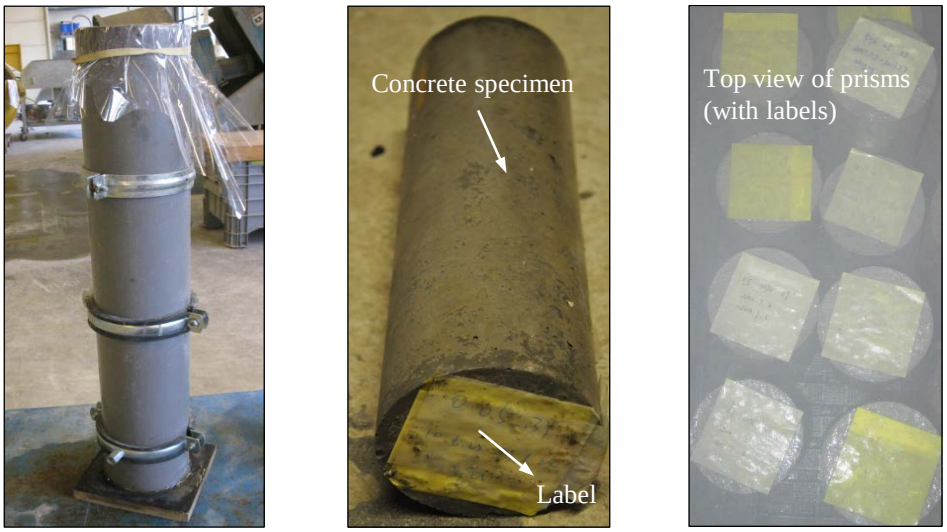

(a) *(b)* *(c)*

Figure 6.2: Concrete specimens casted in the mold (a); demoulded (b); cured in a fog room (c)

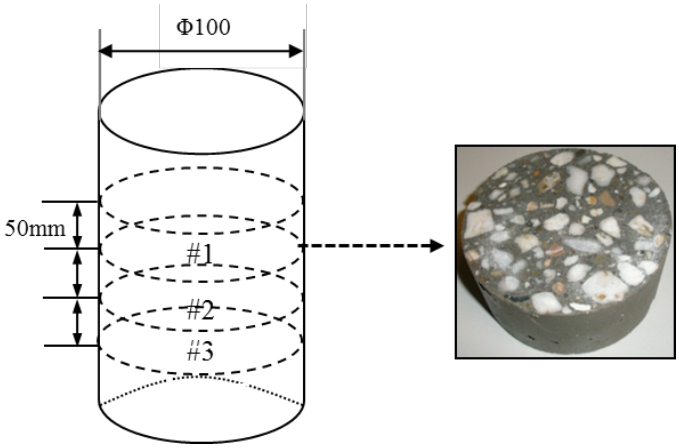

Figure 6.3: The sawing plan of test specimen

Before the RCM-specimens are tested, a preconditioning is required to make the concrete specimen thoroughly saturated. The preconditioning procedure is as follows:

- Sawing, brushing and washing away any burrs from the surfaces of the concrete specimen. Wiping off excess water from the surface of the specimens.
- Keeping the specimens surface-dry and placing them vertically in the vacuum container for vacuum treatment.
- Exposing both end surfaces to air in order to reach saturation.
- Reducing the absolute pressure in the vacuum container with specimens to a pressure in the range of 10-50 mbar (1-5 kPa) within a few minutes.
- Maintaining the vacuum for three hours and then, with the vacuum pump still running, fill the container with the saturated $Ca(OH)_2$ solution (by dissolving an excess of calcium hydroxide in distilled or de-ionized water) so as to immerse all the specimens.
- Maintaining the vacuum for one hour before allowing air to re-enter the container.
- Keeping the specimens in the solution for 18 ± 2 hours.

The experimental set-up is shown in Figure 6.4. The plastic box was filled with about 12 litre catholyte solution, 10% NaCl by mass in tap water (*100 g NaCl in 900 g water, about 2 N*). The prepared concrete specimens were put in a rubber sleeve and fastened with two stainless steel clamps. After placing the specimens in the plastic box, 300 ml anolyte solution, 0.3 M NaOH in distilled water (*approximately 12 g NaOH in 1 litre water*), filled the sleeve above the concrete specimen.

With the preset voltage of 30 V the initial current through each specimen was recorded. The voltage was adjusted if necessary according to Table 6.2. After adjustment a corresponding test duration was applied.

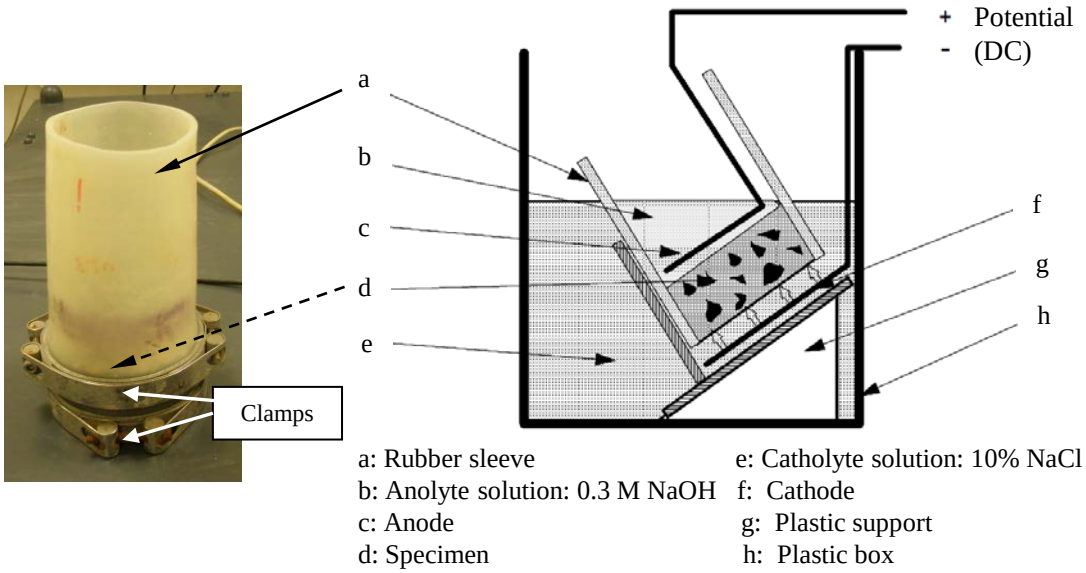

Figure 6.4: The RCM set-up in laboratory

Table 6.2: Test voltage and duration of the test for concrete specimen [NT Build 492 1999]

Initial current I_{30v} (with 30V) (mA)	Applied voltage U (after adjustment) (V)	Possible new initial current I_0 (mA)	Test duration t (hour)
$I_0 < 5$	60	$I_0 < 10$	96
$5 \leq I_0 < 10$	60	$10 \leq I_0 < 20$	48
$10 \leq I_0 < 15$	60	$20 \leq I_0 < 30$	24
$15 \leq I_0 < 20$	50	$25 \leq I_0 < 35$	24
$20 \leq I_0 < 30$	40	$25 \leq I_0 < 40$	24
$30 \leq I_0 < 40$	35	$35 \leq I_0 < 50$	24
$40 \leq I_0 < 60$	30	$40 \leq I_0 < 60$	24
$60 \leq I_0 < 90$	25	$50 \leq I_0 < 75$	24
$90 \leq I_0 < 120$	20	$60 \leq I_0 < 80$	24
$120 \leq I_0 < 180$	15	$60 \leq I_0 < 90$	24
$180 \leq I_0 < 360$	10	$60 \leq I_0 < 120$	24
$I_0 \geq 360$	10	$I_0 \geq 120$	6

When the RCM test was finished three parallel specimens were split and sprayed with 0.1 M silver nitrate ($AgNO_3$) solution to determine the penetration depth of the chloride. Figure 6.5 shows a typical split specimen after spraying with $AgNO_3$. The white silver chloride precipitation on the split surface was clearly visible after 15 minutes. The average penetration depth x_d of the chloride was determined by measuring seven penetration depths of the penetration profile (x_1-x_7) (Figure 6.5).

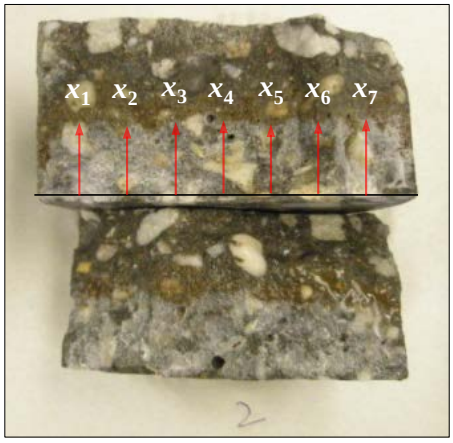

Figure 6.5: Split sample after spraying with $AgNO_3$

The non-steady-state migration coefficient, D_{RCM}, was calculated with Equation 6.1 *[NT Build 492 1999]*:

$$D_{RCM} = \frac{0.0239 \cdot (273+T) \cdot L'}{(U-2) \cdot t_d} \cdot \left(x_d - 0.0238 \sqrt{\frac{(273+T) \cdot L' \cdot x_d}{U-2}} \right) \tag{6.1}$$

where:

D_{RCM} = non-steady-state migration coefficient, $\times 10^{-12}$ m^2/s.
U = absolute value of the applied voltage, *V*.
T = average value of the initial and final temperatures in the anolyte solution, *°C*.
L' = thickness of the specimen, *mm*.
x_d = average value of the penetration depth, *mm*.
t_d = test duration, *hour*.

By comparing D_{RCM} values of Portland cement concrete with those of concrete made with blended cement the effect of fly ash on the resistance of concrete to chloride ingress can be determined. More importantly, the D_{RCM} value measured at an age of 28 days will be used as input parameter to predict the service life of concrete structures. This will be discussed in more detail in chapter 8.

6.3 Experimental Results

6.3.1 Effect of w/c ratio on chloride migration coefficient of Portland cement concrete

Figure 6.6 shows the effect of w/c ratio on the values of the chloride migration coefficient (D_{RCM}) of Portland cement concrete. As expected, the w/c ratio has a significant influence on the D_{RCM} value. At 28 days it varies from 13×10^{-12} m^2/s to 28 $\times10^{-12}$ m^2/s with increasing w/c ratio from 0.4 to 0.6.

However, the evolution of the D_{RCM} values of Portland cement concrete after 28 days is different for different w/c ratios. For w/c ratios 0.4 and 0.5 the D_{RCM} value decreases gradually up to 180 days, then increases to a peak value after about 1 year and then decreases again. In the case of w/c ratio at 0.6, a decrease of the D_{RCM} value is observed from 28 to 90 days. Afterwards, the D_{RCM} value shows an upward trend up to 3 years. As illustrated in Figure 6.6 the development of the D_{RCM} value of Portland cement concrete with time is in accordance with the experimental results of several authors quoted in Figure 2.8 (see chapter 2).

As mentioned in section 6.2.3, the concrete samples were cured in a fog room (100% humidity). In theory, moist curing ensures progress of the hydration of cement clinker resulting in a denser microstructure of the concrete. We would expect, *therefore*, that the D_{RCM} values of Portland cement concrete should decrease with increasing age of the concrete. However, in Figure 2.8 and Figure 6.6 the D_{RCM} values of Portland cement concrete increase after a certain age of the concrete (around 6 months). *The detailed explanation of this behavior will be proposed in chapter 7.*

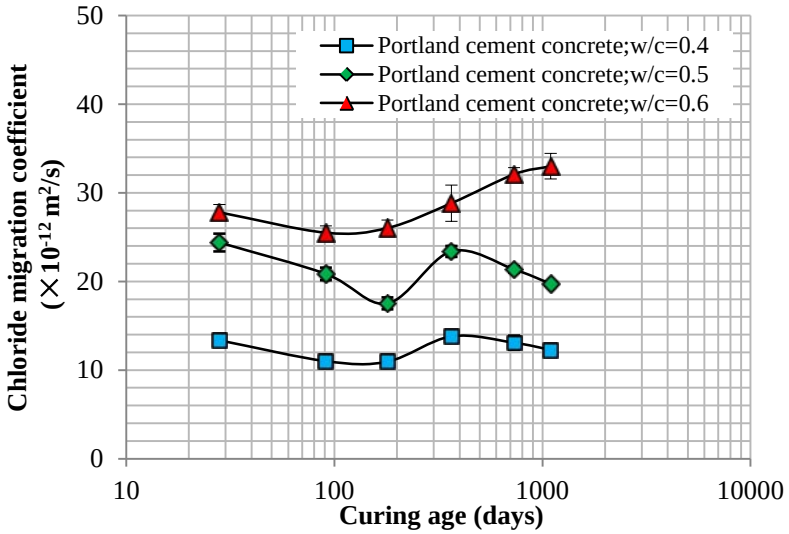

Figure 6.6: D_{RCM} values of Portland cement concrete made with different w/c ratios

6.3.2 Effect of fly ash dosage on chloride migration coefficient of fly ash concrete

Figure 6.7 - 6.9 show the D_{RCM} values of fly ash concrete made with different fly ash dosages and three w/b ratios, together with those of Portland cement concrete. The figures show that for mixtures with different w/b ratios the development of the D_{RCM} values with time exhibit similar trends.

As shown in Figures 6.7- 6.9 the D_{RCM} value of fly ash concrete at 28 days is slightly higher than that of Portland cement concrete. Beyond 28 days the D_{RCM} value of fly ash concrete decreases considerably and is lower than that of Portland cement concrete. At later ages the effect of fly ash on the resistance to chloride ingress becomes even more pronounced.

From Figure 6.7 it can be seen that two concrete mixtures with fly ash content 30% and 50% (w/b=0.4) have similar D_{RCM} values. This also holds for mixtures with w/b = 0.5 (see Figure 6.8). On closer look only a minor difference is found in the development of the D_{RCM} values with time for these two mixtures. That will be discussed below:

- In Figure 6.7 the D_{RCM} value of the mixture made with 50% fly ash exhibits an almost linear relation with time from 28 days to 3 years when plotted on a double logarithmic coordinate, with a R^2 value of 0.96. A similar trend was reported by Maage *[Maage 1996]* of the effect of other Pozzolanic material (condensed silica fume) on the D_{RCM} values of Portland cement concrete (ages from 1 day to 180 days).
- For the concrete with 30% fly ash the D_{RCM} value decreases linearly with time from 28 days to 1 year when plotted on a double logarithmic scale as shown in Figure 6.7. After about 1 year the D_{RCM} value hardly changes. This can be explained by the results of porosity of blended cement paste. As shown in chapter 4 (see Figure 4.13) the total porosity of blended cement paste with 30% fly ash (w/b=0.4) hardly changes in the period from 1 year to 3 years. It suggests that after about 1 year the structure of the fly ash concrete made with 30% fly ash becomes stable, resulting in an almost constant resistance to chloride ingress.

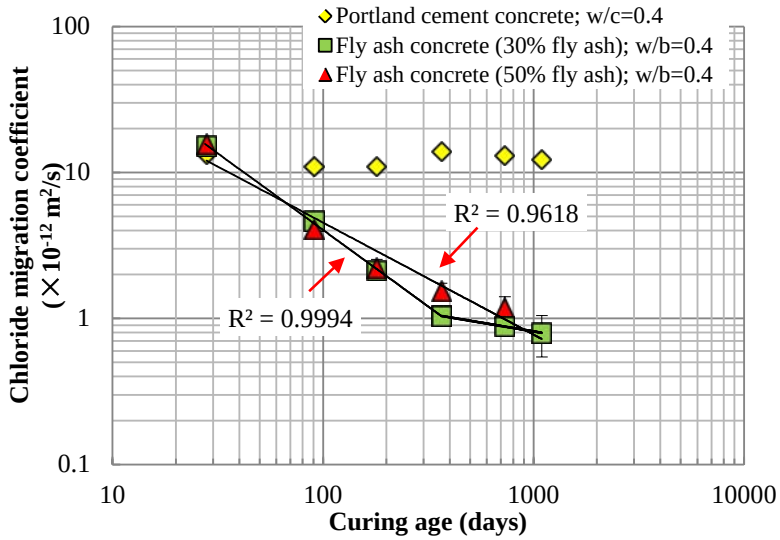

Figure 6.7: The D_{RCM} value relative to the fly ash dosage for concrete with w/b ratio of 0.4

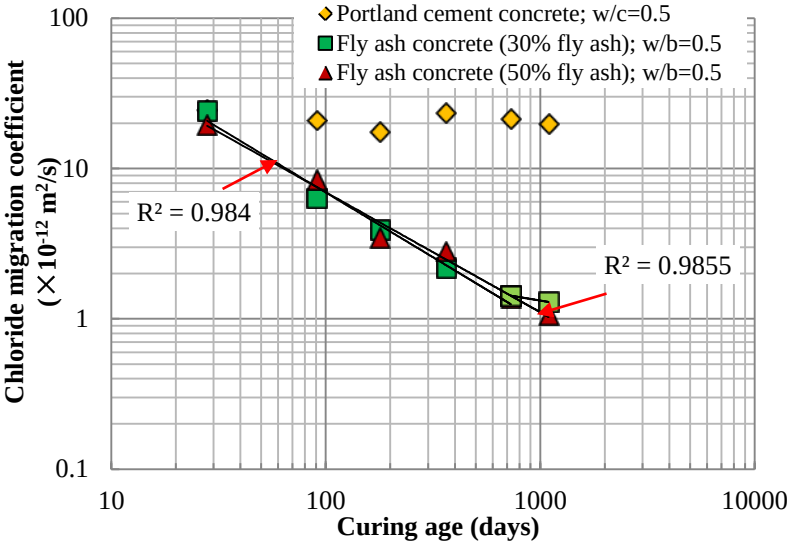

Figure 6.8: The D_{RCM} value relative to the fly ash dosage for concrete with w/b ratio of 0.5

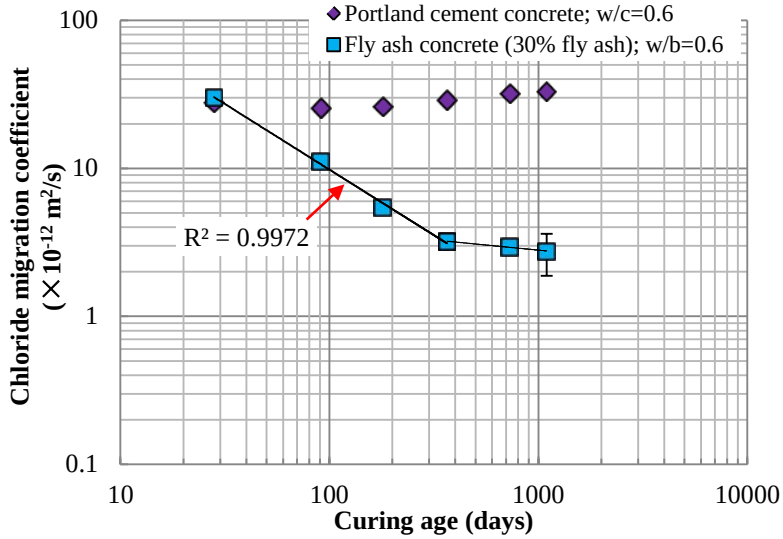

Figure 6.9: The D_{RCM} value relative to the fly ash dosage for concrete with w/b ratio of 0.6

6.3.3 Effect of w/b ratio on chloride migration coefficient of fly ash concrete

Figure 6.10 and Figure 6.11 show the effect of w/b ratio on the D_{RCM} values of fly ash concrete made with 30% and 50% fly ash, respectively.

From Figure 6.10 it is clear that at three w/b ratios, the relation between the D_{RCM} values and time for fly ash concrete made with 30% fly ash is *bilinear*. As expected, the increase of w/b ratio leads to a higher D_{RCM} value at the same age of the concrete.

For fly ash concrete made with 50% fly ash, Figure 6.11 shows that at ages up to 3 years the mixture made with w/b ratio of 0.4 has better resistance to chloride ingress than that with w/b ratio of 0.5.

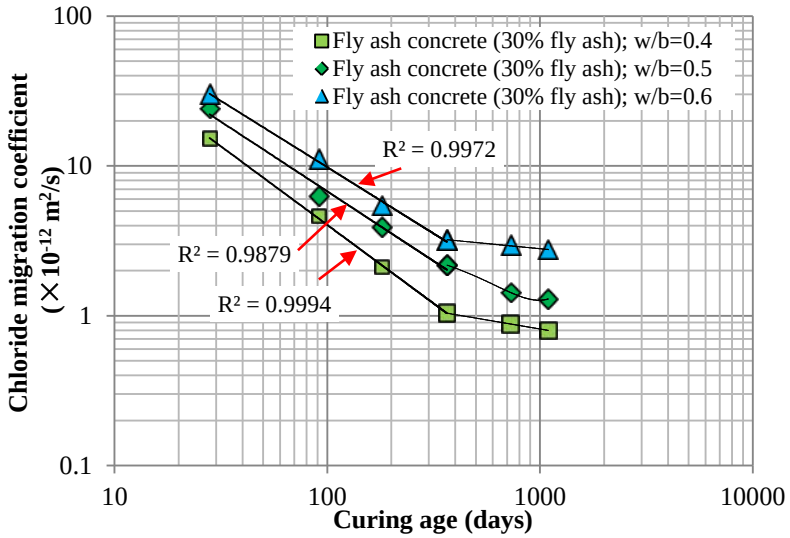

Figure 6.10: Effect of w/b ratio on the D_{RCM} values of fly ash concrete made with 30% fly ash

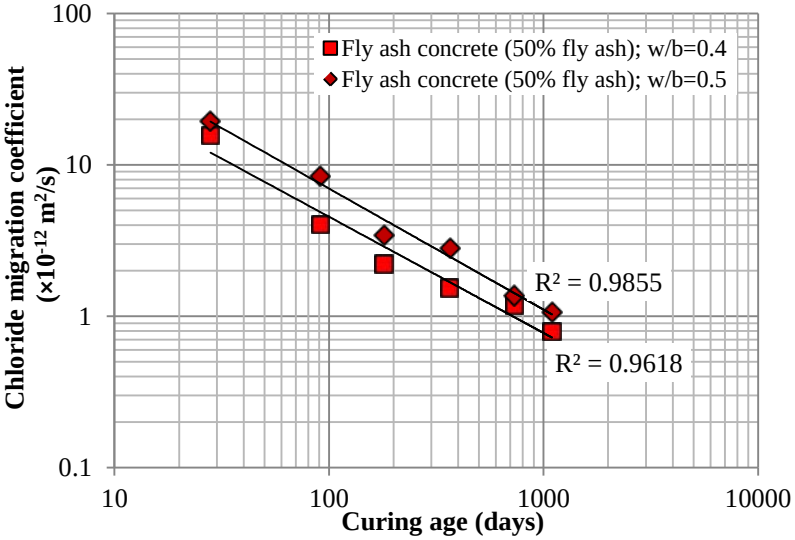

Figure 6.11: Effect of w/b ratio on the D_{RCM} values of fly ash concrete made with 50% fly ash

6.3.4 Correlation between w/b and chloride migration coefficient

It has been reported *[CUR-Bouw&Infra 2009; van Breugel et al. 2009; van der Wegen et al. 2012]* that the D_{RCM} value is linearly related to the w/b ratio for different types of concrete at an age of around 28 days:

$$D_{RCM}(28days) = A(w/b) + B \tag{6.2}$$

where A and B are constants related to particular cement types.

Figure 6.12 shows this linear relation for three binder types (Portland cement concrete, fly ash cement and slag cement concrete).

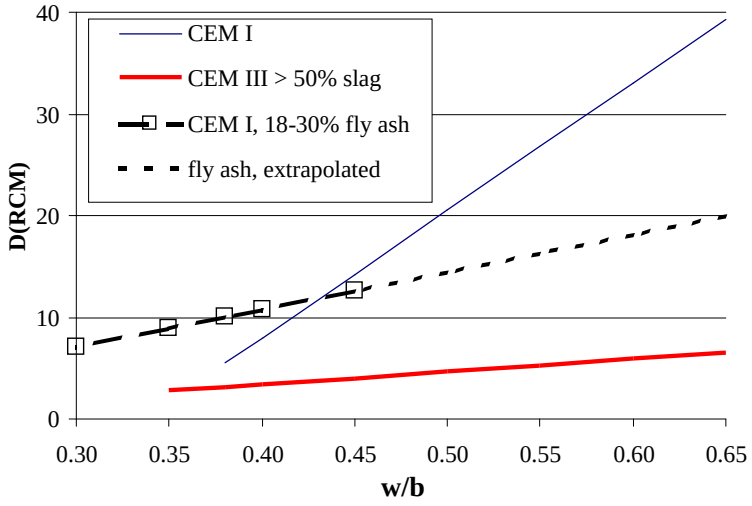

Figure 6.12: Correlation between w/b and D_{RCM} values at about 28 days; all values × 10^{-12} m^2/s [CUR-Bouw&Infra 2009; van Breugel et al. 2009]

In this research it is found that this linear relationship between the D_{RCM} values and w/b ratio for Portland cement concrete and fly ash concrete also applies at later ages of concrete. This is shown in Figure 6.13 and 6.14, respectively. The linear regression equations and the values of R^2 for Portland cement concrete and fly ash concrete are listed in Table 6.3 and 6.4.

For Portland cement concrete the D_{RCM} values depend on the w/c ratio. This dependency remains during the whole period from 28 days to 3 years (see Figure 6.13 and Table 6.3).

For the concrete mixture made with 30% fly ash the D_{RCM} values strongly depend on the w/b ratio at an age of 28 days as well (Figure 6.14). At 28 days the D_{RCM} values increase significantly from 15 ×10^{-12} m^2/s to 31 ×10^{-12} m^2/s with increasing w/b ratio from 0.4 to 0.6. With increasing age of the concrete the effect of the w/b ratio on the D_{RCM} values of fly ash concrete turns out to be less pronounced (Table 6.4). After 1 year the D_{RCM} value of fly ash concrete with 30% fly ash changes *from 0.8×10^{-12} m^2/s to 2.7 ×10^{-12} m^2/s* with increasing w/b ratio. It indicates that at later ages fly ash concrete made with 30% fly ash still has a good resistance to chloride ingress at a high w/b of 0.6. It is emphasized here that prolonged wet curing is essential for fly ash concrete in order to benefit from the pozzolanic reaction of fly ash.

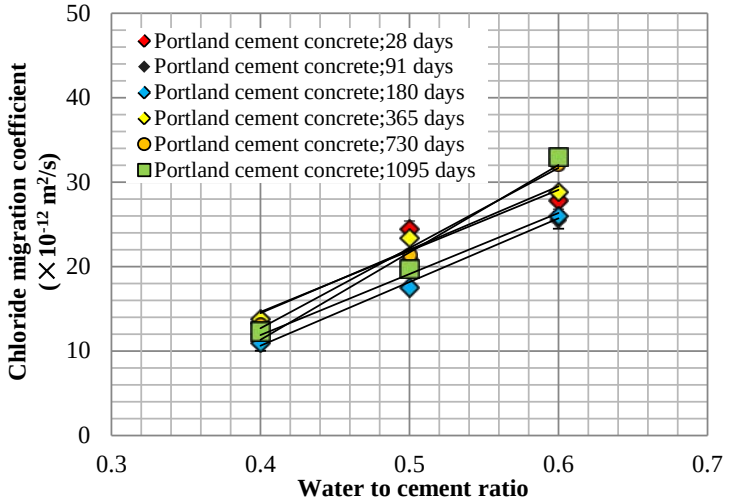

Figure 6.13: Linear relation between the D_{RCM} values and w/c ratio for Portland cement concrete at ages from 28 to 1095 days

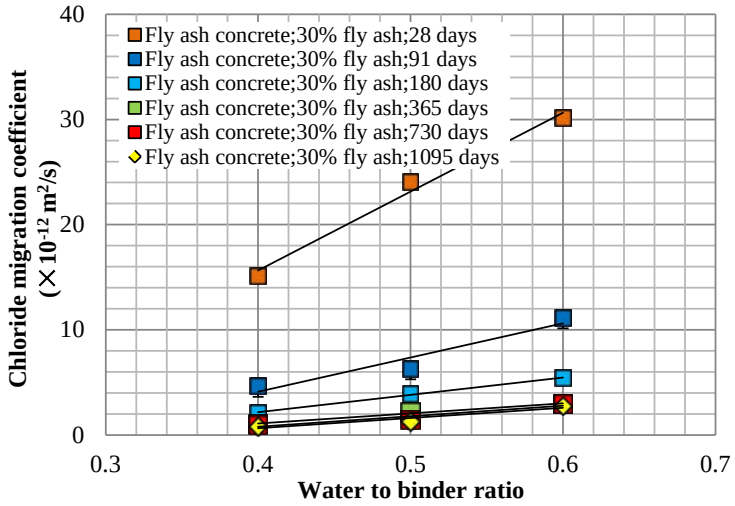

Figure 6.14: Linear relation between the D_{RCM} values and w/b ratio for fly ash concrete (FA30) at ages from 28 to 1095 days

Table 6.3: The linear regression equations and R^2 for Portland cement concrete

OPC / Ages (days)	Linear equation	R^2
28	D_{RCM} = 75.1(w/c ratio) - 15.5	0.9751
91	D_{RCM} = 72.5(w/c ratio) - 17.1	0.9590
180	D_{RCM} = 75.4(w/c ratio) - 19.5	0.9946
365	D_{RCM} = 75.1(w/c ratio) - 15.5	0.9751
730	D_{RCM} = 95.0(w/c ratio) - 25.3	0.9945
1095	D_{RCM} = 103.6(w/c ratio) - 30.1	0.9745

Table 6.4: The linear regression equations and R^2 for fly ash concrete (FA30)

FA30 / Ages (days)	Linear equation	R^2
28	D_{RCM} = 75.0(w/b ratio) - 14.4	0.9877
91	D_{RCM} = 32.5(w/b ratio) - 8.9	0.9261
180	D_{RCM} = 16.6(w/b ratio) - 4.5	0.9978
365	D_{RCM} = 9.5(w/b ratio) - 2.7	0.9868
730	D_{RCM} = 9.9 (w/b ratio) - 3.2	0.9113
1095	D_{RCM} = 9.8(w/b ratio) - 3.3	0.9259

6.4 Discussions

Based on the above obtained RCM-results, the following issues will be discussed in more detail:

- Possible reasons for the difference of the evolution of the D_{RCM} values with time between Portland cement concrete and fly ash concrete (Chapter 7).
- The discussions of the ageing factor in view of service life predictions of concrete structures (Chapter 8).
- Factors influencing the resistance of fly ash concrete to chloride ingress (Par. 6.4.1).

6.4.1 Factors affecting the resistance of fly ash concrete to chloride penetration

The results of the RCM tests show that fly ash concrete has better resistance against chloride penetration than Portland cement concrete at ages beyond about 28 days. This can be explained by differences in the pore structure of Portland cement paste and blended cement paste (as mentioned in chapter 4). In this section the correlation between connectivity of the pores and the chloride migration coefficient is shown. Special attention will be paid to the role of ink-bottle pores, although the ink-bottle pores are considered ineffective to the permeability of paste, as discussed in chapter 4 and 5.

6.4.1.1 Correlation between connectivity of the pores and chloride migration coefficient

The correlation between the chloride migration coefficient D_{RCM} and connectivity of the pores for different fly ash-blended mixtures is shown in Figure 6.15. As observed the D_{RCM} values increase with increasing connectivity of the pores. As discussed in chapter 4, the pore network of blended cement paste is refined by the reaction products of fly ash. The connectivity of the pores of blended cement paste decreases (particularly after 180 days), thus improving the resistance of fly ash concrete to chloride penetration.

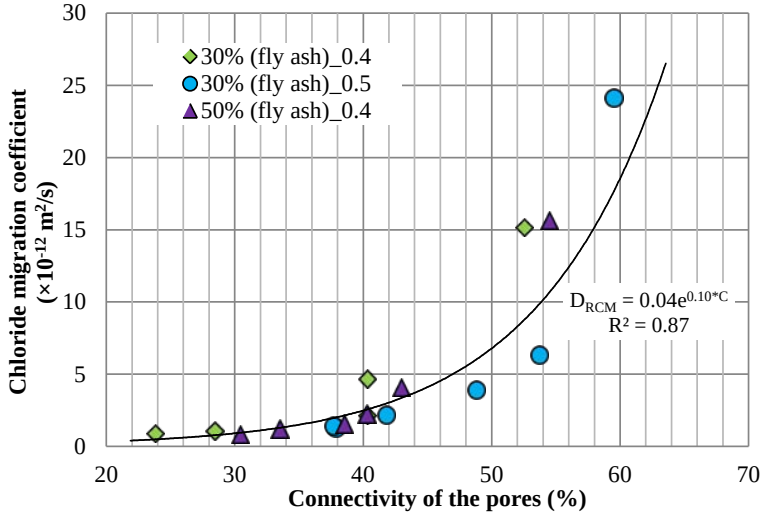

Figure 6.15: The correlation between the D_{RCM} values and connectivity of the pores for binary systems

6.4.1.2 Effect of ink-bottle porosity on resistance to chloride penetration

The ink-bottle porosity represents the pore volume that can only be reached via narrow entrances. When the chloride ions diffuse (or migrate) through a continuous pore to which ink-bottle pores are connected, the effect of ink-bottle pores on chloride transport varies with the concentration of chloride ions in the ink-bottle pores. Two stages can be distinguished (see Figure 6.16):

1) ***Initial stage*** *– The concentration of chloride ions in the ink-bottle pores is less than that in the continuous pore (see Figure 6.16 a).* In this stage chloride ions can diffuse from the continuous pores to the ink-bottle pores. As a result the concentration of chloride ions in the continuous pores decreases.
2) ***Later stage*** *– The concentration of chloride ions in the ink-bottle pores is equal to that in the continuous pore (see Figure 6.16 b).* In this stage the ink-bottle pores will not absorb more chloride ions from the continuous pores. In this period the effect of ink-bottle pores on chloride transport is negligible.

In chapter 4 it was found that fly ash blended cement paste has a higher ink-bottle porosity than pure Portland cement paste at ages beyond 28 days (see Figure 4.21). As suggested above, the resistance to chloride penetration is influenced by the ink-bottle pores, *but* only at initial stage when the ink-bottle pores are able to absorb chloride ions.

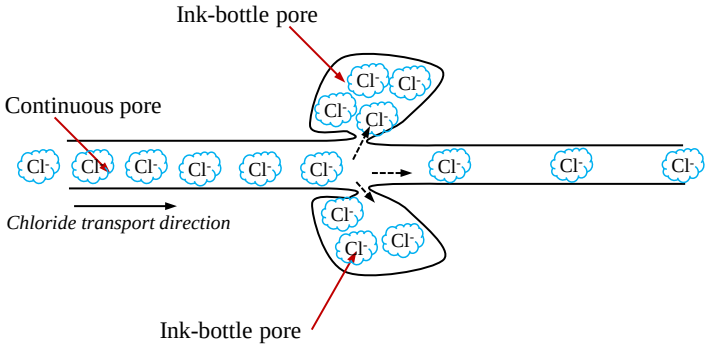

(a) Initial stage. Cl^- concentration in ink-bottle pores < Cl^- concentration in capillary pores

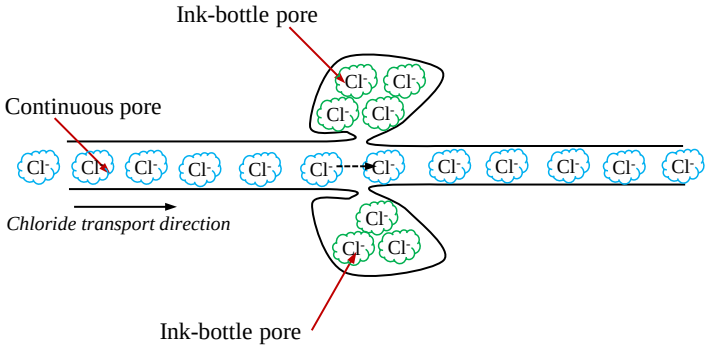

(b) Later stage. Cl^- concentration in ink-bottle pores = Cl^- concentration in capillary pores

Figure 6.16: The transport of chloride ions in a continuous pore to which ink-bottle pores are connected (a) initial stage; (b) later stage

6.5 Concluding Remarks

In this chapter RCM tests were carried out in order to determine the resistance of Portland cement concrete and fly ash concrete to chloride penetration at ages up to 3 years. The major conclusions of this chapter are as follows:

Portland cement concrete

1. Under moist curing conditions the D_{RCM} values of Portland cement concrete made with different w/c ratios (0.4, 0.5 and 0.6) decrease with time from 28 to 180 days. After that the D_{RCM} values increase and then turn to decrease again after around 1 year (Figure 6.6). The possible reasons for this behavior will be discussed in chapter 7.

Fly ash concrete

1. At ages beyond about 28 days the concrete mixtures made with 30% and 50% fly ash (w/b=0.4) have better resistance against chloride penetration than Portland cement concrete. With increasing time the effect of fly ash on the resistance of concrete (w/b=0.4, 0.5 and 0.6) to chloride ingress becomes even more pronounced (Figures 6.7-6.9).

2. At ages up to 3 years concrete mixtures with fly ash content 30% and 50% have similar D_{RCM} values (see Figure 6.7 and 6.8). It holds for mixtures with w/b=0.4 and 0.5.

3. At ages beyond 28 days fly ash concrete has a higher ink-bottle porosity than Portland cement concrete. The effect of ink-bottle porosity on chloride transport varies with the time of exposure. After first exposure to chloride the ink-bottle pores absorb chloride ions, resulting in a decrease of the concentration of chloride ions in the effective capillary pores. After a certain time the pore solution of ink-bottle pores is saturated with chloride ions, and the effect of ink-bottle porosity on chloride transport is negligible.

References

[1] Rilem Report 38: Durability of self-compacting concrete. Edited by G. De Schutter and K. Audenaert. April 2007.

[2] Maage, M., Helland, S., Poulsen, E., Vennesland, O., Carlsen, J.E., 1996. Service life prediction of existing concrete structures exposed to marine environment. ACI Materials Journal, 1996; 93(6): 602-608.

[3] Neville, A. M., 1995. Properties of concrete. 4th and final Ed., Longman's, London.

[4] NT Build 492, 1999. Concrete, mortar and cement-based repair materials: chloride migration coefficient from non-steady-state migration experiments. UDC 691.32/691.53/691.54. Approved 1999-11.

[5] Van Breugel, K., Polder, R., 2009. Probability-based service life design of structural concrete, in Proc. 2nd Int. RILEM Workshop on Concrete Durability and Service Life Planning-ConcreteLife'09, Haifa, Israel.

[6] van der Wegen Gert, Polder Rob B., van Breugel Klaas, 2012. Guideline for service life design of structural concrete - A performance based approach with regard to chloride induced corrosion. HERON, 2012; 57 (3): 153-167.

Chapter 7

Discussion of Chloride Migration Coefficient of Concrete[6]

7.1 Introduction

Wet curing contributes to the reduction of the porosity and drying shrinkage of concrete, and thus achieving high strength *[Neville 1995]* and good resistance to physical or chemical attacks in aggressive environments *[Safiudeen 2007]*. In theory, the resistance of concrete to chloride penetration increases with increasing age of the concrete due to densification of the microstructure. However, as discussed in chapter 2 and chapter 6 (see Figure 2.8 and 6.6), the D_{RCM} values of Portland cement concrete increase after a certain age (around months) when the concrete specimens are cured under moist conditions (fog room: 20 °C, 100% humidity or under water: 20 °C). This behavior has not received much attention by researchers in the past. In order to be sure about the reliability of long-term predictions of the performance of Portland cement concrete, however, it is necessary to know the possible reasons why the resistance of Portland cement concrete to chloride penetration decreases after a certain time, even under a proper curing condition.

In this chapter two possible reasons for the decrease of the resistance of Portland cement concrete to chloride penetration are discussed:

1. Leaching of calcium hydroxide (CH) Par. 7.3
2. Delayed ettringite formation (DEF) Par. 7.4

7.2 Survey of the Results of RCM Test

7.2.1 RCM-results for Portland cement concrete

Figure 7.1 summarizes the D_{RCM} values of Portland cement concrete at ages up to 3 years. These results were presented earlier in chapter 2 and chapter 6. For the presented results the initial D_{RCM} value at 28 days varied from 6.2×10^{-12} m^2/s to 27.8×10^{-12} m^2/s. This variation is due to the difference of the type of Portland cement (*CEM I 32.5 (R), ASTM type I, CEM I*

[6] This chapter is partially based on:

1) Zhuqing Yu, Guang Ye, Martin Hunger, Reinier van Noort. Discussion of the evolution of the chloride migration coefficient of Portland cement concrete tested by the Rapid Chloride Migration (RCM) test at long-term curing periods up to 5 years. CONSEC'13 - 7th International Conference on Concrete under Severe Conditions – Environment and Loading. 23 - 25 September 2013, Nanjing.

2) Zhuqing Yu, Guang Ye, Klaas van Breugel. Ageing of Portland cement concrete cured under moist conditions. 1st International conference on Ageing of Materials and Structures (AMS'14). 26-28 May 2014, Delft, the Netherlands.

42.5 R/N) and the w/c ratio of the mixtures (*from 0.32 to 0.7*). The data gathered in Figure 7.1 suggests that the D_{RCM} values mostly decrease from 28 days to 180 days and then increase. The reasons for this increase are still unknown. After a certain age of the concrete (around 1 year) the D_{RCM} values decrease again.

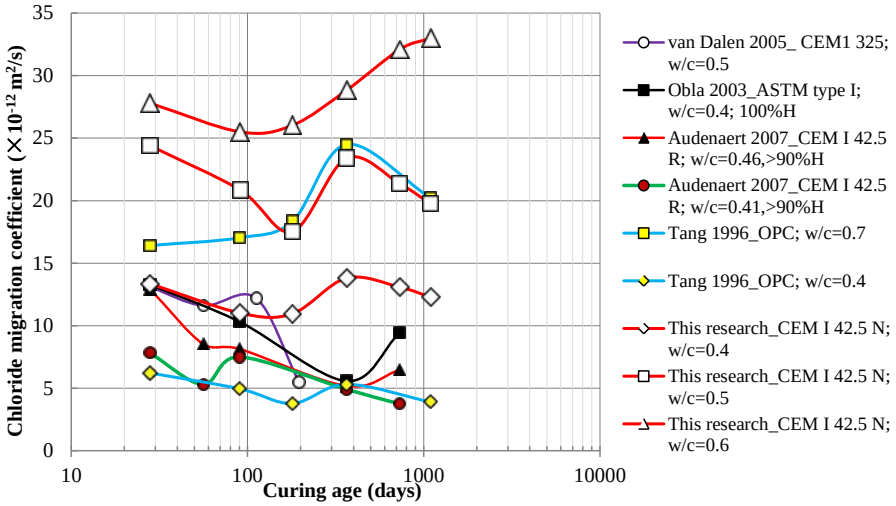

Figure 7.1: The relationship between the chloride migration coefficient, i.e. D_{RCM} values, of Portland cement concrete and time [Tang 1996; Obla 2003; van Dalen 2005; Audenaert 2007; this work]

7.2.2 RCM-results for fly ash concrete

Figure 7.2 presents the development of the chloride migration coefficient of fly ash concrete with time, including the experimental results obtained from chapter 6 and those of Valcke *[Valcke 2012]*. Replacement percentage ranges from 30% to 50%. It is clear that the D_{RCM} values of fly ash concrete decrease gradually at ages from 28 days to 1 year, with little changes at later ages.

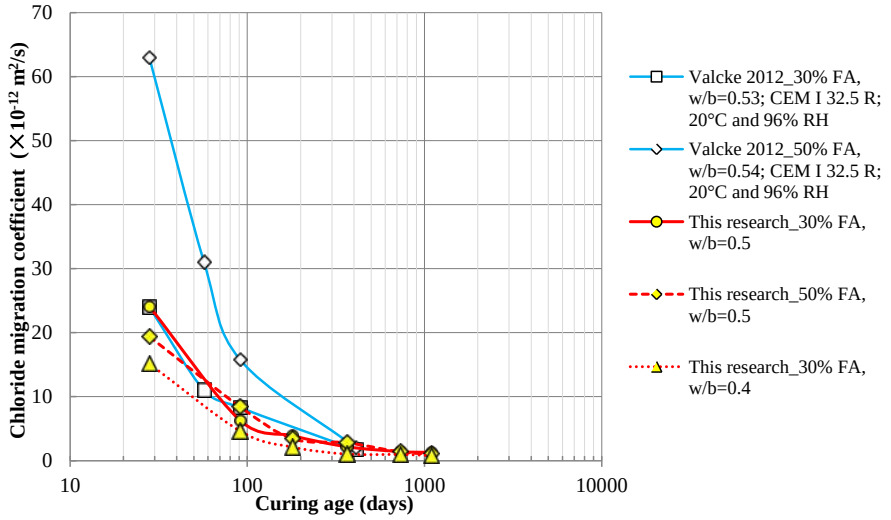

Figure 7.2: The relationship between the chloride migration coefficient, i.e. D_{RCM} values, of fly ash concrete and time [Valcke 2012; Our test results] (Note: FA: fly ash)

7.2.3 Short summary

From Figure 7.1 and 7.2 it can be seen that the evolution of the RCM-results with time for fly ash concrete is different from that for Portland cement concrete. In the following sections the possible reasons for the increase of the D_{RCM} values of Portland cement concrete after about 180 days are discussed, including the leaching of calcium hydroxide and the delayed ettringite formation in concrete.

7.3 Leaching of Calcium Hydroxide

7.3.1 General

Calcium hydroxide (CH) is the most soluble and vulnerable hydration product in hardened cement paste *[Neville 1995]*. The leaching of CH increases the porosity of paste thus making the concrete more vulnerable to further leaching and chemical attack *[Gérard 1996, 1999, 2002; Carde 1997; Torrenti 1999; Ekström 2001]*. This leaching might result in a decrease of the resistance of Portland cement concrete to chloride penetration.

The determination of CH content in concrete is a simple way to assess the leaching of CH. In the following sections the test method is mentioned. Then the CH content in Portland cement concrete is discussed.

7.3.2 Test method

The CH content of concrete was determined by thermogravimetric analysis (TGA). The testing procedure of TGA has been described in chapter 3. The concrete samples used for TGA tests are from those prepared for RCM tests as mentioned in chapter 6.

7.3.3 CH content in concrete

Figure 7.3 shows the TG curves for Portland cement concrete ($w/c = 0.6$) at ages of 2 and 3 years. Based on the method described in Figure 3.10 (chapter 3) the calculated CH content is 11.07% for 2 years old mixture and 11.09% for 3 years old mixture. From these results it can be seen that the CH content in Portland cement concrete does not decrease with increasing age of the concrete from 2 to 3 years. The values of the CH content suggest that the leaching of CH does not take place in Portland cement concrete when it is cured in moist conditions. It is not the reason for the increase of the D_{RCM} values of Portland cement concrete after an age of 180 days.

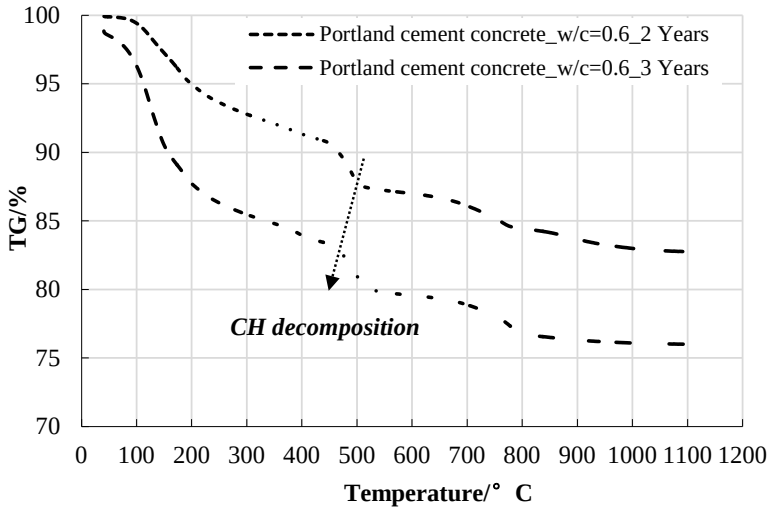

Figure 7.3: TG data of Portland cement concrete at different ages

7.4 Delayed Ettringite Formation (DEF)

7.4.1 General

As mentioned in the introduction (section 7.1) DEF is considered another possible reason for the decrease of the resistance of Portland cement concrete to chloride ingress at later stages. That is because DEF results in cracks *[Diamond 1996]* and increases probability of chloride ingress. In the following sections, the test methods and sample preparation are firstly presented. The mechanisms of early ettringite formation (EEF) and delayed ettringite formation (DEF) are discussed.

7.4.2 Test methods and sample preparation

In order to study DEF in concrete two techniques were used, *i.e.* X-ray diffraction (XRD) analysis and scanning electron microscopy equipped with energy dispersive spectroscopy (SEM/EDS). XRD analysis was used to identify the hydration products of concrete. SEM was used to observe the morphology of hydration products by performing secondary electron (SE) mode (for instance, needle-shaped ettringite in concrete). SEM/EDS technique was used to obtain the chemical analysis of the selected area or spot analyses of concrete specimens. Details of the test methods of XRD and SEM were also described in chapter 3.

The concrete specimens for SE-image observation were split into several small pieces by hammer and dried in a vacuum machine. After drying (around 2 days) carbon coating was applied on the surface of samples to create a conductive layer in order to avoid charging of concrete samples and to improve the SE signal. The carbon coated concrete samples and coating machine are shown in Figure 7.4.

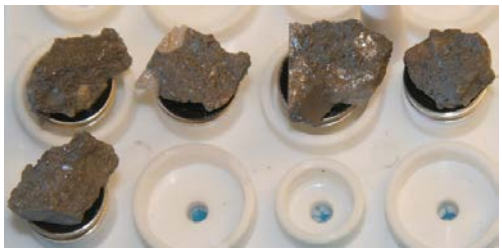

(a)

(b)

Figure 7.4: Carbon-coated samples for SE image observations (a) and carbon coating instrument (b)

7.4.3 Mechanism of early ettringite formation

In a hydrating Portland cement system, ettringite is formed by the reaction of tricalcium aluminate (C_3A) with calcium sulfate (gypsum) in the first few hours after mixing with water *[Collepardi 2001]*. The chemical reaction is shown in Equation 7.1.

$$\underset{C_3A}{3CaO \cdot Al_2O_3} + \underset{Gpysum}{3CaSO_4 \cdot 2H_2O} + 26H_2O \rightarrow \underset{\textbf{\textit{Ettringite}}}{(3CaO \cdot Al_2O_3) \cdot 3CaSO_4 \cdot 32H_2O} \quad (7.1)$$

The formation of ettringite at early age does not cause any significant localized disruptive action since this reaction occurs in a plastic mixture *[Collepardi 2001]*. Once all sulfate (gypsum) is used up ettringite reacts with remaining C_3A and finally converts into monosulphoaluminate (AFm), Equation 7.2 *[Taylor 1997]*:

$$\underset{\textbf{\textit{Ettringite}}}{(3CaO \cdot Al_2O_3) \cdot 3CaSO_4 \cdot 32H_2O} + \underset{C_3A}{2(3CaO \cdot Al_2O_3)} + 4H_2O \rightarrow \underset{AFm}{3(3CaO \cdot Al_2O_3) \cdot CaSO_4 \cdot 12H_2O} \quad (7.2)$$

Normally, most of the sulfate in the cement is consumed to form ettringite at early ages.

7.4.4 Mechanism of delayed ettringite formation

At later stages (after several months or years) ettringite can form again if a new source of sulfate becomes available in the pore solution of the paste *[Stark 1999; Collepardi 2001]*. This is so called delayed ettringite formation (DEF). The chemical reaction is given with Equation 7.3:

$$\underset{AFm}{(3CaO \cdot Al_2O_3) \cdot CaSO_4 \cdot 12H_2O} + 6Ca(OH)_2 + \textbf{\textit{8(CaSO}}_{\textbf{\textit{4}}} \textbf{\textit{} \cdot 2H}_{\textbf{\textit{2}}}\textbf{\textit{O)}} \rightarrow \underset{\textbf{\textit{Ettringite}}}{3(3CaO \cdot Al_2O_3) \cdot 3CaSO_4 \cdot 32H_2O} \quad (7.3)$$

Table 7.1: Molar volume of each substance in Equation 7.3

	Chemical formula	Molar Ratio *Al/S*	Molar Volume (cm^3/mol)
Ettringite (AFt)	$(3CaO \cdot Al_2O_3) \cdot 3CaSO_4 \cdot 32H_2O$	0.67	735
Monosulfoaluminate (AFm)	$(3CaO \cdot Al_2O_3) \cdot CaSO_4 \cdot 12H_2O$	2	313
Gypsum	$CaSO_4 \cdot 2H_2O$	-	74.2
Portlandite	$Ca(OH)_2$	-	33.1

Table 7.1 shows the molar volume of each substance in Equation 7.3. Based on this table the molar volume change of the delayed ettringite formation (Equation 7.3) is shown in Equation 7.4. This equation indicates that the produced ettringite occupies more space than the reactants, around 2 times more. This type of formation of ettringite causes detrimental expansion and cracks in the hardened concrete *[Diamond 1996, Collepardi 2001]*.

$$\begin{aligned} &\textit{Molar volume of reactants}: && (313+6\times 33.1+8\times 74.2)\ cm^3/mol = \mathbf{1105.2}\ cm^3/mol \\ &\textit{Molar volume of reaction product}: && (3\times 735)\ cm^3/mol = \mathbf{2205}\ cm^3/mol \end{aligned} \tag{7.4}$$

7.4.5 Delayed ettringite formation in Portland cement concrete

In this section the secondary electron (SE) image observations and XRD tests are carried out to identify the ettringite formation in concrete. Besides, the conditions for DEF in concrete are also discussed in this section.

7.4.5.1 Identification of ettringite in Portland cement concrete

Figure 7.5 shows the SE image of Portland cement concrete (*w/c=0.4*) at an age of 2 years. The needle-shaped ettringite crystals can easily be observed. An energy dispersive spectroscopy (EDS) analysis is made at the spot of the red square. The EDS spectrum is shown in Figure 7.6. The molar ratio of Al/S is around 1.38:1, which is in the range from 0.67 (molar ratio of Al/S of ettringite) to 2 (molar ratio of Al/S of monosulfatealuminate, AFm) (see Table 7.1). This indicates that the selected area probably includes both ettringite and AFm phases. In Figure 7.6 the Si element peak is also detected, probably from C-S-H phase. Hence, this area might be a mixture of AFm, ettringite and C-S-H. Furthermore, micro-cracks with a width of 3-5 μm can also be observed. Ettringite and micro-cracks are also observed in the images collected from other concrete samples (*w/c=0.6*) at an age of 3 years as shown in Figure 7.7.

Figure 7.8 shows the XRD patterns of Portland cement concrete (*w/c=0.4*) at an age of 215 days and 2 years. At 215 days the characteristic peaks of quartz (Q: from aggregate), portlandite (CH: hydration product) and calcite ($CaCO_3$: from limestone powder, *see section 3.5.1*) are clearly detected. At an age of 2 years another two characteristic peaks are also observed. They are ettringite ($2\theta = 9.09°$) and monocarbonate ($2\theta = 11.7°$).

From the results of XRD test and SE image observations it is clear that ettringite forms in Portland cement concrete at later ages and that formation of ettringite is then accompanied with micro crack formation.

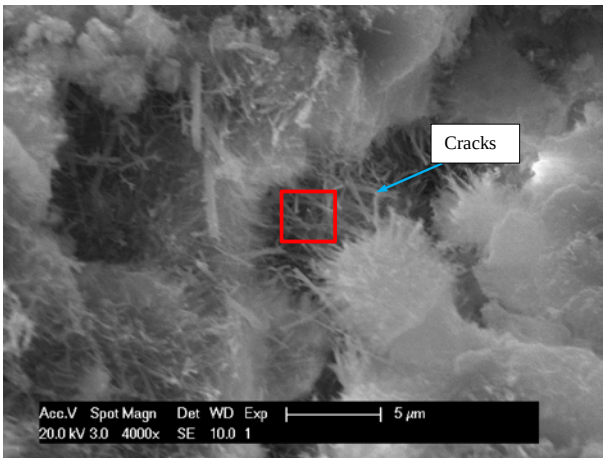

Figure 7.5: SE image of Portland cement concrete (w/c=0.4) at an age of 2 years (4000×)

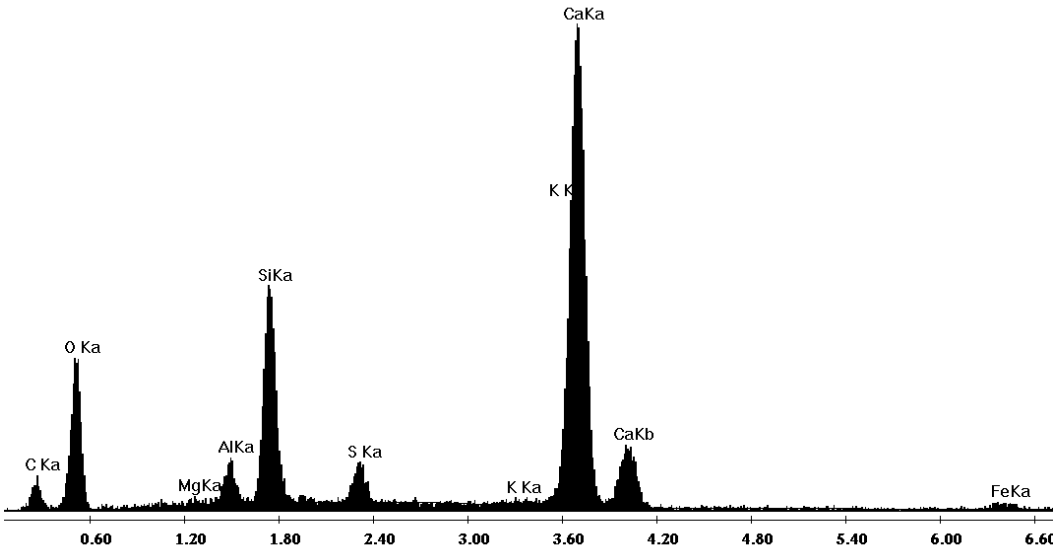

(a) EDS spectrum

Element	C	O	Si	S	Ca	Al	Mg	Fe	K
Wt %	10.80	37.37	10.03	1.98	34.97	2.30	0.55	1.56	0.44
Molar ratio: Al : S=1.38:1									

(b) element analysis

Figure 7.6: EDS spectrum of selected area (a) and element analysis (b)

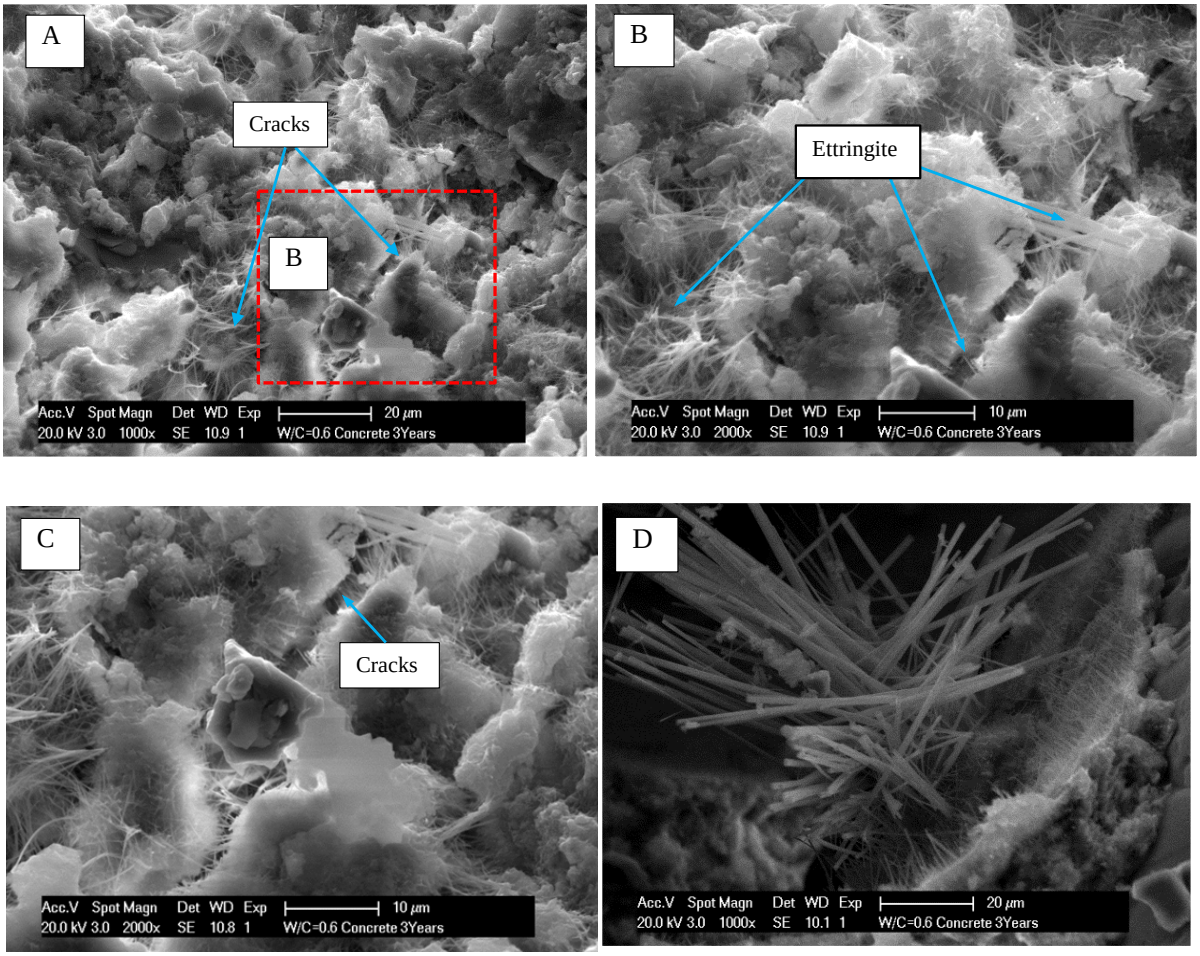

Figure 7.7: SE images of Portland cement concrete: w/c=0.6 at an age of 3 years A: 1000×; B: 2000×; C: 2000×; D: 1000×

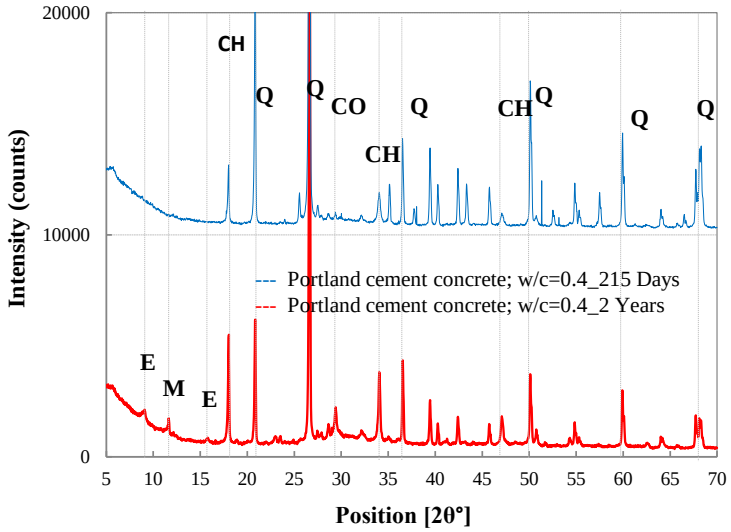

E: ettringite; Q: SiO_2; CH: $Ca(OH)_2$; CO: $CaCO_3$; M: monocarbonate

Figure 7.8: XRD patterns of Portland cement concrete

7.4.5.2 Conditions for the formation of delayed ettringite

As mentioned in section 7.4.4 delayed ettringite formation in concrete normally requires a new source of sulfate in the pore solution of the paste. It has been proposed by Klemm *[Klemm 1990]* that also the presence of limestone powder ($CaCO_3$) in concrete can result in the formation of ettringite if the concrete is cured in wet (moist) conditions. Under moist conditions $CaCO_3$ can slowly dissolve and subsequently react with any calcium monosulfoaluminate hydrate or calcium aluminate hydrate to form ettringite and monocarbonate. The chemical reaction of $CaCO_3$ with monosulfate (AFm) is *[Klemm 1990; Taylor 1997]*:

$$\underset{AFm}{3(3CaO\cdot Al_2O_3)\cdot CaSO_4\cdot 12H_2O} + \mathbf{2CaCO_3} + 18H_2O \rightarrow \underset{Monocarbonate}{2(3CaO\cdot Al_2O_3)\cdot CaCO_3\cdot 11H_2O} + \underset{\mathbf{Ettringite}}{(3CaO\cdot Al_2O_3)\cdot 3CaSO_4\cdot 32H_2O} \quad (7.5)$$

Table 7.2 shows the solubility product of calcite, AFm, monocarbonate and ettringite as determined by Zhang *[Zhang 1980]*. The reaction products *ettringite and monocarbonate* have a lower solubility product and are, *therefore*, more stable products. The reaction of $CaCO_3$ with AFm, *Equation 7.5*, do happen.

Table 7.2: Solubility products of calcite, AFm, monocarbonate and ettringite [Zhang 1980]

Salt		Solubility product at 25 °C
Calcite	$CaCO_3$	8.7×10^{-9}
Monosulfoaluminate (AFm)	$(3CaO\cdot Al_2O_3)\cdot CaSO_4\cdot 12H_2O$	1.7×10^{-28}
Monocarbonate	$(3CaO\cdot Al_2O_3)\cdot CaCO_3\cdot 11H_2O$	1.4×10^{-30}
Ettringite	$(3CaO\cdot Al_2O_3)\cdot 3CaSO_4\cdot 32H_2O$	4.1×10^{-40}

It follows from the above consideration that two factors result in DEF in concrete:

1) *The concrete should contain $CaCO_3$;*
   In section 3.5.1 it was mentioned that commonly used Portland cement is allowed to contain an amount of limestone powder ($CaCO_3$) up to 5%. From the results of XRD tests (see Figure 7.8) it can be seen that the Portland cement used in this study contains $CaCO_3$ and the reaction of $CaCO_3$ with AFm as shown in Equation 7.5 really occurs.

2) *The concrete must be cured in wet (moist) conditions.*
   From Equation 7.5 it can be seen that the reaction of $CaCO_3$ with AFm in Portland cement concrete requires water. To further evaluate the importance of moist conditions, the XRD patterns of Portland cement concrete and Portland cement paste are compared (see Figure 7.9 and Figure 7.10). The paste specimens were cured in sealed plastic bottles (20 ºC) and the concrete specimens were cured in moist conditions (a fog room; 20°C). From these two figures it can be seen that at the age of 2 years and 3 years, the ettringite peak cannot be observed in the XRD patterns of the sealed cured Portland cement paste. The moist cured concrete samples, *however*, do contain ettringite.

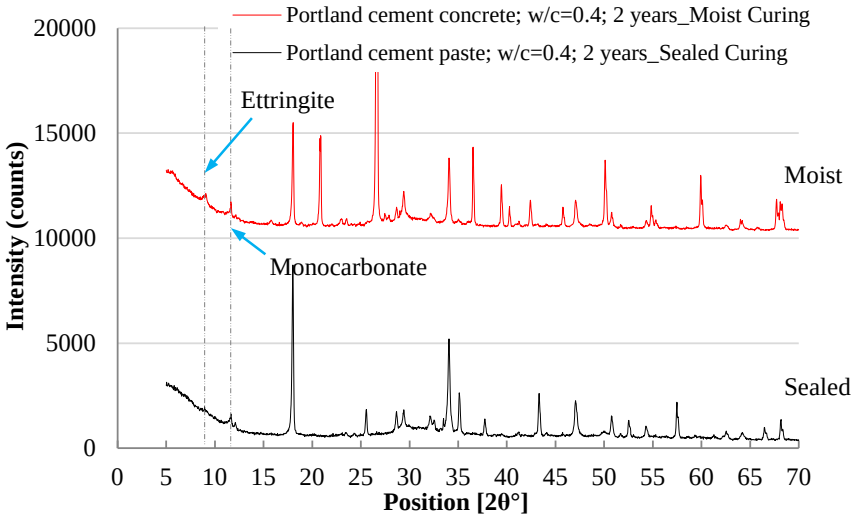

Figure 7.9: XRD patterns of Portland cement paste (w/c=0.4) with sealed curing compared with Portland cement concrete with moist curing at 2 years

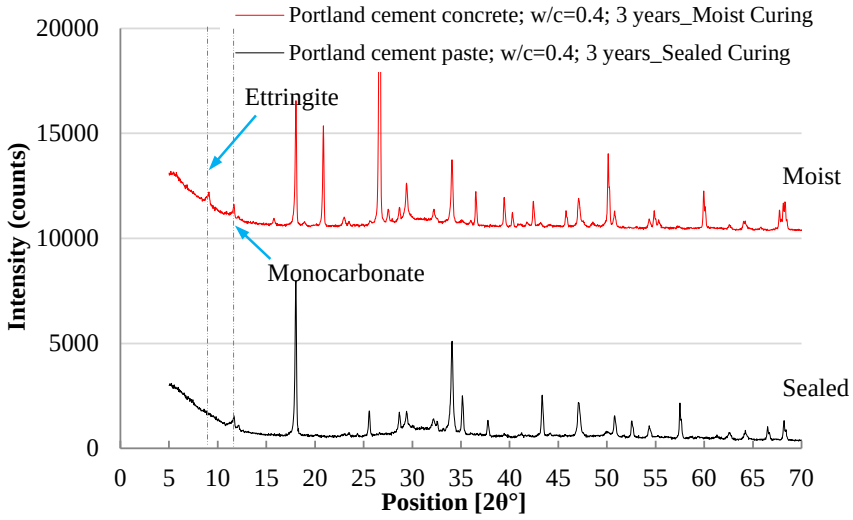

Figure 7.10: XRD patterns of and Portland cement paste (w/c=0.4) with sealed curing compared with Portland cement concrete with moist curing at 3 years

The possibility of thaumasite formation (TF)

It should be mentioned here that an important question is whether we are dealing with DEF or thaumasite[7] formation (TF) since in XRD patterns, the main characteristic peak of thaumasite (2θ = 9.2°) *[Pipilikaki 2008]* is very close to that of ettringite (2θ = 9.09°) *[Möschner 2007]*. Regarding to TF in the presence of limestone, it is commonly believed that TF occurs at low temperatures (*e.g.* 5°C, 10°C) when concrete is exposed to carbonate and sulfate *[Van Aardt 1975; Crammond 1985, Pipilikaki 2008]*. Brown, however, reported that TF can also occur at

[7] Thaumasite: $[Ca_3Si(OH)_6{\cdot}12H_2O]$ (SO_4) (CO_3), has a structure similar to that of ettringite, $(3CaO{\cdot}Al_2O_3)$ $3CaSO_4{\cdot}32$ H_2O, with Si^{4+} replacing Al^{3+} and SO_4^{2-} and CO_3^{2-} groups in the channel sites *[Taylor 1995]*. Thaumasite can form in concrete by reaction of C-S-H with sulfates in the presence of carbonate ions, *i.e.* thaumasite formation (TF). The replacement of C-S-H by thaumasite results in the softening of the cement paste matrix into a white, mushy incohesive mass *[Crammond 2003]*. TF only occurs in very wet environments and the rate of TF is increased at low temperatures. It was reported by Hooton *[Hooton 2002]* that in all of the laboratory and field cases reported, the sulfates for this reaction come from external sources.

ambient temperature, *e.g.* 23°C (exposed to sulfate solution) *[Brown 2002]*. The formation of thaumasite in cement paste (concrete) can be described with Equation 7.6 *[Heinz 2003]*:

$$C-S-H+CaCO_3+CaSO_4+xH_2O \rightarrow CaSiO_3 \cdot CaSO_4 \cdot CaCO_3 \cdot 15H_2O \quad (7.6)$$

According to Hartshorn *[Hartshorn 1998]* thaumasite possibly forms in concrete even without the presence of external sulfate. In those cases some sulfates should have been present with mixtures already. However in the presence of low sulfate concentrations only a few cases of TF were reported *[Schmidt 2007]*. Based on the experimental data as well as thermodynamic modelling results by Schmidt *[Schmidt 2008]* thaumasite can only form at molar SO_3/Al_2O_3 ratio in the cement system higher than 3. For lower amounts of SO_3 only ettringite forms. In this study the molar ratio of SO_3/Al_2O_3 is 0.66 calculated from the data shown in Table 3.1. It means that thaumasite is not likely to be formed in this study.

7.4.5.3 Summary

Since DEF results in a change of the microstructure of cement paste, it is considered a possible reason for an increase of the D_{RCM} values of Portland cement concrete after an age of 180 days. The information presented in this section (7.4.5) shows that delayed ettringite formation occurs in Portland cement concrete when it contains limestone powder and when it is cured under moist conditions. In this study the possibility of thaumasite formation in Portland cement concrete is low.

At present, the use of limestone powder in cement is common in European countries. It brings technical, economic and ecological benefits. However, it appears that the addition of limestone powder in concrete may lead to the formation of delayed ettringite at later ages and decrease the resistance of Portland cement concrete to chloride penetration under moist conditions. It is recommended that more attention should be paid to the impact of limestone powder on the D_{RCM} values of Portland cement concrete when limestone powder is used in concrete mixtures.

7.4.6 Effect of fly ash on delayed ettringite formation

In fly ash concrete the pozzolanic reaction of fly ash consumes calcium hydroxide and forms calcium silicate hydrate, consolidating and densifying the microstructure of concrete. It is generally assumed that the presence of fly ash in concrete can minimize the probability of delayed ettringite formation (DEF) *[Fu 1996; Stark 1999; Dayarathn 2013]*. However, the mechanisms involved are still unclear. In this section the XRD tests and SE image observations are conducted to study the delayed ettringite formation in fly ash concrete. The same batch of cement (CEM I 42.5N) is used to prepare fly ash concrete mixtures. The fly ash concrete specimens are also cured under moist conditions.

7.4.6.1 Results of XRD and SE images

Figure 7.11 shows the XRD pattern of fly ash concrete at an age of the concrete of 3 years. In this figure the characteristic peak of ettringite is found. The SE images of fly ash concrete at an age of 3 years are presented in Figure 7.12 to Figure 7.14. In general, fly ash concrete has a dense microstructure as shown in Figure 7.12. In Figure 7.13, needle-shaped ettringite crystals are observed in voids. Furthermore, ettringite crystals are also observed in the voids left by the reaction of the fly ash particles as shown in Figure 7.14.

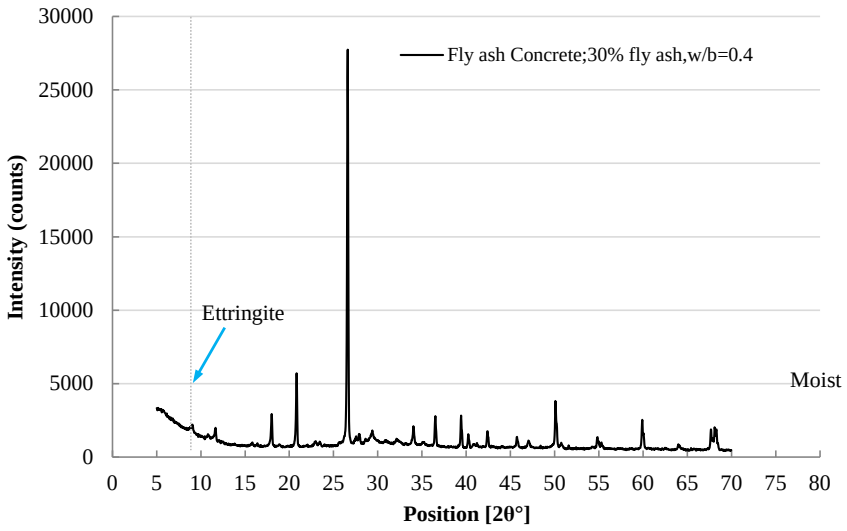

Figure 7.11: XRD pattern of fly ash concrete (30% fly ash; w/b=0.4) at 3 years

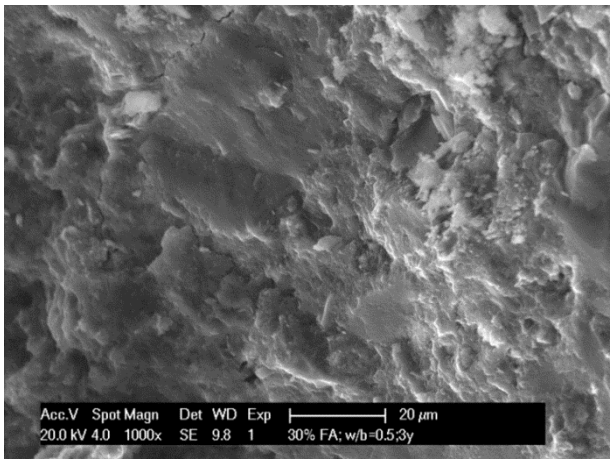

Figure 7.12: SE image of fly ash concrete (30% fly ash; w/b=0.5) 1000×

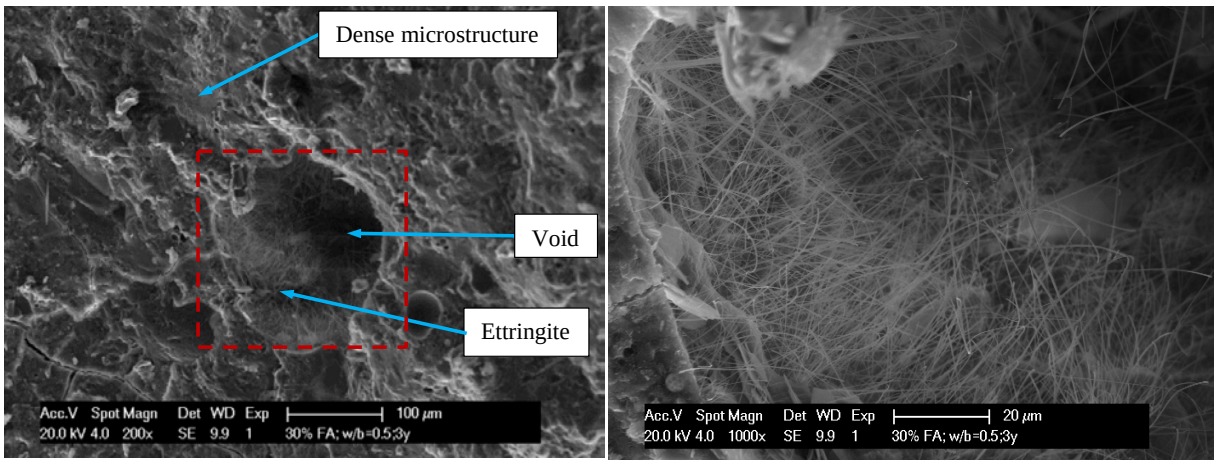

(a) 200 × *(b) 1000×*

Figure 7.13: SE images of fly ash concrete (30% fly ash; w/b=0.5) with Ettringite (a) 200×; (b) 1000×

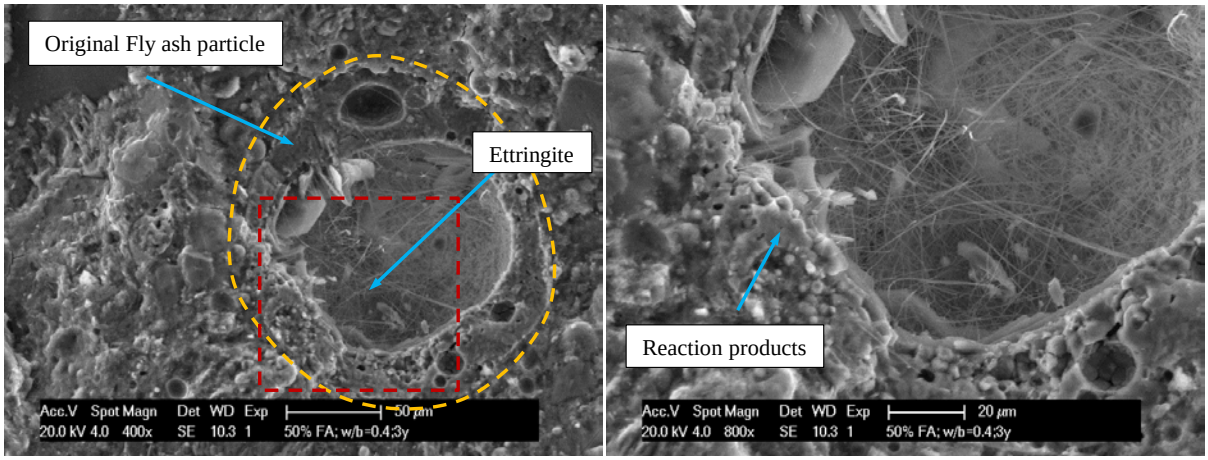

(a) 400 × *(b) 800 ×*

Figure 7.14: SE image of fly ash concrete (50% fly ash; w/b=0.4) with Ettringite (a) 400×; (b) 800×

7.4.6.2 Discussions

Based on the results of XRD tests and SE image observations, it is concluded that delayed ettringite formation also occurs in fly ash concrete. The ettringite tends to form in voids initially present in the paste and in the spaces left after the pozzolanic reaction fly ash particles (as mentioned in Figure 4.8). Since in fly ash concrete more space is present for the formation of delayed ettringite, the expansion due to DEF and an associated probability of the micro-cracking are obviously strongly mitigated.

7.5 Conclusions

In this chapter it was discussed *why the chloride migration coefficient of Portland cement concrete increases at later ages*. The transport of chloride in concrete is strongly related to the microstructure of the cement paste. Two possible reasons resulting in the change of the microstructure of paste, *i.e.* the leaching of CH and the delayed ettringite formation (DEF), were investigated. Meanwhile, fly ash concrete was tested for comparison. The following conclusions have been drawn from the present study:

Leaching of CH

1. When the concrete specimens are cured under moist conditions (in a fog room) over a long period, *viz.* 3 years, leaching of CH does not occur. Hence, the leaching of CH is not considered the reason for an increase of the D_{RCM} values of Portland cement concrete at later age.

Delayed ettringite formation

1. Delayed ettringite formation (DEF) occurs in Portland cement concrete when limestone powder (as filler) is blended with Portland cement clinker and when it is cured under moist conditions. DEF may result in a change of the microstructure of hydrated cement paste and an increase of D_{RCM} at later ages.

2. Ettringite forms in fly ash concrete at later ages. This ettringite is found in voids initially present in the paste and in the spaces left after the reaction of fly ash particles. Formation of ettringite in empty spaces explains why DEF in fly ash concrete does not lead to expansion and micro-cracking and an associated increase of the D_{RCM} values as observed for Portland cement concrete.

References

[1] Audenaert Katrien, Boel Veerle, De Schutter Geert, 2007. Chloride migration in self compacting concrete. CONSEC'07 Tours, France Concrete under Severe Conditions : Environment & Loading F. Toutlemonde et al. (eds)

[2] Brown Paul, Hooton R.D., Ettringite and thaumasite formation in laboratory concretes prepared using sulfate-resisting cements. Cement & Concrete Composites, 2002; 24: 361-370.

[3] Carde Christophe, François Raoul, 1997. Effect of the leaching of calcium hydroxide from cement paste on the mechanical and physical properties. Cement and Concrete Research, 1997; 27: 539-550.

[4] Collepardi M., 2001. Ettringite formation and sulfate attack on concrete. ACI special publication. 2001; 200: 21-38.

[5] Crammond NJ., 1985. Thaumasite in failed cement mortars and renders from exposed brickwork. Cement Concrete Research, 1985; 15:1039-1050.

[6] Crammond N.J. 2003. The thaumasite form of sulfate attack in the UK. Cement & Concrete Composites, 2003; 25: 809-818.

[7] Diamond S., 1996. Delayed ettringite formation-processes and problems. Cement and Concrete Composites, 1996; 18: 205-215.

[8] Ekström Tomas, 2001. Leaching of concrete-experiments and modelling. Report TVBM-3090. Lund institute of technology.

[9] Gérard, B., 1996. Contribution of the mechanical, chemical, and transport couplings in the long-term behaviour of radioactive waste repository structures', Ph.D. Thesis, Civil Engineering Department, Laval University, Quebec City, Canada / ENS Ca&an, France, 1996, (in French).

[10] Gérard, B., Pijaudier-Cabot, G., Le Bellego, C., 1999. Mechanical stability analysis of cement-based materials submitted to calcium leaching. In Proceedings of SMIP. The 15th Conference, Seoul, Korea, 1999; 79-90.

[11] Gérard B., Bellego C. Le, Bernard O., 2002. Simplified modelling of calcium leaching of concrete in various environments. Materials and Structures, 2002; (35): 632-640.

[12] Hartshorn, S. and Sims, I. 1998. "Thaumasite – a brief guide for engineers." Concrete, Vol. 32, pp. 24-27.

[13] Heinz D, Urbonas L., 2003. About thaumasite formation in Portland-limestone cement pastes and mortars-effect of heat treatment at 95 °C and storage at 5 °C. Cem Concr Compos, 2003; 25: 961-967.Hooton R. Doug, Thomas Michael D. A., 2002. The use of limestone in portland cements: effect on thaumasite form of sulfate attack. PCA R&D Serial No. 2658. 2002.

[14] Klemm, Waldemar A., Adams, Lawrence D., 1990. An investigation of the formation of carboaluminates, published in carbonate additions to cement, ASTM STP 1064, P. Klieger and R. D. Hooton, Eds., American Society for Testing and Materials, Philadelphia, 1990; 60-72.

[15] Möschner Göril, 2007. A thermodynamic approach to cement hydration: the role of retarding admixtures and Fe-minerals during the hydration of cements. A dissertation toETH ZURICH.

[16] Neville, A. M. Properties of concrete, 4th and final Ed., Longman's, London. 1995.

[17] Obla Karthik H., Hill Russell L., Thomas Michael D. A., Shashiprakash Surali G., Perebatova Olga., 2003. Properties of Concrete Containing Ultra-Fine Fly Ash. ACI Materials Journal, September-October 2003; 426-433.

[18] Pipilikaki P., Papageorgiou D., Teas Ch., Chaniotakis E., Katsioti M., 2008. The effect of temperature on thaumasite formation. Cement & Concrete Composites, 2008; 30: 964-969.

[19] Safiuddin Md., Raman S. N., Zain M. F. M., 2007. Effect of different curing methods on the properties of microsilica concrete. Australian Journal of Basic and Applied Sciences, 2007; 1(2): 87-95.

[20] Schmidt Thomas, 2007. Sulfate Attack and the Role of Internal Carbonate on the Formation of Thaumasite. EPFL, Swiss Federal Institute of Technology (EPFL), PhD thesis.

[21] Schmidt Thomas, Lothenbach Barbara, Romer Michael, Karen Scrivener, Rentsch Daniel, Figi Renato, 2008. A thermodynamic and experimental study of the conditions of thaumasite formation. Cement and Concrete Research, 2008; 38: 337-349.

[22] Stark Jochen, Bollmann Katrin, 1999. Delayed Ettringite Formation in Concrete. Bauhaus-University Weimar / Germany. Proc. Nordic Concr. Res. Mtg. Island, 1999; 4–28.

[23] Tang, L., 1996. Electrically accelerated methods for determining chloride diffusivity in concrete. Magazine of Concrete Research. 1996; 48(176): 173-179.

[24] Taylor HFW., 1997. Cement chemistry. London: Thomas Telford.

[25] Torrenti, J.M., Didry, O.,Ollivier, J.-P., Has, F., 1999. The degradation of concrete: couplings between cracking and chemical degradation. Hermes Science Press, Paris, Paris, 1999; 128-130, (in French).

[26] Valcke Siska L.A., Polder Rob B., Nijland Timo G., Leegwater Greet A., Visser1 J.H.M., van Vliet A.J. Bigaj, 2012. High filler concrete using fly ash -Chloride penetration and microstructure. HERON, 2012; 57(3): 169-184.

[27] Van Aardt JHF, Visser S., 1975. Thaumasite formation: A cause of deterioration of portland cement and related substances in the presence of sulphate. Cement Concrete Research, 1975; 5: 225-232.

[28] van Dalen Sander M., 2005. Experimenteel onderzoek naar de RCM-methode (In Dutch). Master Thesis. Delft University of Technology. 2005.

[29] Zhang, F., Zhou, Z., and Lou, Z., 1980. Solubility product and stability of Ettringite. Proceedings, Seventh international congress on the chemistry of cement. Vol. II, Paris, 1980; 88-93.

Chapter 8

Ageing Factor for Service Life Prediction of Concrete Structures[8]

8.1 Introduction

In the prevailing Dutch concrete standards corrosion of reinforced concrete caused by chloride penetration is assumed to be the dominant mechanism determining the service life of marine concrete structures *[NEN 6720, NEN-EN 206-1/NEN 8005, NEN 6722]*. In chapter 6 it has been found that at early ages, *i.e.* up to 28 days, fly ash concrete has a higher chloride migration coefficient than Portland cement concrete when cured under moist conditions. As hydration proceeds, the migration coefficient of fly ash concrete decreases significantly with time, particularly at ages beyond 28 days. It was proposed by Maage *[Maage 1996]* that the time-dependent chloride diffusion (migration) coefficient can be described as a function of the initial value of the chloride diffusion (migration) coefficient (normally measured at 28 days) and the ageing factor *n*. The 28 days values of the chloride diffusion (migration) coefficient and the ageing factor are two important input parameters of the DuraCrete methodology to predict the service life of concrete structures.

In this chapter the ageing factor *n* for describing the evolution of the diffusion coefficient *D(t)* with time of Portland cement concrete and fly ash concrete is determined based on the measured RCM-results (see chapter 6). An important question is whether the new *n*-values can directly be adopted in currently used DuraCrete methodology for service life predictions. For answering this question the structure of the DuraCrete methodology has to be looked at in more detail.

8.2 DuraCrete Model

8.2.1 General introduction

The DuraCrete methodology was developed in 1990s in a European research project, "*Probabilistic Performance Based Durability Design of Concrete Structures*" *[DuraCrete 2000]*. The aim of this methodology was to develop a durability design concept, based on realistic and sufficiently accurate environmental and material models, being capable of

[8] This chapter is partially based on:

1) Zhuqing Yu, Guang Ye. New Perspective of Service Life Prediction of Fly Ash Concrete. Construction and Building Materials 48 (2013) 764–771.

2) Zhuqing Yu, Guang Ye. A discussion of service life prediction of fly ash concrete based on DuraCrete. International Congress on Durability of Concrete, Trondheim, Norway. 18-21 June 2012.

predicting the behavior of concrete structures *[DuraCrete 2000]*. Defining the desired performance of the structure is the first step in the process of designing durable concrete structures *[DuraCrete 2000]*. Figure 8.1 schematically shows the performance of a concrete structure when suffering from reinforcement corrosion and related damage. In this figure two main phases are defined in the development of the performance of concrete structures with time, *viz.* the initiation phase and the propagation phase. The initiation period is the time for an aggressive substance to reach the reinforcement and cause corrosion of the steel. During the propagation phase, deterioration develops and loss of function is observed. The propagation phase includes several kinds of damages, such as cracking, spalling and collapse, as shown in Figure 8.1. In our cases it is assumed that the deterioration mechanism of concrete structures is caused only by chloride ingress and subsequent corrosion of steel reinforcement.

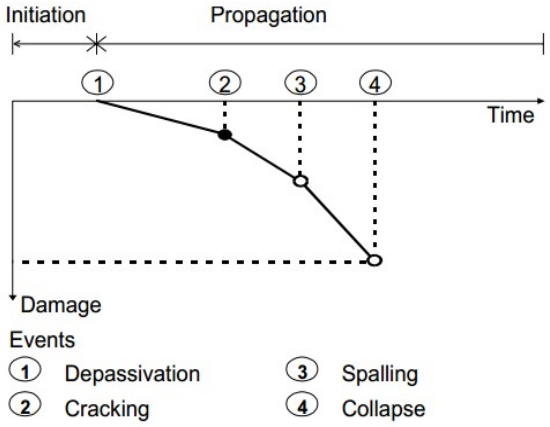

Figure 8.1: The performance of a concrete structure with respect to reinforcement corrosion and related damage [DuraCrete 2000]

8.2.2 Chloride transport in concrete

Chloride ion transport in concrete can be driven by three mechanisms, *i.e.* capillary absorption, hydrostatic pressure and diffusion *[Neville 1995]*. Fick's 2nd law can be used to describe diffusion-controlled chloride ion transport into concrete *[Collepardi 1970; Polder 2003; Polder 2006; van Breugel 2009; Oslakovic 2010]*. When Fick's 2nd law is applied it is implicitly assumed that chloride ion penetration is primarily a diffusion process.

8.2.3 Modelling chloride ingress

In the DuraCrete methodology the development of chloride profiles in time is approximated by:

$$C^d(x,t) = C^d_{s,cl}\left[1 - erf\left(\frac{x^d}{2\sqrt{\frac{t}{R^d_{cl}(t)}}}\right)\right] \tag{8.1}$$

where:

$C^d(x,t)$ = design value of chloride concentration at depth *x* and after time *t*, *% relative to binder*.
$C^d_{s,cl}$ = design value of the chloride surface concentration, *% relative to binder*.
x^d = design value of the cover depth, *mm*.
$R^d_{cl}(t)$ = design value for the resistance to chloride penetration, *year/mm*^{2}.
t = time, *year*.

Corrosion of reinforced concrete is assumed to start when the chloride concentration *C(x,t)* around the surface of the reinforcing bars (*x=concrete cover depth*) exceeds the critical chloride concentration C^d_{cr}. The design equation, *g*, is given by *[DuraCrete 2000]*:

$$g = C^d_{cr} - C^d(x,t) = C^d_{cr} - C^d_{s,cl}\left[1 - erf\left(\frac{x^d}{2\sqrt{\frac{t}{R^d_{cl}(t)}}}\right)\right] \tag{8.2}$$

where:

C^d_{cr} = design value of the critical chloride concentration, *% relative to binder*.

The design value of the critical chloride concentration C^d_{cr}, surface chloride concentration $C^d_{s,cl}$, cover depth x^d and the resistance to chloride penetration $R^d_{cl}(t)$ can be determined with following equations *[DuraCrete 2000]*:

$$C^d_{cr} = C^c_{cr} \cdot \frac{1}{\gamma_{C_{cr}}} \tag{8.3}$$

$$C^d_{s,cl} = A_{C_{s,cl}} \cdot (w/b) \cdot \gamma_{C_{s,cl}} \tag{8.4}$$

$$x^d = x^c - \Delta x \tag{8.5}$$

$$R^d_{cl}(t) = \frac{R^c_{cl,0}}{k^c_{e,cl} \cdot k^c_{c,cl} \cdot (\frac{t_0}{t})^{n_{cl}} \cdot \gamma_{R_{cl}}} \tag{8.6}$$

where:

C^c_{cr} = characteristic value of the critical chloride concentration, *% relative to binder*.
$\gamma_{C_{cr}}$ = partial factor of the critical chloride concentration.
$A_{C_{s,cl}}$ = regression parameter. It is used to determine the chloride surface concentration at a given water-binder ratio, obtained by regression analysis. *% relative to binder*.

w/b = water to binder ratio.
$\gamma_{C_{s,cl}}$ = partial factor for the surface concentration.
x^c = cover depth to reinforcement, *mm*.
Δx = safety margin for the cover depth, *mm*.
$R^c_{cl,0}$ = resistance to chloride penetration determined on the basis of compliance tests, *year/mm*^{2}.
$k^c_{e,cl}$ = environmental factor.
$k^c_{c,cl}$ = curing factor.
t_0 = age of concrete when the compliance test is performed, *years*.
For example, t_0= 0.0767 years (corresponding to 28 *days*).
n_{cl} = ageing factor.
$\gamma_{R_{cl}}$ = partial factor for the resistance with respect to chloride ingress.

With the boundary condition, $C^d_{cr}=C^d(x,t)$, the time to initiation of corrosion, *i.e.* the service life t^d_i, is calculated as follows:

$$t_i^d = \left[\left(\frac{2}{x^c - \Delta x} \cdot erf^{-1}\left(1 - \frac{C^c_{cr}}{\gamma_{C_{cr}}} \cdot \frac{1}{A_{C_{s,cl}} \cdot (w/b) \cdot \gamma_{C_{s,cl}}}\right)\right)^{-2} \cdot \frac{R^c_{cl,0}}{k^c_{e,cl} \cdot k^c_{c,cl} \cdot (t_0)^{n^c_{cl}} \cdot \gamma_{R_{cl}}} \right]^{\frac{1}{1-n^c_{cl}}} \tag{8.7}$$

As mentioned in section 2.6.1 the DuraCrete methodology is a probabilistic approach for service life design of concrete structures (see Figure 2.11). The acceptable probability of failure for corrosion initiation of reinforcing steel may be 10% *[Gjørv 2009; Fluge 2001; van der Wegen 2012]*.

8.2.4 Input parameters

The main input parameters in Equation 8.7 will be discussed in this paragraph, including the critical chloride concentration C^c_{cr}, the resistance to chloride penetration at 28 days t_0, $R^c_{cl,0}$. and the ageing factor *n* (n_{cl}).

Critical chloride concentration

The critical chloride concentration is normally defined in the form of *total chloride by weight of binder [Glass 1997]*. It depends not only on the environment and the type of binder, but also on the w/c (w/b) ratio.

Resistance to chloride penetration

As mentioned in section 2.6.2 both the chloride diffusion coefficient and the chloride migration coefficient can be used to evaluate the resistance of concrete to chloride penetration. As reported by Tang *[Tang 2012]*, the chloride diffusion coefficient and the chloride migration coefficient exhibit a good correlation (see Figure 2.12). In the DuraCrete

methodology the resistance of concrete to chloride penetration at 28 days (t_0), $R^c_{cl,0}$ in the RCM test (NTBuild 492) (see Equation 8.6), is expressed as a function of the chloride migration coefficient measured at 28 days:

$$R^c_{cl,0}\left(year/mm^2\right)=\frac{1}{D_{RCM,28\,days}\left(m^2/s\right)\times 3.1536\times 10^{13}} \tag{8.8}$$

Ageing factor

As mentioned in the literature review (see chapter 2) a time-dependent chloride diffusion (migration) coefficient *D(t)* is used in Fick's 2nd law. A commonly used expression for *D(t)*, as proposed by Maage *[Maage 1996]*, is $D(t)=D_0\left(t_0/t\right)^n$ (see also Equation 2.14). In this equation the ageing factor *n* is used to quantify the effect of ageing of the concrete on the evolution of *D(t)* for a given type of cement. The value of *n* has a significant influence on the evolution of *D(t) [Markeset 2010; van der Wegen 2014]* and of the service life of concrete structures. Figure 8.2 shows the relation between the ageing factor and the chloride diffusion coefficient *[Koenders 2008]*. A high aging factor indicates a more intensive densification of the microstructure, resulting in a lower chloride diffusion coefficient as function of time.

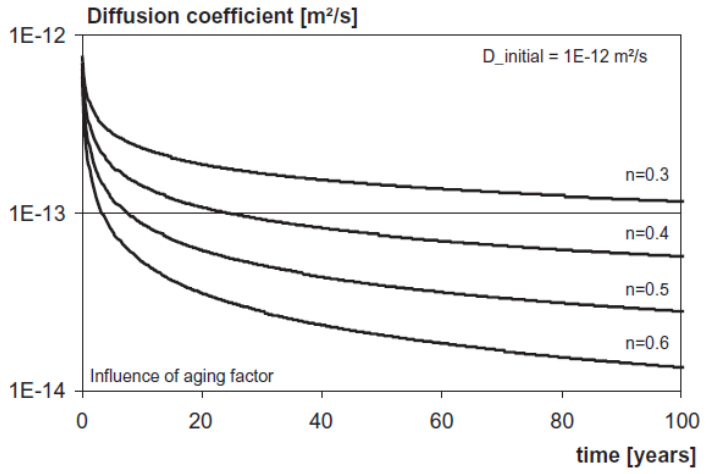

Figure 8.2: Diffusion coefficient for different aging factors by using Equation 2.14 [Koenders 2008]

Table 8.1 shows the reported ageing factors for different types of cement *[DuraCrete 2000; CUR-Bouw&Infra 2009; van der Wegen 2012]*. In general the slow pozzolanic reaction of fly ash results in a relatively high initial chloride diffusion (migration) coefficient (normally at 28 days) as well as in a higher *n*-value than Portland cement concrete and slag cement concrete *[DuraCrete 2000; Gaal 2006]*. The *n*-values shown in the CUR-VC81[9] database are determined from D_{RCM} values of concrete samples that had been cured under water at 20 °C for the period from 28 days to 3 years *[van der Wegen 2012]*.

[9] CUR-VC81 (CUR-Voorschriftencommissie 81): It is a Dutch Regulations Committee working on "design of structural concrete with respect chloride induced corrosion".

Table 8.1: Ageing factor n for different binders [DuraCrete 2000; CUR-Bouw&Infra 2009]

Ref.	CUR-VC81 database	DuraCrete 2000		CUR-VC 81 used in calculations	
Type of binder/storage or exposure conditions/	standard conditions (under water 20 °C)	tidal, splash zone	atmospheric	underground, splash zone	above ground, marine atmospheric
NEN-EN 206				XD2, XS3	XD1, XD3, XS1
CEM I	0.25	0.37	0.65	0.40	0.60
CEM I, 25-50% slag, II/B-S; or III/A, <50% slag	0.30	-	-	0.45	0.65
CEM III 50-80% slag	0.40	0.48-0.6	0.85	0.50	0.70
CEM I with 21-30 % fly ash	0.80	-	0.66	0.70	0.80
CEM V/A (25% slag and 25% fly ash)	0.60	-	-	0.60	0.70

8.2.5 Evaluating comments

Before applying the DuraCrete methodology to predict the service life of concrete structures, two points should be considered carefully:

1. *Is the ageing factor n for describing the time dependency of D(t) really a constant?*
2. *Are environmental factor k_e and curing factor k_c as considered in DuraCrete concept independent of the aging factor n?*

Question 1:

In the DuraCrete methodology, the chloride diffusion coefficient *D(t)* is time-dependent (see Equation 2.14). It is assumed that *D(t)* decreases continuously with age of the concrete. A reasonable explanation for this is, of course, the continuing cement hydration and densification of concrete over time. In Equation 2.14 the value of ageing factor (*n*-value) is considered constant. It means that *D(t)* would go to zero as time tends to infinity ($t \rightarrow \infty$), which is not realistic. From the obtained RCM-results in chapter 6 it can be seen that *D(t)* decreases with time only up to a certain age, for example around 1 year for mixtures made with 30% fly ash (see Figure 6.10). In reality, the chloride diffusion coefficient *D(t)* is directly determined by the microstructure of concrete. This means that, once hydration stops and the microstructure does not densify further, we cannot expect a continuing decrease of the diffusion coefficient.

Question 2:

In the DuraCrete methodology, the environment factor k_e and curing factor k_c are taken into account for service life predictions of concrete structures in the field. Based on Equation 2.14, the chloride diffusion coefficient *D(t)* is modified as *[DuraCrete 2000]*:

$$D(t) = k_e k_c D_0 \left(\frac{t_0}{t} \right)^n \tag{8.9}$$

where:

k_e = environmental factor.
k_c = curing factor.

The environmental factor k_e accounts for the effect of different marine environments (such as submerged zone, tidal zone, splash zone and atmospheric zone) and different cement types (such as Portland cement, blast furnace slag cement and fly ash cement, etc.). The factor k_e is determined from fitting the chloride profiles from practical or laboratory experiments with Equation 8.1 *[CUR-Bouw&Infra 2009]*.

The curing factor k_c allows for the influence of the curing period of concrete before exposure to marine environment. The value of k_c decreases with increasing curing period of concrete, since the longer the curing period, the higher the resistance of concrete to chloride penetration.

From the way in which the parameters, k_e, k_c and n, are obtained it is obvious that these parameters are mutually interdependent. It is not justified, therefore, to change one of them, *i.e.* n, to predict the service life of concrete structures without reconsidering the values of other parameters, *i.e.* k_e *and* k_c.

8.3 The Ageing Factor *n*

In this study the resistance of concrete to chloride penetration was investigated at ages of the concrete up to 3 years in laboratory (see chapter 6). The values of the ageing factor n can be determined from measured RCM-values by least squares regression analysis, based on Equation 2.14. However, the n-values strongly depend on the length of the reference period covered by the measured D_{RCM} values used for fitting Equation 2.14. As discussed in section 6.3.1 the RCM-values of Portland cement concrete with different w/c ratios (0.4, 0.5 and 0.6) increase at later ages, *i.e.* after around 180 days (Figure 6.6). In the following reference periods are considered from 28 days to 180 days and from 28 days to 3 years for Portland cement concrete and fly ash concrete.

8.3.1 Portland cement concrete

Two calculations for the n-values will be given below:

1) *Data set I.* D_{RCM} values from 28 days to 180 days
   By using the measured D_{RCM} values at ages from 28 days to 180 days, the calculated n-values and predicted chloride migration coefficient with time for each mixture are shown in Figure 8.3.

2) *Data set II*. D_{RCM} values from 28 days to 3 years
   By using the measured D_{RCM} values at ages from 28 days to 3 years are used, the calculated n-values and predicted chloride migration coefficient with time for each mixture are shown in Figure 8.4.

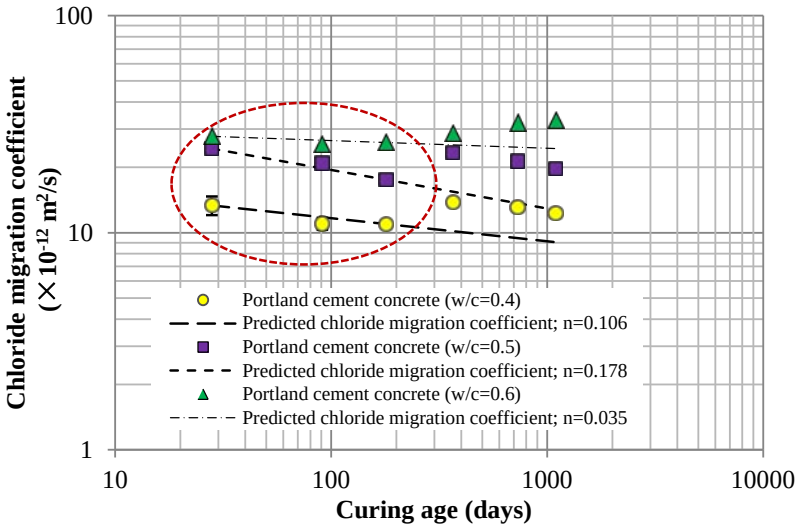

Figure 8.3: Predicted chloride migration coefficient of Portland cement concrete (based on the data at ages from 28 days to 180 days)

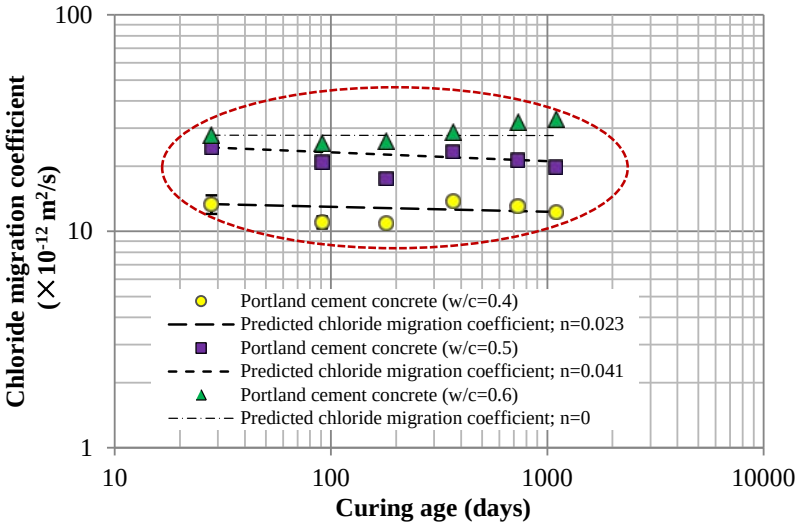

Figure 8.4: Predicted chloride migration coefficient of Portland cement concrete (based on the data at ages from 28 days to 3 years)

Table 8.2 summaries the *n*-values calculated for the data sets I and II. From this Table it can be seen that the *n*-values for Portland cement concrete mixtures (w/c=0.4-0.6) calculated by using the measured D_{RCM} values from 28 days to 3 years, *i.e.* 0-0.041, are much lower than those calculated by using the data from 28 days to 180 days, *i.e.* 0.035-0.178. That is due to the decrease of the resistance to chloride ingress at later ages, *i.e.* after about 180 days. The possible reason for this decrease has been discussed in chapter 7. Compared to the recommended *n*-value, 0.25, for Portland cement concrete mentioned in literature (see Table 8.1), the calculated *n*-values shown in Table 8.2 are all much lower. Such low *n*-values, however, were also observed by other researchers *[Tang 1996; van Dalen 2005; Baert 2008; Maes 2012]*, as shown in Table 8.3.

Table 8.2: Summary of the ageing factor n for Portland cement concrete mixtures

Mixture	w/c ratio	Ageing factor, *n*		
		Data set I (28-180 days)	Data set II (28 days-3 years)	Recommended values (see Table 8.1)
OPC-04	0.4	0.106	0.023	
OPC-05	0.5	0.178	0.041	0.25
OPC-06	0.6	0.035	0.000	

Table 8.3: Ageing factor n for Portland cement concrete mixtures from references

w/c	*n-values*	Reference periods	Reference
0.32	0.004	28-1095 days	*[Tang 1996]*
0.40	0.130	28-1095 days	*[Tang 1996]*
0.40	0.130	28-365 days	*[Baert 2008]*
0.45	0.180	28-224 days	*[Maes 2012]*
0.45	0.236	28-91 days	*[Dalen 2006]*

Figure 8.5 shows the D_{RCM} values at different ages of the concrete, from reference (w/c=0.4) *[Baert 2008]* and this work (w/c=0.4) shown in Figure 8.3. It can be seen that the D_{RCM} values of Portland cement concrete (w/c=0.4) decrease significantly at ages from 28 days to 90 days, resulting from continuing hydration of cement. After about 90 days the D_{RCM} values do not decrease significantly, even an increase of the D_{RCM} values at later ages in our test results. After 90 days the hydration of cement in Portland cement concrete is almost completed if the concrete samples are cured at 20°C and 100% RH *[Patel 1988]*. The microstructure of concrete tends to be stable. The *n*-value of Portland cement concrete mixtures calculated by the measured D_{RCM} from 28 days to 91 days is higher than that calculated from the measured D_{RCM} from 28 days to 1 year (see Figure 8.5). In other words, the *n*-value is variable and depends on the microstructure of concrete, as mentioned in section 8.2.5. Hence, the time dependency of the diffusion coefficient *D(t)* can, in fact, not be described with a constant value of *n*. The changes in the ageing factor definitely influence the service life predictions of concrete structures.

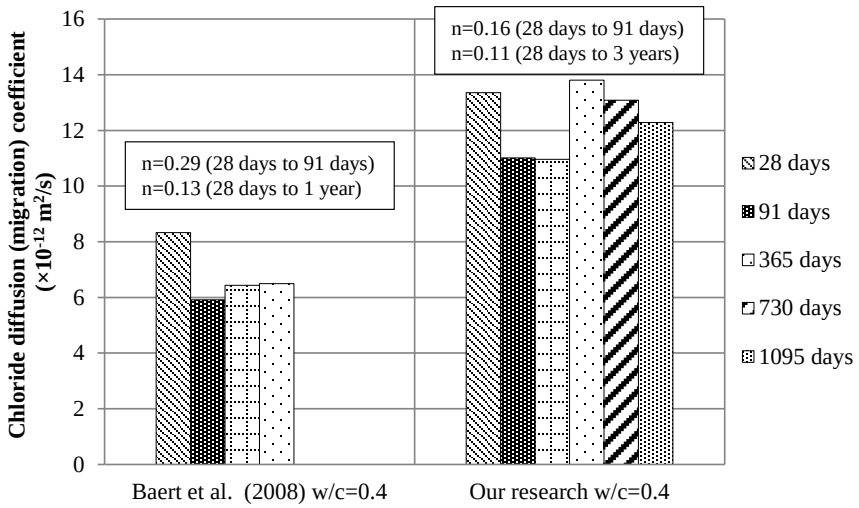

Figure 8.5: D_{RCM} values of Portland cement concrete from reference [Baert 2008] and our data

8.3.2 Fly ash concrete

Like for Portland cement concrete two calculations for the *n*-values of fly ash concrete by using different sets of D_{RCM} values are shown as follows:

1) *Data set I*. D_{RCM} values from 28 days to 180 days
   By using the measured D_{RCM} values at ages from 28 days to 180 days, the calculated *n*-values and predicted chloride migration coefficient with time for each mixture are shown in Figure 8.6. The concrete mixtures are made with 30% and 50% fly ash.

2) *Data set II*. D_{RCM} values from 28 days to 3 years
   By using the measured D_{RCM} values at ages from 28 days to 3 years are used, the calculated *n*-values and predicted chloride migration coefficient with time for each mixture are shown in Figure 8.7. The concrete mixtures are made with 30% and 50% fly ash.

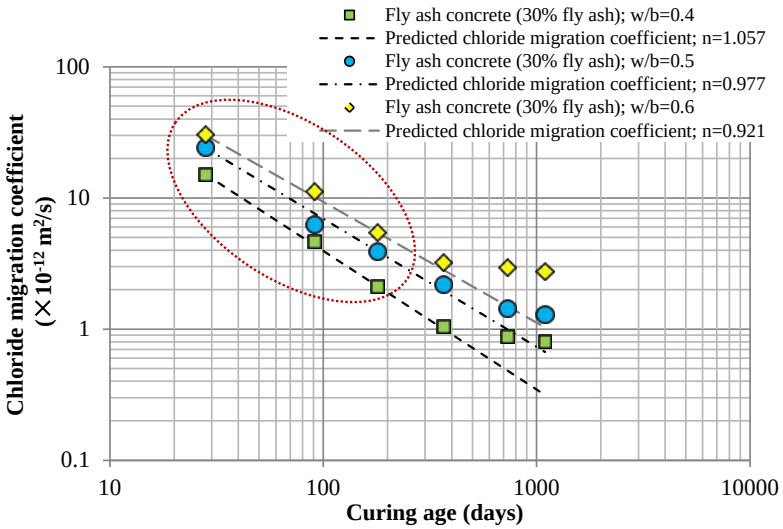

(a) 30% fly ash

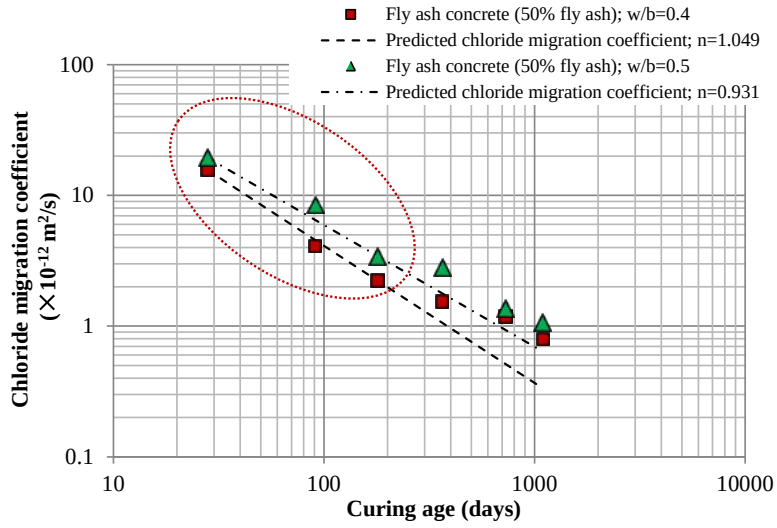

(b) 50% fly ash

Figure 8.6: Predicted chloride migration coefficient of fly ash concrete (a): 30% fly ash; (b): 50% fly ash (based on the data at ages from 28 days to 180 days)

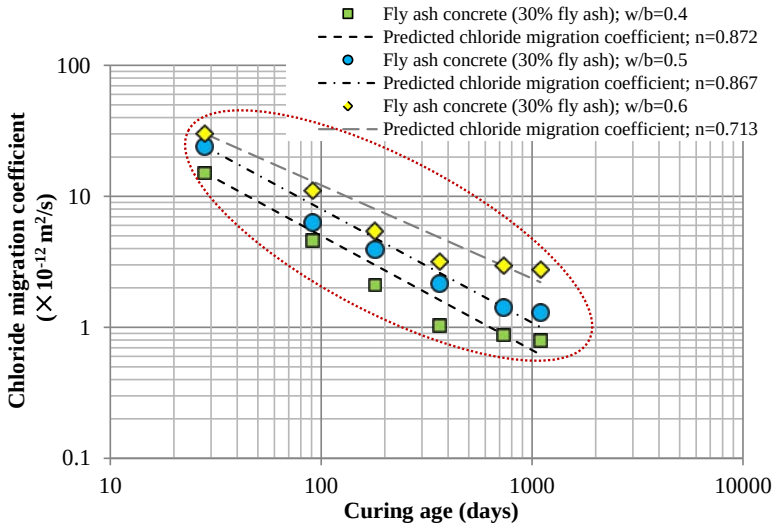

(a) 30% fly ash

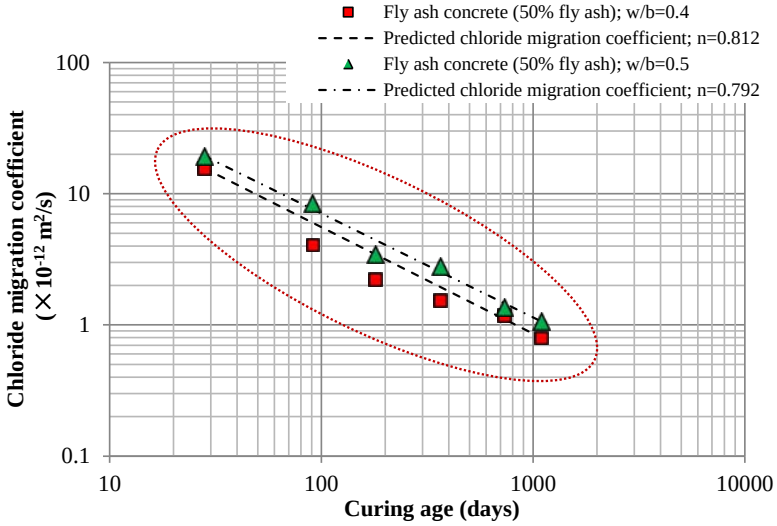

(b) 50% fly ash

Figure 8.7: Predicted chloride migration coefficient of fly ash concrete (a): 30% fly ash; (b): 50% fly ash (based on the data at ages from 28 days to 3 years)

Table 8.4 summaries the *n*-values for fly ash concrete mixtures calculated for the data sets I and II. The *n*-values of fly ash concrete mixtures are much higher than that of Portland cement concrete mixtures. From Table 8.4 it can be seen that for mixtures (30% and 50%) with w/b ratio of 0.4, 0.5 and 0.6 the calculated *n*-values by using the measured D_{RCM} values from 28 days to 180 days do not significantly differ from each other. The *n*-value for fly ash concrete mixtures is taken equal to the average value, *i.e.* 0.987. It indicates that the microstructure of fly ash concrete is becoming denser with time. As shown in Figure 8.6 (a, b), after about 1 year the D_{RCM} values of fly ash concrete are slightly decreasing, particularly for the mixture with 30% fly ash (Figure 8.6a). The relationship between *D(t)* and age of the concrete tends to be bilinear on a double log scale. Hence, the evolution of *D(t)* with time cannot be described accurately with only one value of the ageing factor *n*, *i.e.* 0.987.

By using the measured D_{RCM} values from 28 days to 3 years (data set II), as shown in Figure 8.7 (a, b) and Table 8.4, the average *n*-value for fly ash concrete becomes lower, *i.e.* 0.811. This calculated *n*-value is close to the recommended value in literature (Table 8.1), *i.e.*

0.80. However, the predicted results do not fit satisfactorily to the experimental results (see Figure 8.7 (a, b)).

Table 8.4: Summary of the ageing factor n for fly ash concrete mixtures

Mixture	w/b ratio	Ageing factor, *n*		
		Data set I (28-180 days)	Data set II (28 days-3 years)	Recommended values (see Table 8.1)
FA-30-04	0.4	1.057	0.872	0.80
FA-30-05	0.5	0.977	0.867	
FA-30-06	0.6	0.921	0.713	
FA-50-04	0.4	1.049	0.812	
FA-50-05	0.5	0.931	0.792	
Average value, n		*0.987*	*0.811*	

8.3.3 Evaluation of the ageing factor in view of service life predictions of concrete structures

Figure 8.8 shows the evolution of *D(t)* of the concrete mixture with 30% fly ash and w/b=0.4, including the experimental results and the predicted values with two different values of the ageing factor, *i.e.* 0.987 and 0.811. From this figure it can be seen that the experimental results do not follow these two predicted curves of *D(t)*, *i.e.* curves *a* and *b*. As mentioned above, on a double log scale the observed relationship between *D(t)* and age of the concrete is more bilinear. At later ages, *i.e.* after about 1 year, the evolution of *D(t)* may follow another trend line.

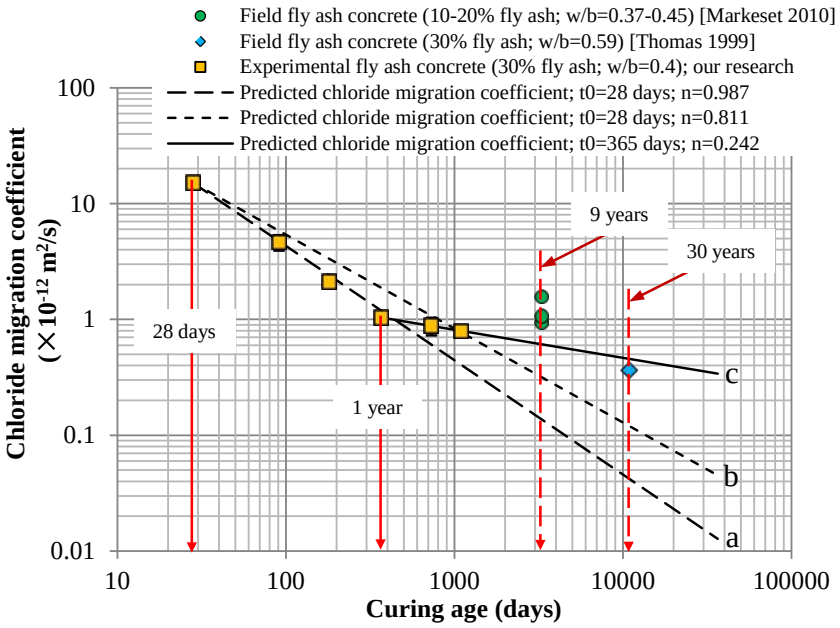

Figure 8.8: Predicted chloride migration coefficient of fly ash concrete structures with time for different n-values and experimental results from our lab (30% fly ash, w/b=0.4) and reference (30 years old field sample from hydraulic dam; 30% fly ash, w/b=0.59; chloride diffusion coefficient) [Thomas 1999]; 9 years old field sample in Norway (10-20% fly ash; w/b=0.37-0.45; Tidal zone; chloride diffusion coefficient) [Markeset 2010]

If a regression analysis is carried out for measured data in the period from 1 year to 3 years, with Equation 2.14, a new *n*-value, *i.e.* n=0.242, is determined (t_0=365 days; $D_{0,\ 365\ days}$=1.04 ×10^{-12} m^2/s), as shown in Figure 8.8 (curve *c*). Although this *n*-value is much lower than the *n*-values presented in Table 8.4, *i.e.* 0.8-0.987 (obtained by t_0=28 days; $D_{0,\ 28\ days}$=15.15 ×10^{-12} m^2/s), it represents the evolution of the chloride migration coefficient for fly ash concrete at later ages, *i.e.* after about 1 year, more accurately. From Figure 8.8 it can be seen that the predicted RCM-value at 30 years using the *n*-value of 0.242, is close to the data tested on the 30 years old sample, obtained from field structures *[Thomas 1999]*. Beside this value, the predicted RCM-value at 9 years is a little bit lower than the data tested on the 9 years old sample, obtained from field structures *[Markeset 2010]*. This can be explained by the fly ash content in concrete mixtures. As mentioned in Figure 2.13, fly ash concrete mixture with 30% fly ash has a better resistance to chloride ingress than the mixture with 10-20% fly ash. Based on above discussions it is believed that the service life of concrete structures will be overestimated if a constant value of the ageing factor *n* is used, unless this is adequately corrected by appropriate values of k_e an k_c.

8.4 Concluding Remarks

In the DuraCrete methodology it is assumed that the chloride diffusion (migration) coefficient of concrete, *D(t)*, decreases considerably with increasing age of the concrete. This decrease is quantified with a constant value of *n*. In this chapter, however, it is demonstrated that the decrease of the diffusion coefficient cannot be described adequately with a constant value of *n*. The changes in the ageing factor *n* may change the predicted service life of concrete structures significantly. The following conclusions about the ageing factor *n* of Portland cement concrete and fly ash concrete are shown*:*

Portland cement concrete

1. The ageing factor *n* can be determined from the measured RCM-values. The *n*-values strongly depend on the length of the reference period covered by the measured D_{RCM} values. For Portland cement concrete (w/c=0.4-0.6) the *n*-values calculated by using the measured D_{RCM} values from 28 days to 3 years, *i.e.* 0-0.041, are much lower than those calculated by using the data from 28 days to 180 days, *i.e.* 0.035-0.178. That is due to the decrease of the resistance to chloride ingress at later ages (about 180 days). The possible reason for this increase of the chloride migration coefficient is the delayed ettringite formation in Portland cement concrete (see chapter 7).

Fly ash concrete

1. Due to the pozzolanic reaction of fly ash, fly ash concrete has a higher ageing factor *n* than Portland cement concrete. It appears that the fly ash content (from 30% to 50%) and w/b ratio (from 0.4 to 0.6) does not significantly affect the *n*-values. The average *n*-value for fly ash concrete mixtures is 0.987, if calculated by using the measured D_{RCM} values from 28 days to 180 days. After about 1 year the D_{RCM} values of fly ash concrete are slightly decreasing, particularly for the mixture with 30% fly ash (w/b ratio = 0.4, 0.5 and 0.6). The relationship between *D(t)* and age of the concrete is more bilinear. By using the measured D_{RCM} values from 28 days to 3 years, the calculated average *n*-value is 0.811. This suggests that the ageing factor *n* decreases over time. It is believed that the service life of concrete structures will be overestimated if a

constant value of the ageing factor is used. In service life predictions of concrete structures the ageing factor n needs to be reconsidered taking into account the actual evolution of $D(t)$ with time. It is emphasized that reconsideration of n-values should be accompanied by reconsidering other model parameters values (*e.g.* k_e an k_c in the DuraCrete model).

References

[1] Baert G., Gruyaert E., Audenaert K., De Belie N., 2008. Chloride ingress in high-volume fly ash concrete. Published in 1st International Conference on Microstructure Related Durability of Cementitious Composites, 13-15 October 2008, Nanjing, China. ed. W. Sun, K. van Breugel, C. Miao, G. Ye and H. Chen, Print-ISBN: 978-2-35158-065-3, e-ISBN: 978-2-35158-084-4, Publisher: RILEM Publications, 2008, pp: 473-482.

[2] Collepardi, M., Marcialis, A., Turriziani, R., 1970. La Cinetica Di Penetrazione Degli Ioni Cloruro Nel Calcestruzzo (The penetration kinetics of chloride ions into concrete), il Cemento, 1970; 67: 157-164.

[3] CUR-Bouw&Infra 2009. Duurzaamheid van constructief beton met betrekking tot chloride-geïnitieerde wapeningscorrosie - Leidraad voor het formuleren van prestatie-eisen – Achtergrondrapport (in Dutch), Tudelft, 19 Mei 2009.

[4] DuraCrete, 2000. Probabilistic Performance based Durability Design of Concrete Structures. Contract BRPR-CT95-0132, Project BE95-1347. Document BE95-1347/R17, May 2000.

[5] Fluge, F., 2001. Marine chlorides – A probabilistic approach to derive provisions for EN 206-1, Third DuraNet Workshop on Service life design of concrete structures, from theory to standardisation, Tromsø, June 10-12.

[6] Gaal GCM, Koenders EAB and Polder RB, 2006. Ageing effect of chloride diffusion coefficient, in ConcreteLife'06 – International RILEM-JCI Seminar on Concrete Durability and Service Life Planning: Curing, crack control, performance in harsh environments, 14-16 March 2006, Dead Sea, pp. 41-50

[7] Gjørv, O.E., 2009. Durability design of concrete structures in severe environments, Taylor & Francis, London and New York.

[8] Glass, G.K., Buenfeld, N.R., 1997. The presentation of the chloride threshold level for corrosion of steel in concrete. Corrosion Science, 1997; 39: 1001-1013.

[9] Koenders E.A.B., Ottelé M., Obladen B., 2008. A spreadsheet model for service-life predictions. The 2nd international conference on Concrete Repair, Rehabilitation and Retrofitting II, eds Alexander et al, published by Taylor & Francis Group, London, ISBN 978-0-415-46850-3. 2008, 289-295.

[10] Maage, M., Helland, S., Poulsen, E., Vennesland, O., Carlsen, J.E., 1996. Service life prediction of existing concrete structures exposed to marine environment. ACI Materials Journal, 1996; 93(6): 602-608.

[11] Maes M., Caspeele R., Van den Heede P., De Belie N., 2013. Influence of sulphates on chloride diffusion and the effect of this on service life prediction of concrete in a submerged marine environment. in: Strauss, A. et al. Life-Cycle and Sustainability of Civil Infrastructure Systems Proceedings of the Third International Symposium on Life-Cycle Civil Engineering (IALCCE'12), Vienna, Austria, October 3-6, 2012. pp. 899-906.

[12] Markeset Gro, Skjølsvold Ola, 2010. Time dependent chloride diffusion coefficient-field studies of concrete exposed to marine environment in Norway. 2nd International Symposium on Service Life Design for Infrastructures. Delft, Nederland. 4-6, October, 2010

[13] NEN 6720:1995 nl TGB 1990 - Voorschriften Beton - Constructieve eisen en rekenmethoden (VBC 1995).

[14] NEN-EN 206-1 Beton – Deel 1: Specificatie, eigenschappen, vervaardiging en conformiteit.

[15] NEN 8005:2008 nl Nederlandse invulling van NEN-EN 206-1: Beton - Deel 1: Specificatie, eigenschappen, vervaardiging en conformiteit.

[16] NEN 6722: 1989 Voorschriften Beton. Uitvoering (VBU 1988), met correctieblad van mei 1989.

[17] NEN-EN 206-1/NEN 8005: Concrete composition.

[18] Neville, A. M., 1995. Properties of concrete. Wiley, New York.

[19] Oslakovic Irina Stipanovic, Bjegovic Dubravka, Mikulic Dunja, 2010. Evaluation of service life design models on concrete structures exposed to marine environment. Materials and Structures. 2010; 43:1397-1412.

[20] Patel, R.G., Killoh, D.C., Parrott, L.J. and Gutteridge, W.A., 1988. Influence of curing at different relative humidities upon compound reactions and porosity of Portland cement paste. Materials and Structures. 1988: 21 (123): 192-197.

[21] Polder Rob B., de Rooij Mario R., de Vries Hans, Gulikers Joost, 2003. Observed Chloride Penetration in Eastern Scheldt Storm Surge Barrier, The Netherlands, after 20 years in North Sea Environment. Workshop "Risk based maintenance of Structures", TU Delft, 21 January 2003.

[22] Polder, R.B, de Rooij, M.R., van Breugel, K., 2006. Validation of models for service life prediction – Experiments from the practice. In Proc. Int. RILEM-JCI seminar Concrete Life'06, Ein Bokek, 2006; 292-301.

[23] Tang, L., 1996. Electrically accelerated methods for determining chloride diffusivity in concrete. Magazine of Concrete Research. 1996; 48(176): 173-179.

[24] Tang Luping, Nilsson Lars-olof, Muhammed Basheer P. A., 2012. Resistance of concrete to chloride ingress testing and modelling. Spon Press.

[25] Thomas Michael D.A., Bamforth Phil B., 1999. Modelling chloride diffusion in concrete effect of fly ash and slag. Cement and concrete research. 1999; 29: 487-495.

[26] van Breugel, K., Polder, R., 2009. Probability-based service life design of structural concrete, in Proc. 2nd Int. RILEM Workshop on Concrete Durability and Service Life Planning-ConcreteLife'09, Haifa, Israel, 2009; 383-391.

[27] van Dalen Sander M., 2005. Experimenteel onderzoek naar de RCM-methode (In Dutch). Master Thesis. Delft University of Technology. 2005.

[28] van der Wegen Gert, Polder Rob B., van Breugel Klaas, 2012. Guideline for service life design of structural concrete - A performance based approach with regard to chloride induced corrosion. HERON, 2012; 57 (3): 153-167.

[29] van der Wegen G.J.L., Boutz M.M.R., Sarabèr A.J., van Eijk R.J., 2014. Ageing coefficient of fly ash concrete and its impact on durability. AMS '14 - Proceedings of the 1st International Conference on Ageing of Materials & Structures, edited by K. van Breugel, E.A.B. Koenders, ISBN: 978-94-6186-314-0, p. 171-178, 26-28 May 2014, Delft, The Netherlands.

Chapter 9

Retrospection, Conclusions, Recommendations

9.1 Retrospection

Fly ash is a by-product of the combustion of coal in electric power generating plants. Since it can chemically react with calcium hydroxide produced by the hydration of cement, *viz. pozzolanic reaction*, fly ash is used as a supplementary cementitious material in concrete. It is generally believed that the pozzolanic reaction of fly ash refines the pore structure of Portland cement-fly ash binary systems, improves the durability of concrete and extends the service life of concrete structures. However, studies on *"how does fly ash refine the pore structure of binary systems? What is the reason why binary systems is less permeable and has better resistance to chloride penetration only at long-term curing period? how does fly ash extend the service life of concrete structures?"* are still insufficient. This study aims to investigate the microstructure development and transport properties of Portland cement-fly ash binary systems at ages up to 3 years in view of service life predictions of concrete structures.

In Portland cement-fly ash binary systems there are two kinds of chemical reactions: *the hydration of cement and the pozzolanic reaction of fly ash*. The bridge between these two reactions is the calcium hydroxide phase. It is produced by the hydration of cement clinker and consumed by the pozzolanic reaction of fly ash in binary systems. In chapter 3 the evolution of calcium hydroxide content in binary systems was studied at ages up to 3 years. Meanwhile, in order to study the influence of fly ash on the hydration process of binary systems, both the degree of the hydration of cement and the degree of the pozzolanic reaction of fly ash were determined.

The hydration of cement goes along with a continuous evolution of the microstructure of the cement paste. In chapter 4, the development of microstructure, *the solid phase and pore phase*, was studied by environmental scanning electron microscope (ESEM) and mercury intrusion porosimetry (MIP) techniques. With MIP the effect of fly ash on the pore structure of blended cement paste was investigated intensively. Various pore structure parameters, *i.e.* the porosity, connectivity of the pores and critical pore width, were determined.

The pore structure determines the transport properties. In chapter 5 the water permeability of binary systems was determined. Based on the information of the pore structure measurements (chapter 4) the crucial factor governing the water permeability of binary systems was discussed.

In chapter 6 the resistance of fly ash concrete to chloride ingress was investigated at ages up to 3 years. Fly ash concrete has an increased resistance to chloride ingress with time. The factor affecting the resistance of fly ash concrete to chloride ingress was also discussed.

In chapter 6 it was found that the chloride migration coefficient of Portland cement concrete increased at later ages, around 180 days. It was expected that for moist cured concrete the D_{RCM} values should decrease with increasing age of the concrete. In chapter 7 the

possible reasons for the increase of the chloride migration coefficient of Portland cement concrete were explored: including the leaching of calcium hydroxide (CH) and the delayed ettringite formation (DEF).

Based on the measured D_{RCM} values, the ageing factor *n* of concrete was determined. It describes how rapidly the chloride diffusion (migration) coefficient, *D(t)*, of concrete decreases with time. In chapter 8 the value of the ageing factor *n* is discussed in view of service life predictions of concrete structures based on the DuraCrete concept.

9.2 Conclusions

The general conclusions of this research are:

- At later ages, *i.e. after 180 days*, the calcium hydroxide (CH) content in Portland cement-fly ash binary systems hardly changes. This can be inferred from a low degree of the pozzolanic reaction of fly ash in binary systems after 180 days.

- The pozzolanic reaction of fly ash particles in binary systems results in the formation of more ink-bottle pores and provides extra space for the accommodation of reaction products, like C-S-H.

- The total porosity of blended cement paste is higher than that of Portland cement paste, *even at an age of 3 years*, since more empty cavities form in blended cement paste due to the pozzolanic reaction of fly ash. At the same time the presence of fly ash results in the formation of a large amount of small capillary pores in the range between 10 nm and 100 nm.

- At later ages, *i.e. after about 180 days*, the connectivity of the pores in fly ash-blended cement paste is lower than that in Portland cement paste.

- The water permeability of fly ash-blended cement paste decreases with time up to 1 year. After 1 year the water permeability of blended cement paste hardly changes.

- At later ages, *i.e.* after 90 days, fly ash-blended cement paste is less permeable than Portland cement paste, although its porosity is higher than Portland cement paste.

- Under moist curing conditions the D_{RCM} values of Portland cement concrete made with different w/c ratios (0.4, 0.5 and 0.6) decrease with time from 28 to 180 days. After that the D_{RCM} values increase and then turn to decrease again after around 1 year. The possible reason is the delayed ettringite formation due to the addition of limestone powder (see later).

- As small amounts of additional constituent, *e.g.* limestone powder ($CaCO_3$), can be blended with Portland cement up to 5%. When concrete is cured under moist conditions $CaCO_3$ reacts with monosulfate to form ettringite and monocarbonate. This delayed ettringite formation (DEF) occurs in Portland cement concrete and may result in a change of the microstructure of hydrated cement paste and an increase of D_{RCM} at later ages.

- Ettringite also forms in fly ash concrete at later ages. This ettringite is found in voids initially present in the paste and in the spaces left after the reaction of fly ash particles. Formation of ettringite in empty spaces explains why DEF in fly ash concrete does not lead to expansion and micro-cracking and an associated increase of the D_{RCM} values as observed for Portland cement concrete.

- In the DuraCrete methodology it is assumed that the chloride diffusion (migration) coefficient of concrete, *D(t)*, decreases considerably with increasing age of the concrete. This decrease is quantified with a constant value of *n*. It means that *D(t)* would go to zero as time tends to infinity ($t \rightarrow \infty$), which is not realistic. In reality, the chloride diffusion coefficient *D(t)* is directly determined by the microstructure of concrete. The decrease of the diffusion coefficient cannot be described adequately with a constant value of *n*. In service life predictions of concrete structures the ageing factor *n* need to be reconsidered taking into account the actual evolution of *D(t)* with time. It is emphasized that reconsideration of *n*-values should be accompanied by reconsidering other model parameters values (*e.g.* k_e an k_c in the DuraCrete model), since these parameter, k_e, k_c and *n*, are mutually interdependent.

9.3 Contribution of This Study

With this research a comprehensive survey of the evolution of the properties of Portland cement-fly ash binary systems at ages up to 3 years was given, including the hydration process, microstructure development and transport properties (water permeability and chloride ingress). The main contribution of this study are listed:

- Normally studies on the pore structure of blended cement paste are limited to short-term tests, *i.e.* up to 90 days. From 90 days to 3 years, *however*, the presence of fly ash hardly further reduces the capillary porosity of binary systems. Fly ash refines the pore structure of binary systems at later ages, resulting in the decrease of the connectivity of the pores after around 180 days.

- Limestone powder is widely used in the concrete industry. However, it was found that the presence of limestone powder, *even less than 5% of the total cement mass*, may lead to delayed ettringite formation in concrete (in moist conditions), resulting in a decrease of the resistance of Portland cement concrete to chloride penetration at later ages (after about 180 days). In practice, when the Portland cement blended with limestone powder are designed to be used in marine environment, more attention should be paid to the possible negative effects of limestone powder.

- In the DuraCrete methodology the ageing factor *n* describes the time dependency of *D(t)*. It is assumed as a constant value in service life predictions of concrete structures. However, the *n*-value depends on the length of the reference period in which the values of *D(t)* are taken as basis for the determination of the *n*-values. It was found that if taking longer reference period (from 28 days to 3 years) the *n*-value decreases. Obviously, the decrease of *D(t)* is less than that predicted with a constant *n-value* obtained with a short reference period (from 28 days to 180 days). In service life predictions of concrete structures the ageing factor *n* need to be reconsidered taking into account the actual evolution of *D(t)* with time. The reconsideration of *n*-values should be accompanied by reconsidering other model parameters values (*e.g.* k_e an k_c in the DuraCrete model). This

study provides incentive for further investigation of the service life predictions of concrete structures based on the DuraCrete methodology.

- The experimental results obtained in this research, particularly the evolution of the pore structure at ages up to 3 years, provide a database for validating hydration, microstructure and transport properties of Portland cement-fly ash binary system.

9.4 Recommendations for Future Work

From this study several aspects are recommended for more detailed investigations.

- *The use of limestone in cement (concrete)*
  Portland cement containing limestone (*CEM II/A(B)-L(LL)* is commonly used in European countries *[EN 197-1:2000]*. We found that the presence of limestone in Portland cement concrete is the possible reason for a decrease of the resistance to chloride ingress at later ages, after around 180 days (in moist conditions). However, the presence of limestone in fly ash concrete (ternary systems: fly ash, Portland cement and limestone) appears not to influence the resistance of concrete to chloride ingress. It is recommended to further investigate the durability of this ternary systems for concrete structures exposed to combined aggressive environments, *e.g.* chloride ingress and carbonation, sulfate and chloride attack.

- *Long-term properties of concrete made of composite cement CEM V/A (B)*
  In cement industry fly ash is used, *together with blast furnace slag* (a type of by-product in industry), to produce composite cement *CEM V/A (B) [EN 197-1:2000]*. This cement is a kind of "green" cement, because it reduces the use of cement clinker, CO_2 emissions and landfill costs of fly ash and blast furnace slag. However, there is a lack of understanding on the long-term properties of concrete made with composite cement *CEM V/A (B)*, such as microstructure development, transport properties and durability.

- *The ageing factor for predicting the service life of concrete structures in view of the microstructure of paste (concrete)*
  In service life predictions of concrete structures according to the DuraCrete methodology the ageing factor *n* is a very important parameter. It describes the time dependency of chloride diffusion coefficient, *D(t)*. In this study it is found that the decrease of *D(t)* cannot be described adequately with a constant value of *n*. In reality, the chloride diffusion coefficient is directly determined by the microstructure of concrete. Hence, in order to predict the service life of concrete structures accurately, the relationship between the ageing factor and the microstructure of paste (concrete) need to be studied in more detail.

References

[1] *European standards EN 197-1 Cement Composition. June 2000.*

Appendix

A: The pore size distribution of Portland cement paste and blended cement paste obtained by MIP technique

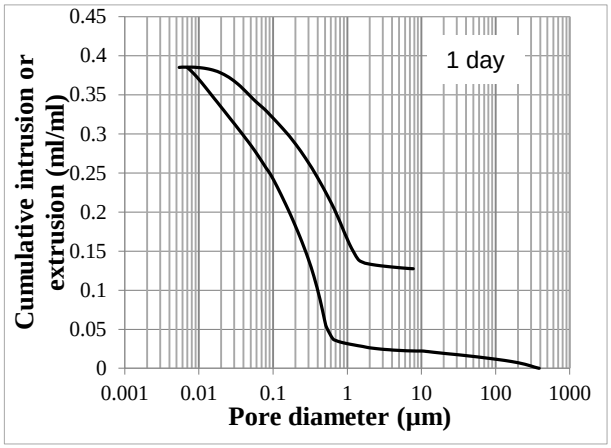

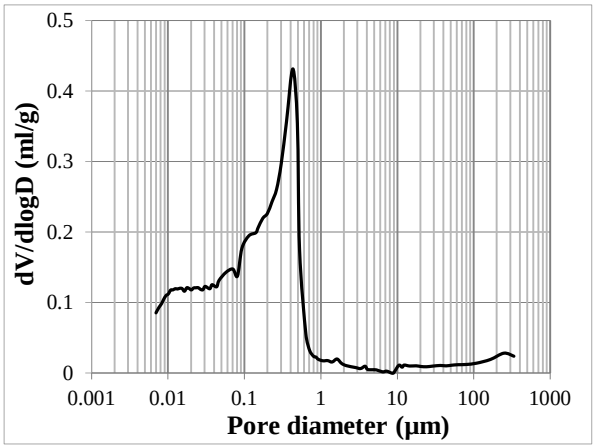

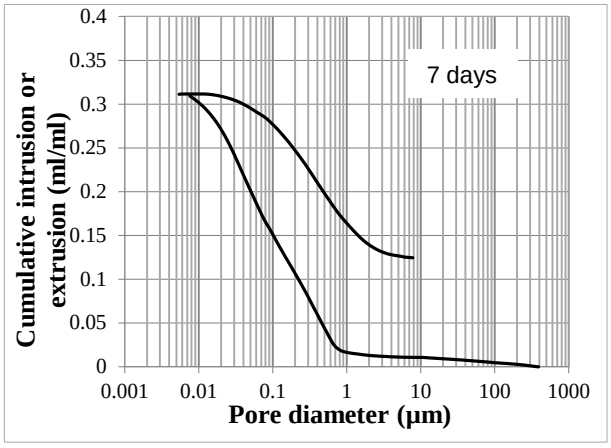

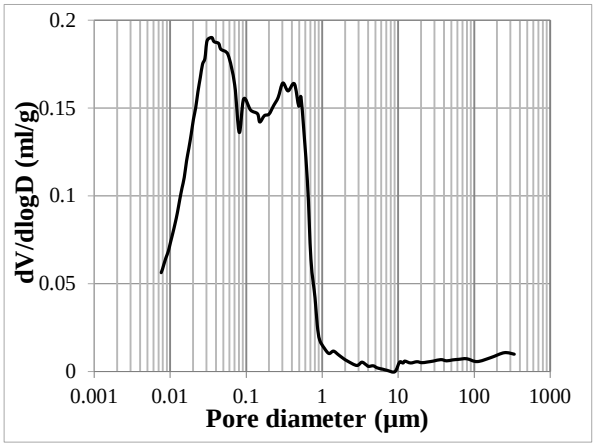

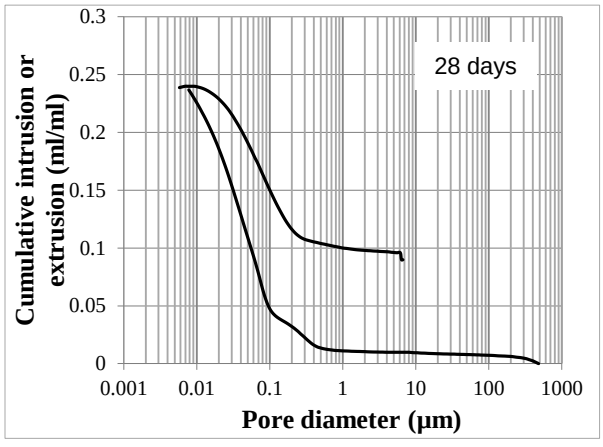

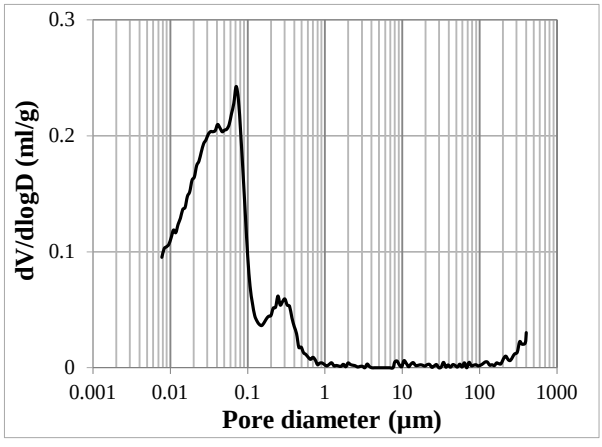

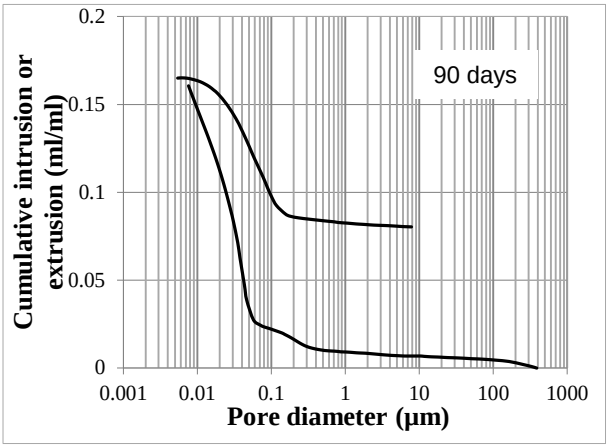
90 days
Cumulative intrusion or extrusion (ml/ml)
Pore diameter (µm)
0.2
0.15
0.1
0.05
0
0.001
0.01
0.1
1
10
100
1000

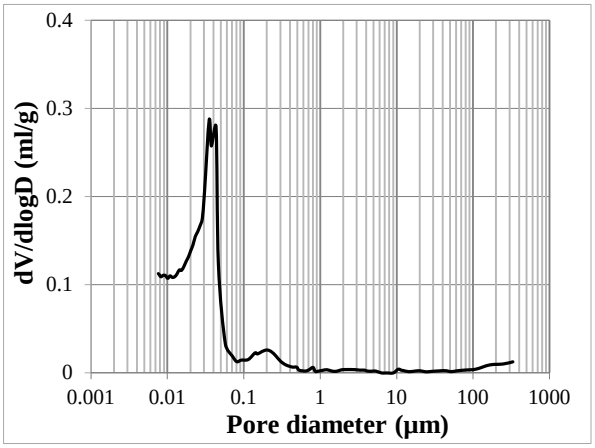
dV/dlogD (ml/g)
Pore diameter (µm)
0.4
0.3
0.2
0.1
0
0.001
0.01
0.1
1
10
100
1000

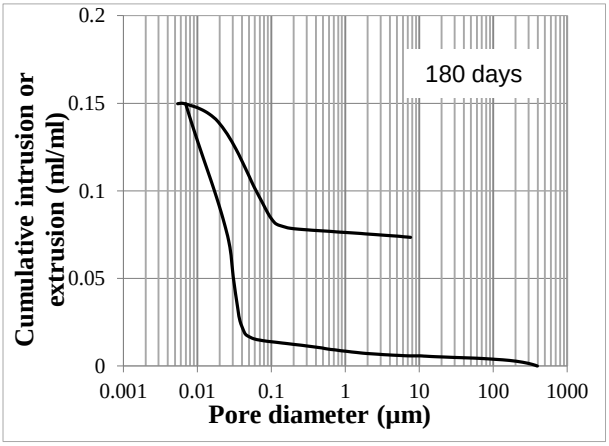
180 days
Cumulative intrusion or extrusion (ml/ml)
Pore diameter (µm)
0.2
0.15
0.1
0.05
0
0.001
0.01
0.1
1
10
100
1000

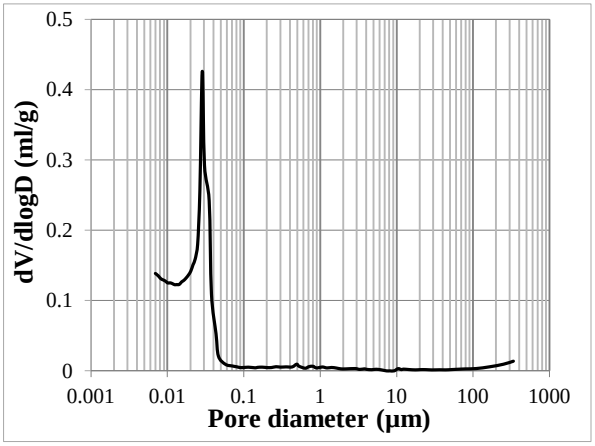
dV/dlogD (ml/g)
Pore diameter (µm)
0.5
0.4
0.3
0.2
0.1
0
0.001
0.01
0.1
1
10
100
1000

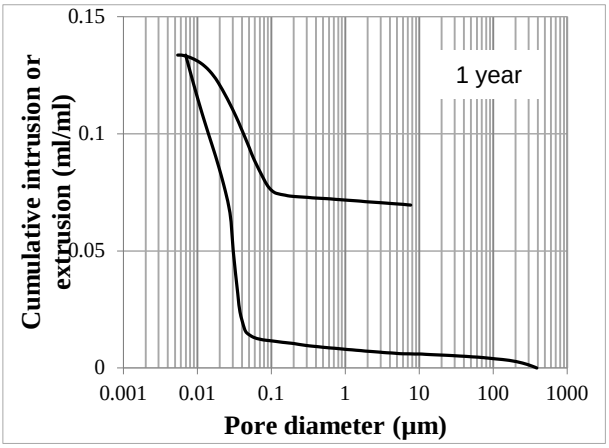
1 year
Cumulative intrusion or extrusion (ml/ml)
Pore diameter (µm)
0.15
0.1
0.05
0
0.001
0.01
0.1
1
10
100
1000

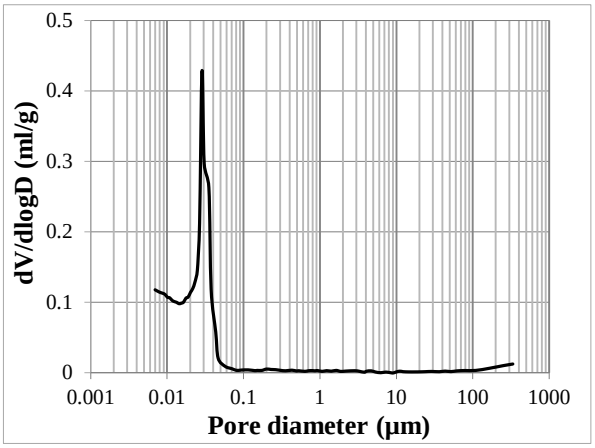
dV/dlogD (ml/g)
Pore diameter (µm)
0.5
0.4
0.3
0.2
0.1
0
0.001
0.01
0.1
1
10
100
1000

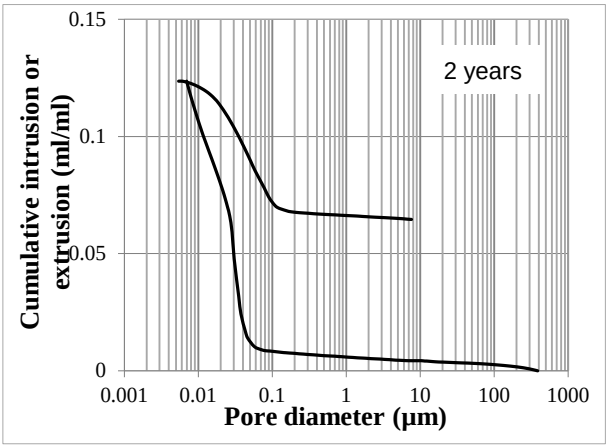
2 years
Cumulative intrusion or extrusion (ml/ml)
Pore diameter (µm)
0.15
0.1
0.05
0
0.001
0.01
0.1
1
10
100
1000

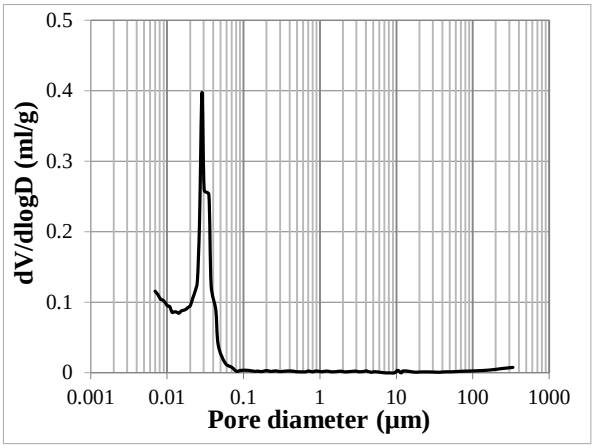
dV/dlogD (ml/g)
Pore diameter (µm)
0.5
0.4
0.3
0.2
0.1
0
0.001
0.01
0.1
1
10
100
1000

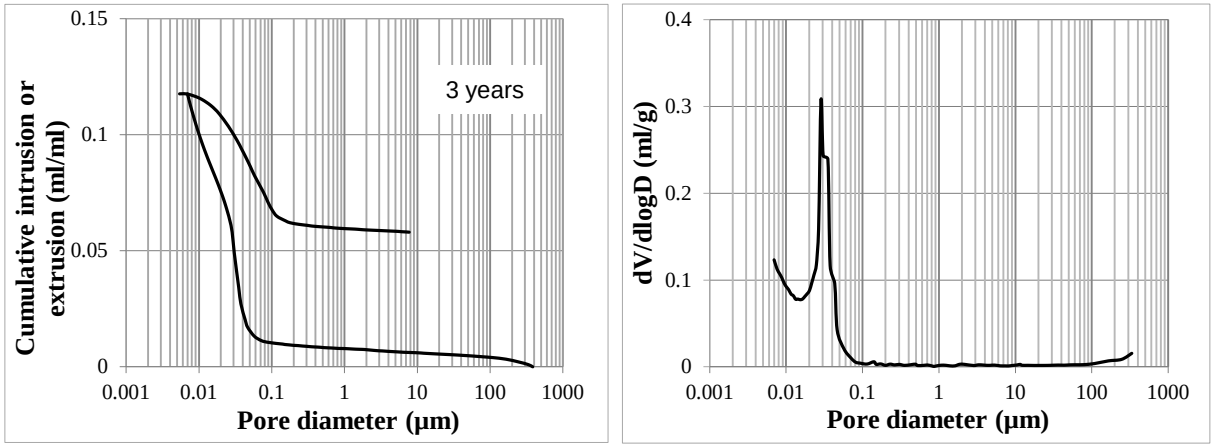

Figure A.1: Cumulative and differential PSD curves of Portland cement paste at different ages

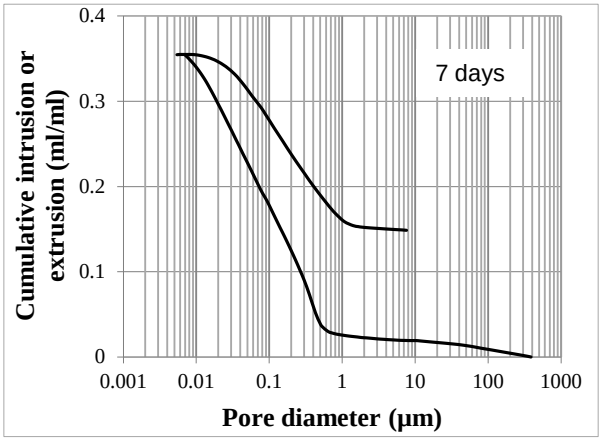
7 days
Cumulative intrusion or extrusion (ml/ml)
Pore diameter (µm)

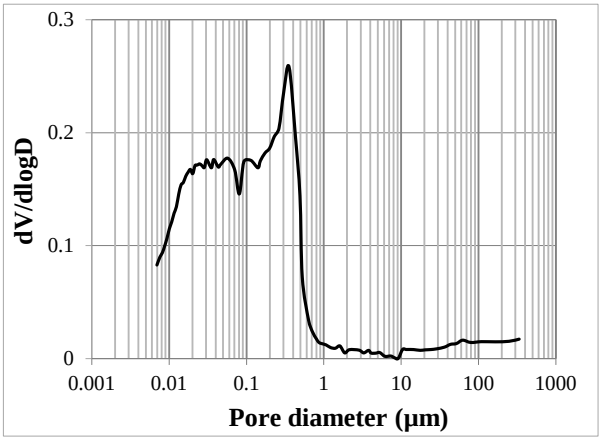
dV/dlogD
Pore diameter (µm)

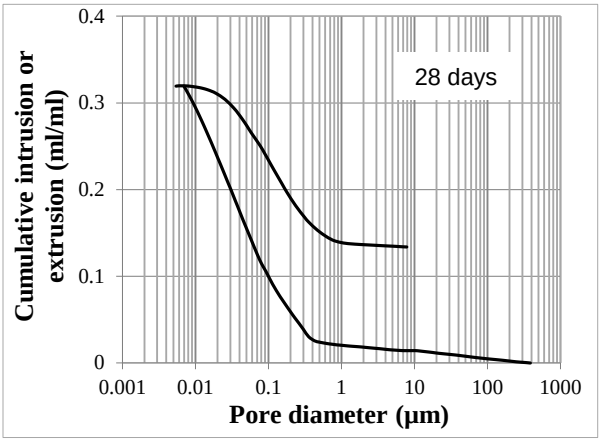
28 days
Cumulative intrusion or extrusion (ml/ml)
Pore diameter (µm)

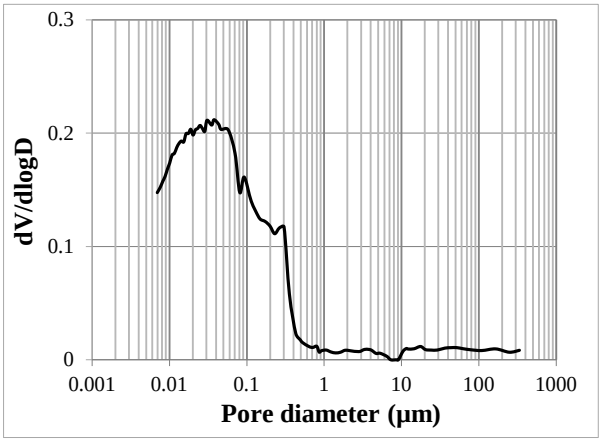
dV/dlogD
Pore diameter (µm)

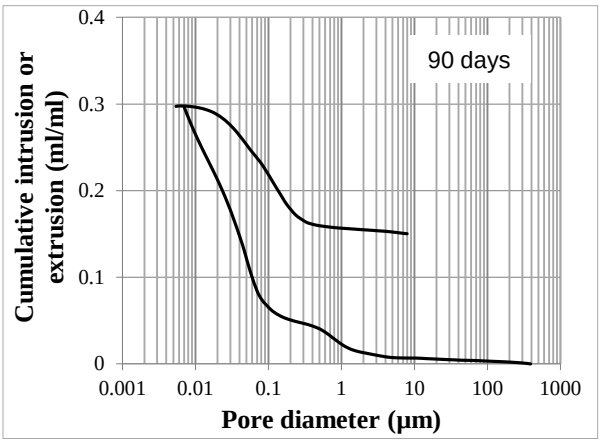
90 days
Cumulative intrusion or extrusion (ml/ml)
Pore diameter (µm)

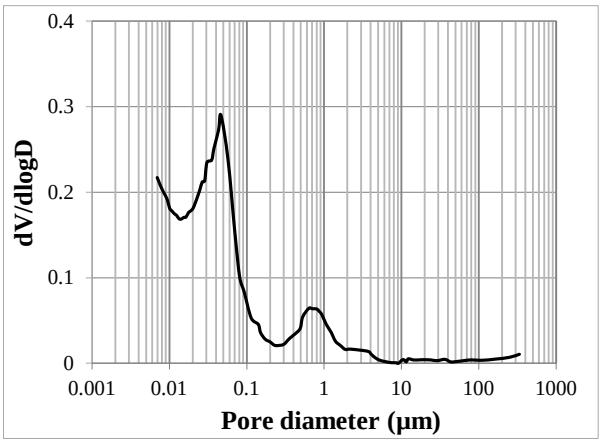
dV/dlogD
Pore diameter (µm)

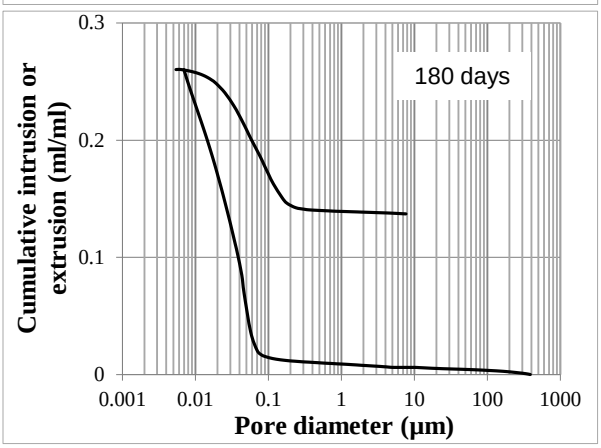
180 days
Cumulative intrusion or extrusion (ml/ml)
Pore diameter (µm)

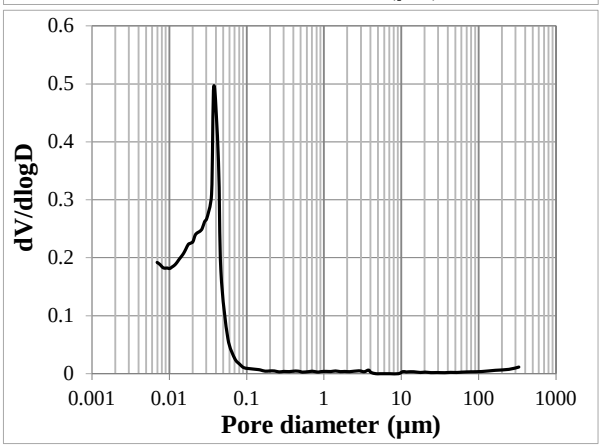
dV/dlogD
Pore diameter (µm)

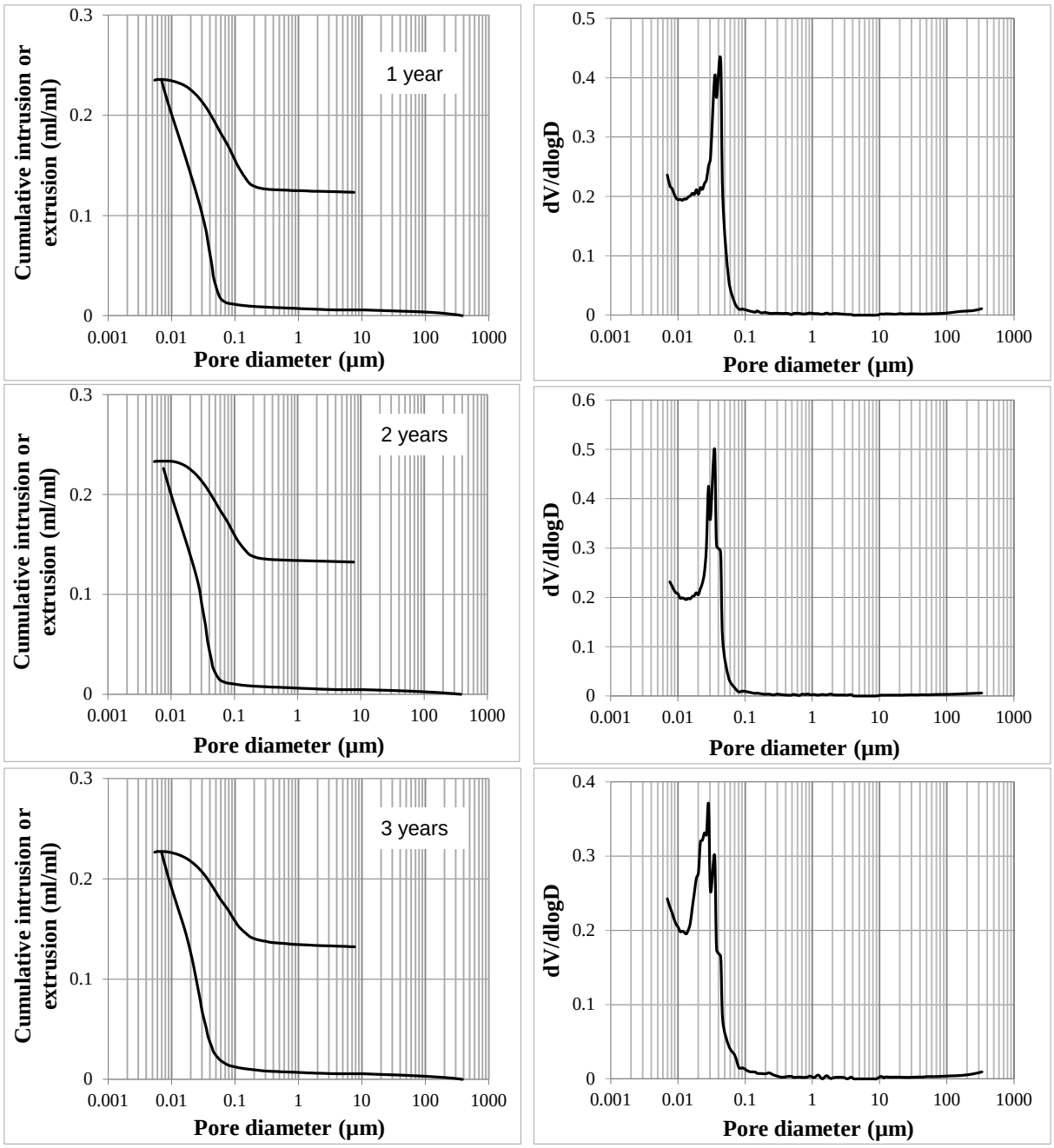

Figure A.2: Cumulative and differential PSD curves of cement paste blended with fly ash (50% fly ash; w/b=0.4) at different ages

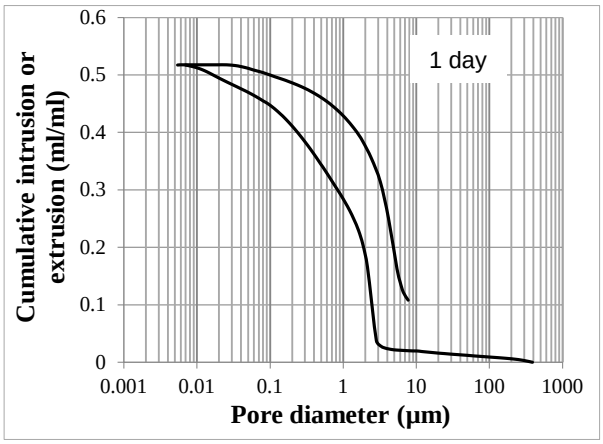
1 day
Cumulative intrusion or extrusion (ml/ml)
0.6
0.5
0.4
0.3
0.2
0.1
0
0.001
0.01
0.1
1
10
100
1000
Pore diameter (µm)

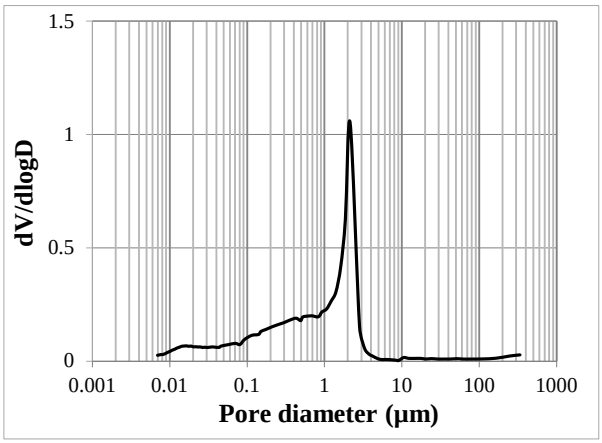
dV/dlogD
1.5
1
0.5
0
0.001
0.01
0.1
1
10
100
1000
Pore diameter (µm)

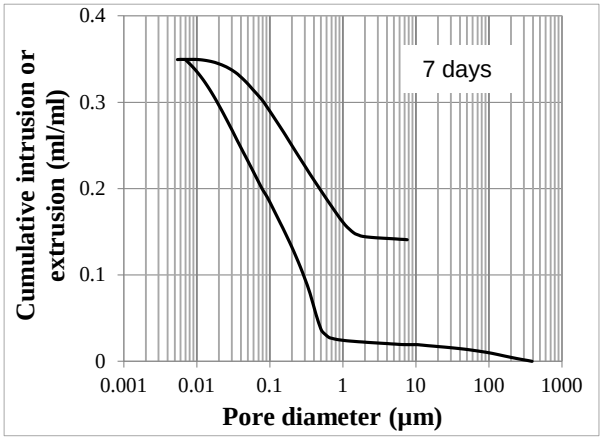
7 days
Cumulative intrusion or extrusion (ml/ml)
0.4
0.3
0.2
0.1
0
0.001
0.01
0.1
1
10
100
1000
Pore diameter (µm)

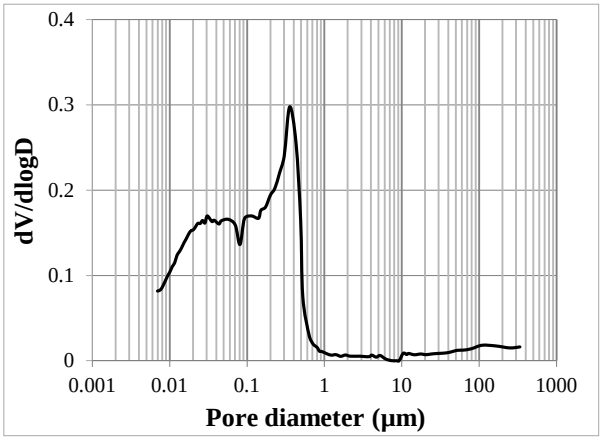
dV/dlogD
0.4
0.3
0.2
0.1
0
0.001
0.01
0.1
1
10
100
1000
Pore diameter (µm)

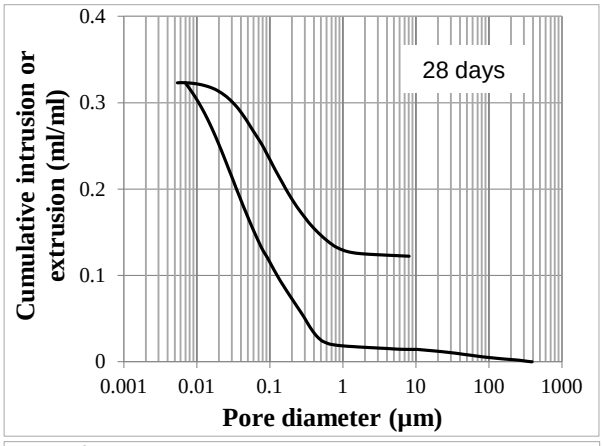
28 days
Cumulative intrusion or extrusion (ml/ml)
0.4
0.3
0.2
0.1
0
0.001
0.01
0.1
1
10
100
1000
Pore diameter (µm)

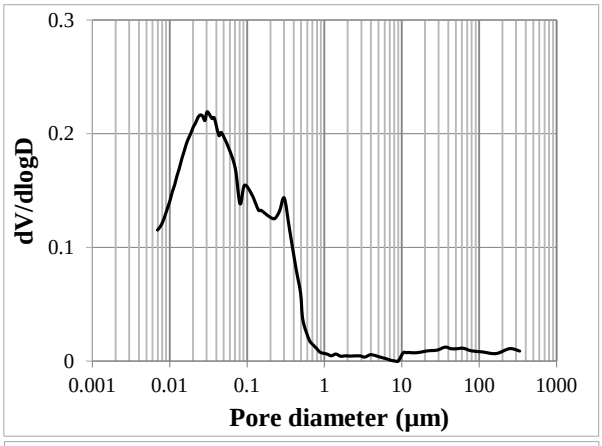
dV/dlogD
0.3
0.2
0.1
0
0.001
0.01
0.1
1
10
100
1000
Pore diameter (µm)

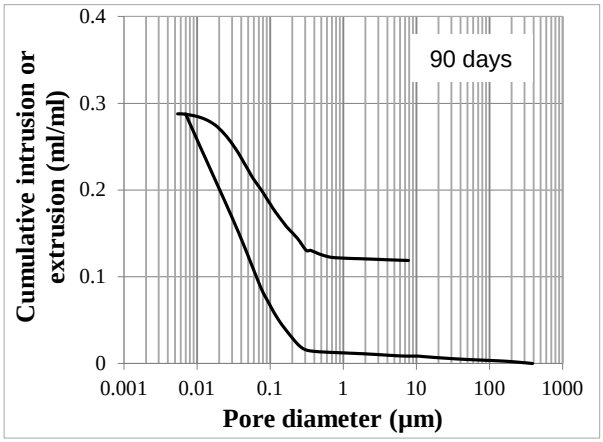
90 days
Cumulative intrusion or extrusion (ml/ml)
0.4
0.3
0.2
0.1
0
0.001
0.01
0.1
1
10
100
1000
Pore diameter (µm)

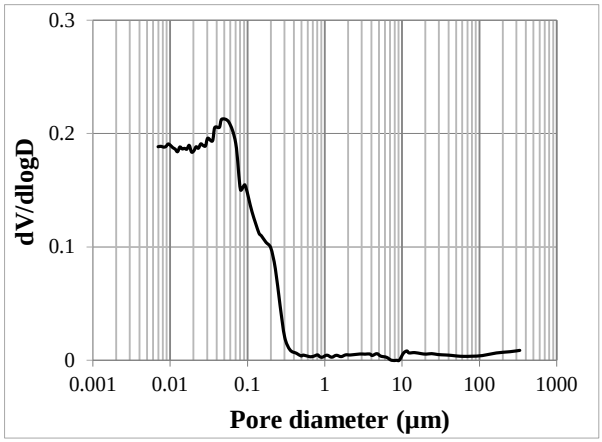
dV/dlogD
0.3
0.2
0.1
0
0.001
0.01
0.1
1
10
100
1000
Pore diameter (µm)

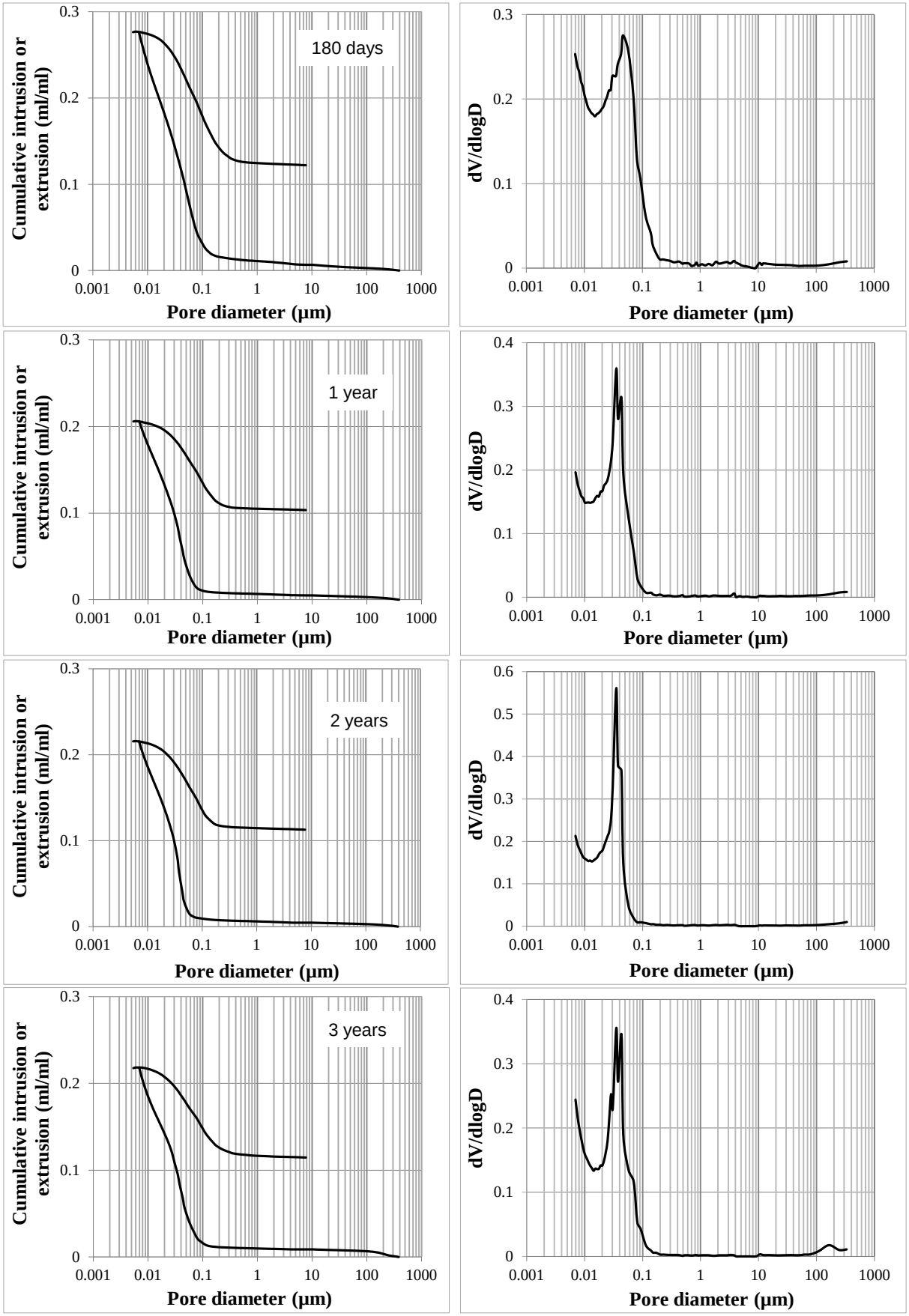

Figure A.3: Cumulative and differential PSD curves of cement paste blended with fly ash (30% fly ash; w/b=0.5) at different ages

B: The regression equations and the values of R^2 for the evolution of the total porosity of all mixtures with time (Figure 4.13 and 4.14)

Mixture	From 1 day to 1 year		From 1 year to 3 years	
	Equation	R^2	Equation	R^2
Portland cement paste w/c=0.4	Total porosity = -4.541ln(age) + 38.858	0.987	Total porosity = -1.455ln(age) + 21.946	1.000
Cement paste blended with 30% fly ash; w/b=0.4	Total porosity = -3.973ln(age) + 40.311	0.985	Total porosity = 0.023ln(age) + 16.045	0.001
Cement paste blended with 50% fly ash; w/b=0.4	Total porosity = -3.154ln(age) + 42.583	0.987	Total porosity = -0.718ln(age) + 27.834	0.794
Cement paste blended with 30% fly ash; w/b=0.5	Total porosity = -4.589ln(age) + 48.626	0.923	Total porosity = 1.103ln(age) + 14.143	0.952

C: The values of chloride migration coefficient of Portland cement concrete and fly ash concrete

Mixture/	Curing age (days)					
$\times 10^{-12}$ m^2/s	*28*	*91*	*180*	*365*	*730*	*1095*
OPC-04	13.36	11.01	10.96	13.81	13.09	12.29
OPC-05	24.40	20.85	17.53	23.40	21.36	19.74
OPC-06	27.80	25.50	26.03	28.83	32.09	32.10
FA-30-04	15.15	4.64	2.12	1.04	0.88	0.80
FA-30-05	24.10	6.30	3.91	2.18	1.43	1.29
FA-30-06	30.15	11.14	5.43	3.28	2.95	2.75
FA-50-04	15.63	4.07	2.22	1.54	1.18	0.80
FA-50-05	19.39	8.43	3.43	2.80	1.37	1.06

Propositions

1. The pore structure is the key to open the secrets of concrete.

2. Moist curing is not always beneficial to the performance of concrete.

3. The use of limestone powder in moist-cured Portland cement concrete may cause deterioration of concrete, resulting in a decrease of the resistance to chloride penetration at later ages (after around 180 days).

4. It is not sufficient to estimate the properties of Portland cement-fly ash binary systems from experimental results of short-term tests, *i.e.* test periods of 3 months or even 1 year.

5. Ignoring abnormal experimental results may keep us thinking in the wrong direction.

6. For a PhD candidate, emotional intelligence quotient *EQ* is more important than intelligence quotient *IQ*.

7. The final year of a PhD study determines the whole personal life.

8. The contribution of a PhD thesis in civil engineering is to expand the current body of knowledge incrementally, rather than establishing a whole new academic framework.

9. Stick to what you know, do the best.

10. You can tell whether a man is clever by his answers. You can tell whether a man is wise by his questions (Naguib Mahfouz: winner of the Nobel Prize for Literature, 1988).

These propositions are regarded as opposable and defendable, and have been approved as such by the promotor Prof. dr. ir. Klaas van Breugel

Stellingen

1. De poriënstructuur is de sleutel tot het openen van de geheimen van beton.

2. Verharding onder water is niet altijd gunstig voor de prestaties van beton.

3. Het gebruik van kalksteenmeel in portlandcementbeton kan degradatie van beton met zich meebrengen als gevolg van een afname van de weerstand tegen chloridepenetratie op latere leeftijd (na ongeveer 180 dagen).

4. Het is niet voldoende om een schatting te maken van de eigenschappen van portlandvliegasbeton op basis van experimentele resultaten van kort lopende proeven, dat wil zeggen een beproevingsduur van 3 maanden of zelfs 1 jaar.

5. Negeren van abnormale experimentele resultaten kan er toe leiden dat wij in een verkeerde richting blijven denken.

6. Voor een promovendus is het emotionele intelligentiequotiënt EQ belangrijker dan intelligentiequotiënt IQ.

7. Het laatste jaar van een promotieonderzoek bepaalt het hele persoonlijke leven.

8. De bijdrage van een proefschrift in de civiele techniek is om de huidige hoeveelheid kennis stapsgewijs uit te breiden en niet het optuigen van een heel nieuw academisch denkkader.

9. Blijf bij wat je weet, doe het beste.

10. Een slim mens herken je aan zijn antwoorden. Een wijs mens herken je aan zijn vragen. (Naguib Mahfouz: winnaar van de Nobelprijs voor de Literatuur, 1988).

Deze stellingen worden opponeerbaar en verdedigbaar geacht en zijn als zodanig goedgekeurd door de promotoren Prof. ir. Klaas van Breugel.

Curriculum Vitae

Personnel Information

Name: Zhuqing Yu (于竹青)
Date of Birth: 07 August 1983
Place of Birth: Yantai, P.R. China
Email: yu.zhuqing@hotmail.com

Education Experience

2002.09-2006.06: Bachelor
Materials Science and Engineering, School of Materials Science and Engineering, Wuhan University of Technology, P.R.China

2006.09-2009.06: Master
Material Science, School of Materials Science and Engineering, Wuhan University of Technology, P.R.China

2009.09-2015.05: PhD
Microlab, Materials & Environment, Faculty of Civil Engineering and Geosciences, Delft University of Technology, the Netherlands

Publication

1. Zhuqing Yu, Guang Ye (2013). New Perspective of Service Life Prediction of Fly Ash Concrete. Construction and Building Materials 48 (2013) 764–771.

2. Zhuqing Yu, Guang Ye (2013). The pore structure of cement paste blended with fly ash. Construction and Building Materials 45 (2013) 30-35.

3. Yun Gao, Geert De Schutter, Guang Ye, Zhuqing Yu, Zhijun Tan, Kai Wu. A microscopic study on ternary blended cement based composites. Construction and Building Materials 46 (2013) 28-38.

4. Yu, Z.Q., Ye, G., van Breugel, K. (2010), A review of the effects of fly ash on durability of concrete: Hydration chemistry and microstructure, Journal of Wuhan University of Technology 32 (17), pp. 235-240. It was also presented in "Int. conference on sustainable construction materials: design, performance and application". August 10-12, 2010, Wuhan, China.

5. Zhuqing Yu, Guang Ye, Klaas van Breugel, Wei Chen. (2014), Ageing of Portland Cement Concrete Cured under Moist Conditions. AMS '14 Proceedings of the Int. Conference on Ageing of Materials & Structures, 26-28 May 2014, Delft, The Netherlands.

6. Zhuqing Yu, Guang Ye, Martin Hunger, Reinier van Noort (2013). Discussion of the evolution of the chloride migration coefficient of Portland cement concrete tested by the Rapid Chloride Migration (RCM) test at long-term curing periods up to 5 years. Proceeding of CONSEC'13 – 7th Int. Conference on Concrete under Severe Conditions – Environment and Loading. September 23-25 2013, Nanjing, China.

7. Zhuqing Yu, Guang Ye (2012). A discussion of service life prediction of fly ash concrete based on DuraCrete. Proceeding of Int. Congress on Durability of Concrete. June 18-21 2012, Trondheim, Norway.

8. Zhuqing Yu, Guang Ye (2012). The pore structure and water permeability of cement paste blended with fly ash over a long period up to one year. Proceeding of Concrete Repair, Rehabilitation and Retrofitting III: 3rd Int. Conference on Concrete Repair, Rehabilitation and Retrofitting, 296-301, September 3-5 2012, Cape Town, South Africa.

9. Zhuqing Yu, Guang Ye (2012). Chloride penetration and microstructure development of fly ash concrete. Proceeding of the 2nd international conference "Microstructure related durability of cementitious composites". April 11-13 2012. Amsterdam, the Netherlands.

10. Zhuqing Yu, Guang Ye (2011). Modeling the Chemical Reaction Process of Fly Ash under Portland Cement Circumstance. Proceeding of XIII Int. Congress on the Chemistry of Cement. July 3-8, 2011. Madrid, Spain.